EXPLORING THE THERAPEUTIC POTENTIAL OF CAR-ENGINEERED T-CELLS TARGETING ENDOTHELIAL MARKERS ON TUMOUR AND INFLAMED VASCULATURE

by

Kristina Petrovic

UNIVERSITY OF BIRMINGHAM

A thesis submitted to the University of Birmingham for the degree of

DOCTOR OF PHILOSOPHY

Institute of Immunology and Immunotherapy

College of Medical and Dental Sciences

University of Birmingham

August 2018

ABSTRACT

T-cells engineered to target tumour antigens through surface-expressed chimeric antigen receptors (CARs) are highly effective in treating some leukaemias. The challenge is to extend this success to solid tumours. Tumour endothelial marker 8 (TEM8) is a conserved transmembrane protein overexpressed on the vasculature of many solid tumours but low or undetectable on healthy tissues, making it a potential CAR T-cell target. This thesis explores the safety and therapeutic efficacy of this approach by generating five human TEM8-specific CARs, expressing them in T-lymphocytes, and characterising their functional responses to TEM8 *in vitro*. Four of the five CARs showed unexpected reactivity to control cells, and in mouse studies some of these proved toxic while most were selectively lost from the circulation, an effect that was TEM8-dependent. Only one CAR selectively responded to target cells overexpressing human TEM8 *in vitro* but was unable to recognise mouse TEM8, so further *in vivo* studies were not possible. These results highlight the sensitivity and potency of CAR-engineered T-cells and demonstrate the need for additional safety measures if targeting TEM8. The thesis also demonstrates that another TEM, CLEC14A, is overexpressed in some inflammatory liver diseases, and identifies a suitable mouse model for exploring the therapeutic potential of CLEC14A-specific CAR-expressing regulatory T-cells.

ACKNOWLEDGEMENTS

First and foremost, I would like to thank my supervisor, Dr Steven Lee, for his invaluable support, guidance and encouragement throughout my time in the lab, his always open doors and for putting up with my incessant questions! It has made all the difference to my work and writing. I would also like to thank the members of the Lee lab, both past and present, for their help and advice along the way – special thanks to Joe and Katie for taking the time to help me with experiments I really couldn't have done by myself. Thank you to our collaborators in the US for sharing their knowledge with us so generously, and the Wellcome Trust for providing the funding for the work described in this thesis.

Thank you also to my second supervisor, Prof Roy Bicknell, for helpful discussions and advice, and to all the lovely people in Cancer Sciences and the IBR who I have worked with at one time or another. Special mentions go to Jamie at the PEF – thank you for all the help with protein work! – to Vas, Ditte, Gary and everyone else in the liver labs whom I pestered for sections, and to Renad for the genuinely enjoyable time spent working on Tregs together and for all the scrumptious food!

To all my friends I met through work but whose company is still making my life that much happier outside it – if I start naming you I just know I will accidentally forget someone, but you all know who you are! Thank you for all the laughs, the lunches & brunches, the board games, the occasional late nights, general philosophising about life and for surviving our PhD days together.

I would like to say a very special thank you to my family, without whose support I would never have been able to be here in the first place – thank you for always being so proud of me and for being my staunchest supporters in everything.

Finally, thank you to Ivan – for encouraging me to keep going, always taking an interest in my work (it seems that T-cells really are your favourite immune cells ever), and for the constant battling with planes & visas to make our time together possible.

CONTENTS

1 INTRODUCTION 1

1.1 T-cells and their role in the immune response 2

1.1.1 Innate and adaptive immunity 2

1.1.2 TCR generation and T-cell development 4

1.1.3 Antigen recognition and T-cell activation 8

1.1.4 TCR signalling, co-stimulation and co-inhibition 9

1.2 Cancer immunoediting 14

1.2.1 Tumour elimination 15

1.2.2 Immunity-induced tumour equilibrium 17

1.2.3 Immunosuppression and tumour escape 19

1.3 Tumour immunotherapy 24

1.3.1 Cancer vaccines 24

1.3.2 Immune checkpoint blockade 26

1.3.3 TIL therapy 31

1.3.4 TCR-engineered T-cell therapy 36

1.4 Chimeric antigen receptor (CAR) therapy 39

1.4.1 CAR design 40

1.4.2 CAR therapy of haematological tumours 44

1.4.3 CAR therapy of solid tumours 46

1.5 Tumour angiogenesis 48

1.5.1 Tumour vasculature targeting 49
1.5.2 Tumour endothelial markers 52
1.5.3 TEM8 53
1.6 Liver inflammation 56
1.6.1 Physiology of the human liver 57
1.6.2 Primary sclerosing cholangitis 61
1.6.3 Mouse models of PSC 62
1.6.4 CLEC14A 64
1.7 Regulatory T-cell therapy 67
1.7.1 Tregs and autoimmunity 67
1.7.2 Adoptive Treg transfer 68
1.7.3 Engineering Tregs to express CARs 70
1.8 Hypotheses and aims 71
2 MATERIALS AND METHODS 73
2.1 Tissue culture 73
2.1.1 Maintenance of adherent cell lines 73
2.1.2 Isolation and maintenance of human PBMCs and T-cells 75
2.1.3 Isolation and maintenance of human Tregs 75
2.1.4 Cryopreservation and revival of cells 76
2.1.5 Mycoplasma testing 77
2.2 Molecular techniques 77

2.2.1 Cloning of TEM8-targeting CAR constructs into MP71 retroviral vector 77

2.2.2 Cloning of mouse TEM8 gBlock fragment into pWPI lentiviral vector.. 78

2.2.3 DNA sequencing 79

2.2.4 Human TEM8 quantitative polymerase chain reaction (qPCR) 79

2.3 TEM8 protein production 81

2.4 Transduction protocols 82

2.4.1 Retroviral transduction of human T-cells and Tregs with CARs 82

2.4.2 Retroviral transduction of mouse T-cells with TEM8 CARs 84

2.4.3 Lentiviral transduction of LS174T cells with mTEM8 84

2.5 Phenotypic and functional analysis of transduced T-cells 85

2.5.1 Flow cytometry of T-cells and target cells 85

2.5.2 IFNγ enzyme-linked immunosorbent assay (IFNγ ELISA)..... 88

2.5.3 Intracellular cytokine staining 90

2.5.4 Proliferation assay..... 90

2.5.5 Chromium release assay..... 91

2.5.6 Treg suppression assay 92

2.6 *In vivo* studies..... 94

2.6.1 Mouse breeding and genotyping 94

2.6.2 Toxicity studies in C57BL/6 WT and TEM8 KO mice 95

2.6.3 Multiple infusion toxicity study in NSG mice 95

2.6.4 Tumour protection study in NSG mice 96
2.6.5 Mouse monitoring, tail bleed staining and ending the experiments 96
2.6.6 Mouse plasma multiplex cytokine analysis 98
2.7 CLEC14A and CD31 staining in liver tissue 98
2.7.1 Immunohistochemistry of fixed human liver tissue 99
2.7.2 Immunofluorescence of frozen mouse liver tissue 101
2.8 Statistical analysis 103
3 GENERATION AND *IN VITRO* TESTING OF TEM8 CAR-ENGINEERED T-CELLS 104
3.1 Human T-cells are successfully transduced with five distinct TEM8 CARs 104
3.2 TEM8 CAR T-cells produce multiple cytokines in response to target cells 111
3.3 TEM8 CAR T-cells proliferate in response to target cells 123
3.4 TEM8 CAR T-cells show specific cytotoxicity in response to target cells . 127
3.5 TEM8 expression on target cells and CAR T-cell cross-reactivity 130
3.6 Discussion 134
3.6.1 CAR T-cell generation methods 134
3.6.2 The affinities and cross-reactivity of TEM8 CARs 138
3.6.3 TEM8 expression on the surface of target cells 140
4 EXPLORATION OF *IN VIVO* TOXICITY AND ANTI-TUMOUR RESPONSE OF TEM8 CAR-ENGINEERED T-CELLS 144

4.1 Early *in vivo* study shows potential toxicity of L2 and L3 CARs 145

4.2 1D2 CAR T-cells persist in the peripheral circulation of healthy mice while other CARs are selectively removed from it 152

4.3 L2 CAR T-cells cause toxicity in healthy NSG mice 161

4.4 L2 CAR T-cells potentially target low-level TEM8 expression on healthy mouse tissue 173

4.5 1D2 CAR T-cells are not tumour-protective in a pilot study in NSG mice . 182

4.6 1D2 CAR T-cells do not respond to mouse TEM8 191

4.7 Discussion 201

4.7.1 Toxicity of high-affinity TEM8 CARs in healthy mice 201

4.7.2 TEM8 expression on healthy mouse tissue 204

4.7.3 Eye toxicity in TEM8 KO mice 206

4.7.4 Tumour protection by TEM8 CARs 208

5 GENERATION AND SUPPRESSIVE POTENTIAL OF CAR-ENGINEERED T_{REGS} TARGETING CLEC14A IN INFLAMED LIVER 210

5.1 CLEC14A is expressed in human inflamed liver 211

5.2 CLEC14A is expressed in the liver of MDR2 KO FVB mice 219

5.3 Human Tregs are successfully engineered to express a CLEC14A CAR. 223

5.4 Pilot studies exploring the suppressive activities of CLEC14A-specific CAR Tregs 228

5.5 Discussion 234

5.5.1 The suitability of the MDR2 KO FVB model 234
5.5.2 Treg stability and in vitro culture methods 236
5.5.3 CAR Treg suppression capacity 238
6 GENERAL DISCUSSION 241
6.1 Metabolic modulation of tumours and CAR T-cell treatment 242
6.2 Antigen specificity and safety of CAR T-cells 245
6.3 Autoimmunity and CAR Tregs 250
6.4 Conclusions 251
7 LIST OF REFERENCES 253

LIST OF ILLUSTRATIONS

Figure 1.1 – T-cell development in the thymus 7

Figure 1.2 – The structure of the αβ T-cell receptor 12

Figure 1.3 – The immunological synapse 13

Figure 1.4 – The process of cancer immunoediting 23

Figure 1.5 – Overview of adoptive cell transfer 35

Figure 1.6 – The structure and main properties of 1st, 2nd and 3rd generation CARs 43

Figure 1.7 – The structural and immune components of the liver 60

Figure 1.8 – Expression of CLEC14A in human hepatocellular carcinoma and healthy liver tissue 66

Figure 2.1 – Schematic representation of the 2nd generation TEM8 CAR construct used in this thesis 80

Figure 3.1 – T-cell gating strategy to identify CAR transduction levels of bulk T-cell populations and their CD8 and CD4 subsets 107

Figure 3.2 – Representative CAR transduction levels in bulk T-cell populations and their CD8 and CD4 subsets 108

Figure 3.3 – IFNγ release of L1 and L2 CAR T-cells at decreasing input numbers in response to target cells 115

Figure 3.4 – TEM8 CAR T-cell IFNγ release in response to target cells 116

Figure 3.5 – Mock, L5 and 1D2 CAR T-cell IFNγ release in response to target cells 117

Figure 3.6 – Sample intracellular cytokine release flow data from mock and two TEM8 CAR T-cell products 118

Figure 3.7 – Multiple cytokine release by TEM8 CAR T-cells in response to target cells 122
Figure 3.8 – Antigen-specific proliferation of one batch of TEM8 CAR T-cells in response to target cells..... 125
Figure 3.9 – Antigen-specific proliferation of a second batch of TEM8 CAR T-cells in response to target cells..... 126
Figure 3.10 – Specific cytotoxicity of TEM8 CAR T-cells in response to target cells 128
Figure 3.11 – Relative hTEM8 mRNA expression of target cells used in T-cell functional assays 132
Figure 3.12 – TEM8 protein expression on the surface of target cells used in T-cell functional assays 133
Figure 4.1 – Mouse body weights over time in pilot CAR T-cell toxicity study in C57BL/6 mice 147
Figure 4.2 – Numbers of infused ($CD45.1^+$) T-cells in mouse peripheral blood and their proportion of the total T-cell population over time in pilot CAR T-cell toxicity study in C57BL/6 mice..... 148
Figure 4.3 – Numbers of transduced ($CD34^+$) CAR T-cells in mouse peripheral blood and their proportion of the infused T-cell population over time in pilot CAR T-cell toxicity study in C57BL/6 mice..... 150
Figure 4.4 – Mouse body weights over time in second CAR T-cell toxicity study in C57BL/6 mice 155

Figure 4.5 – Numbers of infused ($CD45.1^+$) T-cells in mouse peripheral blood and their proportion of the total T-cell population over time in second CAR T-cell toxicity study in C57BL/6 mice 156
Figure 4.6 – Numbers of transduced ($CD34^+$) CAR T-cells in mouse peripheral blood and their proportion of the infused T-cell population over time in second CAR T-cell toxicity study in C57BL/6 mice 158
Figure 4.7 – Levels of selected cytokines measured in the plasma of C57BL/6 mice on days 4 and 9 of the second CAR T-cell toxicity study 160
Figure 4.8 – Mouse body weights over time in multiple infusion CAR T-cell toxicity study in NSG mice 164
Figure 4.9 – Numbers of infused T-cells in mouse peripheral blood over time in multiple infusion CAR T-cell toxicity study in NSG mice 165
Figure 4.10 – Numbers of transduced ($CD34^+$) CAR T-cells in mouse peripheral blood and their proportion of the total infused T-cell population over time in multiple infusion CAR T-cell toxicity study in NSG mice 167
Figure 4.11 – Representative tissue sections from NSG mice in the multiple infusion CAR T-cell toxicity study 170
Figure 4.12 – *In vitro* hTEM8 and target cell responses by CAR T-cells used in multiple infusion CAR T-cell toxicity study in NSG mice 171
Figure 4.13 – Mouse body weights over time in CAR T-cell toxicity study in C57BL/6 WT and TEM8 KO mice 176
Figure 4.14 – Numbers of infused ($CD45.1^+$) T-cells in mouse peripheral blood and their proportion of the total T-cell population over time in CAR T-cell toxicity study in C57BL/6 WT and TEM8 KO mice 177

Figure 4.15 – Numbers of transduced ($CD34^+$) CAR T-cells in mouse peripheral blood and their proportion of the infused T-cell population over time in CAR T-cell toxicity study in C57BL/6 WT and TEM8 KO mice 179
Figure 4.16 – Levels of selected cytokines measured in the plasma of C57BL/6 WT and TEM8 KO mice on days 1 and 6 of the CAR T-cell toxicity study 181
Figure 4.17 – Mouse body weights over time in DLD-1 tumour protection study in NSG mice 184
Figure 4.18 – Numbers of infused T-cells in mouse peripheral blood over time in DLD-1 tumour protection study in NSG mice 185
Figure 4.19 – Numbers of transduced ($CD34^+$) CAR T-cells in mouse peripheral blood and their proportion of the total infused T-cell population over time in DLD-1 tumour protection study in NSG mice 187
Figure 4.20 – Tumour volumes measured in mice over time in DLD-1 tumour protection study 189
Figure 4.21 – TEM8 CAR T-cell IFNγ release in response to hTEM8 and mTEM8-expressing target cells 193
Figure 4.22 – Specific cytotoxicity of TEM8 CAR T-cells in response to hTEM8- and mTEM8-expressing target cells 194
Figure 4.23 – TEM8 CAR T-cell IFNγ release in response to decreasing concentrations of recombinant hTEM8 and mTEM8 protein 195
Figure 4.24 – The results of the transduction of LS174T cells with a GFP^+ lentiviral mTEM8 gBlock construct 198
Figure 4.25 – TEM8 CAR T-cell IFNγ release in response to LS174T cells with or without surface mTEM8 expression 199

Figure 4.26 – Specific cytotoxicity of TEM8 CAR T-cells in response to LS174T cells with or without surface mTEM8 expression 200
Figure 5.1 – Representative normal and donor human liver sections stained for CD31 and CLEC14A by immunohistochemistry..... 214
Figure 5.2 – Representative human liver sections from inflammatory liver conditions stained for CD31 and CLEC14A by immunohistochemistry..... 216
Figure 5.3 – Representative normal, donor and inflamed human liver sections stained with IgG control for CLEC14A by immunohistochemistry 218
Figure 5.4 – Representative liver sections from MDR2 KO FVB mice of various ages stained for CD31 and CLEC14A by immunofluorescence 221
Figure 5.5 – Representative liver sections from 6-8 week old FVB WT mice stained for CD31 and CLEC14A by immunofluorescence..... 222
Figure 5.6 – Gating strategy to identify purified Tregs successfully transduced with a CLEC14A CAR 225
Figure 5.7 – Effect of rapamycin on the maintenance of Treg phenotype with time spent in culture 227
Figure 5.8 – Suppression of proliferation of one batch of conventional CD8 CAR T-cells by their autologous CAR Tregs in the presence or absence of antigen..... 231
Figure 5.9 – Suppression of proliferation of a second batch of conventional CD8 CAR T-cells by their autologous CAR or mock Tregs in the presence or absence of antigen 232

LIST OF TABLES

Table 2.1 – Adherent cells used as T-cell targets in this thesis 74

Table 2.2 – Antibodies used to stain T-cells for transduction efficiency/phenotype and target cells for TEM8 expression 87

Table 2.3 – Reagents used to develop IFNγ ELISA reactions 89

Table 2.4 – Antibodies used for intracellular cytokine staining of T-cells 93

Table 3.1 – The half maximum concentrations (EC_{50}) of five anti-TEM8 Fabs needed to bind recombinant human or mouse TEM8 extracellular domain (ED)..... 110

LIST OF ABBREVIATIONS

Abbreviation	Meaning
ACT	Adoptive cell transfer
AIH	Autoimmune hepatitis
ALD	Alcoholic liver disease
ALL	Acute lymphoblastic leukaemia
Allo-	Allogeneic
ANTXR	Anthrax toxin receptor
APC	Allophycocyanin
APCs	Antigen presenting cells
atRA	All-*trans* retinoic acid
B-	B-cell associated
BMSU	Biomedical Services Unit, University of Birmingham
BSA	Bovine serum albumin
β_2m	Beta 2-microglobulin
C57BL/6	C57 black 6
CAR	Chimeric antigen receptor
CEA	Carcinoembryonic antigen
CFSE	Carboxyfluorescein diacetate succinimidyl ester
CFTR	Cystic fibrosis transmembrane conductance regulator
CHO	Chinese hamster ovary
CLEC14A	C-type lectin domain containing 14A
CLL	Chronic lymphocytic leukaemia
CLR	Centre for Liver Research, University of Birmingham
CMG2	Capillary morphogenesis gene-2
CRC	Colorectal carcinoma
CRS	Cytokine release syndrome
CTL	Cytotoxic T-lymphocyte
CTLA-4	Cytotoxic T-lymphocyte-associated antigen-4
Cy	Cyanine
DC	Dendritic cell
DMEM	Dulbecco's Modified Eagle Medium
ECM	Extracellular matrix

EGFR	Epidermal growth factor receptor
ELISA	Enzyme-linked immunosorbent assay
Fab	Fragment antigen binding
FBS	Foetal bovine serum
Fc	Fragment crystallisable
FDA	Food and Drug Administration
FGF	Fibroblast growth factor
FGFR2	Fibroblast growth factor receptor-2
FITC	Fluorescein isothyocyanate
Foxp3	Forkhead box P3
FVB	Friend leukaemia virus B-type
GFP	Green fluorescent protein
GvHD	Graft-versus-host disease
Gy	Gray (unit)
HBSS	Hank's Balanced Salt Solution
HCC	Hepatocellular carcinoma
HEK293T	Human embryonic kidney 293 (T-antigen)
HER2	Human epidermal growth factor receptor-2
HLA	Human leukocyte antigen
HMEC	Human microvascular endothelial cells
HNSCC	Head and neck squamous cell carcinoma
HRP	Horseradish peroxidase
HSCT	Haematopoietic stem cell transplantation
HUVEC	Human umbilical vein endothelial cells
IBD	Inflammatory bowel disease
IDO	Indoleamine-2,3-dioxygenase
IFNγ	Interferon gamma
Ig	Immunoglobulin
IL	Interleukin
ITAM	Immunoreceptor tyrosine-based activation motif
KO	Knockout
LSEC	Liver sinusoidal endothelial cells
mAb	Monoclonal antibody

MAGE-A	Melanoma-associated antigen
MART-1	Melanoma antigen recognised by T-cells 1
MCA	Methylcholanthrene
MDR2	Multidrug resistance gene-2
MHC	Major histocompatibility complex
MS	Multiple sclerosis
mTCM	Mouse T-cell medium
mTOR	Mammalian target of rapamycin
NCI	National Cancer Institute
NK	Natural killer
NKG2D	Natural killer group 2D
NSCLC	Non-small cell lung cancer
NSG	NOD *scid* gamma
NY-ESO-1	New York esophageal squamous cell carcinoma-1
PBMC	Peripheral blood mononuclear cells
PBS	Phosphate-buffered saline
PD-1	Programmed cell death protein-1
PD-L1	Programmed cell death protein-1 ligand-1
PE	Phycoerythrin
PEF	Protein Expression Facility, University of Birmingham
PSC	Primary sclerosing cholangitis
PSMA	Prostate-specific membrane antigen
qPCR	Quantitative polymerase chain reaction
RCC	Renal cell carcinoma
RPMI	Roswell Park Memorial Institute
RT-PCR	Reverse transcription polymerase chain reaction
scFv	Single chain variable fragment
SDS	Sodium dodecyl sulphate
SDS-PAGE	SDS polyacrylamide gel electrophoresis
SEB	Staphylococcal enterotoxin B
synNotch	Synthetic Notch
T1D	Type 1 diabetes
TanCAR	Tandem chimeric antigen receptor

TBI	Total body irradiation
TCM	T-cell medium
Tconv	Conventional T-cell
TCR	T-cell receptor
TEM	Tumour endothelial marker
TGFβ	Transforming growth factor beta
TIL	Tumour-infiltrating lymphocyte
TME	Tumour microenvironment
TNBC	Triple-negative breast cancer
TNFα	Tumour necrosis factor alpha
Treg	Regulatory T-cell
VEGF	Vascular endothelial growth factor
VEGFR	Vascular endothelial growth factor receptor
WT	Wild-type

1 INTRODUCTION

The innate and adaptive immune system function in concert to protect the host from invading microorganisms, potentially damaging toxins and other foreign substances encountered on a regular basis. The adaptive immune system also has a crucial role in identifying mutated self-antigens expressed by many tumours, with T-lymphocytes – the principal drivers of cell-mediated immunity – playing a central part in the antitumour immune response. While immune attack can lead to tumour elimination, T-cells and other immune effectors also select for less immunogenic malignant cells, which are able to escape destruction and instead contribute to cancer progression and metastasis. This dual role of the immune system in tumour elimination and sculpting is termed 'immunoediting'. Harnessing the potential of the antitumour immune response while finding ways to circumvent tumour resistance has been the principal goal of cancer immunotherapy, which has emerged as a very promising approach to treating cancer. Several immunotherapy treatment modalities have been implemented to date, including cancer vaccines, immune checkpoint blockade and transfer of autologous tumour-specific lymphocytes, to name just a few of the most common ones.

Technological advances led to the emergence of T-cells genetically engineered to express high-affinity T-cell receptors (TCRs) or, more recently, chimeric antigen receptors (CARs), capable of recognising the desired tumour antigen with high specificity and eliciting a potent cytotoxic response. With this as with other immunotherapies, selectivity for tumour tissue is crucial in order to avoid potentially severe toxicities to normal host cells, a task made more difficult by the inhospitable

tumour microenvironment and the fact that truly selective tumour antigens are very difficult to identify. Tumour-associated vasculature is more easily accessible to immune effectors and may be sufficiently different to normal vasculature to permit discrimination in targeting. Tumour endothelial markers (TEMs) markedly overexpressed on tumour-associated vessels but absent from normal blood vessels, in particular TEM8, may represent a novel, highly selective target for cancer immunotherapies including CAR-engineered T-cells. Therefore, the exploration of this particular targeted approach is the major focus of this thesis.

CAR engineering is not limited solely to conventional T-cells; regulatory T-cells (Tregs) can be modified in the same way, and their natural immunosuppressive capacity, so often detrimental in cancer, can be applied to treating inflammatory conditions instead. One such approach, where CAR Tregs are directed against an endothelial marker overexpressed in inflammatory liver conditions, CLEC14A, potentially provides a novel way to treat debilitating immune-mediated diseases and is also explored herein.

1.1 T-cells and their role in the immune response

1.1.1 Innate and adaptive immunity

To ensure host survival, immune cells need to be capable of successfully discriminating between self- and non-self in order to eradicate outside threats while avoiding damage to host's own tissues. This balance between immune destruction of foreign invaders and tolerance (i.e. lack of response) to self-tissues is achieved

through the concerted efforts of two complementary arms of the immune system – innate and adaptive[1,2]. Innate responses are encoded by germ line genes and rely on recognition of broad molecular patterns shared by many different pathogens and toxins which differentiate them from the mammalian host. This means that the innate immune system is antigen-nonspecific but able to react quickly to pathogenic attack, usually within minutes or hours, thus forming the first line of host defence[3]. Components of innate immunity include physical barriers such as the skin and mucosa, soluble factors such as cytokines and chemokines which modulate leukocyte function and migration respectively, and leukocytes of the myeloid lineage as well as natural killer (NK) lymphocytes[1]. All of these have a crucial role in both defending the host and communicating with the adaptive arm of the immune system to prime it for response.

Adaptive immune responses are encoded in gene elements which undergo somatic rearrangement to form highly specific antigen-binding structures capable of recognising virtually any individual foreign invader[2]. This unique feature pertains to the main drivers of adaptive immunity, T- and B-lymphocytes, which are initially present in small numbers but undergo clonal expansion when presented with their cognate antigen in order to effect a temporally delayed but very powerful and antigen-specific immune attack. Another key characteristic of adaptive immunity is the formation of immunological memory, whereby a portion of T- and B-lymphocytes persists in the body after the initial antigen encounter and mounts a very rapid and potent immune response if the same antigen is ever encountered again[1,2]. Even though both types of lymphocytes drive adaptive responses, there are fundamental differences between them. B-cells are characterised by surface expression and secretion of immunoglobulin

(Ig), which binds cognate antigen without any need for previous antigen processing and presentation. On the other hand, T-cells express the membrane-bound T-cell receptor (TCR), which is only able to bind antigen when it is correctly processed and presented on the surface of a cell (see section 1.1.2). In addition, unlike B-cells which develop fully in the bone marrow, T-cells migrate out of it to undergo their maturation in the lymphoid organ known as the thymus[1,2].

1.1.2 TCR generation and T-cell development

Self-tolerance as a hallmark of the whole immune system is particularly important for T-cells, which recognise foreign or mutated peptide antigens only in association with self major histocompatibility complex (MHC) (also known in humans as human leukocyte antigen – HLA) molecules[4]. In fact, the TCR on the surface of T-lymphocytes, which binds the MHC-antigen molecular complex, has very low affinity for antigen alone or for MHC molecules presenting other peptides. It is instead constrained to recognising the antigenic peptide-MHC complex as a whole, a characteristic termed 'MHC restriction' and first demonstrated in a series of experiments in mice in the 1970s[5,6]. This unique ability of the T-cell is achieved through the sophisticated process of thymic selection and maturation which is summarised below and in **Figure 1.1**.

Haematopoietic stem cells give rise to committed T-cell precursors in the bone marrow, which then migrate to the thymus to begin their differentiation into mature T-cells. These precursors, or pro-thymocytes, do not express CD3, CD4 or CD8 surface markers, and are known as 'double-negative' ($CD4^{-}CD8^{-}$)[2]. Upon arrival into the thymic subcapsular zone, the double-negative cells begin the somatic rearrangement

of their numerous variable (V), diversity (D) and joining (J) gene elements into fully formed $V_\alpha J_\alpha$ and $V_\beta D_\beta J_\beta$ chains of the TCR. This process of apparently random combinatorial assembly results in a hugely diverse array of functional antigen-specific TCRs[4]. The β chain of the TCR is the first to undergo rearrangement while the double-negative T-cell precursors are still in the subcapsular zone of the thymus. Provided the rearrangement is productive and results in a functional β chain, the cells progress into the thymic cortex where the same process happens for the α chain; upon formation of a fully functional $\alpha\beta$ TCR, the expression of CD3, CD4 and CD8 is also induced on the cell surface and marks their transition to 'double-positive' T-cells ($CD4^+CD8^+$)[2,4].

While still in the thymic cortex, the developing lymphocytes interact with self MHC molecules found on the surface of the cortical epithelial cells. If they do so with sufficient affinity, they progress into the thymic medulla, while the T-cells that do not bind self MHC molecules are eliminated by apoptosis – this constitutes positive selection[7]. It is at this juncture that double-positive lymphocytes which interact with class I MHC molecules become single positive for CD8, and those that bind class II MHC molecules become CD4 positive only[4]. Finally, the positively selected CD8 and CD4 T-cells that have entered the thymic medulla interact with a vast variety of tissue-specific self-peptides presented in the context of MHC molecules on the surface of medullary epithelial cells. The T-cells that bind self-peptides too strongly are considered autoreactive and are therefore apoptosed (negative selection), while the remainder – approximately 5% of the starting double-negative thymocyte population – are exported into the peripheral circulation[7]. The vast majority of circulating T-cells use the $\alpha\beta$ TCR and are characterised as either $CD4^+$ or $CD8^+$; about 5-10% of them have

an alternate version of the TCR, $\gamma\delta$, do not express surface CD4 or CD8 and are predominantly found in the gastrointestinal tract[2], but are outside the scope of this thesis.

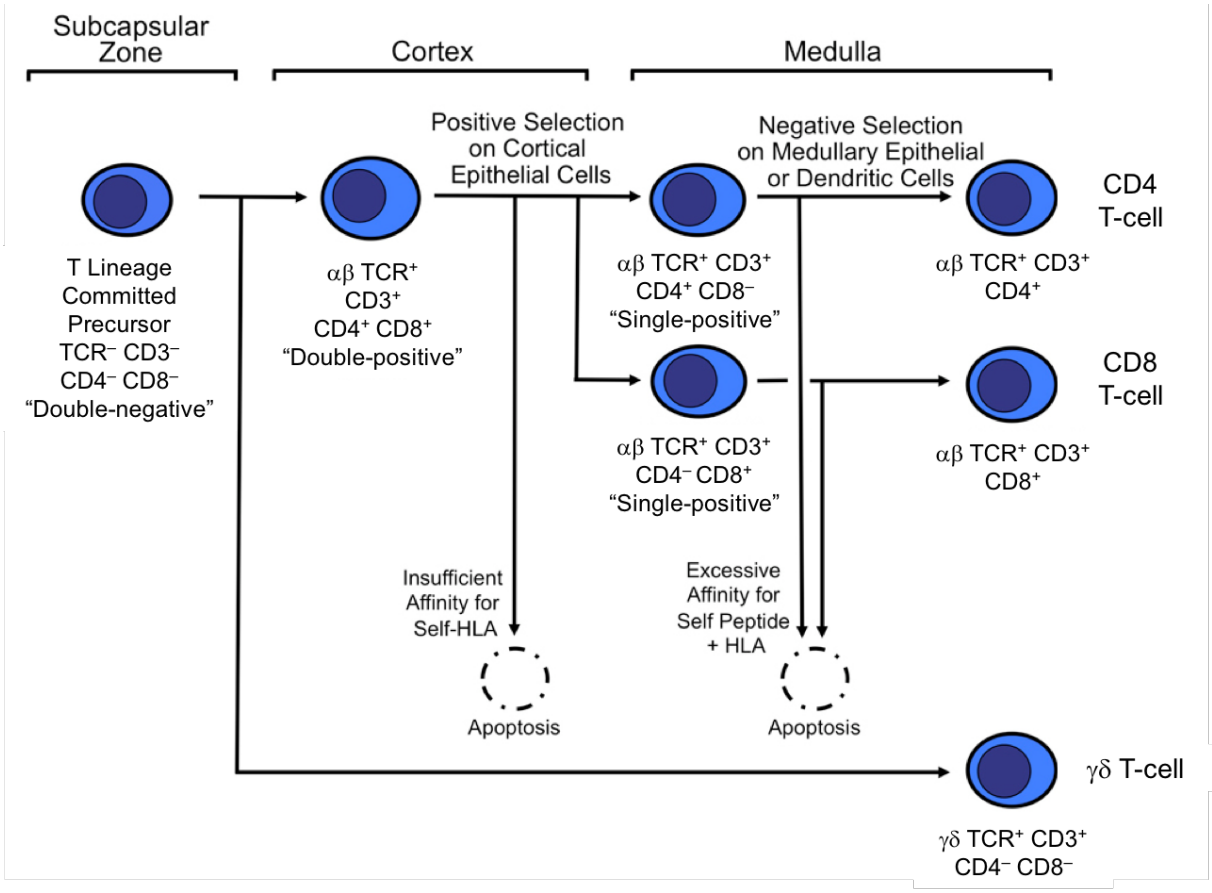

Figure 1.1 – T-cell development in the thymus

Haematopoietic precursors committed to the T-cell lineage leave the bone marrow for the subcapsular zone of the thymus. They then proceed through the thymic cortex and medulla, rearranging their T-cell receptor (TCR) α and β chain gene elements and undergoing positive and negative selection to eliminate those T-cells that respectively show inadequate affinity for self human leukocyte antigen (HLA) molecules or excessive binding to self-peptides expressed in the context of host HLA. During the selection process the lymphocytes become single positive for either CD4 or CD8, finally leaving the thymus as mature CD4 or CD8 T-cells with a fully functional $\alpha\beta$ TCR. A small proportion of T-cells rearrange their γ and δ TCR chains instead, do not express surface CD4 or CD8 and undergo most of their maturation in the extrathymic compartment. Adapted from The Journal of Allergy and Clinical Immunology, 125(2 Suppl 2), David D. Chaplin, Overview of the immune response, S3-23, Copyright (2010), with permission from Elsevier[2].

1.1.3 Antigen recognition and T-cell activation

Mature αβ T-cells, characterised as either $CD4^+$ or $CD8^+$, are antigen-naïve after leaving the thymus. They concentrate in secondary lymphoid organs such as the spleen and lymph nodes where they eventually encounter antigenic peptide-MHC complexes[2]. Depending on the nature of antigenic challenge, two major classes of MHC molecules present the peptide to the T-cells to trigger different kinds of T-cell responses. MHC class I proteins are constitutively expressed on all nucleated cells, and generally present endogenous peptides derived from host cell proteins (including tumour-specific proteins if the cell is cancerous) or from intracellular pathogens such as viruses[4]. MHC class I-peptide antigen complexes are recognised by CD8 T-cells, with the CD8 co-receptor interacting directly with the class I molecule to stabilise the complex and ensure full T-cell activation[8]. Upon engagement of their TCR by peptide-MHC class I, CD8 T-cells become cytotoxic T-lymphocytes (CTLs) which induce target cell apoptosis by direct cell-to-cell contact and release of various pro-apoptotic factors including granzymes and perforin[4].

In contrast to class I, MHC class II molecules are present mainly on the surface of "professional" antigen-presenting cells (APCs), which include dendritic cells (DCs), monocytes, macrophages and B-lymphocytes. APCs are found in large numbers in the skin and mucosa, where they are most likely to encounter pathogens; they specialise in taking up exogenous antigens, such as those derived from bacteria and parasites, by endocytosis or phagocytosis and processing them for presentation in association with MHC class II molecules on the cell surface[9]. APCs are then able to travel from the periphery to the secondary lymphoid organs, where their class II-peptide antigen

complexes interact with the TCR of CD4 T-cells. CD4 αβ T-cells are the most numerous T-cell subset in the body and perform a variety of functions upon activation. Most of them are designated as T-helper cells and enhance T- and B-cell responses through cognate signalling or the secretion of various cytokines, but an important group of CD4 T-cells have a regulatory role and prevent autoimmunity and immune-mediated tissue damage[4] – these regulatory T-cells (Tregs) will be discussed in section 1.7.

1.1.4 TCR signalling, co-stimulation and co-inhibition

In order to achieve full T-cell activation, signalling through the TCR alone is not enough. A host of co-stimulatory molecules is also required – without additional signals, stimulation of TCR in isolation leads to a state of functional unresponsiveness, or 'anergy'[10]. The αβ TCR is associated with the CD3 complex of accessory chains, consisting of transmembrane γ, δ and ε chains and a predominantly intracytoplasmic CD3ζ homodimer (**Figure 1.2**). Each chain contains an immunoreceptor tyrosine-based activation motif (ITAM) on its cytoplasmic portion, with CD3ζ chains containing three ITAMs each. When phosphorylated as a consequence of peptide-MHC binding to the TCR, ITAMs in turn initiate a string of phosphorylation reactions leading to the ultimate activation of genes responsible for T-lymphocyte proliferation and differentiation[2,4].

Perhaps the most well-described co-stimulatory receptor expressed on the surface of T-lymphocytes is CD28, which was found to induce T-cell proliferation, augment lymphocyte interleukin-2 (IL-2) production and cause overall amplification of the antigen response following TCR/CD3 stimulation in primary T-cell cultures[11]. The

importance of CD28 co-stimulation was further shown in studies of $CD28^{-/-}$ mice, which mounted a weak immune response and had impaired T-cell proliferation[12,13]. CD28 binds B7-1 (CD80) on the surface of the APC, as evidenced by B7-specific monoclonal antibodies (mAbs) inhibiting this interaction[14], and by CD28-deficient T-cells exhibiting no B7-dependent co-stimulation[12]. A second ligand for CD28 on the APC was subsequently identified as B7-2 (CD86)[15]. The structural homologue of CD28 – cytotoxic T-lymphocyte associated antigen-4 (CTLA-4) – is also found on the T-cell surface and binds CD80 and CD86, but with the opposite effect of T-cell inhibition rather than stimulation[16]. CD28 and CTLA-4 are therefore mutually antagonistic, with CD28 expressed constitutively on T-cells while CTLA-4 is induced upon activation, and its upregulation in turn downregulates CD28 expression[17].

This already complex picture is further compounded by the presence of numerous other co-stimulatory and co-inhibitory molecules on the surface of T-lymphocytes. These include co-stimulatory molecules 4-1BB (CD137) and OX40 (CD134), which bind their respective ligands 4-1BBL and OX40L on the APC and promote cytokine production and T-cell survival via upregulaton of various anti-apoptotic factors[18]. Conversely, the programmed cell death protein-1 (PD-1) is, like CTLA-4, co-inhibitory, and alongside other surface-expressed inhibitory molecules like lymphocyte-activation gene-3 (LAG-3) and T-cell immunoglobulin mucin-3 (TIM-3) serves as an indicator of T-cell exhaustion[19]. In all cases, upon TCR/CD3 activation, significant rearrangement of the receptors and the various co-stimulatory molecules takes place to form a so-called 'immunological synapse'[20] (**Figure 1.3**). Successful synapse formation is what ultimately leads to T-cell differentiation into T-helper or CTL subsets, their migration to

peripheral tissues, and exertion of their effector functions at the site of antigenic challenge[2].

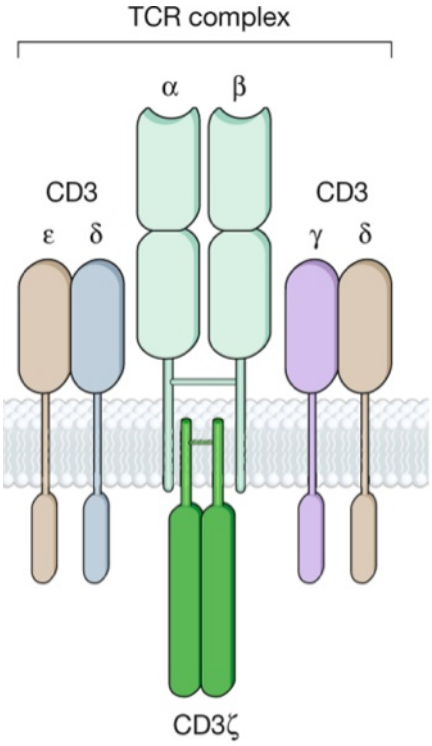

Figure 1.2 – The structure of the αβ T-cell receptor

The αβ T-cell receptor (TCR) consists of the αβ heterodimer together with the CD3 complex of accessory chains: one γ, one ε, two δ (all transmembrane) and a predominantly intracellular CD3ζ homodimer, which signals into the cell once the TCR binds to a peptide-MHC complex. Reprinted by permission from Macmillan Publishers Ltd: NATURE (Sadelain M, Rivière I, Riddell S. Therapeutic T cell engineering. 545(7655):423–31), copyright (2017)[21].

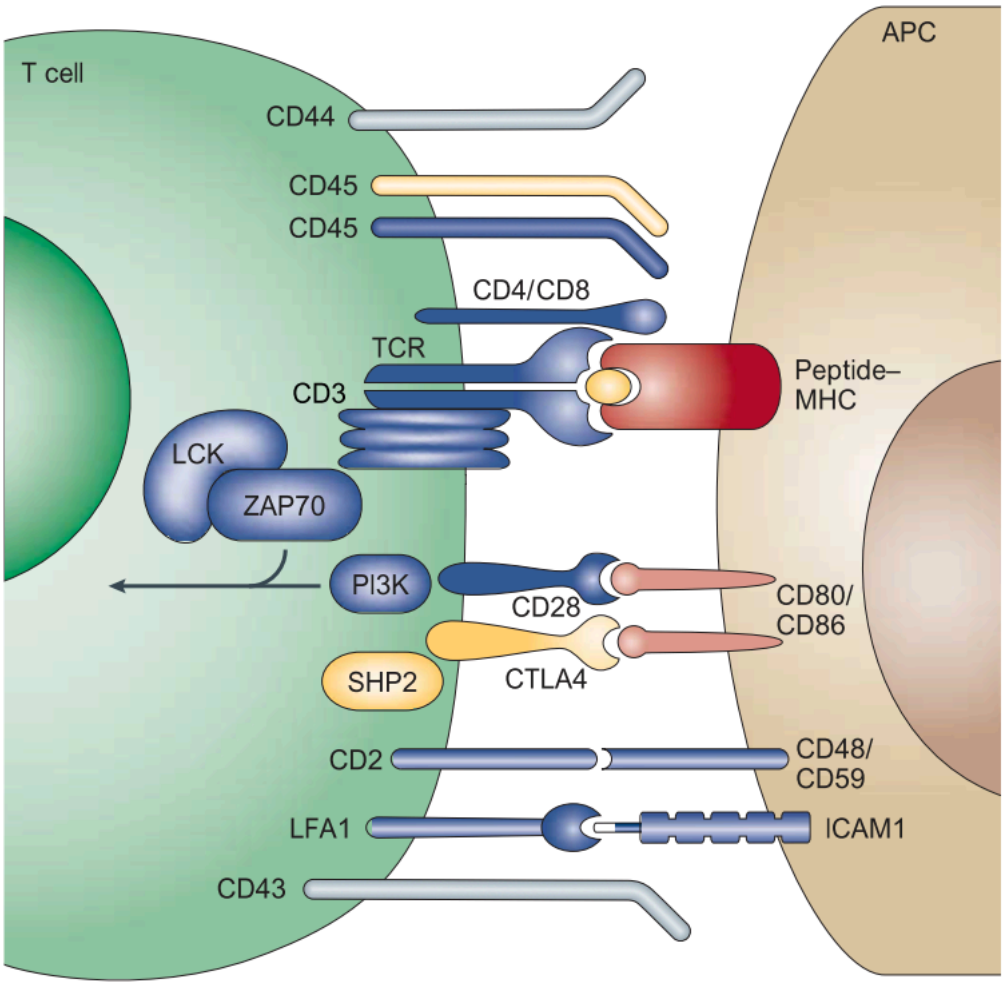

Figure 1.3 – The immunological synapse

The structure of the binding interface between a T-cell and an antigen-presenting cell (APC), termed immunological synapse, showing the interaction between the TCR/CD3 complex on the surface of the T-cell and the peptide-MHC ligand on the APC surface, together with a host of co-stimulatory (blue) and co-inhibitory molecules (yellow) as well as surface markers that do not participate in the signalling (grey). Upon TCR/CD3 binding of the peptide-MHC, the cytoplasmic portions of the CD3 chains are phosphorylated by tyrosine kinases including LCK, which in turn recruit signalling molecules such as ζ-chain associated protein 70 (ZAP70) – this starts a signalling cascade which ultimately leads to T-cell activation. PI3K, phosphatidylinositol 3-kinase; CTLA4, cytotoxic T-lymphocyte associated antigen 4; SHP2, Src homology region 2-containing protein tyrosine phosphatase 2; LFA1, leukocyte function-associated antigen 1; ICAM1, intercellular adhesion molecule 1. Reprinted by permission from Macmillan Publishers Ltd: NATURE REVIEWS IMMUNOLOGY (Huppa JB, Davis MM. T-cell-antigen recognition and the immunological synapse. 3(12):973–83), copyright (2003)[22].

1.2 Cancer immunoediting

It is now widely recognised that the host immune system is heavily involved in tumour regulation. Cells that have escaped intrinsic control mechanisms and started to proliferate without key environmental stimuli, thus acquiring potential to become cancerous, can be recognised through their expression of mutated antigens, or 'neo-antigens', and eliminated by immune effector cells including T-lymphocytes[23]. This elimination of pre-malignant and malignant cells is known as cancer immunosurveillance, and evidence of it in both mice and humans has steadily accumulated over the years (discussed in more detail in section 1.2.1).

More recently it has become apparent that, rather than only being host-protective, the immune system also has the capacity to shape tumour development. Evidence for this was first found in a study of immunodeficient mice that lacked either responsiveness to interferon gamma (IFNγ) or all of their lymphocytes, including T-lymphocytes[24]. These mice were more susceptible to methylcholanthrene (MCA)-induced sarcomas as well as spontaneous development of epithelial carcinomas compared to their wild-type counterparts. Importantly, however, when MCA sarcomas from immunodeficient hosts were transplanted into wild-type mice, 40% were spontaneously rejected, while MCA sarcomas from immunocompetent hosts all exhibited growth and progression in wild-type mice after the same transplantation procedure[24]. This showed the capacity of the immune system to alter tumour immunogenicity, with tumours generated in the presence of an intact immune system being much less immunogenic and therefore exhibiting higher potential for progression and metastasis. Evidence from this study led to the formulation of the cancer immunoediting concept[25], encompassing the immune

system's dual role in immunosurveillance and tumour-sculpting. Cancer immunoediting is divided into three stages, each of which is discussed in more detail below – elimination, equilibrium and escape[26] (**Figure 1.4**).

1.2.1 Tumour elimination

The elimination phase, previously referred to as cancer immunosurveillance, is characterised by cells of both innate and adaptive immunity recognising and killing transformed cells in the host before they become clinically apparent, thus restoring physiological balance[23]. Even though this process has never been visualised, it has been shown *in vivo* in numerous mouse models where parts of the immune system have been abolished by gene knockout or neutralising antibodies, as well as in the more complex and varied settings of human clinical trials. In addition to the study discussed above[24], the heavy implication of T-cells in tumour regulation has been demonstrated in several others, with mice lacking $\alpha\beta$ T-cells[27], the less common $\gamma\delta$ T-cells[27], or T-lymphocytes in general[28] all being more susceptible to chemical carcinogen-induced sarcomas. Furthermore, mice deficient in IFNγ and perforin, two key effector molecules secreted by cytotoxic T-lymphocytes, showed significantly reduced capacity for preventing prostate and mammary tumour metastases to the lung compared to mice lacking only one of the two, with IFNγ also controlling mouse sarcoma growth rate[29]. In fact, IFNγ is an important mediator of immunosurveillance with the capability to enhance tumour cell immunogenicity[30], partly through upregulation of MHC class I expression on tumour cells and consequent better tumour targeting by CD8 T-lymphocytes[24,31]. The role of perforin is also crucial – perforin-deficient mice suffered a much higher incidence rate of spontaneous lymphoma than

their wild-type counterparts[32], which increased further when mice also lacked β_2-microglobulin (β_2m) necessary for MHC class I molecule function[33]. The above studies all demonstrated the importance of CTLs in tumour initiation and progression. Interestingly, defects in perforin cytotoxicity were also shown to increase susceptibility to haematological malignancies in humans[34], providing further evidence for the role of adaptive immunity in tumour elimination.

Advances in human T-cell culture methods, the ability to mimic the immune response *in vitro* with the help of dendritic cells, and screening of serum samples from neoplastic patients for immune reactivity to specific tumour proteins led to the discovery of a multitude of tumour antigens which the human immune system can recognise[35]. Examples include the cancer-testis antigens melanoma-associated antigen-1 (MAGE-A1)[36] and New York esophageal squamous cell carcinoma-1 (NY-ESO-1), the latter of which is found in a wide variety of cancers including those of the breast, prostate, bladder and liver as well as in healthy testes and ovaries[37]. Both MAGE-A and NY-ESO-1 are also expressed in conjunction in metastatic melanoma lesions[38]. Another tumour antigen, cyclin B1, is aberrantly expressed in the cytoplasm of many human tumour cells including those from breast and head and neck cancers while being barely detectable in normal cells[39]. In these and many other cases, the tumour antigens were found to trigger CTL responses *in vitro*. Clinical evidence of cancer immunosurveillance in humans is harder to come by due to the complex nature of the human body compared to mouse models and the requirement for large clinical trials with long-term follow-up. Nonetheless, immunosuppression has been linked to increased incidence of malignancies, such as in the case of AIDS patients who have a

higher risk of virus-associated cancers[40] and smoking-independent lung adenocarcinomas[41,42] than the wider population. A study of heart and lung transplant patients in a 15-year period, all of whom received immunosuppressive treatment to prevent graft rejection, found that their risk of cancer diagnosis was increased sevenfold compared to the general population, with leukaemias and lymphomas being the predominant cancer types diagnosed in this group[43]. In addition, CD8 tumour-infiltrating lymphocytes (TILs), when present in high numbers within the tumour, strongly correlate with favourable clinical outcomes in various cancers. The fact that TILs are good predictors of survival was first observed in melanoma patients[44,45], followed by the finding that nearly 40% of patients with ovarian cancer who had high TIL numbers survived longer than five years post-diagnosis compared to only 4.5% of patients with low TIL numbers[46]. A multi-centre study of patients with colon cancer determined that the presence of tumour-infiltrating cells, including TILs, was a more accurate predictor of clinical outcome than histopathological staining methods[47]. These and other studies highlighted the importance of TILs as a prognostic indicator and influenced their subsequent use in tumour immunotherapy, which is discussed further in section 1.3.3.

1.2.2 Immunity-induced tumour equilibrium

Certain tumour cells are able to evade destruction by the immune system yet remain partially controlled, resulting in incomplete tumour elimination and entry into a state of dynamic balance with host immunity instead. In this equilibrium phase, the antitumour immune response keeps the cancer in a ‘dormant’ state and prevents its outgrowth, but cannot fully eradicate it[23]. Experimental evidence of equilibrium was first found in

a study of wild-type mice injected with low-dose MCA[48], which led to tumour establishment in a small number of treated animals. However, when the remaining mice with no overt tumours were depleted of CD4 and CD8 T-cells, or when cytokines mediating adaptive immunity such as IFNγ or interleukin-12 (IL-12) were blocked using mAbs, approximately half the mice displayed progressive sarcoma. Furthermore, this was only found when mAbs were directed against CD4, CD8 or the above cytokines, with anti-NK cell mAbs showing no effect on tumour progression[48], thus providing evidence for the crucial role of T-lymphocytes in keeping the tumour in check. The fact that T-cells are essential for inducing tumour equilibrium was shown in a further study in a murine model of a p53-mutant tumour, where T-cell cytokines IFNγ and tumour necrosis factor α (TNFα) induced cancer growth arrest and senescence[49]. Another study in a mouse model of metastatic melanoma showed that CD8 T-cell depletion led to significantly faster progression to metastases, and suggested that keeping the disseminated tumour in a dormant state that does not lead to macroscopic metastases is a viable therapeutic strategy in cancer patients[50].

It has been shown that tumours can stay dormant in human hosts for years or even decades before any clinical manifestation, a phenomenon known as minimal residual disease[23]. For example, circulating tumour cells have been detected in former breast cancer patients up to 22 years after mastectomy with no evidence of clinical disease, thus supporting the hypothesis of cancer equilibrium in humans[51]. Evidence implicating the immune system in this process can be found in the rare, but significant cases where an occult tumour was unintentionally transplanted from donor to immunosuppressed recipient along with the transplanted organ. Even though their incidence is small,

donor-related tumours have been detected in the past, some of which never manifested in the donors themselves and only developed many months or years later in the immunosuppressed individual receiving the organ[52]. Several cases have also been reported of patients developing melanoma from transplanted organs originating from donors who underwent successful melanoma surgery and been cleared of cancer years earlier; some of the recipients progressed to metastatic melanoma with fatal outcomes[53]. These reports highlight the existence of a balance between cancer and the human immune system, which is nonetheless broken down once the immune system is compromised. However, long periods of tumour dormancy and apparent lack of clinical disease in many patients suggest that tumour equilibrium is a valid therapeutic endpoint in the cases where cancer elimination cannot be achieved.

1.2.3 Immunosuppression and tumour escape

It has been shown that, in a mouse model of tumour dormancy in acute myeloid leukaemia, residual tumour cells become increasingly resistant to CTL-mediated killing with increased time they spend dormant in the host[54]. In this study, leukaemic cells that persisted upregulated their surface expression of PD-1 ligand-1 (PD-L1) and the CTLA-4 ligand CD80, thus leading to downregulation of the T-cell response. Blocking CTLA-4, CD80 or PD-L1 enhanced T-cell cytotoxicity and led to prolonged mouse survival[54]. It has also been shown that cancer recognition by T-cells is reduced by the promotion of outgrowth of tumour cells lacking strongly immunogenic mutant peptides[55]. These studies provide evidence for the tendency of tumour cells to become less immunogenic under selective pressure by the immune system, ultimately leading to survival of the most aggressive tumour variants and their unrestricted growth and

spreading in the host. This last phase of cancer immunoediting, in which the immune system fails to control the tumour, is termed tumour escape[23], and cancer cells are able to employ a variety of mechanisms to achieve it.

Experiments in mice suggest that, over time, tumours are able to promote their own growth by further inducing the naturally occurring process of tolerance, whereby T-cells responsive to self-antigen – and consequently to antigens expressed by tumours – are eliminated (much like during the process of thymic selection)[23,56,57]. Furthermore, loss of antigen presentation on the surface of tumour cells renders them 'invisible' to immune effectors. For example, downregulation of β_2m in several patient-derived metastatic melanoma cell lines led to loss of MHC class I surface expression and the ability to present endogenous antigen, which in turn resulted in poor recognition by CD8 T-cells[58]. Another study showed that, in the presence of CTLs, the absence of melanocyte differentiation antigens from the surface of patient-derived melanoma cells led to progressive metastases, while one metastasis that persistently expressed antigen underwent regression[59]. Apart from peptide-MHC class I downregulation common to many tumours, other mechanisms of tumour immune evasion include upregulation of anti-apoptotic factors such as BCL-xL[60], deregulation of the Fas-mediated cell death pathway[61], and direct tumour cell contact with, and inhibition of, CTLs via PD-1/PD-L1 and/or CTLA-4 interactions as discussed above[54].

In addition to the described changes in cancer cells themselves, tumours generate an immunosuppressive microenvironment in order to further subvert the host immune system. One example of this, found in both mouse and human tumours, is the secretion

of products of sterol metabolism that inhibit the expression of CC chemokine receptor-7 on the surface of dendritic cells; this in turn renders DCs incapable of migrating to secondary lymphoid organs to present tumour antigens to cells of adaptive immunity[62]. Another important tumour-secreted molecule is vascular endothelial growth factor (VEGF) which plays a crucial role in tumour angiogenesis but also inhibits DC maturation, as evidenced by the combination treatment of anti-VEGF antibody and peptide-pulsed DCs leading to a potent and prolonged antitumour effect in mice[63]. Immunosuppressive cytokines are also heavily implicated, with transforming growth factor beta (TGFβ) capable of inhibiting both DC and T-cell function[64]. A particularly potent immunosuppressive enzyme constitutively expressed by most human tumours is indoleamine-2,3-dioxygenase (IDO), which metabolises tryptophan and has previously been found to suppress T-cell activity in order to prevent maternal rejection of the foetus[65]. In tumours, IDO causes inhibition of CD8 T-cell proliferation and stimulation of CD4 T-cell apoptosis, leading to failure of T-lymphocytes to accumulate at the tumour site[66].

In addition to the above, tumours are able to recruit Tregs, a subset of CD4 T-lymphocytes which, as mentioned previously, are crucial in mediating tolerance to self-antigen and eliminating self-reactive effector cells under physiological conditions. However, in a tumour setting, these regulatory T-cells act to suppress CTLs through various mechanisms, including production of TGFβ and IL-10, expression of CTLA-4 and PD-L1, and consumption of IL-2 which is necessary for continued T-cell activation[67]. There is extensive evidence of increased proportions of Tregs in many progressive human tumours, such as early-stage non-small cell lung cancer (NSCLC)

and late-stage ovarian cancer[68], malignant glioma[69] and head and neck squamous cell carcinoma (HNSCC)[70], all of which are found to suppress cytotoxic CD8 T-cell responses. The presence of Tregs in the tumour also leads to reduced survival in patients with ovarian cancer[71] and represents a marker of poor prognosis in pancreatic ductal carcinoma[72]. More recently, it has been shown that eliminating certain Treg subsets rather than all intratumoural Tregs could provide an effective approach to tumour therapy. Colorectal carcinomas (CRCs) had a much better prognosis if they were predominantly infiltrated by Tregs expressing low levels of the transcription factor forkhead box P3 (Foxp3), termed $Foxp3^{lo}$ Tregs, rather than their $Foxp3^{hi}$ counterparts, suggesting that selective elimination of the $Foxp3^{hi}$ population could boost antitumour responses[73]. Similarly, melanomas and HNSCCs with a high proportion of Tregs expressing neuropilin-1 (NRP-1) also exhibited poor prognosis, and deletion of NRP-1 in a Treg-restricted fashion induced secretion of IFNγ, led to fragility of cancer-promoting wild-type Tregs and increased tumour clearance in a melanoma mouse model[74].

All of the above suggests that targeting the mechanisms of tumour immunosuppression and escape, along with potentiating the antitumour immune response, should be the main approach to developing successful cancer immunotherapy. Many strategies have already been tried, with various degrees of success – these will be discussed next.

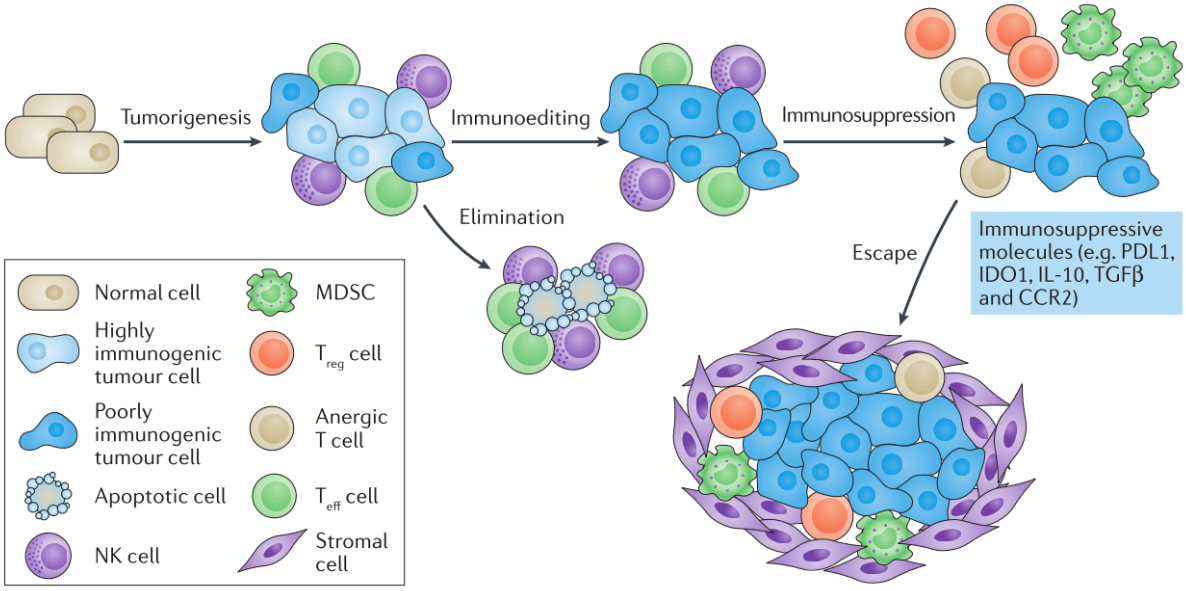

Figure 1.4 – The process of cancer immunoediting

Cancer immunoediting can be divided into three stages: elimination, equilibrium and escape. When normal cells first become cancerous, they are successfully recognised and eliminated by both innate and adaptive immune cells such as natural killer (NK) and effector T-cells (Teff). During this process, however, the immune system targets highly immunogenic tumour cells but is much less effective at killing the poorly immunogenic ones, leading to selection of immune-resistant tumour variants and their establishment in the body. In the equilibrium stage, the immune system keeps the growth of the established tumour in check but is unable to fully eliminate it, mostly due to the tumour activating a host of defence mechanisms such as secretion of immunosuppressive molecules and cytokines, recruiting regulatory T-cells (Tregs) and myeloid-derived suppressor cells (MDSCs) to resist immune attack, and leading to Teff exhaustion in the tumour microenvironment. Once these mechanisms completely overwhelm the host immune response, and the tumour is able to build a protective stroma around itself, it eventually grows and spreads – the phase termed tumour escape. PD-L1, programmed cell death protein-1 ligand-1; IDO1, indoleamine-2,3-dioxygenase 1; IL-10, interleukin-10; TGFβ, transforming growth factor-β; CCR2, C-C motif chemokine receptor 2. Reprinted by permission from Springer Nature: NATURE REVIEWS CANCER (Yarchoan M, Johnson BA, Lutz ER, Laheru DA, Jaffee EM. Targeting neoantigens to augment antitumour immunity. 17(4):209–22), copyright (2017)[75]

1.3 Tumour immunotherapy

Tumour immunotherapy refers to the manipulation of the immune system to treat cancer. The various approaches tried over the years, with increasing promise, rely heavily on rendering established tumours susceptible to immune attack once again and/or boosting the pre-existing or exogenously introduced antitumour immunity. The main approaches to immunotherapy are described below.

1.3.1 Cancer vaccines

One strategy is the use of 'active' immunotherapy, or cancer vaccines, whereby tumour-associated antigens are introduced into patients in order to trigger an immune response from host T-cells and antibodies[35,76]. This has been trialled, for example, in patients with stage III or IV NSCLC immunised with a liposome vaccine derived from the mucin-1 antigen, which is abnormally expressed and glycosylated in NSCLC[77]. In this and a follow-up study of patient survival[78], the 3-year survival rates of patients receiving the vaccine and those that did not were 31% and 17% respectively[77,78]. Even so, a subsequent phase III trial found no significant difference in overall survival when patients with unresectable stage III NSCLC were given the vaccine following chemoradiotherapy compared to those that received placebo instead[79]. Similarly, small-scale evidence of durable clinical response was found in patients with non-Hodgkin's lymphoma vaccinated with recombinant lymphoma-specific idiotype[80], and improved effector T-cell function was observed in trials of DC-based vaccines pulsed with human epidermal growth factor receptor-2 (HER2) peptides and injected into patients with HER2-positive breast cancer[81]. However, all of these would need to be followed up on a larger scale in order to determine actual clinical benefit. In 2010,

sipuleucel-T became the first cancer vaccine to be approved by the US Food and Drug Administration (FDA) for the treatment of prostate cancer. Sipuleucel-T is obtained by *ex vivo* culturing of autologous peripheral blood mononuclear cells (PBMCs), which include T-cells and APCs, with a fusion protein containing prostatic acid phosphatase – a tumour antigen expressed in prostate adenocarcinoma – before injecting the PBMCs back into the patient[82]. Even though this approach induces long-lived immunity *in vivo*[82] and improves overall survival in men with metastatic castration-resistant prostate cancer, it is very expensive – $93,000 for one course of treatment[83] – and does not in fact increase time to disease progression in comparison with placebo[84–86].

The above and the results of many more cancer vaccine trials suggest that, while some therapeutic benefit can certainly be seen, it is generally modest and still far from making a substantial difference in the case of metastatic disease[87]. Combinations of cancer vaccines with classical chemotherapy and other forms of immunotherapy hold some promise for the future. For example, favourable responses to second-line chemotherapy have been observed in patients with advanced small cell lung cancer previously immunised with tumour suppressor protein p53-based cancer vaccine[88]. Furthermore, depletion of Tregs by targeting CD25 on Treg surface, followed by vaccination with melanoma-specific tumour antigens, resulted in induction of tumour-specific CD8 T-cells in 90% of melanoma patients tested[89]. Selecting the most promising antigens for the vaccines to target, which may include those expressed by tumour stromal cells[90], induced neo-antigens on disseminated tumour lesions that are capable of mediating potent immune rejection[91], or even highly personalised, patient-

specific mutations[92], is becoming crucial for the success of this immunotherapeutic modality.

1.3.2 Immune checkpoint blockade

The term 'immune checkpoints' refers to the variety of inhibitory molecules responsible for maintaining the immune system's self-tolerance and avoiding autoimmunity under physiological conditions, and for preventing tissue damage during immune response to infection. However, this essential mechanism is co-opted by many tumours as a way of mediating immune resistance, in particular against tumour-specific T-cells[93]. The vast array of co-inhibitory molecules on the surface of T-lymphocytes all represent immune checkpoint proteins, the inhibition of which has the potential to significantly boost the antitumour immune response; therefore, blocking these using mAbs or otherwise targeting them has become a major focus of cancer immunotherapy. Two immune checkpoint proteins that have been most extensively studied to date are the co-inhibitory receptors CTLA-4 and PD-1[93].

1.3.2.1 Anti-CTLA-4 therapy

CTLA-4 is immensely important physiologically – its role in downregulating the amplitude of T-cell activation is essential for preventing uncontrollable immune responses, as evidenced by *Ctla4*$^{-/-}$ mice all developing lymphoproliferative disease and dying of multiorgan failure caused by lymphocytic infiltration by 3-4 weeks of age[94,95]. However, while CTLA-4 downmodulates the responses of both CD8 CTLs and CD4 T-helper cells, it conversely enhances the immunosuppressive actions of Tregs, thus promoting their role in tumour immune escape. Concomitant CTLA-4 blockade on

effector and regulatory T-cells, which enhances the actions of the former and inhibits the suppressive functions of the latter, has been shown to lead to synergistic antitumour activity in mouse melanoma[96]. CTLA-4 inhibition was first shown to lead to tumour regression, and even to immunity to secondary tumour attack, when the administration of anti-CTLA-4 antibodies to syngeneic mice led to rejection of previously implanted colorectal and fibrosarcoma tumours[97]. Even though there was potential for severe immune toxicity, as previously observed in *Ctla4*$^{-/-}$ mice, this study showed that partial CTLA-4 antibody blockade was able to achieve a therapeutic window[97]. In a further study, mice chronically exposed to ultraviolet (UV)-B radiation developed fewer UV-induced tumours if treated with an anti-CTLA-4 antibody compared to their untreated counterparts, with evidence that the treatment also establishes long-term immune protection against photocarcinogenesis[98]. Moreover, it has been demonstrated that poorly immunogenic tumours do not always respond to CTLA-4 inhibition alone, but become responsive when anti-CTLA-4 therapy is combined with a cancer vaccine, suggesting that, in the absence of significant endogenous immunity, combination treatments that boost immune responses may work better than immune checkpoint inhibition by itself[99].

The accumulated evidence from mice, and the fact that CTLA-4 exhibits 76% overall amino acid homology between mice and humans[100], led to its incorporation into human clinical trials. It was first shown that CTLA-4 antibody blockade could mediate tumour regression in certain metastatic melanoma and ovarian carcinoma patients previously treated with a cancer vaccine[101]. However, serious autoimmune adverse effects, which included dermatitis, hepatitis and enterocolitis, were also observed in similarly treated

metastatic melanoma patients[102]. The evidence that led to FDA approval of a fully humanised anti-CTLA-4 antibody, ipilimumab, in the treatment of metastatic melanoma came from a phase III trial which showed a survival benefit of 3.5 months in metastatic melanoma patients receiving ipilimumab alone or in combination with a melanoma-specific gp100 peptide vaccine compared to those who received the vaccine on its own[103]. What was more prominent was the long-term survival rate, with 18% of ipilimumab patients surviving for more than two years compared with only 5% of those receiving the gp100 vaccine alone[103]. Ipilimumab has since also been approved for adjuvant (i.e. post-surgery) treatment of resected stage III melanoma after a multinational phase III trial showed significantly increased recurrence-free survival in patients treated with adjuvant ipilimumab versus placebo in this setting[104]. Nevertheless, it was noted that more than 50% of patients on ipilimumab discontinued treatment, and five patients (1%) died, due to cutaneous, gastrointestinal, hepatic or endocrine adverse events[104]. Even though this did not translate to a clinically relevant difference in health-related quality of life between ipilimumab- and placebo-treated patients during the 3-year follow-up[105], it is important to bear the potentially life-threatening toxicities of this antibody in mind as it is being tested in other tumour types, including renal cell carcinoma (RCC), ovarian cancer, prostate cancer and urothelial carcinoma[106].

1.3.2.2 Anti-PD-1/PD-L1 therapy

PD-1, like CTLA-4, is a suppressor of T-cell activity, but unlike CTLA-4, it exerts its action through interference with TCR signalling rather than competing with CD28 for binding to ligands CD80 and CD86[106]. There is also evidence that T-cell exhaustion or

anergy, brought about by persistent antigen stimulation, is at least partially mediated by upregulation of PD-1 expression on T-lymphocyte surface, and that blocking the PD-1 signalling pathway leads to restoration of T-cell functional responsiveness[107]. High PD-1 expression has been noted on TILs originating from various tumours, including prostate cancer[108] and melanoma[109], and PD-1 ligands PD-L1 and PD-L2 are commonly overexpressed on the surface of tumour cells. For example, PD-L1 is abundant in samples from human lung, ovary and colon cancers as well as melanoma, and its forced expression on mouse tumour cells mediates tumour-reactive T-cell apoptosis[110]. PD-L2 was found to be upregulated in NSCLC in addition to PD-L1[111], and mAb blockade of both ligands had synergistic effects on the enhancement of T-cell proliferation and effector functions[112]. More recently, it has been shown in a mouse model of progressive sarcoma that T-cells targeting mutant tumour antigens are reactivated inside growing tumours following anti PD-1 and/or anti-CTLA-4 therapy, thus mediating tumour rejection[113]. These and other studies in mouse models of cancer where inhibition of PD-1 and its ligands led to improved antitumour immunity, as well as the much less toxic phenotypes of *Pd1*$^{-/-}$, *Pdl1*$^{-/-}$ and *Pdl2*$^{-/-}$ mice compared to those deficient in CTLA-4, paved the way for human clinical trials[93].

In a phase I study of the anti-PD-1 antibody nivolumab in 39 patients with advanced melanoma, prostate cancer, CRC, RCC or NSCLC, one complete and two partial responses were observed, as well as significant tumour regression in two additional patients; importantly, only one patient suffered a serious adverse event diagnosed as inflammatory colitis[114]. This led to a larger trial of the same antibody in 296 patients with these conditions, where complete or partial responses were observed in patients

with melanoma (28%), RCC (27%) and NSCLC (18%); almost two thirds of responses in patients who were followed up lasted a year or more after therapy was stopped[115]. Even though serious adverse events were noted in 14% of treated patients, with three deaths due to pulmonary toxicity, the safety profile was deemed acceptable[115]. Following a series of phase III clinical trials which all showed the significant survival benefit and better safety profile of nivolumab compared to standard chemotherapy in patients with advanced melanoma[116,117], RCC[118] and both squamous and non-squamous NSCLC[119–121], nivolumab was approved by the FDA for these conditions[106]. Another anti-PD-1 antibody, pembrolizumab, was also trialled in advanced ipilimumab-refractory melanoma[122], NSCLC[123] and various mismatch repair-deficient tumours[124,125], among others. The consistently observed increase in overall and progression-free survival of pembrolizumab-treated patients in all of these led to FDA approval of this antibody for several different cancers, including for any solid tumours characterised by mismatch repair deficiency or high microsatellite instability – the first time a cancer therapy was approved based on a tumour biomarker rather than the location of the tissue involved[126].

Biomarkers are in fact becoming increasingly important in immune checkpoint inhibition, as exemplified by PD-L1 expression on tumour tissue being examined as a prognostic indicator of patient response to immunotherapy in the studies mentioned above. As PD-L1 blockade has the potential to inhibit the interaction of this ligand with both PD-1 and CD80, both of which normally lead to downregulation of antitumour T-cell responses[127], this therapeutic approach has become a very attractive avenue of research in recent years. The anti-PD-L1 antibody atezolizumab has been trialled in

patients with metastatic bladder cancer, demonstrating objective responses in approximately half of the patients who exhibited increased PD-L1 expression in the tumour[128], and in metastatic RCC with promising results[129]. Durvalumab, a second anti-PD-L1 antibody, also led to significantly increased progression-free survival in patients with stage III NSCLC previously treated with chemotherapy in a recent phase III study[130]. Overall, immune checkpoint inhibition of both PD-1 and PD-L1 looks very promising, with many trials ongoing to gauge the full extent of therapeutic benefit to patients. In addition, synergistic blockade of multiple immune checkpoints, of which CTLA-4 and PD-1 are only a small fraction, as well as development of combinatorial approaches incorporating immune checkpoint blockade and cancer vaccines, are all becoming important therapeutic strategies going forward.

1.3.3 TIL therapy

An approach that has shown great promise and even curative potential in recent years is adoptive cell transfer (ACT). ACT involves the *ex vivo* expansion of autologous or HLA-matched tumour-reactive T-cells and their re-infusion back into the patient, where the lymphocytes can subsequently reach the tumour and eliminate it[87]. Usually, ACT is preceded by lymphodepletive chemotherapy with or without total body irradiation (TBI) in order to deplete Tregs from the patient and create “space” in the haematopoietic system, thereby increasing the persistence of transferred T-cells[87] (**Figure 1.5**). ACT therefore has the ability to overcome the major drawback of vaccines, which require *de novo* induction or boosting of immunity in cancer patients who are often already immunocompromised[131], and it also potentially circumvents the

lack of a potent T-cell response to tumour self-antigens resulting from central tolerance[132].

The first clinical report of specifically targeted ACT in humans involved cytomegalovirus (CMV)-specific T-cells being expanded *ex vivo* and administered to bone marrow transplant recipients who are generally at high risk of CMV infection, resulting in the establishment of protective immunity against CMV[133]. This led to efforts to apply ACT to cancer treatment, where a pioneering study demonstrated that adoptive transfer of TILs could be used to successfully treat patients with metastatic melanoma – infusions of autologous TILs and high-dose IL-2 resulted in objective clinical responses in approximately a third of the patients treated[134]. To improve T-cell persistence and increase response rates, a further study by the same group employed an immunodepleting conditioning regimen before adoptive transfer of TILs along with high-dose IL-2 into 13 patients with metastatic melanoma[135]. Six of the 13 patients showed marked tumour regression, and another four had mixed responses; five patients that exhibited regression also developed autoimmune destruction of melanocytes but recovered. The transferred T-cells were specific for the melanoma antigen recognised by T-cells 1 (MART-1) and, apart from mediating the destruction of metastases, also targeted normal tissue expressing the antigen, thus causing autoimmunity[135]. This study showed that targeting self-antigens to destroy tumours was therapeutically feasible as long as autoimmune side effects were minimal or controllable. The same study design was implemented in a larger cohort of 35 patients who demonstrated a similar response rate of 51% (comprising both complete and partial responses)[136], which rose to 72% in a group of 93 patients when high-intensity

TBI was added to lymphodepletive chemotherapy[137]. This last cohort was followed up to reveal that 20 patients (22%) exhibited complete tumour regression, and all but one of these were still in remission after five or more years[138,139]. More recently, it was shown by the same group that this addition of TBI to lymphodepleting regimens may not actually be necessary, with 24% of patients with metastatic melanoma exhibiting complete regression following TIL infusion, and median survival of over 3 years, regardless of whether they received prior TBI or not[140].

The above series of trials, carried out by the Rosenberg group at the National Cancer Institute (NCI), as well as trials in at least three other centres which were able to reproduce high patient response rates[139], showed that TILs could successfully mediate durable complete responses in metastatic melanoma patients regardless of previous cancer treatment received[138]. They also highlighted several drawbacks of this approach and factors to take into account when developing further T-cell-based immunotherapies. *Ex vivo* TIL expansion protocols and tumour-specificity screens prior to re-infusion into patients were initially very labour-intensive, and it soon became obvious that less time-consuming approaches were needed[132]. This was somewhat improved by developing a more rapid TIL generation method that enriches for CD8 T-cells and still produces objective responses in melanoma patients[141], but the therapeutic efficacy of this approach may be inferior to the one seen with standard TIL expansion methods[139]. In addition, a significant positive correlation was observed between the likelihood of complete response to treatment and the administration of TILs which had longer telomeres, were less differentiated, or were present in higher numbers in patient circulation one month post-transfer[138]. This supported the results of

previous studies in mice where less differentiated cells, and those with greater proliferative potential, exhibited more potent antitumour activity upon infusion[142]. Taken together, these findings further highlighted the need to minimise the time TILs spent in culture prior to adoptive transfer as well as to avoid T-cell senescence and anergy, possibly by CD28 co-stimulation to enhance telomere length *in vitro*, or by uncoupling T-cell proliferation from differentiation into effectors[131]. Finally, naturally occurring TILs are only detectable and therapeutically active in a small minority of cancers, mostly melanomas, making their isolation from other tumours, even those that do contain T-cells, impossible or ineffective[87,132]. This is in part because melanoma biopsies can be readily obtained unlike those from most cancers, but the main reason suggested for the presence of therapeutic TILs only in melanoma is the immunogenicity of this tumour, which carries more mutations than any other tumour type[87,131]. In order to target other, less immunogenic tumours, and eliminate the need for isolation of rare TILs, more recent efforts have been directed towards genetic engineering of T-cells resulting in their expression of receptors highly specific for any given tumour antigen. To this end, T-cells purified from patient blood can be engineered to express either tumour antigen-specific TCRs or chimeric antigen receptors (CARs)[87,131,132,139].

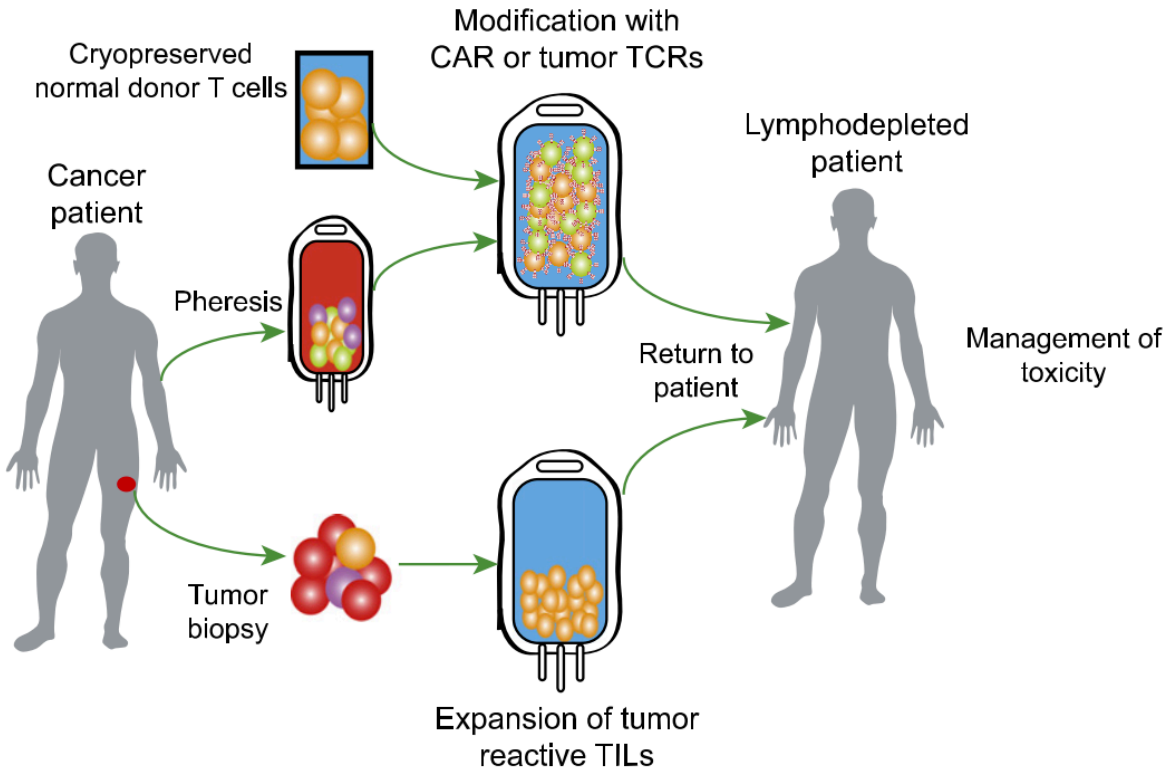

Figure 1.5 – Overview of adoptive cell transfer

Adoptive cell transfer (ACT) can be carried out in several different ways. A patient's own T-cells, or in some instances the T-cells from a healthy donor (either HLA-matched or one whose cells have been modified to switch off alloreactivity) can be engineered *in vitro* to express a tumour-specific high-affinity T-cell receptor (TCR) or chimeric antigen receptor (CAR) before being infused back into the patient. In case of certain solid tumours (e.g. melanoma), the patient's own tumour-infiltrating lymphocytes (TILs) can be harvested from a tumour sample, expanded and re-infused. In the majority of cases, the ACT recipient will undergo some form of lymphodepletion prior to T-cell infusion in order to increase the chance of their successful engraftment. Reprinted by permission from The American Association of Immunologists, Inc.: JOURNAL OF IMMUNOLOGY (Barrett DM, Grupp SA, June CH. Chimeric Antigen Receptor- and TCR-Modified T Cells Enter Main Street and Wall Street. 195(3):755–61), copyright 2015. The American Association of Immunologists, Inc.[143]

1.3.4 TCR-engineered T-cell therapy

The genetic transfer of TCR α and β chains from one T-cell population to another was shown to lead to successful transfer of antigen specificity both for murine[144] and human TCRs[145]. However, the tumour-specific T-cells originally used to obtain TCRs for transfer were isolated from either cancer patients with high antitumour responses or healthy volunteers, where the main obstacles were low frequency in peripheral blood, generally poor affinity for self-antigen due to the effects of central tolerance, and an overall paucity of suitable culture methods[131]. In an effort to increase the potency of tumour antigen recognition by $\alpha\beta$ TCR-engineered T-cells used for ACT, several approaches have been tried, including enrichment for highly specific TCRs through phage displays[146] and introduction of single amino acid modifications into the antigen-binding region of the receptor[147]. While these indeed resulted in increased antigen affinities, such modifications also have the potential to lead to reductions in specificity and a higher propensity towards self-reactivity[87,147]. An alternative approach involves vaccinating human HLA transgenic mice with tumour antigens to induce the clonal expansion of T-cells expressing TCRs with high affinity and specificity for the antigens in question and restricted through common human HLA alleles. Various tumour-specific TCRs have been generated using this method, including those recognising p53 and several melanoma-specific antigens[132].

ACT using TCR-engineered T-cells has shown promising results in several clinical trials, but apart from tumour regression, significant toxicity has also been observed (discussed in more detail below). The main limitation of this approach lies in TCR MHC restriction – tumours frequently downregulate MHC-antigen expression, resulting in

possible lack of response if the tumour has evolved to include antigen-loss variants. In addition, the patients need to possess the restricting MHC allele for that TCR, thus significantly reducing the patient population that can be treated with any one TCR[132,139]. However, MHC dependence of this approach can also be advantageous, as it enables targeting of HLA-peptide complexes derived from intracellular tumour antigens that are otherwise inaccessible to other forms of treatment[139].

The first trial to achieve tumour regression using infusion of autologous, TCR-engineered T-cells targeted the melanoma antigen MART-1. Objective responses were observed in two out of 15 metastatic melanoma patients tested and, importantly, no autoimmune toxicities were reported[148]. Higher-affinity TCRs specific for MART-1 were subsequently generated by transgenic mouse immunisation and used to transduce autologous peripheral blood lymphocytes from 20 metastatic melanoma patients[149]. Here, six patients exhibited partial responses, with three ongoing more than a year post-treatment; however, 16 patients (80%) exhibited one or more adverse events resulting from T-cell mediated autoimmune attack on normal melanocytes, which manifested as damage to the skin (rash followed by vitiligo), eyes (uveitis) or ears (hearing loss)[149]. These trials highlighted the potential of engineered T-cells to mediate both cancer regression and significant toxicity if the tumour antigen targeted is expressed on both normal and tumour tissue.

Unlike the widely expressed MART-1, the cancer-testis antigen NY-ESO-1 is only expressed in healthy testes (where it is protected from T-cell recognition by the lack of MHC molecules on germ cell surface) and in certain malignancies, which include

melanoma and synovial cell sarcoma[139]. High-affinity TCRs specific for NY-ESO-1 were trialled in a cohort of 11 patients with metastatic melanoma and six with metastatic synovial cell sarcoma, where five patients in the former group, and four in the latter, exhibited tumour regression. Two of the five responses in the melanoma patient group were complete and ongoing more than one year after treatment, and none of the patients in the trial experienced autoimmune side effects[150]. In a follow-up trial to this one, it was found that 11/20 melanoma and 11/18 synovial cell sarcoma patients treated with NY-ESO-1 TCR T-cells exhibited objective responses, with approximately a third of the patients in each group surviving for at least 3 years[151]. In a different study, NY-ESO-1 targeting T-cells also induced promising clinical responses in 16/20 patients with multiple myeloma[152].

In contrast to these successes, targeting another cancer-testis antigen, MAGE-A3, led to unexpected toxicity reactions with fatal outcomes. In a trial of a HLA-A2-restricted MAGE-A3-specific TCR in nine cancer patients[153], five experienced clinical regression but three showed severe neural toxicities, and two of the three patients died. Subsequent analyses revealed TCR cross-reactivity with non-identical HLA-A2-restricted epitopes in MAGE-A9 and -A12, with previously undiscovered expression of MAGE-A12 in brain tissue being responsible for the toxicity reactions[153]. Two other trials evaluated a high-affinity HLA-A1-restricted TCR specific for MAGE-A3 in patients with melanoma and myeloma, but the first patient to be treated in each of the trials developed fatal cardiac toxicity[154,155]. High infiltration of engineered T-cells into myocardial tissue was reported, which was subsequently discovered to be due to off-target recognition by the TCR of a related epitope of titin, a protein selectively

expressed by beating, but not resting, cardiac myocytes[154,155]. These trials highlighted the need for high-sensitivity testing of target antigen expression in vital normal tissues in order to predict on-target/off-tumour toxicities. In addition, it is necessary to assess the cross-reactivity of TCRs generated in human HLA transgenic mice, as these would not have been subjected to thymic selection in humans and therefore may exhibit high affinity to certain normally occurring human proteins[139]. Applying these essential tests prior to TCR-based ACT should mitigate for severe adverse reactions in what otherwise continues to be a very promising approach.

1.4 Chimeric antigen receptor (CAR) therapy

Instead of highly specific TCRs, T-cells can be genetically engineered to express CARs – recombinant receptors which bring together the antigen-binding specificity of an antibody or of a natural ligand receptor and the T-cell activating properties of a TCR. Unlike TCRs, CARs can recognise native antigens (including proteins, glycolipids and carbohydrates) on the tumour cell surface in a MHC-independent fashion[156]. Even though they are limited to the recognition of surface antigens alone, without the means to detect intracellular antigens like TCRs, the MHC independence of CAR recognition eliminates the need for patient HLA haplotype matching and circumvents the downregulation of the MHC-antigen processing pathway employed by many tumours[156]. CARs tested in clinical trials to date have led to very encouraging outcomes in patients with haematological malignancies, with increasing potential to expand this success to the therapy of solid tumours as well.

1.4.1 CAR design

CARs are modular receptors consisting of an antigen-binding extracellular domain linked via a transmembrane region to an intracellular signalling domain, sometimes with a 'hinge' or 'spacer region' between the extracellular domain and the transmembrane one[156–158] (**Figure 1.6**, left). The extracellular moiety is most commonly a single-chain variable fragment (scFv) incorporating antigen-binding sequences of both heavy and light chains of a human or murine antibody, although fragment antigen binding (Fab) regions of antibodies as well as natural ligand receptors have also been used[156,158]. The CAR intracellular domain overwhelmingly comprises the CD3ζ chain originating from the TCR/CD3 receptor complex or, less commonly, the Ig fragment crystallisable (Fc) receptor γ chain[156]. A crucial consideration is the position of the CAR-targeted epitope and its distance from the target cell surface, where the CAR spacer region becomes important. The length and flexibility of the CAR, altered by changing the length of the spacer, is likely to affect immunological synapse formation[156,157]. For example, introducing a spacer into a CAR specific for the tumour-associated antigen neural cell adhesion molecule (NCAM) enhances cytokine release and cytotoxicity of NCAM-specific CAR-transduced T-cells[159], possibly because the target epitope is found close to the cell surface and thus requires a more flexible CAR to interact with it. Conversely, a CAR specific for carcinoembryonic antigen (CEA), which binds to the easily accessible CEA amino terminal, exhibits optimum activity without a spacer[159]. Direct comparative studies to assess the different affinities and specificities of CARs binding the same epitope, but that differ in all the above variables, would be needed before a more streamlined CAR design protocol can be established.

Studies in transgenic mice revealed that, while able to support proliferation and effector functions of pre-activated T-cells, signalling through the CAR CD3ζ chain alone was not sufficient to activate resting T-lymphocytes, thus rendering them susceptible to anergy[160]; cytokine release in response to target cells was also much more robust in the presence of CD80-mediated co-stimulation than with CD3ζ signalling alone[161]. These observations led to engineering the 1st generation CARs, which contained CD3ζ as the sole intracellular signalling domain, into 2nd generation CARs that also incorporated the cytoplasmic domain of a co-stimulatory molecule, such as CD28, 4-1BB or OX40[156] (Figure 1.6). The dual signalling provided by CD3ζ and CD28 resulted in more potent and persistent CAR-transduced T-cells, as evidenced by rapid proliferation rates and significant IL-2 production *in vitro*[162] and greater antitumour activity *in vivo*[163,164]. Furthermore, autologous T-cells transduced with CD28/CD3ζ 2nd generation CARs specific for the B-lymphocyte surface antigen CD19 showed significantly enhanced persistence and expansion after infusion into patients with B-cell lymphomas compared to T-cells expressing 1st generation CD19-specific CARs[165]. 4-1BB is another commonly used co-stimulatory domain in CAR constructs instead of CD28. There is as yet no clear consensus on which one is optimal, with *in vivo* studies demonstrating that 4-1BB/CD3ζ CAR T-cells exhibit greater persistence and can, given time, eliminate the targeted tumour, but that CD28/CD3ζ CAR T-cells are able to do so more quickly owing to their more potent anti-tumour effect[166].

3rd generation CARs, comprising two co-stimulatory domains (most commonly CD28 and 4-1BB) in addition to the CD3ζ activation domain (Figure 1.6), seemingly confer even greater antitumour potency on human CAR-transduced T-lymphocytes

adoptively transferred into tumour-bearing mice[167,168]. However, their infusion into three B-cell and mantle cell lymphoma patients in a pilot clinical trial only gave one partial response in a patient who eventually relapsed[169]. A 4th generation of CAR-transduced T-cells, termed T-cells redirected for universal cytokine killing (TRUCKs), has also been described[170]. These 'armoured CAR' T-lymphocytes are engineered to release a transgenic product, commonly a pro-inflammatory cytokine such as IL-12, once their CAR is activated by the target antigen. This in turn results in further enhancement of T-cell proliferation and function and, more importantly, in the additional recruitment of innate immune effectors specifically to the tumour microenvironment, thus inducing superior tumour killing while limiting cytokine-mediated systemic toxicity[156,170]. Preclinical studies of IL-12-secreting CAR-transduced T-cells targeted against CD19[171] and VEGF receptor-2 (VEGFR-2)[172], and further studies of armoured CAR T-cells with alternative genetic payloads such as 4-1BBL and CD40L[173], have all highlighted the increased efficacy and promise of this approach in targeting otherwise poorly treatable tumours.

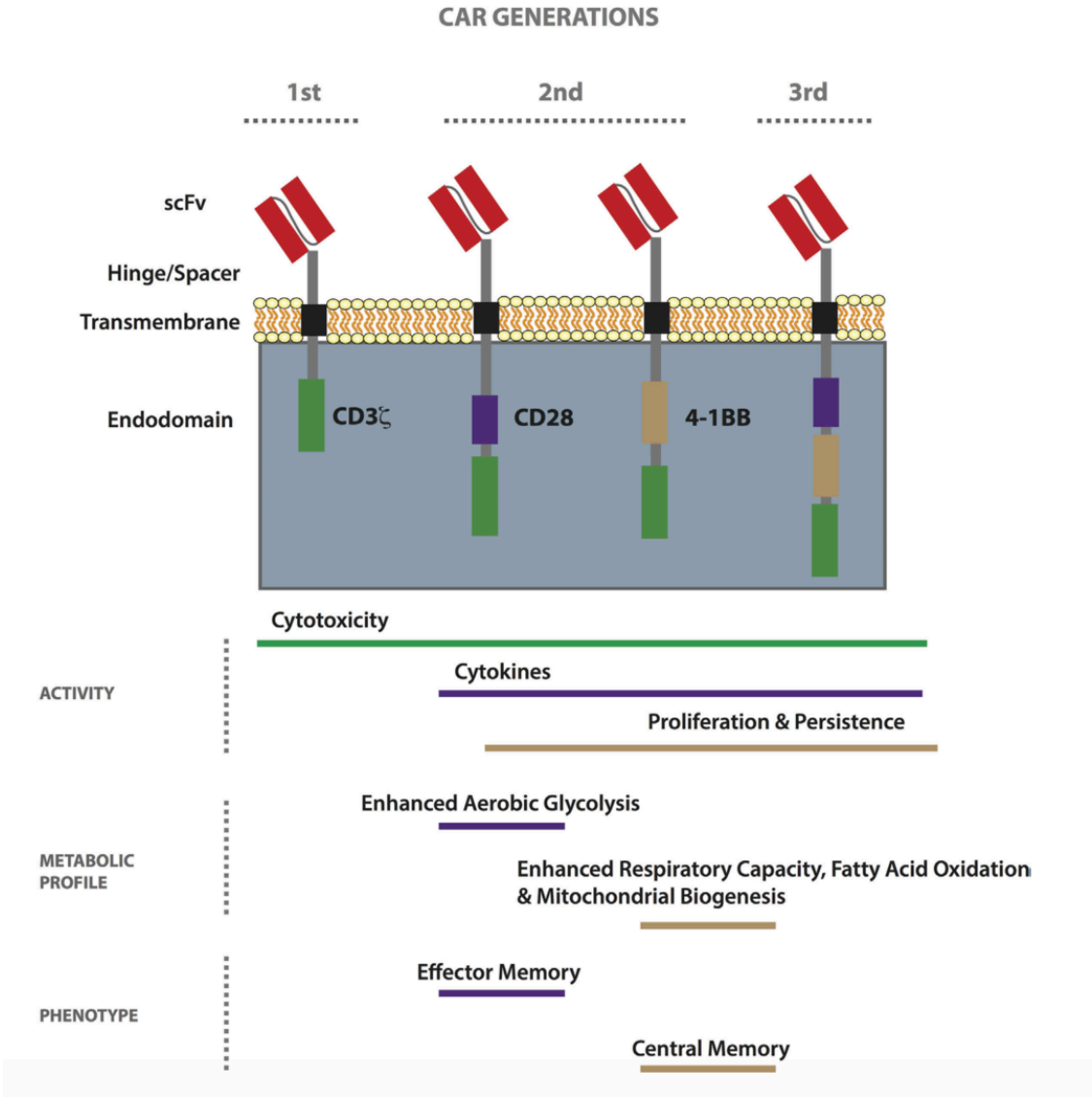

Figure 1.6 – The structure and main properties of 1st, 2nd and 3rd generation CARs All CARs consist of an extracellular region – usually an antibody-derived single-chain variable fragment (scFv) – linked via a hinge/spacer (if present) to a transmembrane and an intracellular region, the latter signalling into the T-cell upon antigen binding. The intracellular region always comprises a signalling domain such as CD3ζ, which is present either alone (1st generation) or together with one or two co-stimulatory domains (2nd and 3rd generation CARs respectively). The most widely used co-stimulatory domains are CD28 and 4-1BB, both of which increase the capacity of the T-cell to release cytokines and proliferate, but the presence of 4-1BB may lead to greater CAR T-cell persistence in the circulation after infusion. Each co-stimulatory domain also results in a different metabolic and phenotypic profile of the engineered T-cell. Reprinted from Irving M, Vuillefroy de Silly R, Scholten K, Dilek N and Coukos G (2017) Engineering Chimeric Antigen Receptor T-Cells for Racing in Solid Tumors: Don't Forget the Fuel. *Front. Immunol.* 8:267[174]

1.4.2 CAR therapy of haematological tumours

The current paradigm for CAR therapy is the targeting of CD19, which is expressed on healthy B-cells but is also overexpressed in the majority of B-cell leukaemias and lymphomas[156]. CD19-specific CAR-engineered T-cells were first shown to successfully eliminate B-cell malignancies in several mouse studies[163,164,175] before being tested in human clinical trials, where they gave highly promising patient outcomes. As of January 2018, over 250 CAR T-cell trials have been reported worldwide[176], the majority of which are directed against haematological tumours; the main CAR target in these remains CD19, but alternative ones include CD20, CD30 and Lewis-Y antigen[177].

The most striking results with CD19-specific CARs have been observed by the groups working at the NCI, the Memorial Sloan-Kettering Cancer Center (MSKCC) and the University of Pennsylvania (UPenn). In an initial study by the NCI group, a patient with advanced follicular lymphoma experienced dramatic tumour regression following the administration of autologous CD28/CD3ζ CD19-specific CAR T-cells[178]. The same group followed this up with a series of trials in advanced B-cell lymphomas or chronic lymphocytic leukaemia (CLL) and observed remissions in the majority of patients in each, most recently demonstrating that this CAR achieved long-term responses in patients with diffuse large B-cell lymphoma[179–181]. The MSKCC group focused on trialling their CD28/CD3ζ CD19-specific CAR in patients with CLL and B-cell acute lymphoblastic leukaemia (B-ALL), achieving modest responses in CLL[182] but highly promising response rates of up to 88% in patients with B-ALL, enabling them to subsequently undergo allogeneic haematopoietic stem cell transplantation (allo-HSCT)[183,184]. Finally, the UPenn group tested their 4-1BB/CD3ζ CD19-specific CAR in

small-scale trials in CLL[185,186] and pre-B-cell ALL[187] with very promising results, culminating in a striking 90% complete response rate when 30 children and adults with relapsed ALL were treated with the same CAR[188]. More recently, this group also reported a 57% overall response rate in treated patients with relapsed/refractory CLL, half of which were complete remissions[189].

Taken together, these very promising results from several trials, along with many others reported or ongoing[177,190–192], highlight the potential of CAR T-cell therapy in $CD19^+$ and other haematological malignancies. However, they also point to several important issues that need to be addressed. Comparisons between the different trials are difficult as each one uses different CAR and T-cell manufacturing methods, lymphodepletion regimens and dosing schedules. It is therefore challenging to draw definitive conclusions regarding the varying patient outcomes, making future standardisation of CAR T-cell therapy a top priority[156]. Moreover, CAR T-cells caused substantial side effects in a significant portion of patients treated in all of the trials above, with the two main safety issues being on-target/off-tumour toxicity and cytokine release syndrome (CRS). Predictably, targeting CD19 not only led to antitumour activity but also to normal B-cell depletion and consequently hypogammaglobulinaemia. While this side effect is readily manageable with intravenous Ig infusions, other CAR targets expressed on normal as well as tumour tissue may result in much less tolerable adverse events, making the target choice a highly important consideration[193]. The other major patient safety concern, “cytokine storms” – the release of large amounts of cytokines causing high fever, hypotension, and potentially fatal organ failure – was also observed in some of the trials described

above and mostly managed with corticosteroids and the anti-IL-6 antibody tocilizumab[187,188]. However, since this severe side effect cannot be controlled by simply reducing treatment dose as T-cells continually proliferate, strategies such as split dosing or the introduction of suicide genes may mitigate for this toxicity to some extent[156]. Ultimately, designing highly tumour-specific CARs, the potential toxicity of which can be regulated with reasonable ease, represents the definitive aim in the use of this treatment modality.

1.4.3 CAR therapy of solid tumours

One reason why CAR T-cells have proven so successful in haematological malignancies is the ease with which they can reach their target antigens on B-cells, the blood and lymphatic system being where both T-cells and B-cells naturally reside. Solid tumours, however, represent an entirely distinct set of challenges, not least of which are the highly immunosuppressive tumour microenvironment and the lack of known target antigens expressed on malignant but absent from normal cells[156]. Nevertheless, recent studies in tumour-bearing mice do show some promise. Tumour control or eradication has been reported in mice treated with CAR T-cells targeting glypican-3 in the treatment of hepatocellular carcinoma (HCC)[194] and lung squamous cell carcinoma[195], mucin-1 in pancreatic cancer[196], and both L1 cell adhesion molecule[197] and the tumour antigen 5T4 in ovarian cancer[198]. CAR-mediated rejection of large established $HER2^+$ tumours[199] and control of large pancreatic and lung tumours[200] in mice have also been described. The promising results of these *in vivo* studies cannot always be safely and effectively translated into the clinic, however, especially since a number of toxicity issues in humans have been raised. HER2-

specific CAR T-cells administered to a patient with metastatic CRC led to off-tumour recognition of low-level HER2 on lung epithelial cells, resulting in a severe cytokine storm and the patient's death[201]. In another trial, half the examined patients with RCC who were administered carboxyanhydrase-IX (CAIX) CAR T-cells had their treatment stopped due to CAIX expression on bile duct epithelial cells leading to liver enzyme disturbances[202], and patients have been reported to develop anaphylaxis[203] or compartmental CRS[204] after being injected with mesothelin-targeted CARs. Despite this, promising results from human clinical trials in solid tumours have also been reported, such as three of 11 children with active neuroblastoma achieving complete remission in response to CAR T-cells targeting the G_{D2} ganglioside[205], and HER2-targeted CARs proving safe and showing therapeutic potential in the same condition[206].

For more successful solid tumour targeting in the future, choosing the correct target antigen and improving tumour specificity of transduced T-cells will be crucial. One approach to achieving this is using low-affinity scFv regions in CARs such that they only respond to their target antigen when it is highly expressed on a given tissue (such as a tumour)[174]. Many novel technologies are also being employed to improve the safety of CAR T-cells. One example is combinatorial antigen recognition, whereby T-cells are engineered to express an antigen-specific CAR and a separate chimeric costimulatory receptor (CCR) binding to a second antigen; T-cell activation is then rendered ineffective upon CAR binding unless simultaneous CCR recognition of the second antigen is also present to provide rescue[207]. Interestingly, it was also recently shown that CARs targeting prostate-specific membrane antigen (PSMA) expressed on

blood vessels supplying ovarian cancer in mice were able to cause vessel ablation, consequent tumour cell depletion and overall reduction in tumour burden[208]. This, along with the previously reported success of 4th generation anti-VEGFR-2 CARs in the treatment of established solid tumours in mice[172], suggested that tumour vasculature could be a very promising and much more easily accessible CAR target.

1.5 Tumour angiogenesis

Angiogenesis is the formation of new blood vessels from pre-existing ones which is essential for the physiological processes of development, pregnancy and wound healing. However, angiogenesis is also exploited by tumours, where a blood supply is crucial for their large-scale growth and metastasis[209–211]. The process is initiated by vasculogenesis, which refers to *de novo* endothelial cell production. This is followed by sprouting angiogenesis involving the activation of endothelial cells on existing blood vessels and their subsequent migration, which results in 'sprouting' of new blood vessels and their remodelling into a functional network[209]. Tumour angiogenesis is driven by pro-angiogenic factors such as VEGF and fibroblast growth factor (FGF), which manage to outweigh the effects of endogenous anti-angiogenic factors including thrombospondin-1 and endostatin[212]. In all cases, the resulting tumour vasculature is disorganised, tortuous and leaky, frequently exhibiting vascular shunts and sluggish blood flow through capillaries. In addition, the microenvironment is profoundly deprived of oxygen and nutrients, with hypoxia leading to acidity due to the presence of lactic acid from anaerobic metabolism[213]. Under these conditions, endothelial cells on tumour vasculature are very different to the quiescent endothelium in normal tissue,

instead proliferating rapidly and actively contributing to the angiogenic process. Their differential transcription profile and resulting phenotype therefore make them a very attractive candidate for selective tumour targeting[209,213].

1.5.1 Tumour vasculature targeting

The appeal of tumour vasculature as a target of anticancer therapy lies in its many favourable characteristics over those of the tumours themselves. Endothelial cells are genetically stable, making their targeting unlikely to lead to resistance as well as widely applicable to multiple tumour types[211]. Being directly exposed to blood also makes these cells easily accessible to therapeutics and immune effectors, which can otherwise have considerable difficulty gaining access to the inhospitable tumour microenvironment. In addition, destroying tumour vascular endothelium is very likely to lead to a potent bystander effect, as the targeted blood vessel supports the growth of many tumour cells[211]. Proof of principle that large solid tumours can be eradicated by targeting their vasculature originally came from a study in which expressing IFNγ on a neuroblastoma cell line in immunocompromised mice led to MHC class II expression on tumour vasculature; injecting the mice with anti-MHC class II antibodies coupled to the immunotoxin ricin led to ricin internalisation into the vascular endothelium, subsequent vascular collapse and dramatic tumour regression[214]. While this and other early studies were certainly very promising, the main challenge for the application of such findings to humans has been the identification of target antigens selectively expressed on tumour vasculature.

One obvious target is the VEGF family of angiogenesis-promoting proteins, of which VEGF-A was the first to be isolated and most extensively studied[215]. VEGF-A is induced by oncogenic genetic mutations and tumour hypoxia, which in turn leads to upregulation of its receptors on the tumour endothelium. As such, both VEGF-A and its receptors are overexpressed in many different cancers, including breast, lung, bladder, ovary, kidney and gastrointestinal tumours, where they correlate with increased risk of recurrence and generally poor prognosis[215]. Some of the principal actions of VEGF-A include inhibition of endothelial cell apoptosis and increase in vascular permeability, which it effects through interaction with its two receptors, VEGFR-1 and VEGFR-2; VEGFR-2 is perceived as crucial for mediating most of these pro-angiogenic effects[213,215].

Early studies in mice found that mAbs binding the VEGF-A/VEGFR-2 complex selectively localised to tumour endothelium[216] and inhibited the growth of both newly injected and established human tumour xenografts[217]. These and other studies that observed potent antitumour effects and endothelial selectivity of anti-VEGF antibodies led to human clinical trials, culminating in FDA approval of the humanised anti-VEGF antibody bevacizumab for first-line treatment of metastatic CRC[218]. Its use has since been expanded to include second-line treatment of metastatic CRC, NSCLC, metastatic RCC, metastatic breast cancer and glioblastoma, while a number of small-molecule receptor tyrosine kinase inhibitors targeting VEGFR-2 such as sunitinib have also shown clinical efficacy, particularly in renal cancer[212,215]. These anti-angiogenic agents are only a few among a multitude of others available, including aflibercept, the 'VEGF trap' which binds VEGF-A with greater affinity than its endogenous receptors[219]

and which has been approved for the treatment of metastatic CRC[220]; trebananib – a peptide-Fc fusion protein that prevents the interaction between pro-angiogenic factors angiopoietins and their receptors[221]; and anti-epidermal growth factor receptor (EGFR) antibodies such as cetuximab, which indirectly inhibit angiogenesis through their EGFR inhibition[215]. Vascular disrupting agents – compounds that target tumour vasculature directly and cause central tumour necrosis – have also been tested in several cancers, both as single agents and in combination with conventional chemotherapy, however they have so far shown little survival benefit and mostly prohibitive toxicity[222].

Despite the reasonable success of current anti-angiogenic therapy, the two main issues it faces are still limited efficacy and toxicity. Trial data have pointed to the fact that anti-VEGF antibodies mostly show clinical benefit as part of combination therapy and not as single agents. Furthermore, inhibiting VEGF proteins or their receptors usually only reduces the rate of angiogenesis rather than eliminates it entirely, prompting research into alternative tumour angiogenic pathways and novel ways to target them[212]. Side effects such as hypertension and, rarely, thromboembolic events are also reported with VEGF-targeted therapies, owing at least in part to their on-target/off-tumour recognition of VEGF, now well known for its critical role in physiological vascular homeostasis independently of any tumour pathology[212,223]. To avoid toxicity issues and increase treatment efficacy, an ideal target of anti-angiogenic or vascular-targeting therapy would be highly selective for tumour vasculature and therefore absent from normal blood vessels, as well as dispensable for all physiological functions such as neovascularisation during ovulation or tissue repair[212]. Such targets

are very difficult to find and hard to validate, but a very promising avenue of research has emerged which may eventually lead to truly selective tumour vasculature targeting.

1.5.2 Tumour endothelial markers

Advances in bioinformatics and gene expression analysis have led to important discoveries of molecular targets differentially expressed on tumour compared to normal endothelium. For example, roundabout-4 (ROBO4) was identified as a smaller, endothelial-specific member of the roundabout receptor family, which is normally localised to neuronal tissue[224]. ROBO4 showed strong expression during embryogenesis but was virtually absent from all adult human tissues except for those undergoing active angiogenesis such as tumours[213,224]. The C-type lectin CLEC14A has also been identified as highly expressed on the vasculature of various solid tumours, in contrast to its low or undetectable expression on normal blood vessels[225]. In another study, serial analysis of gene expression was applied to human endothelial isolates from both healthy colon and colorectal tumour samples to identify 46 transcripts elevated at least 10-fold in tumour-associated compared to normal endothelium[226]. Nine of these tumour endothelial markers (TEMs), TEM1-TEM9, were validated further, and seven of them shown to be characteristic of both primary and metastatic CRC endothelium as well as found in liver metastases and in primary lung and brain tumours among others, confirming their general tumour-associated endothelial distribution[226]. With the exception of TEM8, all the TEMs were also found to be upregulated in physiological angiogenesis required for corpus luteum development and wound healing[226].

Four TEMs were subsequently characterised as cell-surface proteins and therefore deemed most relevant for therapeutic targeting[211]. In order to establish their significance in animal models, mouse counterparts of each of the four were identified, and three of them – designated mTEM1, mTEM5 and mTEM8 – found to be highly expressed on mouse tumour vasculature and the vasculature of developing embryos, but almost undetectable on normal vessels of adult mice[227]. Of all the TEMs investigated, TEM8 was the most intriguing for two reasons. It exhibited the highest interspecies conservation among the cell-surface markers with 96% amino acid identity between mouse and man[227], thus warranting the applicability of future mouse studies to humans. Its expression pattern was also the most favourable, as it was the only human TEM undetectable in physiological angiogenesis, including the vessels of the ovaries at either mRNA or protein level[211,212]. Its potential for highly specific association with tumour vasculature led to further studies of its distribution and function, with a view to designing highly tumour-selective targeting strategies in the future.

1.5.3 TEM8

TEM8 is a single-pass membrane protein consisting of 564 amino acid residues, with a von Willebrand factor type A (vWA) domain in its extracellular region[212]. Shortly after it was first identified, TEM8 was found to be an anthrax toxin receptor, mediating anthrax toxin cell entry via binding of the toxin's protective antigen subunit to the vWA extracellular domain of TEM8[228]. Its subsequently identified closest homologue of 40% shared amino acid identity, capillary morphogenesis gene-2 (CMG2), was discovered to bind anthrax toxin using the same mechanism[229], leading to the alternative naming of TEM8 and CMG2 as anthrax toxin receptors 1 and 2 respectively (ANTXR1 and

ANTXR2)[212]. Unlike TEM8 and its apparent restricted expression to human tumour endothelium, CMG2 is widely expressed in many human tissues[229] and exhibits 11-fold higher affinity for anthrax toxin compared to TEM8, two factors that contribute to CMG2 being the main mediator of anthrax lethality *in vivo*[230]. Apart from its minor pathological function in this disease, and its newly reported role as the receptor of the oncolytic Seneca Valley virus[231], the physiological role of TEM8 is not yet fully understood. Consistent with its previously identified role in angiogenesis, it has been shown to bind to the α3 subunit of collagen type VI, which is also overexpressed on tumour endothelium[232], as well as to collagen type I, thus promoting endothelial cell migration[233] and acting as an adhesion molecule[234]. It has recently been proposed that TEM8 is also required for arteriogenesis following arterial ligation in mice[235]. Even though one study suggested that TEM8 was in fact widely expressed on normal mouse and human epithelial cells lining the lungs, small intestine and skin – the three main entry sites of the anthrax toxin-producing bacterium, *Bacillus anthracis*[236] – these findings were later not reproducible[212].

A number of studies in mice and humans were able to demonstrate the tumour-promoting characteristics of TEM8 and the antitumour effects produced by its targeting. Its downregulation has been linked to a substantial reduction in tumour growth in mouse models of osteosarcoma[237] and HCC[238], and significant TEM8 overexpression was observed in the tumour stroma of patients with triple-negative breast cancer (TNBC)[239] and on the tumour endothelium of gallbladder carcinoma patients[240]. A soluble TEM8-Fc fusion protein successfully suppressed the growth and metastases of human liver, colon and breast tumour xenografts in athymic nude mice, possibly by

diverting and trapping the M2 isoenzyme of pyruvate kinase which is important in tumour development[241]. Vaccinating mice against TEM8 induced potent TEM8-specific CTL responses, suppressed tumour angiogenesis and resulted in protection of the mice from lethal tumour challenges, including that of HCC, with no obvious side effects[242,243]. An anti-TEM8/truncated tissue factor fusion protein administered to mice bearing CRC xenografts resulted in approximately 50% reduction in both tumour volume and tumour growth rate compared to untreated mice; the fusion protein selectively targeted tumour vasculature, decreased its density and promoted targeted rather than non-specific thrombosis[244]. The same NCI group which initially identified TEM8 was able to show that TEM8$^{-/-}$ mice challenged with melanoma exhibited delayed tumour growth and, importantly, showed no developmental defects or faults in physiological angiogenesis[245]. The only physiological difference between wild-type and TEM8$^{-/-}$ mice was the presence of extracellular matrix (ECM) accumulation in the latter which manifested as dental dysplasia, an effect possibly due to the absence of TEM8 interaction with collagen[245].

More recently, the same group generated monoclonal anti-TEM8 antibodies which displayed inhibition of tumour angiogenesis and potent antitumour activity against, among others, syngeneic or human xenogenic melanoma, colon and lung cancers in mice without affecting physiological processes such as wound healing[246]. In fact, wild-type mice treated with anti-TEM8 antibodies exhibited similar delays in tumour growth to that observed in TEM8$^{-/-}$ mice. While anti-TEM8 antibodies did not lead to tumour regression or complete growth inhibition on their own, they considerably augmented the effect of established cancer therapies such as anti-VEGFR-2 and conventional

chemotherapy agents, with anti-TEM8 antibody/irinotecan combination leading to complete cures in 5 of 11 mice treated[246]. Importantly, antibody treatment did not result in any observable toxicity in mice, even after 6 weeks of follow-up[246].

Overall, the most important aim of cancer immunotherapy is the achievement of truly selective tumour targeting. With the discovery of tumour endothelial markers and specifically TEM8, which has so far been detected as overexpressed only on tumour vasculature, this aim may be within reach. Further studies of TEM8 distribution, function and targeting strategies are needed before human clinical trials can be considered. CAR T-cells have emerged as a very promising immunotherapeutic modality in recent years, already showing potential for successful tumour vasculature targeting in various *in vivo* studies directed against PSMA[208], VEGFR-2[172] and even in combination therapies targeting both tumour vasculature and the tumour itself in mouse melanoma[247]. Thus, anti-TEM8 CARs, which unlike anti-TEM8 mAbs would be capable of eliciting the full spectrum of T-cell effector and immune-mobilising functions in the tumour vasculature, may provide an even more potent tumour-targeted approach and are therefore well worth exploring.

1.6 Liver inflammation

The power of the immune system has been harnessed to treat various forms of cancer with some remarkable recent successes with engineered T-cells. This has prompted interest in using similar approaches to treat other diseases. Inflammatory and autoimmune conditions, caused by the overactivity of various immune components

towards the host's own tissues, could be amenable to immunotherapies that aim to suppress rather than boost the immune response – for example, by using immunosuppressive elements such as Tregs instead of immunostimulatory T-cell effectors. One such example includes inflammatory conditions of the liver, where the progressive damage to the organ invariably results in the requirement for liver transplantation in order to ensure the patient's survival. Therefore, identification of a selective marker of liver inflammation, and how it can be targeted using therapeutic Tregs, is another important focus of this thesis.

1.6.1 Physiology of the human liver

The liver is the largest organ in the human body. It carries out a multitude of crucial functions which include nutrient metabolism, elimination of toxins, synthesis of important proteins and immune surveillance[248]. In fact, it is specifically designed as the primary immune surveillance organ of the body, being densely populated by both innate and adaptive immune cells which normally reside in its vasculature, including the largest single population of macrophages – called Kupffer cells in the liver – and NK cells. Receiving both arterial and venous blood, the liver is constantly exposed to a flow of blood-borne exogenous matter, including non-harmful food particles but also potentially harmful pathogens; its ability to differentiate between these and activate immune defences when needed, or retain immune tolerance when not, is crucial for its proper functioning[248]. The importance of a healthy liver has been demonstrated in many *in vivo* studies – for example, depletion of Kupffer cells from the livers of mice infected with a normally sublethal dose of *Listeria monocytogenes* resulted in deaths of these mice within 3 days of infection[249].

The liver is supplied by the portal vein, which absorbs nutrients and other substances from the gut and delivers them to the liver, and the hepatic artery, which provides the liver with oxygenated blood from the systemic circulation. The deoxygenated blood resulting from liver metabolism is then carried away by the hepatic vein back into the circulation[250]. Between these three main vessels, within the organ itself, lies the complex network of capillary-like vessels called sinusoids (**Figure 1.7**). Liver sinusoidal endothelial cells (LSECs), which line the sinusoids, do not form a continuous layer but instead contain gaps (fenestrae), which allow the blood to pass through easily and reach the liver epithelial cells – hepatocytes. This fenestrated endothelium therefore allows the efficient exchange of nutrients and waste products between the blood and liver epithelium underneath[250]. Sinusoids also serve to significantly slow down the flow of blood through the liver – blood pressure in the organ is up to 50 times lower than in the systemic circulation – allowing enough time for the pathogens and other foreign substances passing through to be recognised by resident immune cells[248]. In fact, LSECs, hepatocytes and Kupffer cells, among others, are all specialised APCs, capable of successfully presenting antigen to resident T-lymphocytes and priming them for response[248,250] (Figure 1.7).

The immune environment of the liver is quite different to the one found in the rest of the body. T-cells comprise almost 50% of the entire lymphocyte population in the liver and demonstrate enrichment for CD8 and memory T-cell subsets as well as activated T-cells[251]. Furthermore, unlike antigen presentation in secondary lymphoid organs which includes co-stimulation and results in full T-cell activation, the same process in the liver under regular conditions leads to activated, but not fully “licensed” CD8 T-

cells. Such T-cells proliferate but do not produce IFNγ or induce specific cytotoxicity[252], indicating the presence of a tolerogenic environment. However, in the case of inflammation or infection, upregulation of MHC class I and induction of MHC class II receptors on the surface of liver cells, together with increased co-stimulatory and reduced inhibitory molecule expression, all lead to CD4 T-cell activation and CD8 T-cell licensing into effectors[248]. One of the most important functions of the liver, therefore, is successful maintenance of the balance between immune tolerance under physiological conditions and immune response under pathological ones; the breakdown of this balance ultimately leads to chronic inflammation and autoimmunity.

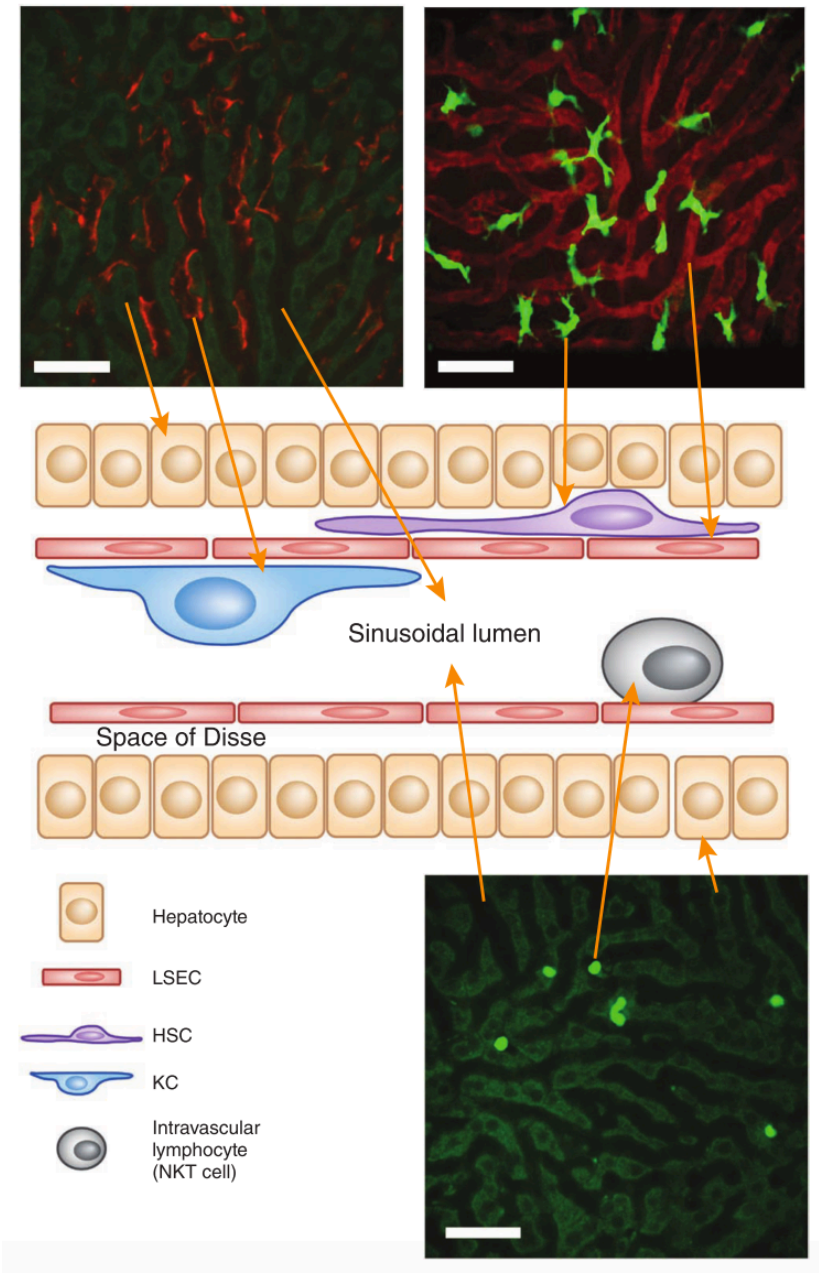

Figure 1.7 – The structural and immune components of the liver

Diagram of a liver sinusoid in cross-section (centre) showing the liver cells and immune cells resident in the hepatic vasculature, with images of mouse livers obtained by intravital microscopy surrounding it. Top left, autofluorescent green hepatocytes surround the sinusoids, with fluorescent red Kupffer cells (KC) lining the interior sinusoidal walls; top right, hepatic stellate cells (HSC, bright green) are found in the space of Disse, between the hepatocytes and the liver sinusoidal endothelial cells (LSEC, red); bottom right, bright green natural killer T (NKT) lymphocytes patrol the sinusoids between rows of dim green hepatocytes. Scale bars, 50μm. Reprinted by permission from Springer Nature: NATURE IMMUNOLOGY (Jenne CN, Kubes P. Immune surveillance by the liver. 14(10):996-1006), copyright (2013)[248]

1.6.2 Primary sclerosing cholangitis

An important function of the liver is the synthesis of bile acids from cholesterol[253]. Bile acids serve as metabolic regulators that facilitate nutrient absorption in the small intestine and, once synthesised by the liver, are stored in the gallbladder as bile. They are transported through conduits known as bile ducts into the intestine after every meal to aid digestion, following which they are recirculated back into the liver[253]. As it travels through the biliary network, bile is modified by the physiological action of the epithelial cells lining the bile ducts – cholangiocytes[254]. Damage to cholangiocytes and bile ducts can lead to bile flow obstruction (cholestasis), resulting in the build-up of toxic metabolites in the liver with simultaneous absence of bile from the intestine[253].

Primary sclerosing cholangitis (PSC) is a chronic, progressive inflammation of the liver characterised by bile duct destruction and frequently culminating in end-stage liver disease[255]. The inflammation is immune-mediated, as evidenced by immune cell infiltrates (including lymphocytes) predominantly around bile ducts, and eventually leads to inflammation and disorganised proliferation of cholangiocytes; this in turn results in bile duct loss, cholestatis and cirrhosis. As a result, more than half of the patients need a liver transplant 10-15 years after their PSC diagnosis[255]. A systematic review of worldwide PSC incidence and prevalence rates found that these vary widely with geographical region, but can reach 1.3 per 100,000 inhabitants (incidence) and 16.2 per 100,000 inhabitants (prevalence) in Northern European countries[256]. The majority of patients – 60% on average – are men, with a peak incidence age of about 40[256], and approximately 60-80% of PSC patients also report inflammatory bowel disease (IBD)[257]. In addition, significant correlations have been found between gene

loci linked with PSC and those associated with HLA, as well as with a number of autoimmune conditions such as type 1 diabetes (T1D), rheumatoid arthritis and psoriasis[257]. In fact, up to 25% of PSC patients are also affected by an autoimmune condition outside the liver and colon[258].

Sclerosing cholangitis is diagnosed as primary only when there is no identifiable precipitating factor; thus, secondary causes such as autoimmune hepatitis (AIH), infection or hereditary disorders need to be excluded in order to treat PSC appropriately[255,259]. However, there is still no cure or even a universally agreed medical treatment for the condition. Anti-inflammatory and immunosuppressive drugs, such as corticosteroids and transplant rejection treatments, have been trialled with little success or withdrawn due to prohibitive adverse events; treatment with ursodeoxycholic acid, usually given for cholestatic disease, is controversial and generally not recommended[260]. Patients who reach end-stage liver disease require liver transplantation; however, rates of post-transplantation PSC recurrence are high, with the results of a large multicentre study suggesting that this happens in approximately 20% of patients after less than 5 years[261]. This, along with PSC carrying an increased risk of cholangiocarcinoma, gallbladder cancer, HCC and CRC[262], demonstrates the increasing importance of identifying new and successful therapeutic approaches for this debilitating disease.

1.6.3 Mouse models of PSC

In order to study the aetiology and pathology of PSC as well as new treatment strategies, it is essential to have a representative animal model. The ideal model would

be immunologically and genetically predisposed to develop bile duct fibrosis and destruction, showcase all the hallmarks of sclerosing cholangitis (such as immuno-inflammatory infiltrates concentrating around bile ducts, duct strictures and dilatations, and cholangiocyte atrophy), and develop concurrent IBD, more specifically colitis. The disease would also ideally progress to cholangiocarcinoma and, as in humans, predominantly affect males[263]. Unfortunately, such an all-encompassing model does not yet exist, even though many murine models of PSC have been developed and allowed the study of one or more aspects of the disease. It may be that, due to the complex nature of PSC, no single model will ever be truly representative, and the study of various combinations of models will have to suffice instead[263].

Currently available mouse models fall into several categories. Those relying on chemical induction of cholangitis are hampered by the lack of complete PSC phenotype or high mortality rates, while those induced by infectious agents are generally too complex for manageable study. On the other hand, antigen-driven or direct biliary injury in mice leads to the development of a relatively mild PSC phenotype, while models of colitis do not develop liver fibrosis at all[263]. Several knockout mouse models have also been generated which, while not ideal, provide an opportunity for longitudinal study of PSC and its treatment options. One such model is the multidrug resistance gene-2 (Mdr2) knockout (MDR2 KO) mouse, which lacks the MDR2 phospholipid transporter normally found on the apical membrane of hepatocytes; as this membrane faces the bile canaliculi (small channels that transport bile and eventually merge into bile ducts), the lack of the transporter results in complete absence of phospholipid from bile[264]. Mice homozygous for the Mdr2 gene disruption

are unable to form mixed phospholipid-bile acid micelles in the bile, which normally function to protect cholangiocytes from bile acid-induced damage. This results in cholangiocyte injury, bile duct disruption and bile acid leakage, inflammatory infiltration, fibrosis and finally cholangiocyte death – thus, a spontaneous phenotype develops which is both macroscopically and microscopically similar to PSC in humans[265]. The model, which is generated on a Friend leukaemia virus B-type/N (FVB/N, or simply FVB) background, does not develop IBD or cholangiocarcinoma but does progress to HCC[263], and has proven suitable for testing novel PSC therapeutic strategies in a number of studies already[266–268]. The MDR2 KO FVB mice were therefore chosen as an appropriate animal model of liver inflammation for the purpose of this thesis.

1.6.4 CLEC14A

The C-type lectin CLEC14A is a single-pass transmembrane protein consisting of 490 amino acid residues, with 67% sequence homology between mice and humans[225]. It is expressed at low or undetectable levels in healthy adult tissues but can be overexpressed on the vasculature of multiple solid tumour types as measured by both immunohistochemistry and immunofluorescence – for example, it was highly expressed on endothelial cells in HCC but absent from adjacent healthy liver tissue (**Figure 1.8**)[225]. A similar pattern was observed in samples from human prostate, breast, kidney and bladder tumours among others, identifying CLEC14A as a novel TEM[225]. Similar to TEM8, it has been found to promote endothelial cell migration and tube formation, with polyclonal antiserum to CLEC14A impairing both of these. Interestingly, it was also upregulated on endothelial cell surface under conditions of low shear stress, such as those that might be found in disorganised and leaky tumour

vasculature; this further confirmed its pro-angiogenic role and highlighted it as a promising target of vascular targeting therapy[225]. More recently, it was confirmed to mediate sprouting angiogenesis both *in vitro* and *in vivo*, and genetic disruption or antibody blockade of CLEC14A in tumour-bearing mice resulted in disruption of both tumour growth and vascularity[269].

Based on the above, as well as early immunofluorescence staining carried out in our lab, we hypothesised that CLEC14A is also upregulated on the vasculature of inflamed liver. Due to the chronic biliary injury which eventually leads to end-stage liver disease, cirrhosis and even cancer in patients with PSC, it is reasonable to expect a degree of disturbance in normal hepatic blood flow, potentially leading to low shear stress conditions required for CLEC14A upregulation. Its expression on liver vasculature in PSC, if present, would provide a promising target which could be tackled using immunotherapeutic approaches, one of which is described below.

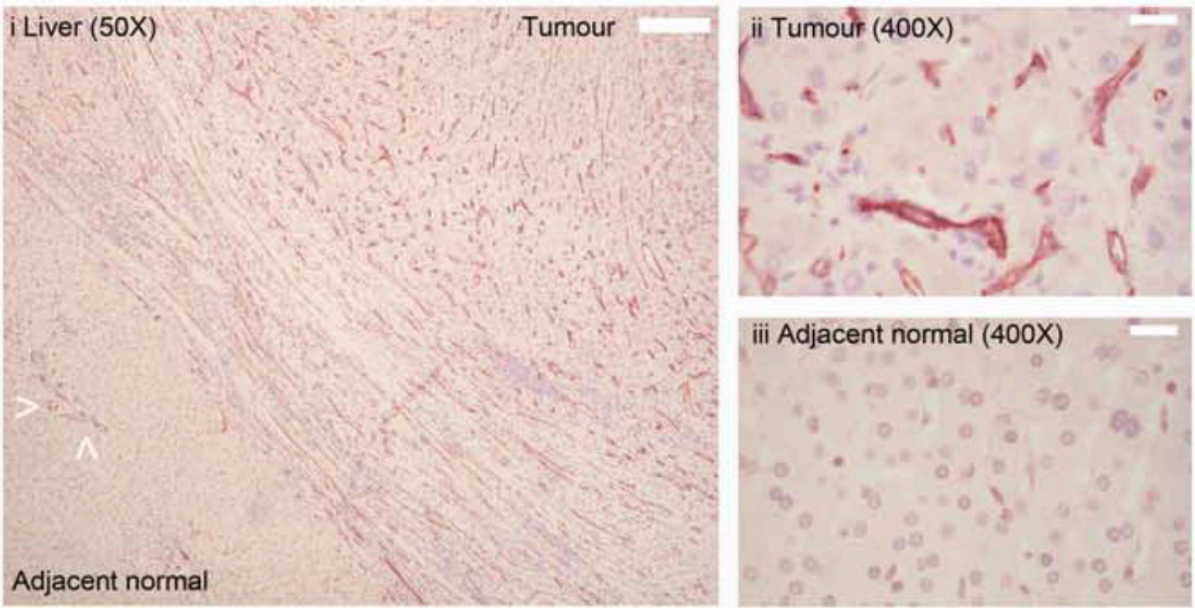

Figure 1.8 – Expression of CLEC14A in human hepatocellular carcinoma and healthy liver tissue

Immunohistochemical staining of human hepatocellular carcinoma (HCC) and adjacent healthy liver tissue using polyclonal CLEC14A antiserum (red) and haematoxylin counterstain (purple). (i), white arrows show invasion of HCC into normal tissue. Scale bar, 200μm. (ii) and (iii), higher magnification shows CLEC14A staining in tumour but not in normal tissue. Scale bars, 25μm. Reprinted by permission from Springer Nature: ONCOGENE (Mura M, Swain RK, Zhuang X, Vorschmitt H, Reynolds GM, Durant S, et al. Identification and angiogenic role of the novel tumor endothelial marker CLEC14A. 31:293–305), copyright (2012)[225]

1.7 Regulatory T-cell therapy

There is evidence of significant T-cell infiltration in the liver of PSC patients, with the inflammation and biliary injury being heavily T-cell mediated[270]. Such damaging action of T-cells directed against host's own tissues would normally be supressed by Tregs, whose main function is to prevent overactive immune responses. However, it has been found that the proportion of Tregs in both peripheral blood and liver of PSC patients is substantially lower than expected, and that the suppressive capacity of Tregs isolated from these patients is also impaired[271]. Treg-based immunotherapy would therefore represent a potentially effective treatment approach in PSC, especially if it can be specifically targeted to the liver, and as such merits further investigation.

1.7.1 Tregs and autoimmunity

Tregs are generally defined as $CD4^+$ $CD25^{high}$ $CD127^{low}$ T-cells which also express the intracellular transcriptional activator Foxp3, the master regulator of their function and development[272,273]. Representing a small part of the CD4 T-cell population – 5-10% – they develop in the thymus and constitutively express IL-2 receptor α chain (CD25) and CTLA-4 among other surface molecules, as well as produce immunosuppressive cytokines such as TGFβ and IL-10[272]. A proportion of Tregs also arises in the periphery upon Foxp3 induction resulting from antigen exposure, and in view of this there has been a recent move towards differentiating between thymic (tTregs) and peripheral Tregs (pTregs)[274]. Consistent with the importance of Tregs in maintaining peripheral tolerance and suppressing self-reactive T-cells, mutations in the Foxp3 gene have been found to cause profound immune dysregulation in both mice and humans[275–277], and depletion of Tregs led to spontaneous development of multiple autoimmune

diseases in mice[278]. Evidence from animal studies also suggests that both tTregs[279] and pTregs[280] are essential for effective immune self-tolerance.

In humans, Tregs are implicated in many autoimmune diseases. They are deficient both in numbers and function in AIH[281] and exhibit impaired suppressive capacity in polyglandular syndrome type II[282], while effector T-cells are less responsive than normal to Treg control in T1D[283] and systemic lupus erythematosus[284]. Significant functional impairments in Tregs have also been documented in patients with multiple sclerosis (MS)[285], myasthenia gravis[286] and rheumatoid arthritis[287]. Therefore, in a wide range of autoimmune conditions including those of the liver, it could be therapeutically beneficial to restore Treg functionality. One way to achieve this in the liver would be to selectively enrich hepatic Tregs by redirecting functional, *in vitro*- or *ex vivo*-expanded regulatory T-cells to the inflamed organ[273].

1.7.2 Adoptive Treg transfer

Targeting autoimmune conditions by adoptive transfer of therapeutic Tregs is not a new concept. It has already been successfully demonstrated, for example, in mouse models of autoimmune gastritis where Tregs targeted the autoantigen H^+/K^+ ATPase[288], and mouse models of MS where the Tregs were directed against a major protein component of the myelin sheath[289]. As with conventional T-cells, TCR gene transfer can also be carried out in Tregs to redirect them to an antigen of choice, as has already been demonstrated in a murine model of arthritis where joint inflammation and bone destruction were both significantly reduced by TCR-engineered Tregs[290]. In humans, a phase I trial of adoptively transferred autologous polyclonal (i.e. non-antigen

specific) Tregs in T1D patients showed that these cells are safe, remain phenotypically stable and persist in the circulation long-term, warranting further phase II studies[291]. Methods are also being developed for Treg expansion that would lead to their increased long-term phenotypic stability in autoimmune conditions where this is particularly important, such as Crohn's disease[292]. Overall, there are a variety of approaches to adoptive Treg therapy, using polyclonal or antigen-specific cells; even though both have shown promise, there is evidence to suggest that antigen-specific Tregs are superior in controlling disease compared to their non-specific counterparts[289,293,294].

For autoimmune conditions of the liver, the goal of ACT would be to target a purified and expanded Treg population specifically to the organ, thus enriching hepatic Tregs and tipping the balance in favour of immune control. Peripheral tolerance and disease remission have already been achieved in a mouse model of AIH treated with adoptively transferred autologous Tregs which were successfully directed to the inflamed liver[295]. Even though the liver-homing chemokine receptor CXCR3 is highly expressed on some Tregs in both mice and humans, and its corresponding ligands are upregulated on inflamed liver sinusoids[273], the best way to achieve specific hepatic targeting in patients would be to render the therapeutic Tregs antigen-specific. Unfortunately, the paucity of disease markers in autoimmune liver conditions makes this strategy difficult, although in some cases – such as in a subset of AIH which exhibits T-cell reactivity to the liver metabolic enzyme CYP2D6 – there is an autoantigen to which Tregs can be redirected[296]. In other cases, polyclonal Treg infusion is the best available option for patients who have failed previous immunosuppressive treatments[273]. In a condition

such as PSC, however, where CLEC14A serves as a potential marker of liver inflammation, there is also the possibility of engineering autologous Tregs to express high specificity receptors such as CARs targeting this endothelial marker, and thus the liver, in a selective way.

1.7.3 Engineering Tregs to express CARs

Since the success of conventional CAR T-cells in haematological malignancies, and their increasing promise in solid tumour treatment, the same genetic engineering approach has become of great interest in Treg immunotherapy of autoimmune diseases. A number of studies of both murine and human CAR Tregs have been carried out, all using the 2nd generation CD28 CAR construct and achieving transduction by retroviral or lentiviral gene transfer. The first CAR Treg study used a transgenic mouse model to show that 2,4,6-trinitrophenol-specific CAR Tregs suppressed effector T-cell responses *in vitro* in an antigen-dependent manner, as well as induced resistance to experimental colitis *in vivo*[297]. A follow-up study of the same antigen-specific CAR showed that it could be retrovirally engineered into mouse Tregs, and that their adoptive transfer into mice resulted in improvement of colitis which was superior to that induced by their unmodified counterparts[298]. Similarly promising findings in mouse colitis were seen with CEA-targeted CAR Tregs[299], while in a mouse model of MS, intranasally- and intraperitoneally-administered myelin-targeted CAR Tregs successfully homed to the central nervous system and cured mice of their encephalomyelitis[300].

Human Tregs have also been successfully engineered with CARs and targeted to an antigen of choice; however, few if any of these studies are in the context of autoimmunity. Nevertheless, CEA-redirected CAR Tregs have been shown to suppress the effector functions of autologous antigen-specific T-cells in a CEA^+ tumour *in vivo*, leading to substantial tumour outgrowth[301]. More recently, a HLA-A2-specific CAR was generated which, when transduced into Tregs and injected into mice, prevented graft-versus-host disease (GvHD) caused by $HLA\text{-}A2^+$ cells much more efficiently than Tregs expressing an irrelevant CAR[302]. Similarly, factor VIII-specific CAR Tregs were able to suppress effector T-cell responses that commonly arise in haemophilia A patients treated with this essential replacement therapy, thus inducing therapeutic immune tolerance[303]. Taken together, these studies provide the proof of principle needed to push CAR Tregs further towards the clinic, including for the treatment of autoimmune conditions.

As of February 2018, 49 clinical trials of Treg infusions are registered on clinicaltrials.gov, most of which are for the treatment of GvHD, transplant rejection or malignancies. Only a small proportion are being carried out in autoimmune conditions, none of which are in the liver. None of the Treg populations currently being trialled are genetically engineered to induce antigen specificity.

1.8 Hypotheses and aims

This thesis consists of two projects. The first project examines the hypothesis that TEM8-specific CARs can be successfully transduced into primary human T-cells, with the resulting CAR T-cells able to selectively and safely target TEM8 expressed on both

mouse and human tumour vasculature. If successful, the findings would potentially pave the way for future clinical studies of this therapeutic modality. To that end, the aims of the project are:

1) To generate TEM8-specific CAR T-cells and extensively test their target responses, functionality and specificity *in vitro*;
2) To study the safety of TEM8 CARs in healthy mice;
3) To examine the anti-tumour potential and responses of TEM8 CARs in tumour-bearing mouse models.

The second project begins to explore the potential for CAR Treg therapy in autoimmune liver inflammation with a focus on PSC, and hypothesises that CLEC14A is a promising CAR target for Tregs in this condition. The project aims are:

1) To examine the expression of CLEC14A in both human inflamed liver tissue and a PSC mouse model;
2) To generate CLEC14A CAR Tregs and test their suppressive capacity *in vitro*;
3) To carry out a pilot study of CLEC14A CAR Tregs in mice with PSC.

2 MATERIALS AND METHODS

2.1 Tissue culture

2.1.1 Maintenance of adherent cell lines

All the adherent cell lines used in this thesis and their appropriate media are listed in **Table 2.1**. All cell media were supplemented with 10% foetal bovine serum (FBS), 100 IU/mL penicillin, 100µg/mL streptomycin, and 2mM L-glutamine (all Gibco, Paisley, UK). Phoenix A (amphotropic) and Phoenix E (ecotropic) retroviral packaging cells[304] and human embryonic kidney (HEK) 293T cells were transferred to antibiotic-free Dulbecco's Modified Eagle Medium (DMEM) prior to transfection with relevant DNA (see sections 2.4.1 and 2.4.3). The only exception to the supplementation described above were the human umbilical vein endothelial cells (HUVEC), which were cultured in Human Large Vessel Endothelial Cell Basal Medium supplemented with growth factors and amphotericin B/gentamycin according to manufacturer's instructions (Cellworks, Buckingham, UK). All adherent cells were passaged by dissociation from plastic with trypsin-ethylenediaminetetraacetic acid (0.5% Trypsin-EDTA [10X], Gibco; diluted to 1X in phosphate-buffered saline [PBS]), neutralisation with excess medium, washing and resuspension in fresh medium every 2-5 days (cell-dependent), and were incubated at 37°C/5% CO_2 when not in use.

Table 2.1 – Adherent cells used as T-cell targets in this thesis

Cell line	Description	Source	Cell medium
CHO-TEM8	Chinese hamster ovary (CHO) cells stably expressing human TEM8	Brad St Croix, National Cancer Institute, National Institutes of Health (NIH), Frederick, MD	F-12 Nutrient Mixture (Ham), Gibco, Paisley, UK
CHO-CMG2	CHO cells stably expressing human CMG2	Brad St Croix, NIH	F-12 Nutrient Mixture (Ham)
CHO-PR230	CHO control cells for CHO-TEM8 and CHO-CMG2	Brad St Croix, NIH	F-12 Nutrient Mixture (Ham)
DLD-1	Human colorectal adenocarcinoma cell line	Brad St Croix, NIH	DMEM, Sigma-Aldrich, Poole, UK
HEK293T	Human embryonic kidney 293 (HEK293) cells containing the SV40 T-antigen	Roy Bicknell, University of Birmingham	DMEM
HEK293-hTEM8	HEK293 cells stably expressing human TEM8	Brad St Croix, NIH	DMEM
HEK293-mTEM8	HEK293 cells stably expressing mouse TEM8	Brad St Croix, NIH	DMEM
HUVEC	Human umbilical vein endothelial cells	Gibco	See section 2.1.1
LS174T	Human colorectal adenocarcinoma cell line	American Type Culture Collection (ATCC)	DMEM
MDA-MB-231	Human breast adenocarcinoma cell line	Fedor Berditchevski, University of Birmingham	DMEM
Phoenix A	HEK293T cells containing amphotropic viral packaging proteins	Indiana University National Gene Vector Biorepository (NGVB)	DMEM
Phoenix E	HEK293T cells containing ecotropic viral packaging proteins	NGVB	DMEM

2.1.2 Isolation and maintenance of human PBMCs and T-cells

Whole blood from healthy consenting donors was collected into apheresis cones and subjected to density centrifugation to isolate the PBMCs. Donor blood samples were first diluted with an equal volume of Roswell Park Memorial Institute (RPMI) medium (Sigma-Aldrich), layered onto Lymphocyte Separation Medium (LSM 1077; GE Healthcare, Buckinghamshire, UK) and centrifuged at 800g for 30 minutes with the brake off. The PBMCs were aspirated from the resulting buffy layer at the interface of separated plasma and LSM and washed with RPMI by centrifugation at 600g for 10 minutes, followed by another wash at 400g for 5 minutes. The cells were then resuspended in RPMI with 10% FBS and the contaminating platelets removed by centrifugation at 250g for 5 minutes. Finally, the resulting PBMCs were counted and either cryopreserved at $1x10^8$ cells/vial for future use (see section 2.1.4) or activated for transduction straight away (see section 2.4.1). T-cells obtained from these PBMCs after transduction were cultured in RPMI supplemented as described in section 2.1.1, with the addition of 1% pooled human serum (TCS Biosciences, Buckingham, UK) to give T-cell medium (TCM). IL-2 (Proleukin®, Novartis, Basel, Switzerland) was also added to TCM at 100 IU/mL for the duration of the culture period to maintain the T-cells.

2.1.3 Isolation and maintenance of human Tregs

Human Tregs were purified from fresh or frozen PBMCs using the $CD4^+CD25^+CD127^{dim/-}$ Regulatory T Cell Isolation Kit II, human (Miltenyi Biotec, Bisley, UK) according to manufacturer's instructions. The resulting Tregs were cultured at $1x10^6$ cells/mL in TCM with the addition of Human T-Activator CD3/CD28 Dynabeads

(Gibco) at 1:1 bead:cell ratio, 1,000 IU/mL IL-2 and 100nM rapamycin (Sigma-Aldrich) to prevent conventional T-cell outgrowth[305].

2.1.4 Cryopreservation and revival of cells

Prior to freezing, cells were harvested from their culture flasks and chilled at 4°C for 15-20 minutes to reduce cellular metabolic rate. They were subsequently centrifuged at 400g for 5 minutes, the supernatant discarded and the cells resuspended at the desired concentration in freezing medium, which consisted of 50% FBS, 40% RPMI and 10% dimethyl sulfoxide (DMSO). The cells were then immediately transferred into sterile 1.8mL CryoTube vials (Thermo Fisher Scientific [Nunc], Roskilde, Denmark) and frozen at -80°C inside an isopropanol-filled freezing container designed to reduce the temperature of the vials by 1°C/minute. After a minimum of 4h at -80°C, the cells were deposited into long-term storage in liquid nitrogen.

To revive previously frozen cells, the desired cryovials were removed from liquid nitrogen and placed in a pre-heated 37°C water bath until the cell suspension within was fully thawed. The cells were immediately transferred into sterile centrifuge tubes and relevant culture medium added to them gradually (dropwise at first). Once the cells were diluted in an excess of culture medium, they were centrifuged at 400g for 5 minutes, resuspended in fresh medium and incubated in a suitable culture flask at 37°C/5% CO_2.

2.1.5 Mycoplasma testing

Periodic testing was carried out on the cell lines in use to check for contamination with the mycoplasma bacterium. Culture supernatant was centrifuged at 600g for 5 minutes and 15µL of it mixed with 15µL of MycoAlert reagent (Cambrex, East Rutherford, NJ) in an OptiPlate-96 (Perkin Elmer, Coventry, UK). The plate was counted using the TopCount NXT microplate scintillation and luminescence counter (Perkin Elmer) and the counts recorded, before 15µL of MycoAlert substrate (Cambrex) was added to the culture supernatant and the plate counted again. If the second count was higher than the first for a given culture, it was considered mycoplasma-positive and was discarded. If the ratio of first to second count was 0.7-1, the relevant culture was quarantined in a separate incubator and re-tested a few days later. A mycoplasma-infected culture supernatant was used as a positive control in all assays. All cell lines tested were negative for mycoplasma.

2.2 Molecular techniques

2.2.1 Cloning of TEM8-targeting CAR constructs into MP71 retroviral vector

The second-generation TEM8 CAR construct used throughout this thesis is shown in **Figure 2.1**. To obtain it, pUC57 plasmid constructs encoding the scFv for one of five TEM8-specific mAbs – L1, L2, L3, L5 or 1D2 (antibody sequences: gift from Brad St Croix, NIH) were synthesised by GenScript (Piscataway, NJ). *Cla*I/*Not*I restriction enzyme digestion (both enzymes from Roche, Basel, Switzerland) was used to cleave these plasmids as well as a MP71 CAR expression retroviral vector which included the

CD28 co-stimulatory and CD3ζ signalling domains (original MP71 vector including the truncated CD34 marker and the subsequent CAR expression construct were kind gifts from Christopher Baum[306] and David Gilham[307] respectively). Following digestion, the five scFv inserts and the CAR expression vector were run on a 0.8% agarose gel (SeaKem GTG agarose, Lonza, Basel, Switzerland), the appropriate bands excised and the DNA extracted using the QIAquick Gel Extraction Kit (Qiagen, Hilden, Germany). Each insert was ligated to the vector using the Rapid DNA Ligation Kit (Roche) and supercompetent *E.coli* DH5α bacteria were transformed with the resulting constructs. DNA was isolated from bacterial colonies that grew overnight on ampicillin selection plates using the QIAprep Spin Miniprep Kit (Qiagen) according to manufacturer's instructions. Following confirmation of the correct DNA sequence of all CAR constructs (see section 2.2.3), the EndoFree Plasmid Maxi Kit (Qiagen) was used to obtain larger quantities of the purified plasmids for the purpose of T-cell transduction.

2.2.2 Cloning of mouse TEM8 gBlock fragment into pWPI lentiviral vector

The mouse TEM8 (mTEM8) gBlock was synthesised by Integrated DNA Technologies (IDT, Coralville, IA) using the mTEM8 sequence (gift from Brad St Croix) flanked by sequences that anneal to the pWPI lentiviral vector. The vector, previously obtained from Roy Bicknell (University of Birmingham) and containing an unrelated insert, was digested using *Pac*I and *Pme*I restriction enzymes (both from New England BioLabs [NEB], Ipswich, MA), run on a 0.6% agarose gel and the vector DNA band excised and purified using the Monarch DNA Gel Extraction Kit (NEB). The mTEM8 gBlock insert and pWPI lentiviral vector were then ligated at a 2:1 insert:vector ratio and competent bacteria transformed with the ligated construct using the NEBuilder HiFi DNA

Assembly Cloning Kit (NEB) according to manufacturer's instructions. DNA from bacterial colonies that grew overnight on ampicillin selection plates was purified using the EndoFree Plasmid Maxi Kit, the DNA sequence confirmed as correct (see section 2.2.3), and the resulting construct used to transfect LS174T target cells for use in T-cell assays (see section 2.4.3).

2.2.3 DNA sequencing

DNA was sequenced either by the Functional Genomics and Proteomics Facility (University of Birmingham) or by Source BioScience (Nottingham, UK) using primers custom-made by Sigma-Aldrich.

2.2.4 Human TEM8 quantitative polymerase chain reaction (qPCR)

qPCR to detect human TEM8 (hTEM8) mRNA in specified target cells was performed using qScript cDNA SuperMix (Quantabio, Beverly, MA) and TaqMan Gene Expression Assay no. Hs00216777_m1 (Life Technologies, Paisley, UK) according to manufacturer's instructions. Relative quantitation was performed using the standard curve method[308].

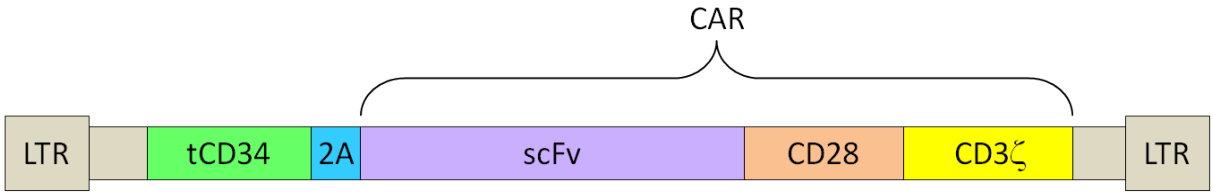

Figure 2.1 – Schematic representation of the 2nd generation TEM8 CAR construct used in this thesis

The CAR sequence consists of a region encoding the single chain variable fragment (scFv) derived from one of five anti-TEM8 monoclonal antibodies (L1, L2, L3, L5 or 1D2), followed by genes for the human CD28 co-stimulatory and human CD3ζ signalling domains. The self-cleaving 2A peptide linker derived from porcine teschovirus-1 ensures equimolar expression of the CAR with a truncated human CD34 (tCD34) molecule, which acts as a non-functional marker of transduced T-cells detectable by flow cytometry. LTR, long terminal repeats.

2.3 TEM8 protein production

The NEBuilder HiFi DNA Assembly Cloning Kit was used to transform competent bacteria with hTEM8-Fc/pFUSE-mIgG2A or mTEM8-Fc/pFUSE-mIgG2A plasmid vectors, both containing Zeocin resistance genes (plasmids: gift from Brad St Croix containing original pFUSE-mIgG2A-Fc1 vector from InvivoGen, San Diego, CA). Bacterial colonies that grew overnight on Fast-Media Zeo Agar plates were further grown in large-scale liquid cultures using Fast-Media Zeo Terrific Broth (both from InvivoGen). hTEM8-Fc and mTEM8-Fc DNA was purified from the resulting bacterial cultures using the Plasmid Maxi Kit (Qiagen).

Recombinant hTEM8-Fc and mTEM8-Fc proteins were produced with kind help from Jamie Webster at the Protein Expression Facility (PEF, University of Birmingham). 2L roller bottles were coated with 1% w/v solution of poly-L-lysine (Sigma-Aldrich) in PBS for 2-4h at 37°C. They were then washed with PBS and HEK293T cells seeded into them in sufficient numbers to allow the cells to reach 80-90% confluence in 48-72h (250mL DMEM supplemented as described in section 2.1.1 in each bottle). The roller bottles were incubated at 37°C in a rotating incubator (1rpm) during this time. When the desired cell confluence was reached, a mix of 435µg hTEM8-Fc or mTEM8-Fc DNA and 2.7mL linear polyethylenimine (PEI 25000; Polysciences, Warrington, PA) in 27mL Opti-MEM Reduced Serum Medium (Gibco) was prepared for each bottle, and the media in the bottles changed to 250mL Opti-MEM before adding the correct transfection mix to each. The roller bottles were incubated at 37°C in the rotating incubator for 7 days, after which the supernatants were harvested and the proteins from them purified using the Protein A Sepharose CL-4B (GE Healthcare) according

to manufacturer's instructions. The eluted hTEM8-Fc and mTEM8-Fc protein fractions were pooled and concentrated using the Amicon Ultra-15 Centrifugal Filter Units with Ultracel-30 Membrane, followed by further concentration with the Amicon Ultra-0.5 Centrifugal Filter Units (both from Merck Millipore, Watford, UK). When run on a 10% SDS-PAGE gel (Mini-PROTEAN Electrophoresis System, Bio-Rad, Watford, UK), the resulting recombinant hTEM8-Fc and mTEM8-Fc proteins gave bands of approximately 70kDa in size (confirmed as correct with Brad St Croix, personal communication 12/10/2016), and the final concentrations of both were determined using the PHERAstar FS microplate reader (BMG LABTECH, Offenburg, Germany).

2.4 Transduction protocols

2.4.1 Retroviral transduction of human T-cells and Tregs with CARs

The following quantities are given for Phoenix A cells growing in T75 flasks; if the process was scaled up to T150 flasks, the quantities of reagents were doubled accordingly. Phoenix A retroviral packaging cells in 4.5mL antibiotic-free DMEM were transfected with 1.8mL Opti-MEM containing 6µg L1, L2, L3, L5 or 1D2 TEM8 CAR or CRT3.2 CLEC14A CAR plasmid construct, 6µg pCL-Ampho retroviral packaging vector (NGVB) and either 72µg PEI (Sigma-Aldrich) or 60µL FuGENE 6 Transfection Reagent (Promega, Southampton, UK). The 2nd generation CRT3.2 CAR construct was the same as the one shown in Figure 2.1, with the scFv region derived from the CRT3 mAb specific for human and mouse CLEC14A obtained as described previously[269]. Mock-transfected controls were generated by adding Opti-MEM alone to

the Phoenix A cells. Both CAR DNA- and mock-transfected cells were incubated at 37°C/5% CO_2 for 48h, with the media changed to 10.5mL fresh antibiotic-free DMEM after the first 24h. Previously isolated PBMCs (section 2.1.2) adjusted to a concentration of $1x10^6$ cells/mL TCM were activated by the addition of 30ng/mL anti-CD3 antibody (OKT3; eBioscience, San Diego, CA), 30ng/mL anti-CD28 antibody (R&D Systems, Abingdon, UK) and 300 IU/mL IL-2, followed by incubation at 37°C/5% CO_2 for 48h before transduction. On the day of transduction, non-tissue culture-treated 6-well plates were coated with 30µg/mL RetroNectin (recombinant human fibronectin fragment; Takara Bio, Japan) for at least 3h, blocked with 2% w/v solution of bovine serum albumin (BSA; Sigma-Aldrich) in PBS for 30min, and washed once with PBS to prepare them for administration of retrovirus-containing and mock supernatants. The supernatants were then harvested from transfected Phoenix A cells, centrifuged at 400g for 5 minutes to remove any cells, and placed in the RetroNectin-coated plates (2mL/well). The plates were centrifuged at 2000g for 2h at 32°C, the supernatant was removed, the wells washed once with PBS and activated T-cells seeded into them at $2\text{-}2.5x10^6$/well ($1x10^6$/mL). The plates were centrifuged again at 400g for 5 minutes and incubated at 37°C/5% CO_2. The next day additional TCM + IL-2 (100 IU/mL) was added to the T-cells to allow them to expand, and the cells were transferred into tissue culture-treated 6-well plates 4-5 days later. They were maintained in culture as described in section 2.1.2.

For retroviral transduction of Tregs isolated as described in section 2.1.3, the Tregs were activated using Human T-Activator CD3/CD28 Dynabeads according to the manufacturer's protocol, with the addition of 1,000 IU/mL IL-2 and 100nM rapamycin.

The transduction process was carried out using the CRT3.2 CLEC14A CAR construct and in non-tissue culture-treated 24-well plates, but was otherwise identical to the one described above.

2.4.2 Retroviral transduction of mouse T-cells with TEM8 CARs

Phoenix E cells were transfected with each of the five TEM8-specific CARs in the same way as Phoenix A cells (section 2.4.1), using pCL-Eco (NGVB) as the retroviral packaging vector instead of pCL-Ampho. Spleens were harvested from healthy 6-8 week old BoyJ mice and mashed through a 70µm cell strainer (Greiner Bio-One, Stonehouse, UK) into a sterile Petri dish containing mouse TCM (RPMI supplemented with 10% FBS, 100 IU/mL penicillin, 100µg/mL streptomycin, and 2mM L-glutamine). The resulting suspension of mouse splenocytes was washed with RPMI by centrifuging at 700g for 5 minutes, the supernatant was discarded and the pellet resuspended in 1X solution of BD Pharm Lyse lysis buffer (BD Biosciences, Oxford, UK) in sterile distilled water in order to lyse the red blood cells. After incubation at 37°C for 4 minutes, the splenocytes were washed with mouse TCM (mTCM) by another centrifugation at 700g for 5 minutes and counted. Their concentration was adjusted to $3x10^6$ cells/mL mTCM, they were activated with 2µg/mL concanavalin A and 1ng/mL IL-7 (both Sigma-Aldrich) and incubated at 37°C/5% CO_2 for 48h, after which the transduction was carried out as for human T-cells (section 2.4.1).

2.4.3 Lentiviral transduction of LS174T cells with mTEM8

HEK293T cells growing in 10cm dishes and placed in 4.5mL antibiotic-free DMEM were transfected with 1.8mL Opti-MEM containing 12µg in total of the pWPI-mTEM8

construct (section 2.2.2), the psPAX2 lentiviral packaging vector (Didier Trono lab, Addgene plasmid #12260) and the pMD2.G envelope expression plasmid (Trono lab, Addgene plasmid #12259), together with 60µL FuGENE 6. The cells were incubated at 37°C/5% CO_2 for 48h, with the media changed to fresh 10.5mL antibiotic-free DMEM after the first 24h. When the incubation was finished, lentiviral supernatant was harvested, centrifuged at 300g for 5 minutes to remove any cells, and 8µg/mL Polybrene Infection/Transfection Reagent (hexadimethrine bromide; Merck Millipore) added to it. The supernatant was passed through a Minisart 0.45µm syringe filter (Sartorius, Goettingen, Germany) and applied in place of regular DMEM to LS174T target cells seeded the previous day into 6cm dishes (3mL/dish). After 2-3 days, the newly generated LS174T-mTEM8 cells were analysed by flow cytometry – the presence of a green fluorescent protein (GFP) marker in the pWPI lentiviral vector allowed for the detection of successfully transduced target cells in the fluorescein isothyocyanate (FITC) channel. The parent LS174T cell line was used as the negative control.

2.5 Phenotypic and functional analysis of transduced T-cells

2.5.1 Flow cytometry of T-cells and target cells

All the antibodies used to label both human and mouse mock- and CAR-transduced T-cells and human Tregs are specified in **Table 2.2**. When labelling, the cells were first washed with PBS by centrifuging at 400g for 5 minutes and resuspended in 40µl of 1/1,000 dilution of viability dye in PBS (LIVE/DEAD Fixable Violet Dead Cell Stain Kit,

Thermo Fisher Scientific, Waltham, MA; reconstituted according to manufacturer's instructions). They were incubated in the dark at room temperature for 20 minutes before being washed with MACS buffer by another centrifugation at 400g for 5 minutes. The cells were then labelled with appropriate dilutions of antibodies specific for relevant T-cell surface markers (Table 2.2) and incubated in the dark on ice for 30 minutes, followed by another wash with MACS buffer as before and final resuspension in 200µl MACS buffer. When labelling human Tregs, the last wash was followed by fixation, permeabilisation and staining for Foxp3 using the Anti-Human Foxp3 Staining Set Alexa Fluor 488 (eBioscience) according to manufacturer's instructions before the final resuspension. The T-cells were then analysed for transduction efficiency and phenotype using the BD LSRII Flow Cytometer (BD Biosciences) and FlowJo software (FlowJo LLC, Ashland, OR). Successful CAR transduction was identified by positive staining for the CD34 marker, which is included in its truncated form in the CAR gene construct and is co-expressed in equimolar quantities to the CAR (Figure 2.1). Mock-transduced T-cells, or in specified instances staining with a concentration- and isotype-matched control antibody (Table 2.2), was used for negative control CD34 staining.

When stated, staining was also performed on relevant target cells to confirm their surface expression of the TEM8 protein. The above staining process was employed for this purpose, with the antibodies used also specified in Table 2.2.

Table 2.2 – Antibodies used to stain T-cells for transduction efficiency/phenotype and target cells for TEM8 expression

Antibody	Clone	Conjugated dye	Manufacturer	Dilution/amount*
Staining of human T-cells				
Mouse anti-human CD4	RPA-T4	FITC	BD Biosciences	1/40
Mouse anti-human CD8a	RPA-T8	PE	eBioscience	1/40
Mouse anti-human CD34	561	APC	BioLegend, San Diego, CA	1/20
Staining of mouse T-cells				
Rat anti-mouse CD4	H129.19	PE	BD Biosciences	1/40
Rat anti-mouse CD8a	53-6.7	FITC	BD Biosciences	1/40
Mouse anti-human CD34	561	APC	BioLegend	1/20
Staining of human Tregs				
Mouse anti-human CD3	UCHT1	Alexa Fluor 700	BioLegend	1/20
Mouse anti-human CD4	RPA-T4	PE	BD Biosciences	1/40
Mouse anti-human CD127	eBioRDR5	PE-Cy7	eBioscience	1/20
Mouse anti-human CD34	561	APC	BioLegend	1/20
Mouse IgG2a, κ isotype control	MOPC-173	APC	BioLegend	1/40
Rat anti-human Foxp3	PCH101	Alexa Fluor 488	eBioscience	5μL
Rat IgG2a, κ isotype control	eBR2a	Alexa Fluor 488	eBioscience	5μL
Staining of target cells				
L2 anti-TEM8 mAb 2mg/mL (primary)	N/A	Unconjugated	Gift from Brad St Croix	2μL
Mouse IgG2a, κ isotype control 1mg/mL (primary)	ZX4	Unconjugated	Thermo Fisher Scientific	4μL
Goat anti-mouse IgG (secondary)	Polyclonal	PE	Bio-Rad	1/20

*for a 40μL cell sample

2.5.2 IFNγ enzyme-linked immunosorbent assay (IFNγ ELISA)

Specified target cells were seeded into 96-well flat-bottom plates, left to adhere for 3-4h, and mock or TEM8 CAR-transduced T-cells added to them (seeding densities are stated in the relevant figure legends). CAR T-cells were equalised for transduction efficiency by adding autologous mock T-cells to each, such that all five CAR T-cell lines had equal proportions of transduced cells. Target cells and T-cells seeded alone were included as controls. Alternatively, decreasing concentrations of recombinant hTEM8-Fc and mTEM8-Fc proteins, generated as described in section 2.3, were left to adhere to 96-well MaxiSorp Nunc-Immuno Plates (Thermo Fisher Scientific) for 3-4h before the plates were washed with PBS and the T-cells added to them as above. T-cells seeded alone and with the recombinant mouse IgG2a Fc fragment (R&D Systems) were included as controls. The T-cell/target cell or T-cell/protein co-cultures were then incubated overnight at 37°C/5% CO_2 in 200µL/well ELISA medium (RPMI supplemented with 10% FBS, 100 IU/mL penicillin, 100µg/mL streptomycin, 2mM L-glutamine and 25 IU/mL IL-2), and the supernatants were assayed for IFNγ release the following day according to the Thermo Fisher Scientific IFNγ ELISA protocol. The exact reagents used in the assay are listed in **Table 2.3**. The absorbance of the plates was read at 450nm and 655nm using the iMark Microplate Absorbance Reader (Bio-Rad) and the readings used to generate a standard curve and calculate IFNγ concentrations in pg/mL.

Table 2.3 – Reagents used to develop IFNγ ELISA reactions

Type of reagent	Reagent	Manufacturer	Working concentration	Amount (µL/well)
Coating antibody	Human IFNγ mAb (2G1)	Thermo Fisher Scientific	0.75µg/mL in coating buffer	50
Coating buffer	Na_2HPO_4 adjusted to pH 9.0 using 0.1M NaH_2PO4	BDH Laboratory Supplies, Poole, UK	0.1M	50
Blocking buffer	1% w/v BSA + 0.05% v/v Tween 20 + 0.1% w/v NaN_3 in PBS	Sigma-Aldrich	See under 'Reagent'	200
Wash buffer	Tween 20 in PBS	Fisher Scientific	0.05% v/v	250
Standard	Human recombinant IFNγ	Sigma-Aldrich	20,000 to 312.5pg/mL by two-fold dilutions*	50
Detection antibody	Human IFNγ mAb (B133.5), biotin-labelled	Thermo Fisher Scientific	0.375µg/mL in blocking buffer	50
Streptavidin-HRP	ExtrAvidin-Peroxidase (buffered aqueous solution)	Sigma-Aldrich	1/1,000 in blocking buffer	50
Substrate solution	Tetramethylbenzidine (TMB) Single Solution	Life Technologies	Neat	50
Stop solution	Phosphoric or sulphuric acid	Sigma-Aldrich	1M	50

*in ELISA medium

2.5.3 Intracellular cytokine staining

Mock or TEM8 CAR-transduced T-cells equalised for transduction efficiency were co-cultured with specified target cells, previously left to adhere for 3-4h, in 48-well plates. All the cells were seeded at $5x10^5$ cells/well in 1mL/well TCM, and T-cells cultured alone or in the presence of 200ng/mL Staphylococcal enterotoxin B (SEB) as positive control were included. After 90 minutes, 10µg/mL brefeldin A (Sigma-Aldrich) was added to all the wells and the plate incubated overnight at 37°C/5% CO_2. The following day the T-cells were harvested, washed with MACS buffer by centrifugation at 400g for 5 minutes and labelled for surface markers using the antibodies specified in **Table 2.4**. They were incubated in the dark on ice for 30 minutes, washed again and fixed using 4% paraformaldehyde (Fisher Scientific). After another incubation in the dark at room temperature for 15 minutes, the cells were washed once more and resuspended in 0.5% saponin (Fisher Scientific) for 5 minutes before the addition of intracellular staining antibodies (Table 2.4). The T-cells were then incubated in the dark at room temperature for 30 minutes, washed as before and finally resuspended in 200µl MACS buffer containing 1% paraformaldehyde. They were analysed by flow cytometry, with fluorescence minus one controls used to determine levels of background staining for IFNγ, IL-2 and TNFα.

2.5.4 Proliferation assay

Mock and transduction-equalised TEM8 CAR T-cells were labelled with 5µM carboxyfluorescein diacetate succinimidyl ester (CFSE) intracellular dye (CFSE Cell Division Tracker Kit, BioLegend) according to manufacturer's instructions. After two wash steps – in PBS and TCM – by centrifugation at 400g for 5 minutes, the T-cells

were resuspended in TCM containing 15 IU/mL IL-2 and co-cultured with specified target cells previously left to adhere for 3-4h in 96-well flat-bottom plates (T-cells: $3x10^5$ cells/well, target cells: $2x10^4$ cells/well, 250µL total medium/well). T-cells alone in TCM containing 600 IU/mL IL-2 were included as a positive control, and the plate incubated at 37°C/5% CO_2 for four days. On day 4, the T-cells were removed and labelled as specified in Table 2.2 ('Staining of human T-cells'), with the anti-CD4 FITC antibody substituted with the anti-CD4 PE-Texas Red one (Beckman Coulter) in order to avoid a clash with CFSE dye detection in the FITC channel. T-cell proliferation was then analysed by flow cytometry.

2.5.5 Chromium release assay

All radioactive work was carried out in accordance with University policies and protocols after appropriate training and authorisation had been given. Indicated target cells were centrifuged at 400g for 5 minutes and the resulting cell pellets labelled with 50-100µCi chromium-51 (^{51}Cr) radionuclide (Perkin Elmer). The cells were resuspended in the chromium-containing supernatant and incubated at 37°C/5% CO_2 for 2h with occasional agitation. They were subsequently given two washes with TCM by centrifugation at 400g for 3 minutes and seeded into 96-well conical bottom MicroWell plates (Nunc) at $2.5x10^3$ cells/well. Mock or transduction-equalised TEM8 CAR T-cells were added to each of the target cells at decreasing effector:target (E:T) ratios, with target cells alone in TCM or in 1% sodium dodecyl sulphate (SDS) included as spontaneous and maximum lysis controls respectively (200µL total TCM/well). The plates were then centrifuged at 400g for 3 minutes and incubated at 37°C/5% CO_2 for 12h. Following the incubation, the cell supernatants were transferred to round base

test tubes (Sterilin, Newport, UK) and analysed for released chromium as a direct measure of target cell lysis using the Cobra II Auto-Gamma Counter (Packard). Specific lysis for each target cell line was calculated using the following formula (cpm = counts per minute, a measure of ionising radiation as reported by the Cobra Counter):

$$\% \text{ specific lysis} = \frac{\text{sample cpm} - \text{spontaneous cpm}}{\text{maximum cpm} - \text{spontaneous cpm}} \times 100$$

2.5.6 Treg suppression assay

96-well MaxiSorp Nunc-Immuno Plates were coated with 10µg/mL recombinant human full-length CLEC14A-Fc (PEF) or purified human IgG-Fc fragment control (Bethyl, Montgomery, TX) for 3-4h. CRT3.2 CLEC14A-specific CAR-transduced T-cells (generated as described in section 2.4.1) were labelled with CFSE as specified in section 2.5.4 and added to protein-containing wells either alone or in co-culture with autologous CRT3.2 CLEC14A-specific CAR-transduced or mock Tregs at increasing T-cell:Treg ratios (200-300µL total medium/well, TCM with 10 IU/mL IL-2 used throughout). The plates were incubated at 37°C/5% CO_2 for 3-4 days, after which the T-cells were harvested, labelled with viability dye, anti-human CD3 Alexa Fluor 700, anti-human CD8a PE and anti-human CD34 APC (see section 2.5.1 for the labelling procedure), and their proliferation analysed by flow cytometry.

Table 2.4 – Antibodies used for intracellular cytokine staining of T-cells

Antibody	Clone	Conjugated dye	Manufacturer	Dilution/amount*
Surface stain antibodies				
Mouse anti-human CD4	SFCI12T4D11	PE-Texas Red	Beckman Coulter, High Wycombe, UK	1/40
Mouse anti-human CD8	SK1	AmCyan	BD Biosciences	1/80
Mouse anti-human CD34	581	PE-Cy5	BD Biosciences	1/40
Intracellular stain antibodies				
Mouse anti-human IFNγ	45.15	FITC	Beckman Coulter	6µL
Rat anti human IL-2	MQ1-17H12	PE	BD Biosciences	3µL
Mouse anti-human TNFα	MAb11	PE-Cy7	eBioscience	1/80

*for a 40µL cell sample

2.6 *In vivo* studies

All animal experiments were conducted at the University of Birmingham Biomedical Services Unit (BMSU) in accordance with the Animals (Scientific Procedures) Act 1986 and under the United Kingdom Home Office-approved project licence P32634CE8 (held by Dr Steven P. Lee) and personal licence. The mice used in all experiments were either the highly immunodeficient NOD *scid* gamma (NSG) mice (bred in-house) or the immunocompetent C57 black 6 (C57BL/6) mice (purchased from Charles River, Wilmington, MA). T-cells for transduction and injection into C57BL/6 mice were isolated from the spleens of BoyJ mice (bred in-house) – this congenic C57BL/6 strain has a distinct pan-leukocyte marker, CD45.1, which allows the tracking of $CD45.1^+$ T-cells when injected into wild-type (WT) C57BL/6 mice (whose congenic marker is CD45.2). Unless otherwise specified, all experimental animals were 6-12 week old females with free access to food and water between experiments and, if ordered externally, were allowed to rest for at least 4 days after arriving at the facility before any procedures were carried out.

2.6.1 Mouse breeding and genotyping

All in-house breeding was performed by qualified BMSU staff under project licence 70/8198 (held by BMSU director Caroline Chadwick). For experiments involving TEM8 KO mice, male $TEM8^{+/-}$ mice (gift from Brad St Croix) were re-derived locally and bred as described before[245] to generate homozygous TEM8 KO progeny on a C57BL/6 background. During re-derivation and subsequent breeding, ear clips were collected from these mice and sent to Transnetyx (Cordova, TN), who genotyped the samples

using custom-made TEM8 probes. The genotype information was then used to inform further breeding.

2.6.2 Toxicity studies in C57BL/6 WT and TEM8 KO mice

One day after TEM8 CAR transduction as described in section 2.4.2, mock or specified CAR-transduced mouse splenocytes were layered onto Histopaque-1083 (Sigma-Aldrich) and centrifuged at 400g for 30 minutes at the lowest brake setting. The lymphocytes were aspirated from the resulting buffy layer and washed with RPMI by centrifugation at 400g for 10 minutes, then once again with mTCM at 250g for 10 minutes. The purified lymphocytes were then resuspended in Hank's Balanced Salt Solution (HBSS; Lonza), counted and, unless otherwise specified, 10-20x10^6 T-cells/mouse centrifuged once more at 700g for 5 minutes. The cells were resuspended in up to 200µL HBSS/mouse (for a mouse weighing ≥20g – scaled down accordingly if weights were <20g), transported on ice to the BMSU and injected intravenously into the tail of healthy, sublethally irradiated (4-5 grays [Gy]) C57BL/6 WT or, if present in the study, TEM8 KO mice.

2.6.3 Multiple infusion toxicity study in NSG mice

Mock or specified TEM8 CAR-transduced human T-cells were pooled one day after transduction (which is described in section 2.4.1) and washed twice with PBS by centrifugation at 400g for 5 minutes. After the second wash the T-cells were counted and 20x10^6 T-cells/mouse centrifuged once more at 400g for 5 minutes, resuspended in HBSS and injected into healthy NSG mice as described in section 2.6.2. This process of T-cell preparation was repeated and the mice injected in the same way on

days 5 and 9 of the study (the day of first injection was counted as day 0). In this study, therefore, the mice were injected with three separate doses of $20x10^6$ T-cells each.

2.6.4 Tumour protection study in NSG mice

DLD-1 human colorectal carcinoma cells, previously shown to generate TEM8-positive vasculature *in vivo*[246], were dissociated from their culture flasks, counted and centrifuged at 400g for 5 minutes before being resuspended in HBSS at $2.5x10^6$ cells/mouse. They were transported on ice to the BMSU and injected subcutaneously into the flank of healthy NSG mice. 3 days later, 1D2 TEM8 CAR or 'no scFv' CAR T-cells ('no scFv' - control CAR which does not contain a scFv region) were prepared as described in section 2.6.3 and injected into the tail vein of the tumour-bearing NSG mice. Tumour size was monitored by regular calliper measurements and not allowed to go above $1250mm^3$, specified in the project licence as the maximum tumour volume before culling would need to take place.

2.6.5 Mouse monitoring, tail bleed staining and ending the experiments

In all the studies described above, mice were closely monitored throughout and weighed at regular intervals. Weekly tail bleeds were also performed to track the fate of the injected T-cells. The blood was collected into pre-weighed microcentrifuge tubes containing 20µL heparin sodium (Wockhardt UK, Wrexham; stock: 1,000 IU/mL, diluted in PBS to 50 IU/mL), the tubes weighed again to calculate the exact volume of blood in each one (assuming 1mg = 1µL) and 100µL of 50 IU/mL heparin in PBS added to each. The tubes were centrifuged at 600g for 3 minutes to separate the plasma from the cells, 100µL of the resulting plasma collected and the samples stored at -80ºC for

subsequent multiplex cytokine analysis (see section 2.6.6). Another 100µL of 50 IU/mL heparin in PBS was then added to the remaining cell pellets in each microcentrifuge tube and all the tail bleed samples transferred into a 96-well conical bottom MicroWell plate, which was centrifuged at 600g for 3 minutes. The samples were resuspended in 200µL/well BD Pharm Lyse lysis buffer, incubated at 37°C for 4 minutes and centrifuged as before – this was repeated once in order to lyse the majority of red blood cells. The samples were then stained as described in section 2.5.1, with the addition of 20µL Flow-Count Fluorospheres (Beckman Coulter) to each sample after the last wash to determine absolute T-cell counts during flow cytometric analysis; these, together with blood volumes calculated as explained above, were subsequently used to determine T-cell numbers and proportions/mL mouse blood. The antibodies used to stain the samples are listed in Table 2.2 ('Staining of human T-cells' and 'Staining of mouse T-cells'), with mouse T-cells also being labelled with the mouse anti-mouse CD45.1 (clone A20) conjugated to PE-Cy7 (BD Biosciences) to differentiate between infused and host T-lymphocytes.

If major health issues or toxicity were observed in the mice during any of the above studies, the mice in question were culled immediately using a Schedule 1 method approved by the Animals (Scientific Procedures) Act 1986. Otherwise, all mice were euthanised by Schedule 1 at the end of the experiment. Where specified, major mouse organs were harvested and fixed in neutral buffered formalin solution 10% (Sigma-Aldrich) for subsequent sectioning, haematoxylin and eosin (H&E) staining and histopathological analysis. Sectioning and H&E staining were performed by the Human Biomaterials Resource Centre (University of Birmingham), the resulting sections were

kindly imaged by Katharine Whitworth (Lee lab) using the Zeiss Axioskop 40 brightfield microscope (air objective at 10X magnification), after which they were examined for histopathology.

2.6.6 Mouse plasma multiplex cytokine analysis

Stored plasma samples from specified mouse experiments were thawed, processed and analysed for a panel of 26 cytokines using the Mouse Magnetic Luminex Assay (LXSAMSM; R&D Systems) according to manufacturer's instructions. The mouse samples and cytokines analysed are stated when discussing relevant experiments in chapter 4. During processing, the samples were further diluted 2-fold as recommended in the provided Luminex protocol and subsequently run on the Bio-Rad Bio-Plex analyser. The original plasma volumes for each sample, as calculated in section 2.6.5, were used to determine the actual dilution factor of the samples before analysis; these were then used in conjunction with the results generated by the Bio-Plex analyser to calculate the exact amount of each cytokine in pg/mL.

2.7 CLEC14A and CD31 staining in liver tissue

All human inflamed liver samples from patients with PSC and alcoholic liver disease (ALD), as well as samples from liver donors whose organs were not accepted for transplantation (donor livers), were obtained from Gary Reynolds at the Centre for Liver Research (CLR, University of Birmingham) with all ethical approval in place. The liver disease tissue array LVD481 and normal human tissue array MNO1021 were purchased from Pantomics, Inc (Richmond, CA). All samples were provided as fixed

tissue sections and stained alongside fixed placenta samples (Human Biomaterials Resource Centre) as a positive control for the immunohistochemistry procedure. This staining was performed with kind help from Katharine Whitworth (Lee lab).

All mouse inflamed liver samples were obtained as frozen sections from male MDR2 KO FVB mice (mouse model of PSC), and were kind gifts from Vasanthy Vigneswara at the CLR. Frozen liver sections from male WT and MDR2 KO C57BL/6 mice (Ditte Hedegaard, CLR) and frozen C57BL/6 placenta samples (Andrea White, University of Birmingham) were stained alongside as controls.

2.7.1 Immunohistochemistry of fixed human liver tissue

Sample and control slides were first baked at 60°C for 30 minutes. They were then dewaxed and rehydrated in a fume hood by submerging in xylene for 3 x 2 minutes, isopropanol (propan-2-ol) for 3 x 2 minutes (both reagents from Fisher Scientific), and finally in deionised water (dH_2O) for 2 x 2 minutes. Chilled 30% hydrogen peroxide (Sigma-Aldrich) was diluted 1/10 in chilled methanol (AnalaR NORMAPUR, VWR, Lutterworth, UK) and the slides submerged in the resulting 3% hydrogen peroxide for 5 minutes. They were transferred to a suitable container and washed with a 0.1% solution of Tween 20 (Sigma-Aldrich) in PBS for 3 x 5 minutes using a stirrer. The slides were then removed from the fume hood and antigen retrieval performed by placing them in an unmasking solution, which was made by diluting the tris-based antigen unmasking solution (Vector Laboratories, Peterborough, UK) to 1% in 1L dH_2O and heating it in a microwave at 850W for 5 minutes. Once in the solution, the slides were heated in the microwave for a further 15 minutes and allowed to cool for 10

minutes before excess dH_2O was added to them to bring the solution to room temperature. Each slide was then fitted onto a Shandon glass coverplate and placed into a Sequenza slide holder (both from Fisher Scientific), after which each one was washed 3 times with 0.1% PBS-Tween (2mL/wash). Normal horse serum blocking solution (Vector Laboratories) was diluted to 10% in PBS and 100µL added to each section, followed by incubation at room temperature for 30 minutes. The slides were then labelled as follows:

- Polyclonal human CLEC14A antibody or normal sheep IgG control (both from R&D Systems) were diluted to 1.7µg/mL in PBS containing 2.5% v/v horse serum and 200µL added to the appropriate slides, followed by incubation at room temperature for 1h;

  OR

  Mouse anti-human CD31 antibody (clone JC70A, Dako/Agilent Technologies, Stockport, UK) was diluted 1/40 in PBS containing 2.5% v/v horse serum and 200µL added to the appropriate slides, followed by incubation at 4°C for 18h (performed overnight);
- Polyclonal donkey anti-sheep IgG (R&D Systems; secondary antibody for the CLEC14A antibody and the sheep IgG control) conjugated to horseradish peroxidase (HRP) was diluted 1/100 in PBS containing 2.5% v/v horse serum and 200µL added to the appropriate slides, followed by incubation at room temperature for 30 minutes;

  OR

  ImmPRESS HRP anti-mouse IgG (Vector Laboratories; secondary antibody for the mouse anti-human CD31 antibody) was diluted 1/4 in PBS containing 2.5%

v/v horse serum and 200µL added to the appropriate slides, followed by incubation at 4°C for 3h.

3 x 2mL wash steps with 0.1% PBS-Tween were performed on all slides after each incubation. After the last set of washes, the ImmPACT NovaRED HRP substrate (Vector Laboratories) was made up according to manufacturer's instructions and 300µL added to each section, followed by incubation at room temperature for 3 minutes (CLEC14A) or 5 minutes (CD31). The slides were then removed from the slide rack and coverplates, transferred to a container and washed with dH_2O for 5 minutes using a stirrer. They were subsequently immersed in filtered Mayer's haematoxylin (pfm medical, Poynton, UK) for 30 seconds, dH_2O for 5 seconds, and in 1/10 dilution of Scott's tap water substitute (Sigma-Aldrich) in dH_2O for 1 minute. Finally, they were washed once more with dH_2O for 5 minutes using a stirrer and dehydrated in the fume hood by immersion in isopropanol for 2 x 2 minutes and xylene for 3 x 2 minutes. Each slide was then pressed down onto an appropriately sized coverslip containing a drop of DPX Mounting Medium (CellPath, Powys, UK), left to dry for at least 24h at room temperature and imaged using the Zeiss Axioskop 40 brightfield microscope (air objective at 10X magnification).

2.7.2 Immunofluorescence of frozen mouse liver tissue

Sample and control slides were first fixed by immersion in -20°C acetone (Fisher Scientific) in a covered glass slide holder for 10 minutes, then transferred to a suitable container and washed with PBS for 3 x 5 minutes using a stirrer. Each slide was fitted onto a Shandon glass coverplate and placed into a Sequenza slide holder, after which 100µL of 2.5% v/v normal horse serum blocking solution (Vector Laboratories) was

added to each and left to incubate at room temperature for 30 minutes. All slides were then taken through the following four steps of the labelling procedure:

- Polyclonal CLEC14A antibody (section 2.7.1; cross-reactive with mouse CLEC14A) or normal sheep IgG control were diluted to 10µg/mL in PBS and 100µL added to the appropriate slides, followed by incubation at 37°C for 1h;
- Rabbit anti-sheep IgG cross-adsorbed secondary antibody, DyLight 550 (Life Technologies) was diluted to 10µg/mL in PBS and 100µL added to each slide, followed by incubation at room temperature in the dark for 1h;
- Purified rat anti-mouse CD31 antibody (clone MEC13.3; BioLegend) was diluted to 10µg/mL in PBS and 100µL added to each slide, followed by incubation at room temperature in the dark for 1h;
- Chicken anti-rat IgG cross-adsorbed secondary antibody, Alexa Fluor 488 (Life Technologies) was diluted to 10µg/mL in PBS and 100µL added to each slide, followed by incubation at room temperature in the dark for 1h.

The slides were washed 3 times with PBS (2mL/wash) after each of the above incubations, followed by a single wash with 2mL dH_2O per slide at the end of the staining procedure. They were removed from the slide rack and coverplates and partially dried off, pressed down onto appropriately sized coverslips each containing a drop of ProLong Gold Antifade Mountant (Invitrogen) and left to dry at room temperature for at least 30 minutes. They were stored in the dark at -20°C and imaged using the Zeiss LSM 510 Meta confocal microscope (air objective at 20X magnification).

2.8 Statistical analysis

Where indicated, statistical analysis was performed using GraphPad Prism 7 software, with statistical significance assumed if P values were less than 0.05. The exact tests performed on the data are indicated in the appropriate figure legends.

3 GENERATION AND *IN VITRO* TESTING OF TEM8 CAR-ENGINEERED T-CELLS

As discussed extensively in section 1.5 of the Introduction, targeting the tumour vasculature – and in particular a selectively expressed tumour endothelial marker such as TEM8 – seems a very promising avenue of further research. In view of the reported success of CAR T-cells, and the encouraging data obtained with TEM8 antibody targeting, the therapeutic potential of CARs redirected towards TEM8 warrants in-depth exploration. The results described in this and next chapter therefore provide insight into the *in vitro* functionality and *in vivo* therapeutic capacity of TEM8-targeted CAR T-cells and can be used to inform decisions about their further testing, both in the lab and, potentially, in the clinic.

3.1 Human T-cells are successfully transduced with five distinct TEM8 CARs

To construct TEM8 CARs, the sequences of five anti-TEM8 mAbs were first obtained as a kind gift from our collaborator Brad St Croix at the NIH, whose lab had previously described making and using them in mouse anti-tumour studies[246]. The antibodies, termed L1, L2, L3, L5 and 1D2, are all cross-reactive with both hTEM8 and mTEM8 at varying affinities in their Fab form, with 1D2 of notably lower affinity for both versions of the protein[246] (**Table 3.1**). The five antibody sequences were used to generate five anti-TEM8 scFvs, which were successfully cloned into a retroviral vector and stably transduced into primary human T-cells as described in detail in sections 2.2.1 and 2.4.1. The construct used for each of the five CARs is shown in Figure 2.1. CD34 expression on the surface of transduced T-cells served as a marker of successful CAR

transduction and, due to the nature of the construct, as a direct measure of CAR levels on the T-cell surface. The full gating strategy routinely used to detect CAR T-cells is shown in **Figure 3.1**.

Bulk populations of primary human T-cells were consistently successfully transduced with all five CARs, as shown in **Figure 3.2A**. For each transduction carried out, a mock T-cell population was also generated as described in section 2.4.1 which served as a CAR-negative control for both flow cytometry and in all subsequent functional assays. CD8 and CD4 T-cell subsets within a given T-cell population were both successfully transduced throughout, although CD4 T-cells consistently exhibited a somewhat higher level of CAR surface expression compared to the CD8 subset (**Figure 3.2B**). Once transduced, the generated CAR T-cells grew well in culture for at least 2-3 weeks, sometimes exhibiting a gradual loss of CAR surface expression over time of up to 10%. They were therefore used in functional assays within the first two weeks of their transduction whenever possible, or cryopreserved early and revived when needed – re-staining of CAR T-cells upon thawing showed very little or no loss in CAR expression.

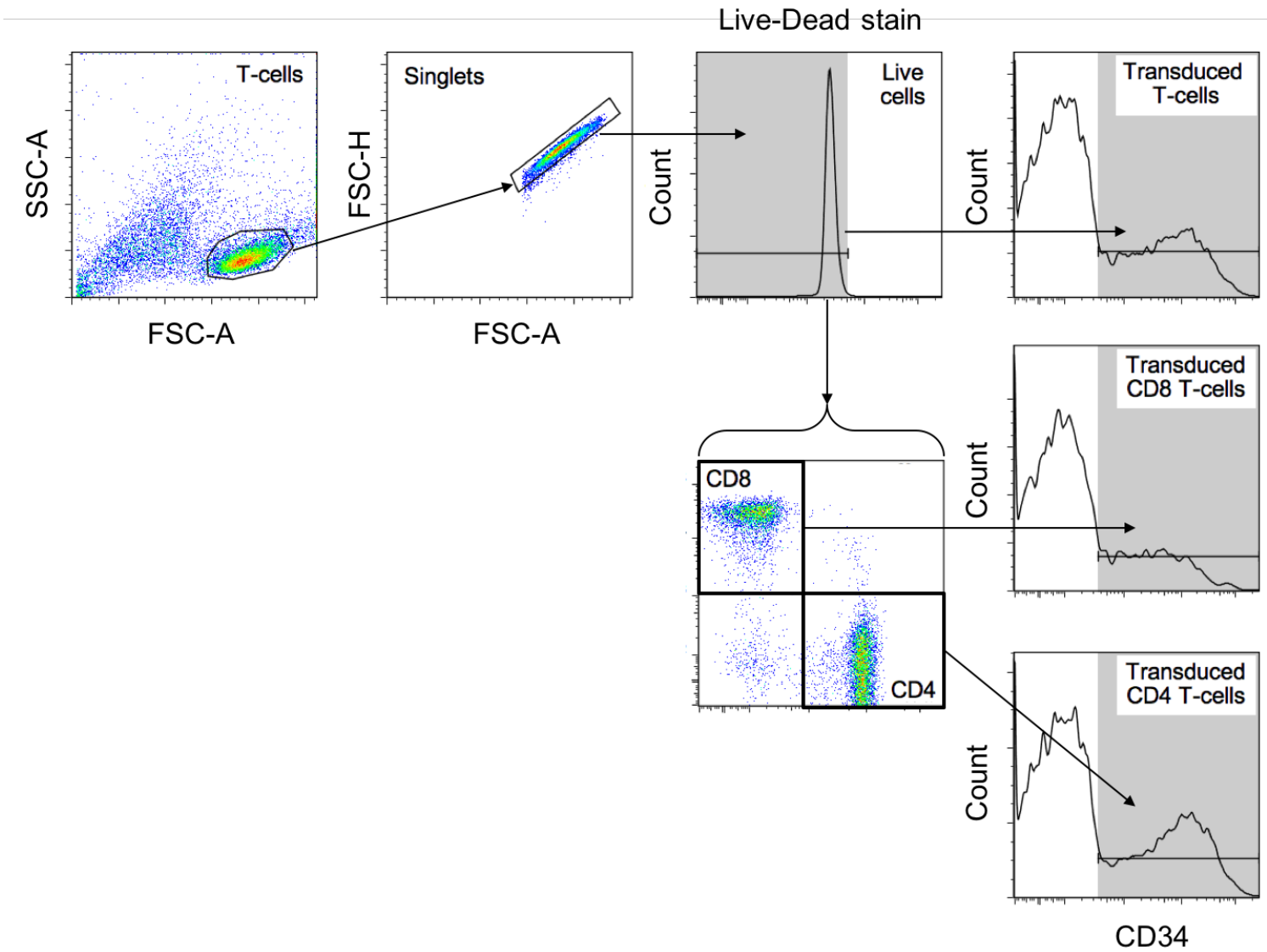
Live-Dead stain
T-cells
SSC-A
FSC-A
Singlets
FSC-H
FSC-A
Count
Live cells
Count
Transduced T-cells
CD8
CD4
Count
Transduced CD8 T-cells
Count
Transduced CD4 T-cells
CD34

Figure 3.1 – T-cell gating strategy to identify CAR transduction levels of bulk T-cell populations and their CD8 and CD4 subsets

L1, L2, L3, L5 and 1D2 CAR T-cells and mock T-cell controls were labelled with viability dye, anti-CD8, anti-CD4 and anti-CD34 antibodies and analysed on the flow cytometer, with CD34 acting as a surface marker of CAR expression. After gating on the T-cell population, singlets (to exclude cell clumps) and live cells (viability dye-negative) sequentially, mock T-cells were used to determine the position of the CD34-negative population and thus allow correct positioning of the CD34 gate. In the CAR T-cell populations, the bulk T-cells within this gate were considered CAR-positive. Live T-cells were also further analysed for CD8 and CD4 expression, and each T-cell subset also examined for CAR transduction in the same way.

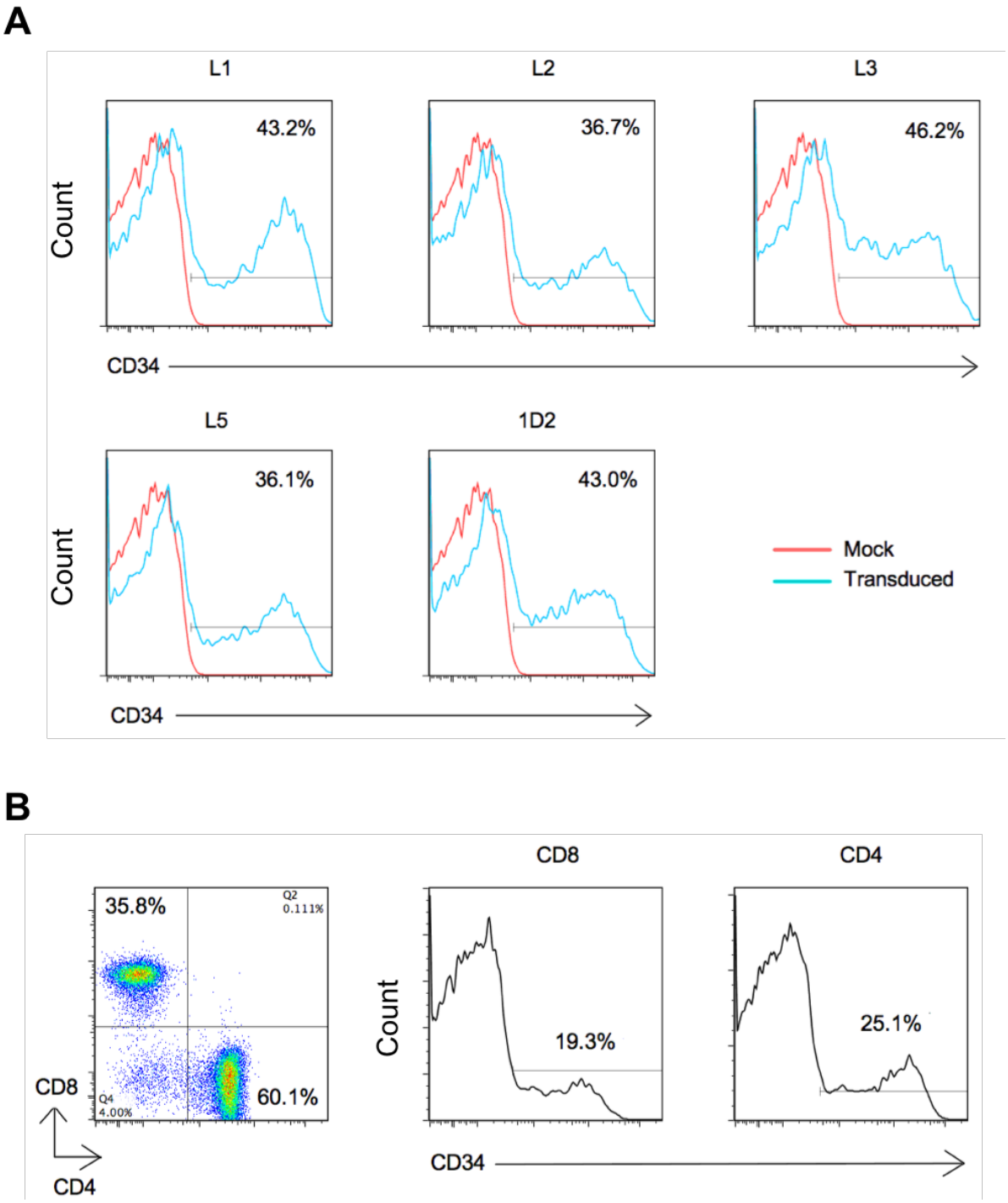

Figure 3.2 – Representative CAR transduction levels in bulk T-cell populations and their CD8 and CD4 subsets

L1, L2, L3, L5 and 1D2 CAR T-cells and mock T-cell controls were labelled with viability dye, anti-CD8, anti-CD4 and anti-CD34 antibodies and analysed on the flow cytometer, with CD34 acting as a surface marker of CAR expression. **(A)** Histograms showing representative CAR transduction levels for each of the five CARs (blue line), gated based on the mock T-cell population (red line). **(B)** L5 CAR T-cells derived from a

different donor to the one in A, showing a representative breakdown of CD8 and CD4 populations and their respective CAR transduction levels. The overall CAR transduction of the bulk T-cell population was 22.7%. Data in A and B are representative of 14 different donors.

Table 3.1 – The half maximum concentrations (EC_{50}) of five anti-TEM8 Fabs needed to bind recombinant human or mouse TEM8 extracellular domain (ED)

EC_{50} (nM) for binding of anti-TEM8 Fabs to recombinant TEM8-ED by ELISA

	L1	L2	L3	L5	1D2
hTEM8	0.18	0.24	0.33	0.24	7.6
mTEM8	0.21	0.28	0.36	0.22	31.2

Reprinted from Cancer Cell, 21(2), Chaudhary A, Hilton MB, Seaman S, Haines DC, Stevenson S, Lemotte PK, et al, TEM8/ANTXR1 blockade inhibits pathological angiogenesis and potentiates tumoricidal responses against multiple cancer types, 212-26, Copyright (2012), with permission from Elsevier[246].

3.2 TEM8 CAR T-cells produce multiple cytokines in response to target cells

Upon successful transduction, TEM8 CAR T-cells and their mock T-cell controls were tested for response to various targets through a series of functional assays. In a preliminary ELISA, mock, L1 and L2 CAR T-cells were analysed for their IFNγ release in the presence of CHO cells stably overexpressing human TEM8 on their surface (CHO-TEM8), and CHO-PR230, a spontaneous TEM8-deficient mutant of CHO cells[309] that served as the TEM8-negative control. While a strong response to CHO-TEM8 was observed for both CARs, an unexpectedly high T-cell response was also seen in the presence of CHO-PR230 (**Figure 3.3A**). To ascertain whether this occurrence was limited to CHO cells, the experiment was repeated with the introduction of two further unrelated targets – Phoenix A[304] (derived from HEK293T cells) and HUVEC. Once again, both L1 and L2 CAR T-cells responded strongly to all target cells, with the highest IFNγ release still observed in the presence of CHO-TEM8 (**Figure 3.3B**). The fact that mock T-cells released little or no IFNγ throughout suggested that this unexpected cross-reactivity was a feature of CAR T-cells alone.

Next, all five CAR T-cells were tested for IFNγ release in response to a range of different target cells once more. The response pattern consistently observed in all the repeats of this IFNγ ELISA is shown in a representative graph in **Figure 3.4A**. All CARs showed specific responses to CHO-TEM8 compared to those seen to CHO-PR230. Nevertheless, L1 and L2 CAR T-cells, as before, responded to all targets (including CHO-PR230), with especially high IFNγ levels released in the presence of HUVEC. L3 and L5 CAR T-cells did not exhibit background responses to CHO-PR230 but still responded to everything else, with the L3 CAR showing higher levels of cross-reactivity

to HUVEC compared to L5. The only CAR to respond solely to its intended TEM8-positive target, CHO-TEM8, was 1D2. It repeatedly released IFNγ in significant amounts only in the presence of this hTEM8-overexpressing cell line, with its responses to the other targets comparable to the low-level background response seen in mock T-cells. Consistent with the lower TEM8 affinity of the 1D2 antibody this CAR is derived from[246], however, it was also the least strong responder to CHO-TEM8 of all the CARs tested. In an attempt to find the cause of the cross-reactivity in the remaining four CARs, the T-cells were also tested for response to CHO cells stably overexpressing human CMG2 – the closest TEM8 homologue which has a much wider tissue distribution[229] – on their surface. However, none of the CAR T-cells released any significant amounts of IFNγ when exposed to this cell line, showing that the responses to the other targets were not due to cross-reactivity with CMG2 (**Figure 3.4B**).

As the most selective TEM8 CAR, 1D2 warranted further investigation of its responses to other target cells. It was therefore tested in another IFNγ ELISA together with the least cross-reactive of the other CARs, L5. In addition to the target cells tested before, two more were included – MDA-MB-231, a breast adenocarcinoma cell line previously shown to express low levels of TEM8 *in vitro*[246], and the colorectal carcinoma cell line LS174T which was TEM8-negative[246]. In accordance with this, neither L5 nor 1D2 CAR T-cells responded to LS174T, but interestingly, only L5 CAR T-cells exhibited IFNγ release in the presence of MDA-MB-231 (**Figure 3.5**). In the case of the 1D2 CAR, there was no response to these cells above background, indicating that this CAR may

only recognise and respond to overexpressed TEM8 rather than lower levels of the protein that may be present on the surface of the other targets.

To examine the release of other pro-inflammatory cytokines by TEM8 CAR T-cells when exposed to target cells, an intracellular cytokine release assay was performed to test for the proportions of each T-cell population that secreted TNFα, IFNγ and/or IL-2. A sample of the obtained flow data is shown in **Figure 3.6** and the cumulative data for all CAR T-cells are presented in **Figure 3.7**. The pattern observed in the IFNγ ELISA was repeated here – L1 and L2 CAR T-cells were the highest responders and secreted one, two or all three cytokines in the presence of all targets apart from the TEM8-negative LS174T. Particularly high responses were once again observed in the presence of HUVEC. A similar pattern was seen in L3 and L5 CAR T-cells but with reduced T-cell proportions secreting each cytokine or cytokine combination, reflecting their lower reactivity compared to the first two CARs. Once again, 1D2 CAR T-cells were the lowest responders to CHO-TEM8, but responded nonetheless; the proportions of these T-cells that exhibited cytokine release when exposed to other targets was low or undetectable. The most commonly secreted cytokine by all activated CAR T-cells was TNFα alone followed by the TNFα/IFNγ combination, although cells secreting all three cytokines were also observed, particularly among the high responders. As before, mock T-cells were not activated by any of the targets, and T-cells alone, whether mock or CAR, mostly secreted single cytokines in very small proportions, confirming that the responses seen were dependent on the presence of TEM8 CARs and the targets that triggered them.

A

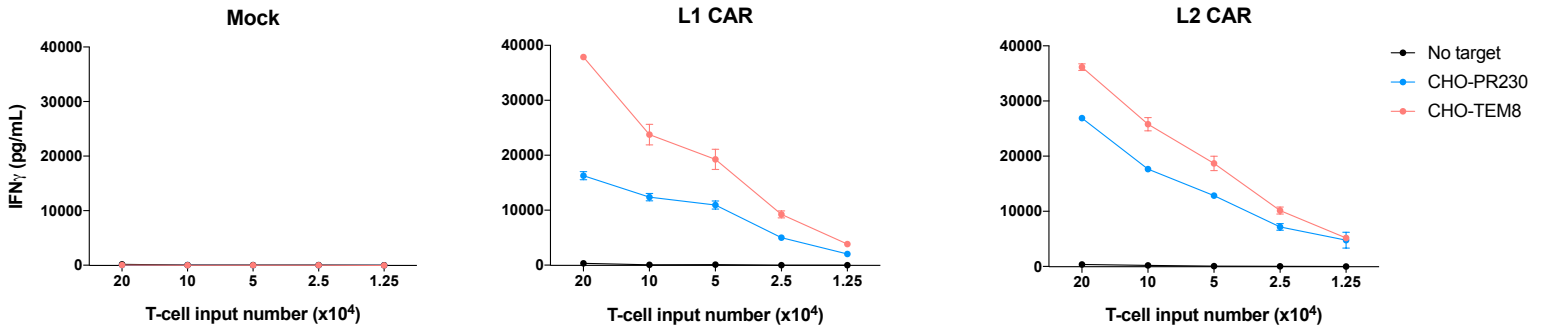
Mock
L1 CAR
L2 CAR
IFNγ (pg/mL)
40000
30000
20000
10000
0
20
10
5
2.5
1.25
T-cell input number (x10⁴)
No target
CHO-PR230
CHO-TEM8

B

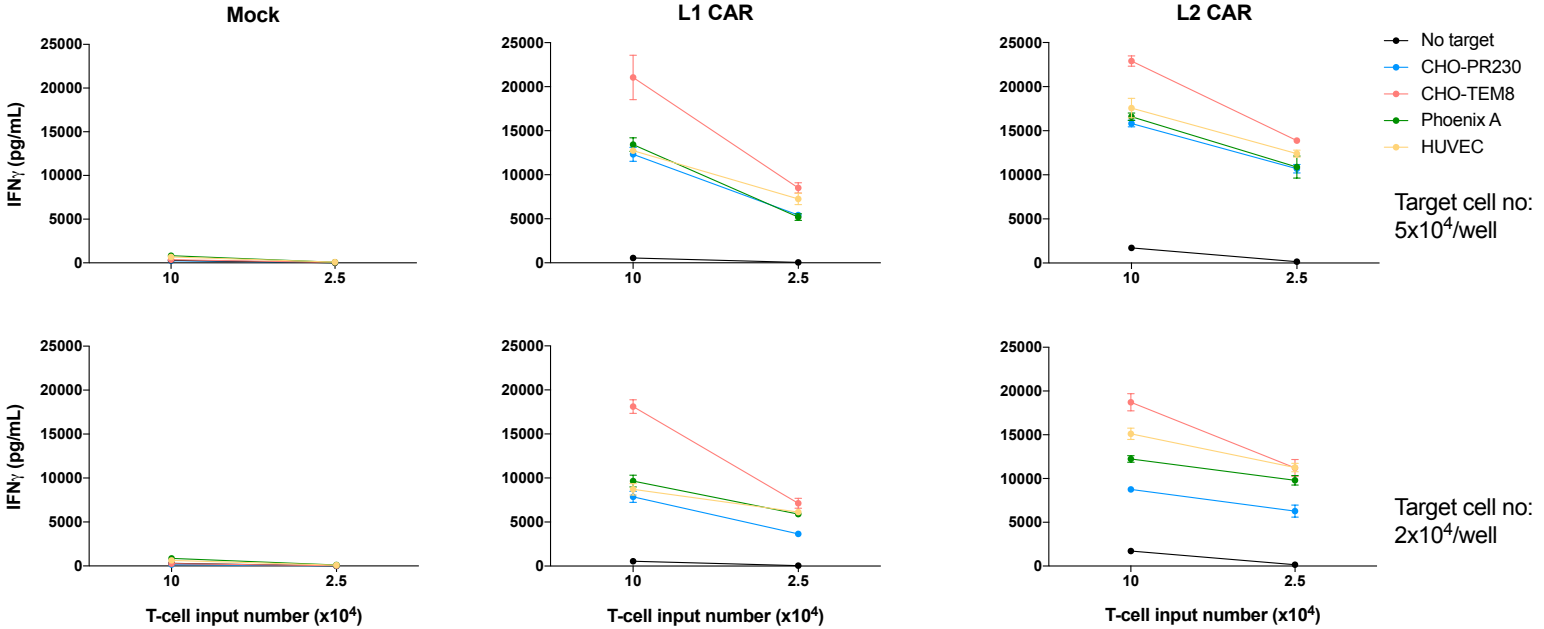
Mock
L1 CAR
L2 CAR
IFNγ (pg/mL)
25000
20000
15000
10000
5000
0
10
2.5
T-cell input number (x10⁴)
No target
CHO-PR230
CHO-TEM8
Phoenix A
HUVEC
Target cell no: 5x10⁴/well
Target cell no: 2x10⁴/well

Figure 3.3 – IFNγ release of L1 and L2 CAR T-cells at decreasing input numbers in response to target cells
Mock, L1 or L2 CAR-transduced T-cells at the indicated input numbers/well were incubated overnight with **(A)** CHO-PR230 or CHO-TEM8 ($5x10^4$ cells/well) or **(B)** CHO-PR230, CHO-TEM8, Phoenix A or HUVEC at high ($5x10^4$ cells/well) or low ($2x10^4$ cells/well) target cell concentration in a 96-well plate. T-cells alone were included as a control. Supernatants were assayed by IFNγ ELISA the following day and the resulting T-cell IFNγ production expressed in pg/mL. Data in A are representative of two independent experiments. All data points were measured in triplicate and expressed as mean ± SD.

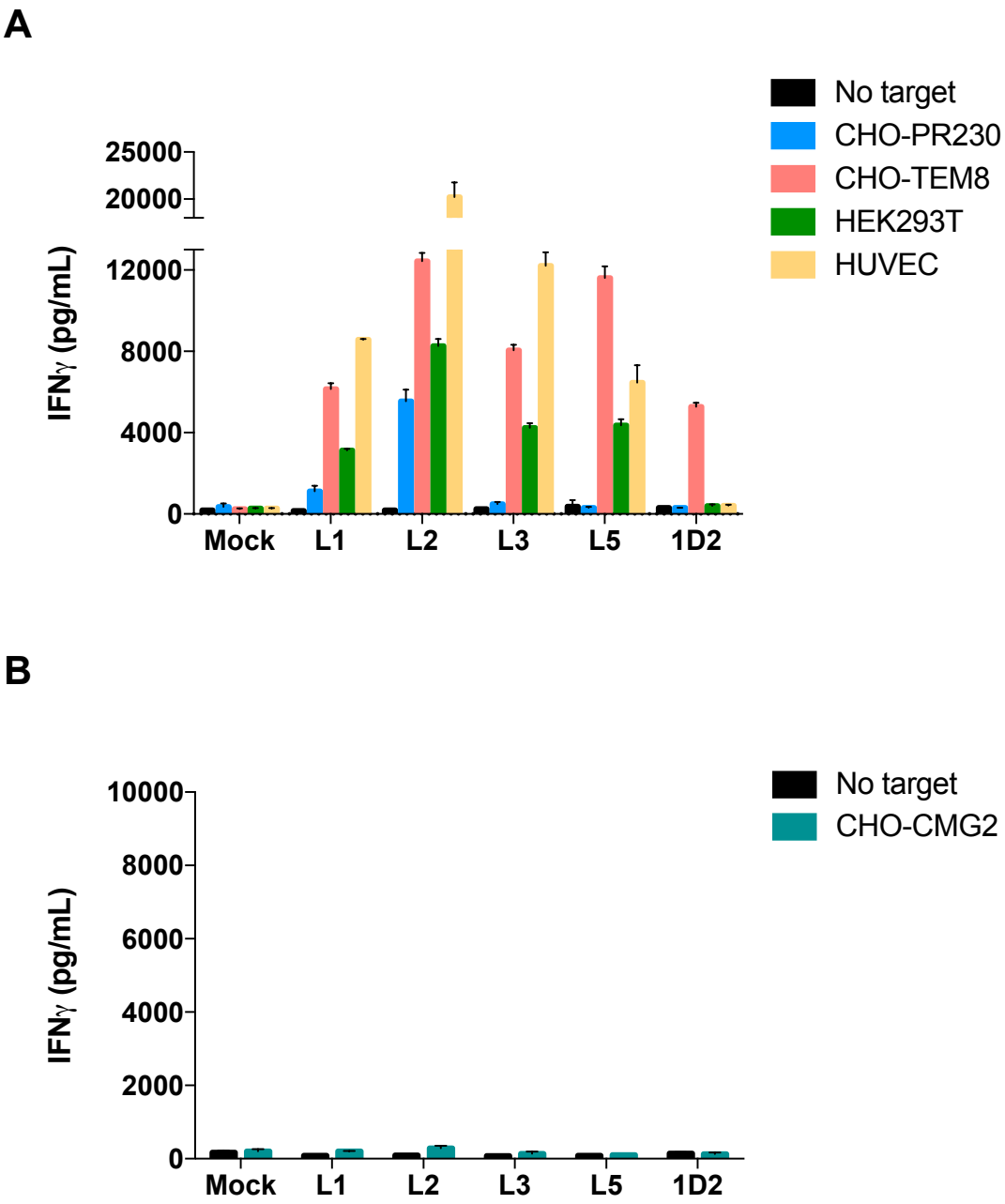

Figure 3.4 – TEM8 CAR T-cell IFNγ release in response to target cells
(A) Mock or TEM8 CAR-transduced T-cells ($5x10^4$ cells/well) were incubated alone or with indicated target cells ($2x10^4$ cells/well) in a 96-well plate overnight. Supernatants were assayed by IFNγ ELISA the following day and the resulting T-cell IFNγ production expressed in pg/mL. Data are representative of 14 independent experiments using T-cells derived from 10 different donors. All data points are measured in triplicate and expressed as mean + SD. **(B)** Mock or TEM8 CAR-transduced T-cells ($2x10^5$ cells/well; different donor to the one in A) were incubated alone or with CHO-CMG2 ($2x10^4$ cells/well) in a 96-well plate overnight and assayed as in A. All data points were measured in triplicate and expressed as mean + SD.

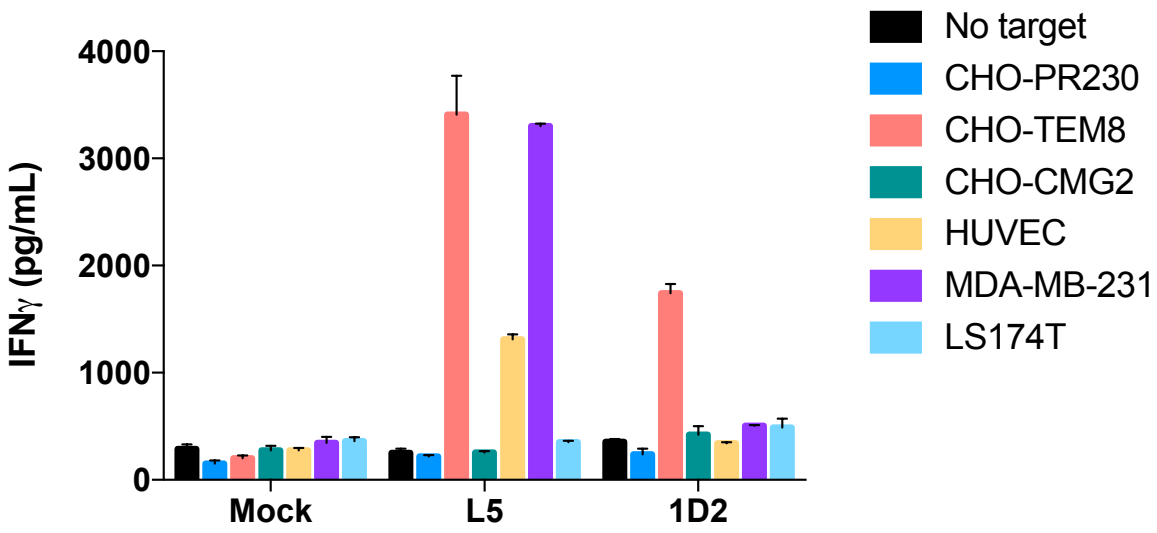

Figure 3.5 – Mock, L5 and 1D2 CAR T-cell IFNγ release in response to target cells
Mock, L5 or 1D2 CAR-transduced T-cells ($2x10^5$ cells/well) were incubated alone or with indicated target cells ($2x10^4$ cells/well) in a 96-well plate overnight. Supernatants were assayed by IFNγ ELISA the following day and the resulting T-cell IFNγ production expressed in pg/mL. All data points were measured in triplicate and expressed as mean + SD.

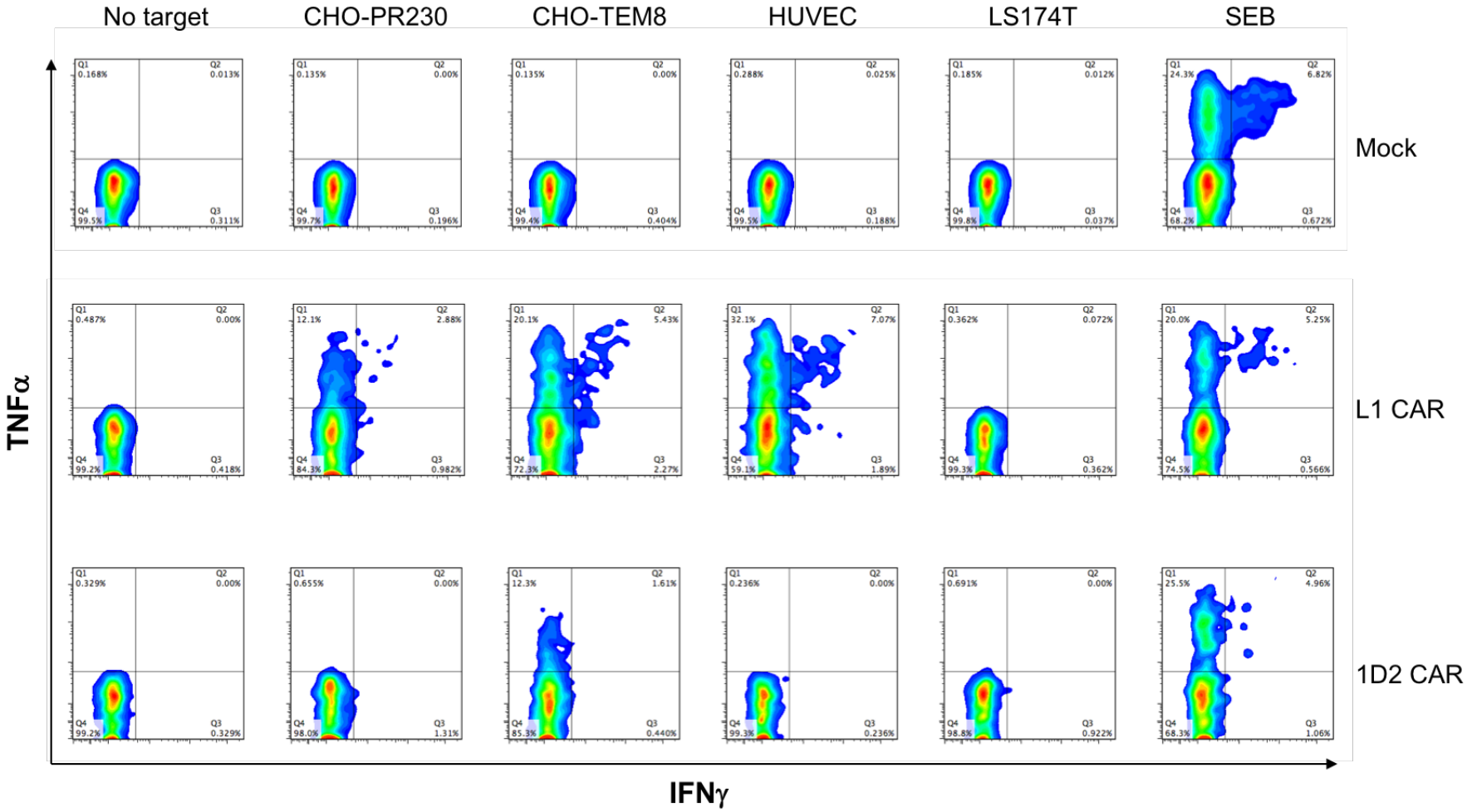

Figure 3.6 – Sample intracellular cytokine release flow data from mock and two TEM8 CAR T-cell products
Mock or TEM8 CAR-transduced T-cells were incubated alone or with indicated target cells (all at $5x10^5$ cells/well) in a 48-well plate overnight. T-cells stimulated non-specifically with the superantigen Staphylococcal enterotoxin B (SEB) were included as

a positive control. The next day the T-cells were harvested, stained with anti-CD34 surface antibody and anti-TNFα, anti-IFNγ and anti-IL-2 intracellular antibodies and analysed on the flow cytometer. Gate thresholds were set using unstimulated T-cells and fluorescence minus one controls. Data show sample TNFα vs IFNγ flow plots of mock, L1 and 1D2 CAR T-cells pre-gated on $CD34^+$ T-cell singlets (or only T-cell singlets in the case of mock T-cells). Data are representative of two independent experiments.

A

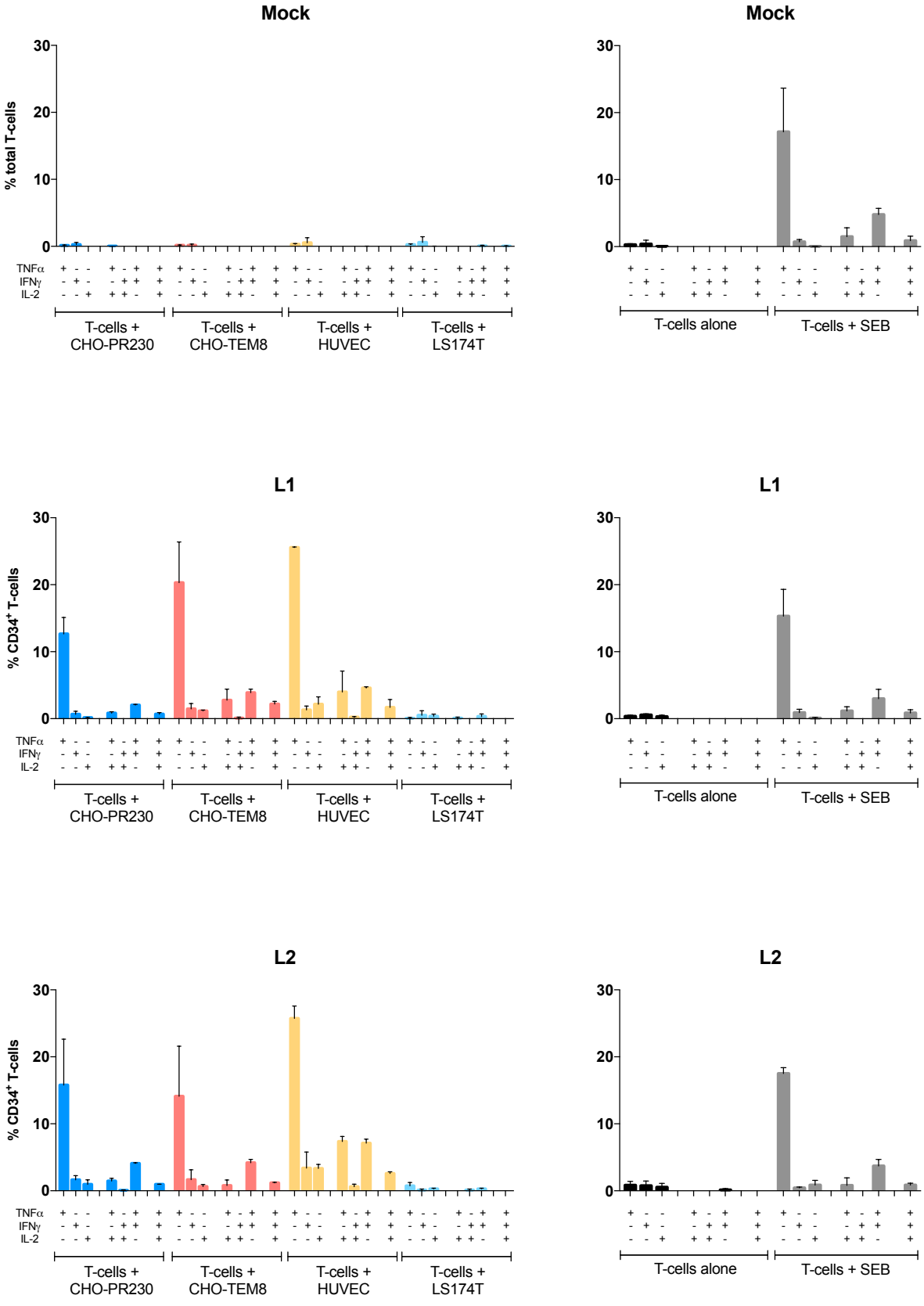
Mock
Mock
% total T-cells
30
20
10
0
TNFα
IFNγ
IL-2
T-cells + CHO-PR230
T-cells + CHO-TEM8
T-cells + HUVEC
T-cells + LS174T
T-cells alone
T-cells + SEB
L1
L1
% CD34+ T-cells
L2
L2

B

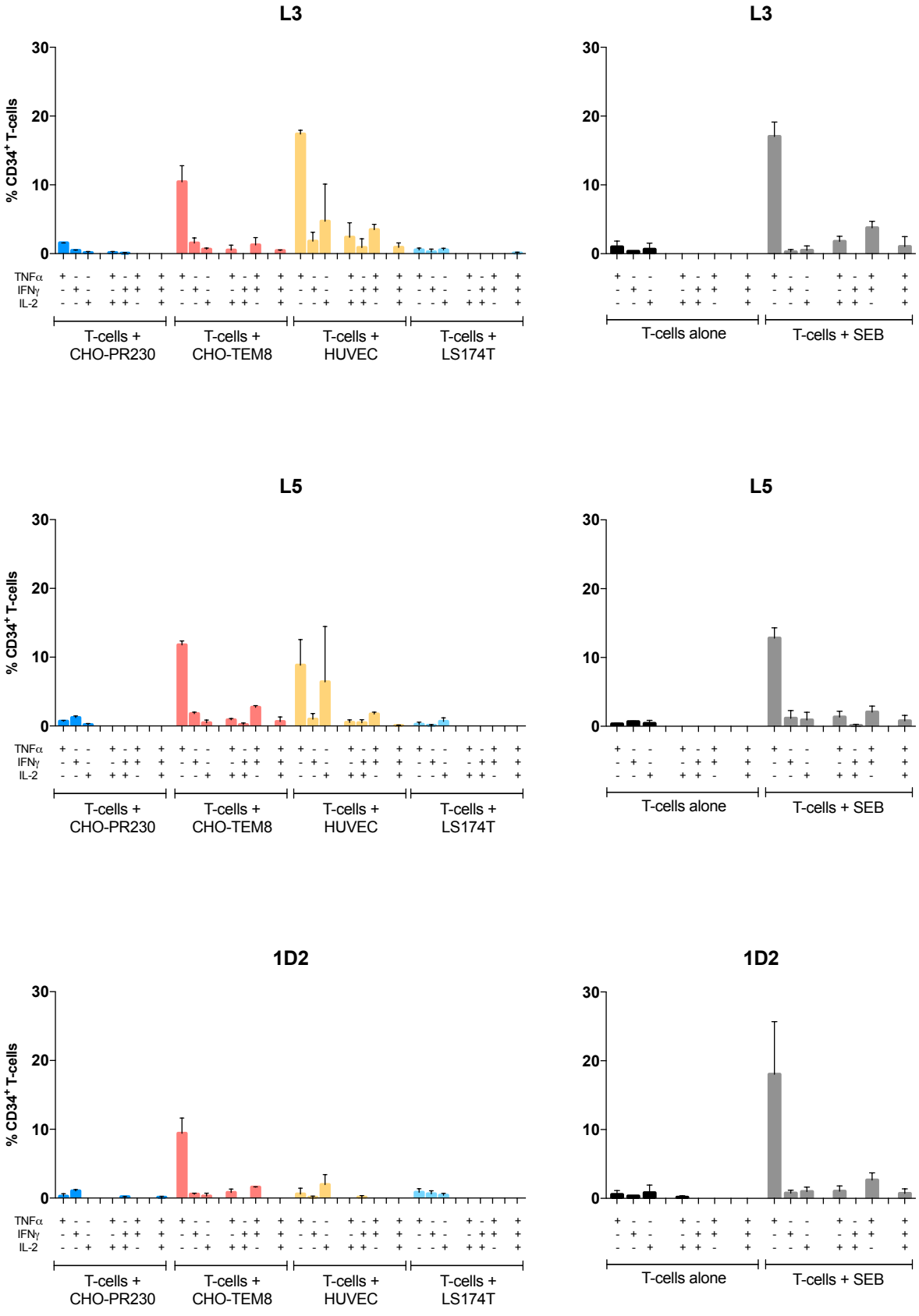
L3
L3
L5
L5
1D2
1D2
% CD34+ T-cells
30
20
10
0
TNFα
IFNγ
IL-2
T-cells + CHO-PR230
T-cells + CHO-TEM8
T-cells + HUVEC
T-cells + LS174T
T-cells alone
T-cells + SEB

Figure 3.7 – Multiple cytokine release by TEM8 CAR T-cells in response to target cells

Mock or TEM8 CAR-transduced T-cells were incubated alone or with indicated target cells (all at $5x10^5$ cells/well) in a 48-well plate overnight. T-cells stimulated non-specifically with the superantigen Staphylococcal enterotoxin B (SEB) were included as a positive control. The next day the T-cells were harvested, stained with anti-CD34 surface antibody and anti-TNFα, anti-IFNγ and anti-IL-2 intracellular antibodies and analysed on the flow cytometer. Gate thresholds were set using unstimulated T-cells and fluorescence minus one controls. Data are represented as the proportion of mock or $CD34^+$ T-cells secreting one, two or all three cytokines for **(A)** mock, L1 and L2 and **(B)** L3, L5 and 1D2 CAR T-cells. Data are cumulative from two independent experiments and expressed as mean + SD.

3.3 TEM8 CAR T-cells proliferate in response to target cells

To test antigen-specific proliferation of TEM8 CAR T-cells, they were labelled with CFSE dye and incubated with their targets for four days after which CFSE expression was assayed by flow cytometry. Sequential dilution of the dye induced by cell division allowed the shift of the signal from bright to dim to serve as a direct measure of cell proliferation, and CAR-positive ($CD34^+$) and non-transduced ($CD34^-$) subsets of each T-cell population were analysed separately to gain a better understanding of CAR-specific antigen-dependent responses. The proliferation patterns of two distinct batches of TEM8 CAR T-cells and their mock controls are shown in **Figure 3.8** and **Figure 3.9**, segregated due to the difference in target cells tested and the presence of significant background T-cell proliferation in one of them. The overall pattern of CAR T-cell responses, however, was very similar to the one observed before. Mock T-cells alone or in the presence of targets did not proliferate, or else showed background proliferation consistent with all CAR T-cells produced in that batch. L1 and L2 CARs were yet again the most cross-reactive ones, exhibiting high responses to CHO-TEM8 as well as to HUVEC, MDA-MB-231 and the control cell line CHO-PR230, but not to the TEM8-negative LS174T cells. The responses of L3 and L5 CAR T-cells were mostly equivalent to those of mock T-cells in the presence of CHO-PR230, but significantly higher to all other target cells except LS174T. 1D2 CAR T-cells were once more the only ones to exhibit selectivity, with CHO-TEM8 being the sole target to elicit consistently high proliferation in this T-cell population.

The response pattern described above was mostly confined to the $CD34^+$ fraction of all TEM8 CAR T-cells, with the $CD34^-$ T-cell populations presenting low or background-

level proliferation regardless of the target they were exposed to. Certain responses were higher than expected in $CD34^+$ T-cells, however, such as the low but noticeable proliferation to CHO-PR230 in L3, L5 and 1D2 CARs, and to MDA-MB-231 and HUVEC in 1D2 CAR T-cells (Figure 3.8). Additionally, some of the $CD34^-$ T-cells exhibited what looked like the usual target-specific response patterns even though they did not express the TEM8 CARs on their surface (Figure 3.8 and Figure 3.9). On closer inspection, however, these unexpected observations were all confined to the CD8 T-cell compartment, which appeared both much more reactive in general than its CD4 counterpart, and accounted for most of the high background proliferation seen in one of the CAR T-cell batches. It is possible that the production of cytokines by $CD34^+$ T-cells in response to antigen led to a bystander effect in $CD34^-$ cells, causing them to proliferate as well; this effect seemed to be much more pronounced in the highly reactive CD8 T-cell subset. The complete absence of antigen-specific responses in the CD4 $CD34^-$ T-cells, and their clear presence in the $CD34^+$ ones, suggest that TEM8 CAR T-cells do indeed respond to their target in a manner dependent on both CAR and target antigen expression.

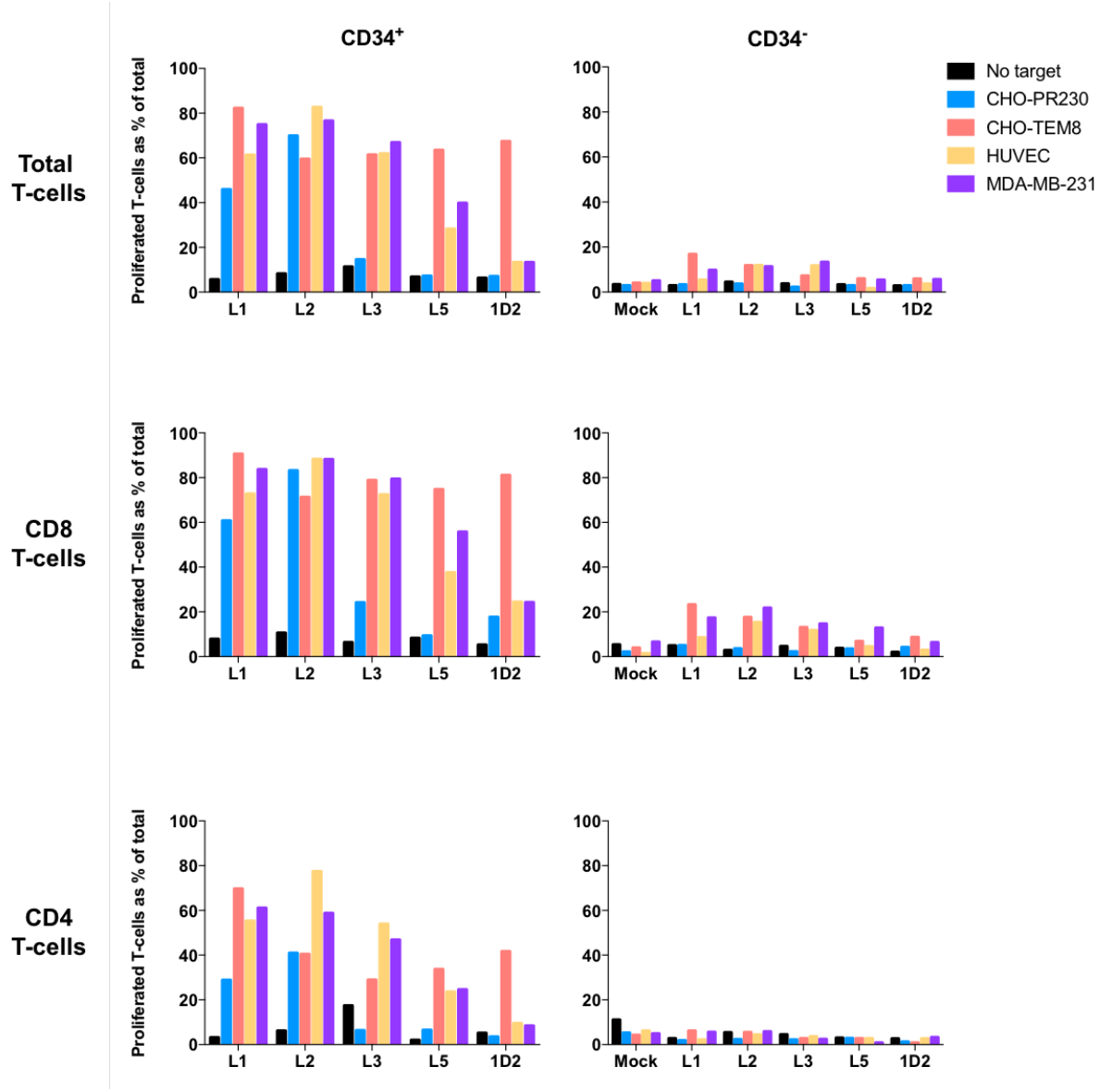

Figure 3.8 – Antigen-specific proliferation of one batch of TEM8 CAR T-cells in response to target cells

Mock or TEM8 CAR-transduced T-cells ($3x10^5$ cells/well) were labelled with CFSE intracellular dye and incubated alone or with indicated target cells ($2x10^4$ cells/well) in a 96-well plate for four days. On day 4 the T-cells were harvested, labelled with anti-CD8, anti-CD4 and anti-CD34 antibodies and analysed by flow cytometry. CFSE-bright mock T-cells were used to correctly position the CFSE-dim proliferation gate – sequential dilution of the dye induced by cell division allowed the shift of the signal from bright to dim to serve as a direct measure of T-cell proliferation. The proportion of T-cells shifting into the CFSE-dim gate was considered to be the proportion of the total $CD34^+$ or $CD34^-$ T-cell population that had proliferated. The bulk, CD8 and CD4 CAR T-cell subsets were each analysed for CD34 expression and proliferation separately.

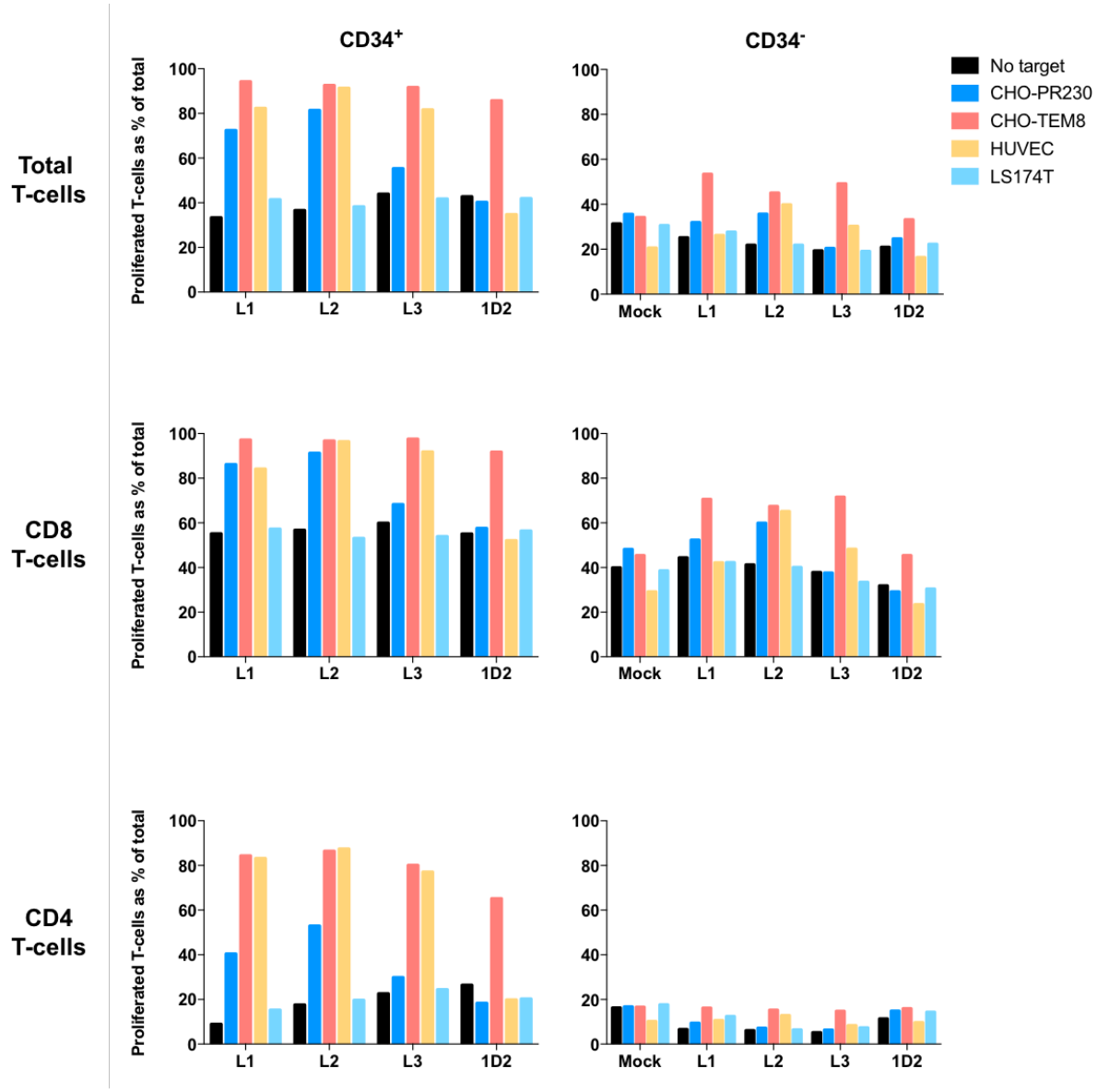

Figure 3.9 – Antigen-specific proliferation of a second batch of TEM8 CAR T-cells in response to target cells

Mock or TEM8 CAR-transduced T-cells ($3x10^5$ cells/well) were labelled with CFSE intracellular dye and incubated alone or with indicated target cells ($2x10^4$ cells/well) in a 96-well plate for four days. On day 4 the T-cells were harvested, labelled with anti-CD8, anti-CD4 and anti-CD34 antibodies and analysed by flow cytometry. The bulk, CD8 and CD4 CAR T-cell subsets were each analysed for CD34 expression and CFSE expression/proliferation separately, as described in Figure 3.8. L5 CAR T-cells did not transduce successfully in this T-cell batch and were therefore not analysed. Data are representative of two independent experiments.

3.4 TEM8 CAR T-cells show specific cytotoxicity in response to target cells

As a final *in vitro* examination of TEM8 CAR T-cell responses to their targets, the target cells were labelled with ^{51}Cr radionuclide and co-cultured with the T-cells; the amount of chromium released from the lysed target cells into the supernatant was a direct measure of T-cell-mediated killing. The pattern observed in all the previous functional assays was once more recapitulated here, and is shown in **Figure 3.10**. All TEM8 CAR T-cells specifically lysed CHO-TEM8, with L1 and L2 also exhibiting significant killing of CHO-PR230; all but 1D2 CAR T-cells also lysed HUVEC. In contrast, there was no specific T-cell cytotoxicity in response to LS174T, as evidenced by the lysis of this cell line being comparable in the presence of both mock and CAR T-cells. This response pattern was consistently observed in repeated chromium release assays. Taken together with the data from previous functional experiments, it confirmed the marked TEM8-specific responses and significant cross-reactivity of L1 and L2 CARs, slightly lower cross-reactivity of L3 and L5 CARs, and the specificity of 1D2 CAR T-cells for the overexpression of the target that is only present on CHO-TEM8.

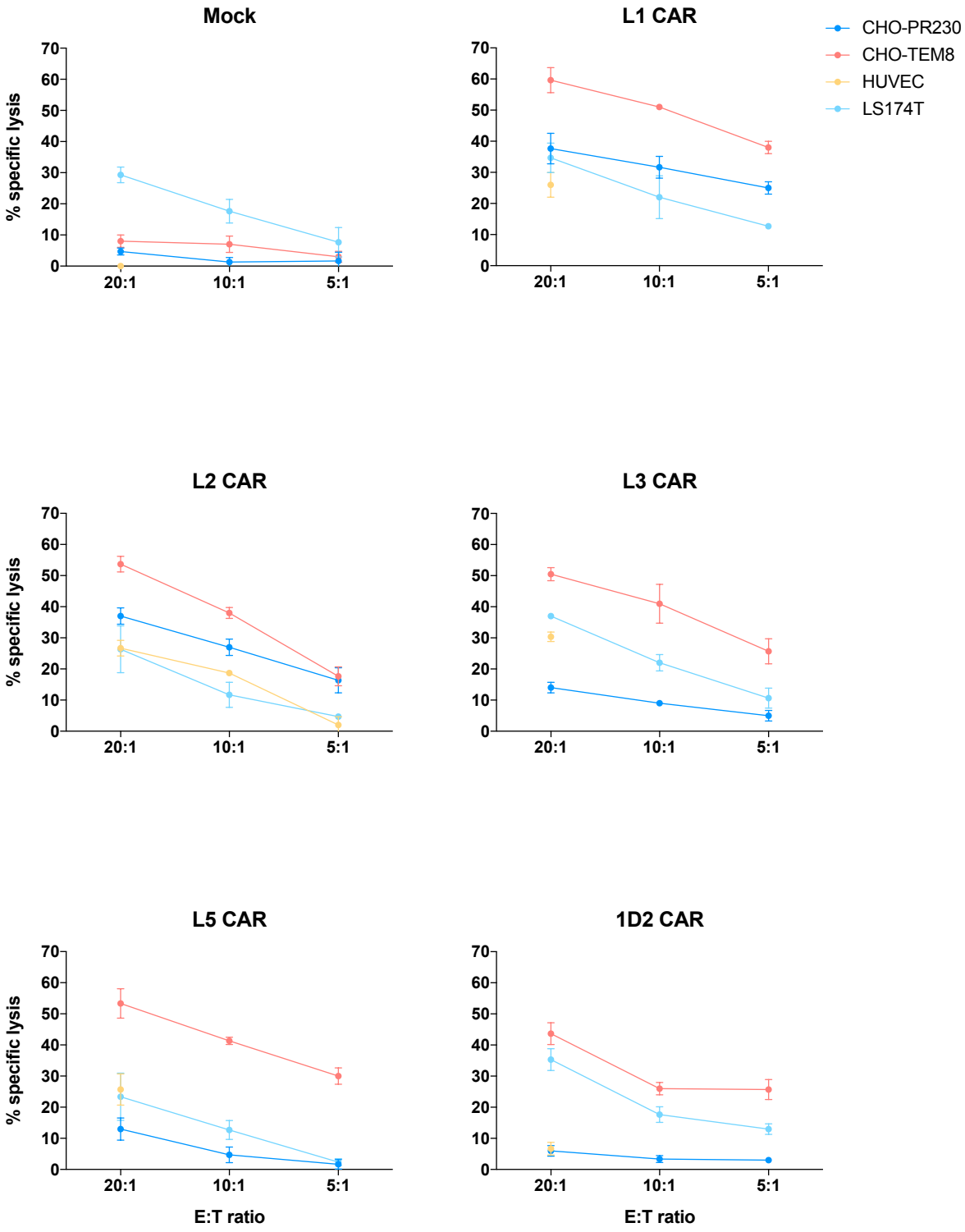

Figure 3.10 – Specific cytotoxicity of TEM8 CAR T-cells in response to target cells

Mock or TEM8 CAR-transduced T-cells were incubated at decreasing effector:target (E:T) ratios with indicated chromium-labelled target cells ($2.5x10^3$ target cells/well of a 96-well plate), and supernatants harvested and analysed for released chromium after

12 hours. % specific lysis for each target was calculated from spontaneous (targets alone) and maximum lysis values (targets incubated with 1% sodium dodecyl-sulphate). Note: in this particular experiment there were enough HUVEC cells to test only the highest E:T ratio for each of the T-cells, except L2 CAR T-cells where all ratios were assessed. Data are representative of four independent experiments using T-cells derived from three different donors. All data points were measured in triplicate and expressed as mean ± SD.

3.5 TEM8 expression on target cells and CAR T-cell cross-reactivity

The persistent *in vitro* cross-reactivity of four of the five TEM8 CAR constructs to cell lines other than their intended target, CHO-TEM8, warranted further investigation of such CAR T-cell behaviour. All the target cell lines tested were therefore examined for human TEM8 mRNA expression by qPCR (**Figure 3.11**). As expected, hTEM8 mRNA was clearly overexpressed in CHO-TEM8, but none was detectable in CHO-PR230 or CHO-CMG2. Interestingly, however, HEK293T, HUVEC and MDA-MB-231 cells all expressed very small, but detectable levels of hTEM8 mRNA, suggesting that TEM8 protein expression could also be present on the surface of these targets. LS174T cells did not exhibit any TEM8 mRNA expression, which correlated with their previously observed inability to elicit specific CAR T-cell responses.

To supplement the obtained data and verify expression of the TEM8 protein on the target cell surface, the cells were stained using the same L2 mAb which had been used to make the L2 CAR (the staining procedure is described in section 2.5.1). The results of L2 staining are shown in **Figure 3.12**. Consistent with the qPCR data, TEM8 was highly expressed on the surface of CHO-TEM8, and present at extremely low levels or completely undetectable on CHO-PR230 and LS174T cells. HEK293T and MDA-MB-231 cells did stain with the L2 antibody, despite the very low hTEM8 mRNA levels present in these targets, possibly indicating that their surface expression of the protein was very stable. Curiously, however, the surface levels of TEM8 on HUVEC detected by the L2 mAb were extremely low.

Taken together, these results could at least partly explain the T-cell cross-reactivity consistently observed *in vitro*, such as the responses seen to HEK293T and MDA-MB-231 and the lack of response to LS174T. However, they still failed to clarify the very high reactivity of L1 and L2 CAR T-cells to CHO-PR230, a cell line that appeared to be completely TEM8-negative, as well as the potent responses of all but 1D2 CAR T-cells to HUVEC, which did not express TEM8 on their surface to any appreciable degree. These responses would therefore need to be discussed in more depth in order to elucidate their impact on further TEM8 CAR T-cell studies.

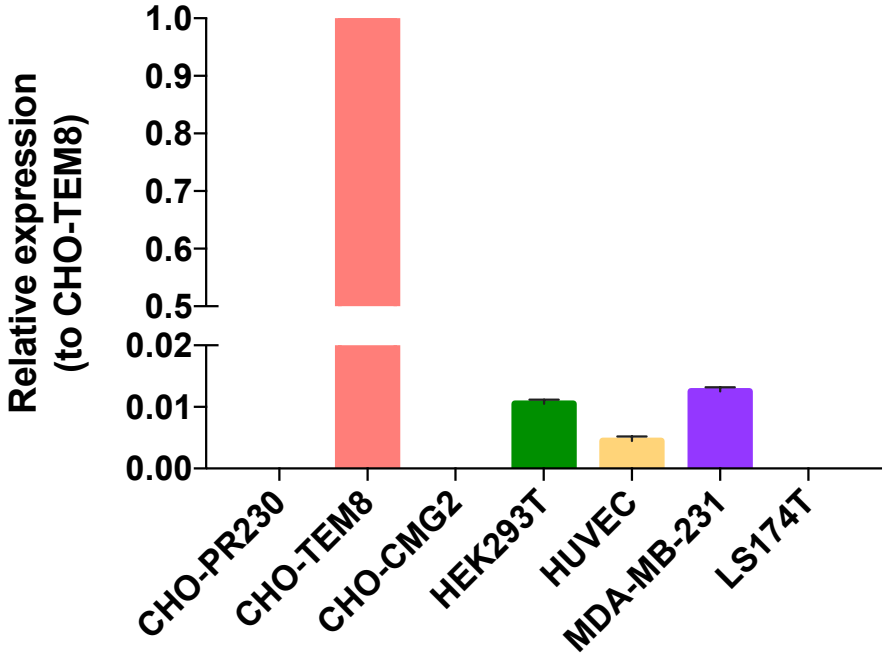

Figure 3.11 – Relative hTEM8 mRNA expression of target cells used in T-cell functional assays

Cell lysates from indicated target cells were examined by qPCR for their expression of hTEM8 mRNA. The mRNA expression levels are shown relative to those obtained for CHO-TEM8, which were assigned the value of 1. All data points were measured in duplicate and expressed as mean + SD.

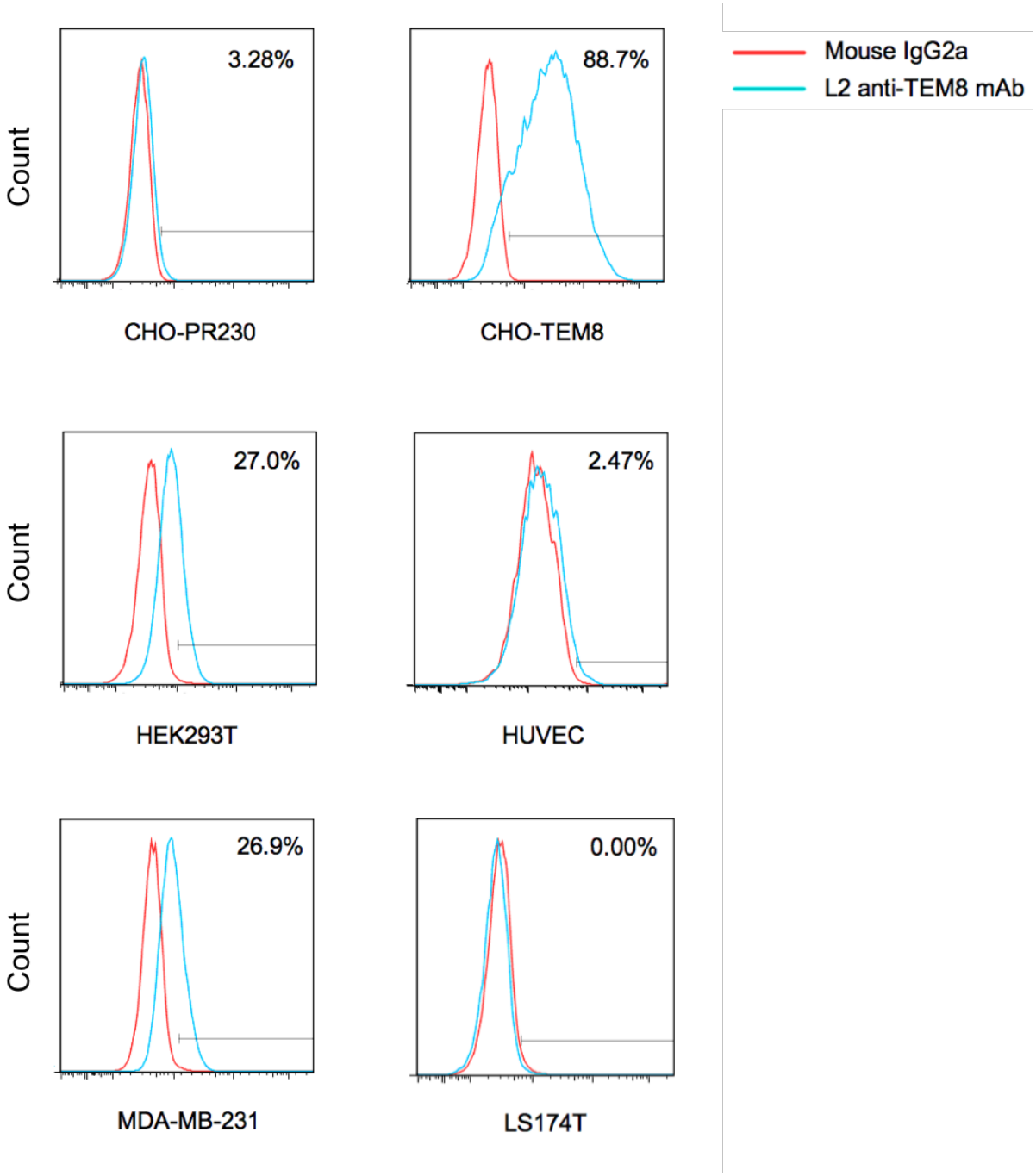

Figure 3.12 – TEM8 protein expression on the surface of target cells used in T-cell functional assays

Indicated target cells were labelled with the primary L2 anti-TEM8 mAb (chimeric antibody with mouse IgG2a constant domain and human variable regions; blue line), or with the primary mouse IgG2a isotype control (red line), before being labelled further with the secondary fluorophore-conjugated anti-mouse IgG. TEM8 expression on the cells was then assayed by flow cytometry. Data are representative of three independent experiments.

3.6 Discussion

This chapter describes the generation of five TEM8-targeted CARs and the successful transduction of human T-cells with each one, resulting in potent TEM8-redirected CAR T-cells which release multiple cytokines, proliferate and exhibit specific lysis in response to TEM8-expressing target cells. However, four of the five CARs – derived from the L1, L2, L3 and L5 anti-TEM8 mAbs – also exhibit significant levels of reactivity to control cell lines, some of which do not express detectable levels of the target protein on their surface. The only CAR that consistently responds solely to the CHO cells that were engineered to overexpress TEM8 is 1D2. This is consistent with the fact that this CAR, when expressed in T-cells, showed the lowest avidity for TEM8, which is in turn consistent with the antibody upon which the CAR was based having the lowest affinity for the protein. The reactivity and response patterns of the five TEM8-targeted CARs will be discussed later, but initially the discussion will focus on the methods available for generating CAR expressing T-cells.

3.6.1 CAR T-cell generation methods

Retroviral transduction is a well-established method of T-cell genetic engineering. The MP71 retroviral vector, which forms the basis of all CAR expression constructs in this thesis, has previously proven superior to alternative vectors in producing highly stable gene expression in both murine and human T-lymphocytes[310]. Initially, there were concerns over the use of such viral vectors due to reports of retroviral gene transfer in the treatment of patients with X-linked severe combined immunodeficiency (SCID) that resulted in insertional oncogenesis and development of T-cell leukaemia[311]. However, while gene transfer into stem cells used to treat these patients carried a high risk of T-

cell leukaemia/lymphoma development, it was subsequently shown in mice that mature T-cells are much less susceptible to insertional mutagenesis, with mice subjected to engineered T-cell transplants showing no signs of resultant cancer[312]. In fact, a decade-long follow-up study of human immunodeficiency virus (HIV) patients treated with retrovirally-engineered CAR T-cells demonstrated that the T-cells were safe and exhibited no signs of oncogenesis or immortalisation over time[313]. Even though newer methods of T-cell transduction have been developed in recent years, such as RNA electroporation for transient CAR expression or the Sleeping Beauty transposon/transposase system for efficient and cost-effective DNA integration[174], retroviruses remain one of the mainstays of stable T-cell genetic engineering. It has been suggested that lentiviruses are safer than retroviruses and may achieve higher CAR expression levels, but are currently more expensive to produce. The relatively low cost and proven safety of retroviral vectors has resulted in their routine use for T-cell transduction in this thesis instead.

There is an ongoing debate over the superiority of CD28 or 4-1BB as the co-stimulatory domain of choice in 2nd generation CARs. Greater persistence in the circulation has been reported for 4-1BB/CD3ζ CAR T-cells compared to their CD28-containing counterparts in several clinical trials of CD19 CARs, which could be explained by CD28 co-stimulation leading to increased T-cell exhaustion while 4-1BB ameliorates it instead[314]. It has also been found that the two co-stimulatory domains lead to different T-cell metabolic profiles, with the presence of 4-1BB resulting in increased oxidative respiration and a CD8 central memory phenotype while CD28 led to glycolysis and the development of effector memory T-cells[315]. Despite these findings, both CD28 and 4-

1BB 2nd generation CARs are still in use in equal measure by the labs which study this therapeutic modality[177], and it is likely that the optimal construct will depend on the clinical situation in which it is being employed. The TEM8-targeted CARs described in this thesis include a CD28/CD3ζ domain, which has previously been used successfully by our lab for CARs specific for another TEM, CLEC14A, to mediate safe anti-tumour responses in several mouse models. Due to the established protocol working well, and the finding that CD28/CD3ζ CAR T-cells may possess more potent anti-tumour function and therefore eliminate tumours more quickly than 4-1BB/CD3ζ CARs[166], the former was decided upon as the construct of choice.

Another well-established protocol used herein is the CD3/CD28 stimulation of T-cells prior to transduction, which has been employed in several patient studies to generate large numbers of T-cells with extensive proliferative potential, the ability to persist *in vivo* and potent anti-tumour effects[186,187,316,317]. Furthermore, using bulk populations containing both CD4 and CD8 T-cells for transduction, rather than selecting for a particular T-cell subtype, has been shown to lead to a more potent response to antigen[132,186,187]. The more contentious issue is the subsequent *in vitro* maintenance of CAR-transduced T-cells in the presence of a reasonably high dose of IL-2 (100 IU/mL). Even though this concentration of the cytokine is conducive to higher cell yields and optimal T-cell responses in functional assays, it also drives differentiation into effectors and results in a reduced memory T-cell population, which in turn promotes *in vitro* exhaustion and possibly poorer *in vivo* persistence[318]. The rapid expansion and high functional responses but eventual exhaustion of the generated TEM8 CAR T-cells have all been observed in this thesis, as the T-cells were only likely to give good *in*

vitro reactivity in the first 2-3 weeks post-transduction. To improve this, and promote the development of a memory rather than effector T-cell phenotype in culture, it might be beneficial to reduce maintenance IL-2 concentration in future studies. The suggested dose of IL-2 that gives reasonable cell expansion rates while maintaining T-cell memory is 20-30 IU/mL[318]. Alternatively, expansion of T-cells using cytokines other than IL-2, such as IL-7 or IL-21, has been found to generate a preferred phenotype for their increased persistence[319].

Overall, the molecular cloning and transduction methods employed here were established, safe and predominantly supported by the available literature, ensuring that the final CAR T-cell product was suitable for the studies conducted. If TEM8 CARs were to reach the clinic, however, the methods could be adjusted depending on the clinical situation in question. For example, lentiviral instead of retroviral vectors can be employed for CAR transduction to achieve higher CAR expression levels on T-cell surface, potentially resulting in greater therapeutic efficacy. If toxicity is anticipated, however, RNA electroporation could provide a safer alternative to stable genetic integration as it results only in transient CAR surface expression, ensuring timely disappearance of the CAR T-cell product from the circulation if toxicity does occur. If tumour relapse is a big concern, 4-1BB/CD3ζ CARs may be more desirable due to their superior persistence; conversely, if the tumour has responded poorly after the first CAR T-cell infusion, better responses may be achieved with the CD28/CD3ζ construct due to its greater anti-tumour potency.

3.6.2 The affinities and cross-reactivity of TEM8 CARs

Although there are various ways in which CAR T-cells can be generated for clinical use, before progressing to clinical studies the likely toxicity of any CAR must first be considered. In this regard, the observed responses of four out of five TEM8-specific CARs generated in this project to various cell lines that were not expected to express high levels of TEM8 is a cause for concern. Elucidating the reason for the observed T-cell reactivity, and its physiological importance going forward, is difficult in part because low-level TEM8 expression has been detected in cell lines in culture but not necessarily reflected in the same tissues *in vivo*. For example, certain human colon cancer cell lines express detectable levels of surface TEM8 *in vitro*, possibly as a method of adapting to growth on plastic, but human colon cancer tumour cells have never shown TEM8 expression in an *in vivo* setting (Brad St Croix, personal communication). It is therefore challenging to predict how any *in vitro* TEM8 CAR cross-reactivity may translate to the clinic, but it is nevertheless an important issue to examine with a view to preventing any potential toxicity if patients are treated with this therapy.

In the first instance, it was suspected that engineering the five antibodies into CARs may have inadvertently modified their TEM8 specificity and resulted in recognition of CMG2, the closest TEM8 homologue, even though there was no evidence of CMG2 recognition in the original mAbs[246]. The ubiquitous expression profile of this anthrax toxin receptor[229], unlike the apparently restricted one of TEM8, made it possible that CMG2 was expressed on the surface of the target cell lines used in this thesis, thus triggering CAR T-cell reactivity in their presence. However, when the five TEM8 CARs were tested against a CHO cell line engineered to overexpress human CMG2, no

significant responses were observed (Figure 3.4B and Figure 3.5), rendering it unlikely that the recognition of this protein was accountable for the prominent CAR T-cell reactivity to control cell lines.

Another explanation may be that the more reactive CARs were able to recognise low-level TEM8 expression on target cells. CAR T-cells require lower expression thresholds of their target antigen than the antibodies from which they are derived and are more potent in mediating immune effects, leading to instances of serious adverse events in patients treated with CARs engineered from previously clinically approved antibodies[132,202]. It is possible, therefore, that the four original high-affinity anti-TEM8 mAbs – L1, L2, L3 and L5 – were converted to very potent CARs responsive to exceedingly low levels of surface TEM8 expression. On the other hand, the 1D2 antibody, the affinity of which for human TEM8 was 20-40 times lower in its Fab form than that of the other four antibodies[246] (Table 3.1), gave a CAR which was only capable of recognising overexpression of the target protein such as the one found on CHO-TEM8. In fact, a similar observation was recently made by another group, which found that the different affinities of two anti-EGFR antibodies, cetuximab and nimotuzumab, resulted in very different specificities for the target antigen when the antibodies were converted to 2nd generation CD28/CD3ζ CARs[320]. While both CARs triggered efficient T-cell activation in the presence of cell lines expressing high densities of EGFR on their surface, the nimotuzumab-CAR, derived from the antibody with much lower affinity for EGFR than cetuximab, resulted in significantly lower or non-existent T-cell responses to targets with reduced expression of the protein. The response of cetuximab-CAR T-cells, on the other hand, was consistently strong

regardless of EGFR density on target cell surface[320], much like the responses observed for the four TEM8 CARs derived from high-affinity anti-TEM8 mAbs.

The above observations support the recently introduced approach of CAR 'affinity tuning' – adjusting the affinity of the scFv domain so as to allow the CAR T-cells to efficiently recognise high levels of target expression on tumour tissue while sparing normal cells, which frequently express low levels of the target, from deleterious T-cell-mediated toxicity. As suggested by the study described above[320], the low affinity of the deriving antibody may in fact be the strength of the resultant CAR, which is subsequently much less likely to mediate on-target, off-tumour toxicity. Affinity tuning based on target antigen density has also been proposed elsewhere, supported by findings that high-affinity CAR T-cells recognise any level of expression of their target, including that which is undetectable by flow cytometry; low-affinity CARs, however, cause robust T-cell responses to high target antigen levels while sparing cells with physiological-level expression[321,322]. A tool for modelling T-cell antigen recognition has also been described which has found that low-affinity receptors perform better than high-affinity ones at high doses of target antigen[323] – all of which suggests that the 1D2 CAR is the most promising TEM8 CAR going forward, and that affinity tuning is an essential consideration for future CAR T-cell therapy.

3.6.3 TEM8 expression on the surface of target cells

CAR T-cell affinities notwithstanding, it is challenging to explain some of the highest cross-reactivity observed in the more potent TEM8 CARs, L1 and L2 CARs in particular. Throughout the experiments described in previous sections, these two

CARs triggered very high T-cell responses to CHO-PR230 – a cell line which does not contain any human TEM8 mRNA (Figure 3.11) or express any appreciable levels of the corresponding protein by flow cytometry (Figure 3.12), and which has also previously proven to be TEM8-negative when tested by Western blotting[246]. Despite all this, CHO-PR230 has been shown to maintain low expression of full-length TEM8 by Northern blotting[309], suggesting that the gene is expressed and therefore may be responsible for the recognition of this cell line by the most high-affinity CARs, L1 and L2. Another possibility is the expression of endogenous hamster TEM8 by CHO-PR230 cells *in vitro* which, if similar enough to mouse TEM8 which L1 and L2 mAbs are both cross-reactive with, could also trigger responses in these CAR T-cells. Finally, it has previously been reported that human microvascular endothelial cells (HMEC) upregulate their *in vitro* TEM8 expression in response to serum deprivation[212,246]. It is possible that reaching confluence while growing in culture temporarily deprived CHO-PR230 of optimal amounts of growth factors and induced cell stress, which in turn caused them to express endogenous TEM8. However, the fact that this has not been observed before for this cell line (Brad St Croix, personal communication), and that L1 and L2 CARs consistently responded to CHO-PR230 to a high degree regardless of the confluency of the target cells or the level of exhaustion of their media, renders this unlikely.

The CAR T-cell responses observed to other cell lines are mostly consistent with what is known about TEM8 expression on these target cells. HEK293T and MDA-MB-231 both express low but detectable levels of human TEM8 protein, as observed both here (Figure 3.12) and elsewhere (ref. 246 and Brad St Croix, personal communication),

explaining the responses of L1, L2, L3 and L5 CAR T-cells to them – and the absence of 1D2 CAR T-cell responses due to low target density. LS174T cells have been consistently identified as TEM8-negative (ref. 246 and Figure 3.12) and accordingly none of the CAR T-cells responded to this cell line, demonstrating that even high-affinity CARs are not activated when their target is truly absent. The particularly high responses to HUVEC by four of the CARs, however, are still difficult to explain. Despite low-level TEM8 mRNA expression (Figure 3.11), corresponding protein expression is not detectable on these cells by flow cytometry (Figure 3.12). Even though serum starvation may induce *in vitro* TEM8 expression on HUVEC, especially since they are closely related to HMEC in which this has already been demonstrated[212,246], it is unlikely that this would be the case as the cells were regularly passaged and fed to avoid exhaustion of the media. An interesting possibility, however, is that TEM8 is able to exist on the cell surface in different forms, depending on its interaction with components of the actin cytoskeleton – this can result in the protein being shielded from recognition by detection antibodies[324]. It is therefore possible that the L2 antibody used here for flow cytometric detection is only able to bind to a particular configuration of TEM8 which may not be the predominant one on the surface of HUVEC. In fact, the same study which reported the above finding also found TEM8 expression by reverse transcription PCR (RT-PCR) in HUVEC[324], confirming the data described in this thesis and increasing the possibility of the TEM8 protein being present on these cells, even if it has not yet been detected.

Interestingly, as this thesis was being written, a group working on a similar project to the one described herein published their findings concerning 2nd and 3rd generation L2-

derived TEM8 CARs, focusing on the potential use of the CARs in triple-negative breast cancer (TNBC)[325]. Even though the range of target cells tested was not the same as the one presented here, there were some similarities allowing for comparisons to be drawn. For example, in the *in vitro* T-cell functional assays, both 2nd generation (CD28/CD3ζ) and 3rd generation (CD28/4-1BB/CD3ζ) L2 CARs secreted cytokines, proliferated and exhibited cytotoxicity in response to a range of TEM8-positive tumour endothelial and TNBC cell lines, including MDA-MB-231. This study reported that MDA-MB-231 was positive for TEM8 expression by flow cytometry, confirming our own data (Figure 3.12). They also demonstrated that endothelial cell lines including HUVEC were TEM8-negative by flow cytometry, but did not report whether their L2 CAR T-cells responded to HUVEC[325]. It was interesting to note, however, that the paper also showed that both 2nd and 3rd generation L2 CAR T-cells responded to b.END3, a murine brain tumour endothelial cell line which expressed very low or undetectable levels of TEM8 according to their flow cytometric analysis[325]. Another point of interest in the paper is that both CARs proliferated in response to low and high concentrations of recombinant TEM8 protein alike, with the 2nd generation CAR exhibiting almost equal proliferation at both concentrations. In fact, the 2nd generation L2 CAR exhibited stronger responses than its 3rd generation counterpart in all functional studies, which was suggested to be due to its lower activation threshold[325]. Taken together, and coupled to the data presented so far in this thesis, the findings strongly suggest that high-affinity CARs are able to detect and respond to exceedingly low levels of their target antigen, even when its expression is undetectable by flow cytometry, and that the CD28/CD3ζ L2 CAR in particular is one such example.

4 EXPLORATION OF *IN VIVO* TOXICITY AND ANTI-TUMOUR RESPONSE OF TEM8 CAR-ENGINEERED T-CELLS

Having performed the *in vitro* studies and determined that TEM8 CAR T-cells successfully and strongly responded to TEM8 on a range of target cells, with the 1D2 CAR especially selective for overexpression of the protein, it was necessary to examine their toxicity and anti-tumour effects *in vivo*. 1D2 was considered particularly promising of the five CARs precisely due to its consistently demonstrated specificity for high levels of surface-expressed TEM8, such as the ones that might be found on tumour vasculature. Cross-reactivity remained a concern with the other four CARs, however, rendering toxicity studies in healthy mice essential before any tumour challenge was also introduced. Even though pre-existing evidence argued against TEM8 expression on healthy mouse tissue, or indeed anywhere except on murine embryonic and tumour vasculature[227,246], the data presented in the previous chapter meant that *in vivo* safety studies became the first priority.

Depending on the mouse strain in the experiments described in this chapter – C57BL/6 or NSG – murine or human CAR T-cells were used respectively. Murine T-cells were transduced with the CARs in a similar way to human T-cells (as described in section 2.4.2) but often exhibited much higher levels of resultant CAR expression than their human counterparts, commonly being over 60% $CD34^+$. If C57BL/6 mice were used, they were irradiated prior to CAR T-cell infusion to aid T-cell engraftment. The infused murine T-cells were derived from BoyJ mouse splenocytes which carry the congenic

marker CD45.1, and could therefore be tracked in the circulation of C57BL/6 mice which express CD45.2 instead.

4.1 Early *in vivo* study shows potential toxicity of L2 and L3 CARs

In a pilot toxicity study in healthy C57BL/6 mice, mock, L1, L2, L3, L5 and 1D2 CAR T-cells were injected into the tail vein of one mouse each with the intention of tracking their fate in the circulation by regular tail bleeds, and of monitoring the health of the mice over time by observation and weighing at regular intervals. The detailed preparation and injection procedure was described in section 2.6.2. Within the first hour of the T-cell injection, the mice were closely observed for post-infusion reactions but did not show any ill effects. Within the first 24h, however, L2 and L3 CAR-injected mice developed signs of toxicity, including general lethargy to a sufficiently high extent that the experienced animal technicians in the BMSU required the mice to be culled. All the other mice appeared healthy, but on the day of the first tail bleed the 1D2 CAR-injected mouse died suddenly during the bleeding procedure. This occurrence, though uncommon, had been documented previously in unrelated animal experiments and was not therefore considered to be caused by the CAR T-cell treatment. The remaining three mice were monitored over the following weeks but remained healthy and active, with their weight steadily growing over time after the initial drop commonly seen in mice following irradiation (**Figure 4.1**).

The tail bleed data obtained from the three mice revealed that the total numbers of infused T-cells steadily rose over a period of four weeks, showing that they were persisting and proliferating in the circulation; their proportion of the total T-cell

population gradually dropped over time, however, which was in accordance with the host immune system being repopulated following the irradiation (**Figure 4.2**). This pattern was more pronounced in CD8 T-cells, which were present in higher numbers than their CD4 counterparts in the infused T-cell product. Interestingly, mock T-cells were much more numerous in the blood of the relevant mouse than L1 and L5 CAR T-cells were in their respective mice. This could point towards the tendency of the host immune system to eliminate significant numbers of infused T-cells carrying TEM8 CARs, or else show that many CAR T-cells had left the circulation early on. In fact, when only $CD34^+$ T-cell numbers and proportions were examined in each CAR T-cell-injected mouse over time, there seemed to be a selective deletion of this subset from the peripheral circulation (**Figure 4.3**). As noted before for human T-cells, mouse CD4 T-cells transduced better than the CD8 subset, as evidenced by higher CD34 expression within the infused CD4 T-cell population. However, for both L1 and L5 CAR T-cells, whether CD4 or CD8, $CD34^+$ cells were virtually undetectable in the peripheral circulation of the mice by day 28.

From the single tail bleed performed on the 1D2 CAR-injected mouse, it was very interesting to observe that the number of $CD34^+$ T-cells in this population, as well as their proportion within infused T-cells, were both much higher than those recorded for L1 and L5 CAR T-cells in the same tail bleed (Figure 4.3). The data, however limited, pointed to 1D2 CAR T-cells being more able to persist at least in the circulation, and the lack of toxicity such as that observed in L2 and L3 CARs was very encouraging. Nevertheless, further studies were needed to examine this in more depth.

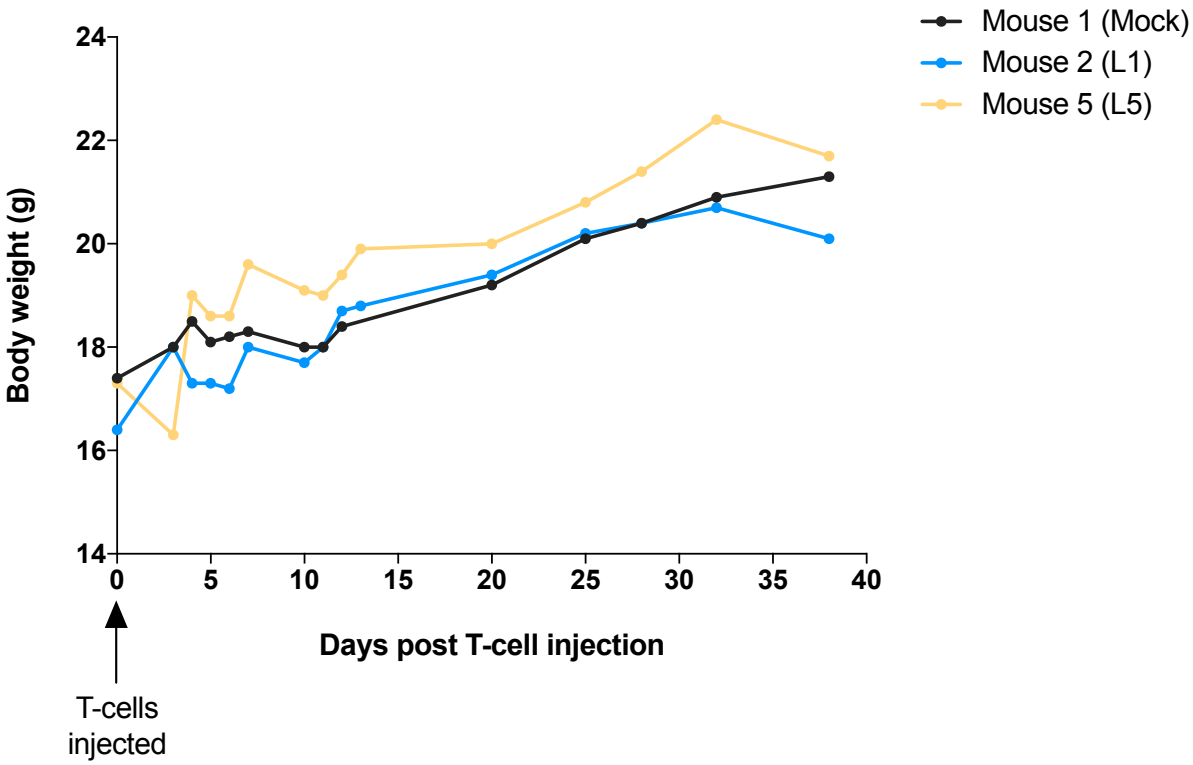

Figure 4.1 – Mouse body weights over time in pilot CAR T-cell toxicity study in C57BL/6 mice

Healthy, sublethally irradiated (4Gy) C57BL/6 mice were injected with $20x10^6$ mock or CAR T-cells which were 55.0% (L1), 64.3% (L2), 39.9% (L3), 54.6% (L5) and 59.4% (1D2) $CD34^+$ (one mouse per condition). L2 and L3 CAR-injected mice exhibited toxicity and were culled within the first 24h, and the 1D2 CAR-injected mouse died during the first tail bleed, leaving three mice in the experiment. These were weighed at regular intervals for 38 days after T-cell injection.

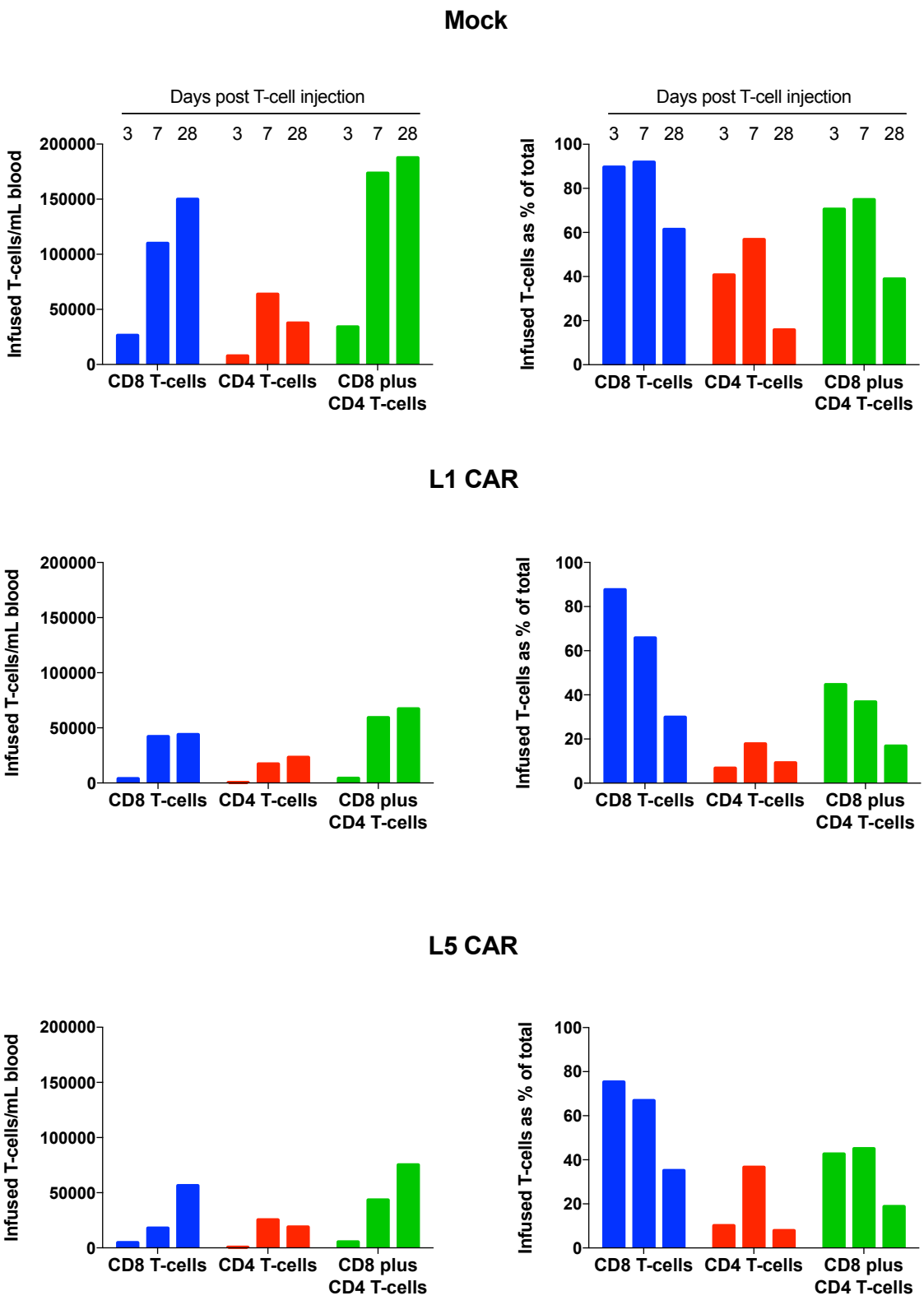

Figure 4.2 – Numbers of infused (CD45.1^{+}) T-cells in mouse peripheral blood and their proportion of the total T-cell population over time in pilot CAR T-cell toxicity study in C57BL/6 mice

Healthy, sublethally irradiated (4Gy) C57BL/6 mice were injected with $20x10^6$ mock or CAR T-cells which were 55% (L1), 64.3% (L2), 39.9% (L3), 54.6% (L5) and 59.4% (1D2) $CD34^+$ (one mouse per condition). L2 and L3 CAR-injected mice exhibited toxicity and were culled within the first 24h, and the 1D2 CAR-injected mouse died during the first tail bleed, leaving three mice in the experiment. On days 3, 7 and 28 after T-cell injection, tail bleed samples were collected and stained with anti-CD45.1, anti-CD8, anti-CD4 and anti-CD34 antibodies. Flow-count beads were included in the samples to calculate absolute T-cell counts during flow cytometric analysis. The analysis was performed by gating on T-cells, singlets, live cells and CD8/CD4 subsets sequentially, followed by $CD45.1^+$ gating on each subset individually and on the two together. The data are presented as numbers of infused ($CD45.1^+$) T-cells/mL blood, calculated using flow-count beads and corresponding tail bleed volumes, over time (left) or as % $CD45.1^+$ T-cells in the CD8, CD4 or both CD8 and CD4 T-cell subsets together over time (right).

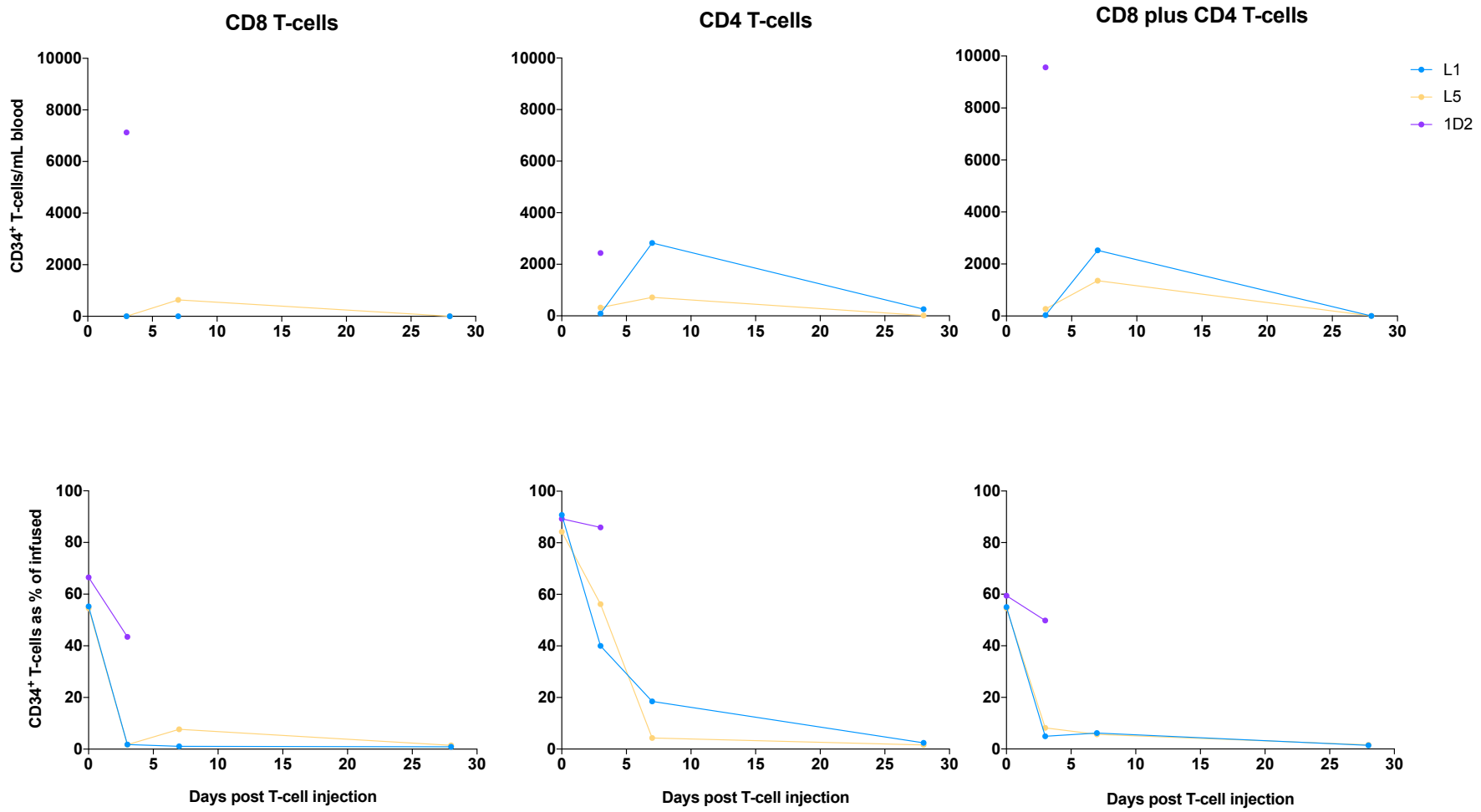

Figure 4.3 – Numbers of transduced ($CD34^+$) CAR T-cells in mouse peripheral blood and their proportion of the infused T-cell population over time in pilot CAR T-cell toxicity study in C57BL/6 mice

Healthy, sublethally irradiated (4Gy) C57BL/6 mice were injected with $20x10^6$ mock or CAR T-cells which were 55% (L1), 64.3% (L2), 39.9% (L3), 54.6% (L5) and 59.4% (1D2) $CD34^+$ (one mouse per condition). L2 and L3 CAR-injected mice exhibited toxicity and were culled within the first 24h, and the 1D2 CAR-injected mouse died during the first tail bleed, leaving three mice in the experiment. On days 3, 7 and 28 after T-cell injection, tail bleed samples were collected and stained with anti-CD45.1, anti-CD8, anti-CD4 and anti-CD34 antibodies. Flow-count beads were included in the samples to calculate absolute T-cell counts during flow cytometric analysis. The analysis was performed by gating on T-cells, singlets, live cells and CD8/CD4 subsets sequentially, followed by $CD45.1^+$ gating on each subset individually and on the two together. Each $CD45.1^+$ gate was then examined further by gating on $CD34^+$ T-cells. The data are presented as numbers of transduced ($CD34^+$) T-cells/mL blood, calculated using flow-count beads and corresponding tail bleed volumes, over time (top) or as % $CD34^+$ T-cells in the infused ($CD45.1^+$) fraction of CD8, CD4 or both CD8 and CD4 T-cell subsets together over time (bottom). In the bottom graphs, % $CD34^+$ values on day 0 correspond to the CAR transduction levels of mouse T-cells immediately prior to T-cell infusion. Tail bleed data obtained from the 1D2 CAR-injected mouse on day 3 are included.

4.2 1D2 CAR T-cells persist in the peripheral circulation of healthy mice while other CARs are selectively removed from it

The toxicity study that followed the pilot one focused on repeating the same experimental setup as before in a larger group of mice while being careful to account for the possibility of repeated toxicity. An additional control was also introduced – a 'no scFv' CAR – where the T-cells were transduced with a CAR that lacked the scFv domain, and was therefore not specific for any given antigen. This was used to assess whether any effects seen were dependent on the specific TEM8-binding domain of the CAR construct.

In the study, healthy male C57BL/6 mice were injected with mock, 'no scFv' CAR- or one of five TEM8 CAR-transduced T-cells as before. Two mice were injected with each CAR T-cell treatment apart from L2 and L3 CARs, which were given only to one mouse each due to previously observed toxicity. This time, however, none of the mice developed overt toxicity reactions within the first 24h or for the entire duration of the experiment. Except for the usual drop in weight in the first few days following irradiation, the mice were active and healthy and for the most part steadily gained weight over time (**Figure 4.4**). The smaller of the two 'no scFv' CAR-injected mice never fully gained its initial weight back and was transiently unwell several days into the experiment, however it recovered quickly and exhibited no further symptoms of distress. The staff in charge of animal welfare observed that this occasionally happened in the animals regardless of their treatment and did not consider it a cause for concern once it passed.

Tail bleeds were performed on all mice at regular intervals and, as before, it was noted that CD8 T-cells were present in higher numbers and proportions in all the infused T-cell populations (**Figure 4.5**). The number of infused mock T-cells rose over time while the CAR T-cell numbers remained relatively steady, but their proportion of the total T-cell population gradually dropped in all the treated mice as the host immune systems recovered once again. Even though this indicated that the injected T-cells persisted well in the peripheral circulation, focusing on the CAR-expressing ($CD34^+$) subset of each T-cell population yielded a very interesting pattern once more. The proportions of $CD34^+$ T-cells within the infused cell populations showed that all but 'no scFv', 1D2 and, interestingly, L2 CAR T-cells were almost completely undetectable at day 21 (**Figure 4.6**). As consistently observed before, the $CD34^+$ % was higher in the CD4 than the CD8 T-cell subset for all CARs examined, and in the case of L2 CAR T-cells, their persistence at day 21 was only apparent in the CD4 compartment; the CD8 $CD34^+$ % was comparatively very low. This was in contrast to the persistence of 1D2 and 'no scFv' CAR T-cells, which was clearly present in both T-cell subsets.

Taken together, the data indicated that 1D2 CAR T-cells persisted in the peripheral circulation when all the other TEM8 CARs were selectively removed from it. The presence of L2 CAR-expressing CD4 T-cells was also of note, although previously observed toxicity and the clear elimination of the cytotoxic CD8 T-cell compartment in the L2 $CD34^+$ T-cell population suggested that these T-cells were also susceptible to deletion from the periphery. The persistence of the non-antigen-specific CAR confirmed that CAR expression itself did not cause $CD34^+$ T-cell elimination, but rather

that this effect was dependent on the scFv moiety present and, possibly, to its affinity for the target antigen.

The fact that no mice in the study succumbed to toxicity, and that tail bleeds were therefore carried out on all of them, afforded the opportunity to explore the cytokines secreted by the injected T-cells. The rapidity of onset of the toxicity reaction in the previous experiment bore the hallmarks of CRS, and although the mice in this study showed no macroscopic signs of it, the first two tail bleeds (taken on days 4 and 9 post T-cell injection) were analysed for the presence of cytokines to explore the possibility of occult T-cell responses. Mouse plasma samples were assayed for a panel of 26 cytokines as described in section 2.6.6, and the results obtained for the ones most relevant to mouse CRS[307,326–328] are shown in **Figure 4.7**. On day 4, the plasma samples from the mice injected with L2 and L3 CARs both showed detectable levels of IFNγ, IL-5 and to a lesser extent IL-6, although these all dropped or were completely undetectable by day 9. Even though TNFα and IL-2 were not recorded in any of the samples, the presence of IFNγ and IL-6 (both of which have been strongly correlated with CRS in other studies) in the two CAR T-cell treatments which previously showed toxicity, potentially pointed to these CARs mediating an asymptomatic CRS in this particular experiment.

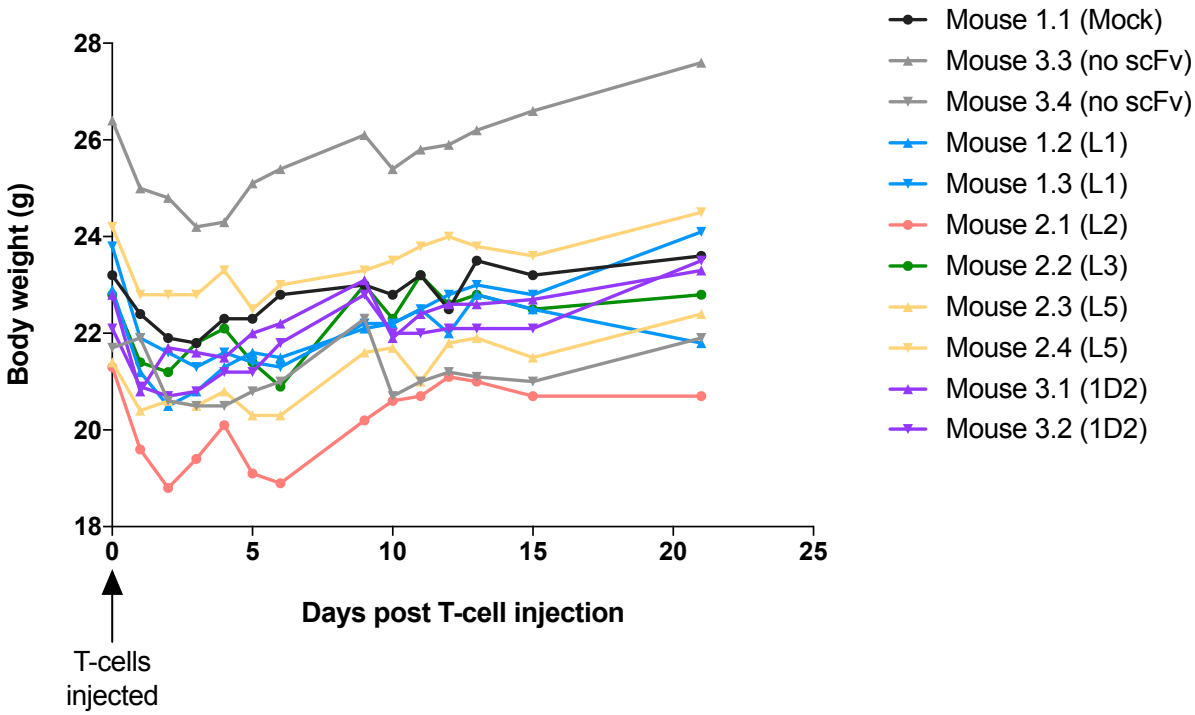

Figure 4.4 – Mouse body weights over time in second CAR T-cell toxicity study in C57BL/6 mice

Healthy, sublethally irradiated (5Gy) C57BL/6 mice were injected with 18-25x10^6 mock or CAR T-cells which were 76.9% (no scFv), 80.7% (L1), 85.1% (L2), 80.0% (L3), 70.1% (L5) and 83.5% (1D2) $CD34^+$ (two mice per condition, except for mock, L2 CAR and L3 CAR T-cells – one mouse per condition). The mice were weighed at regular intervals for 21 days after T-cell injection.

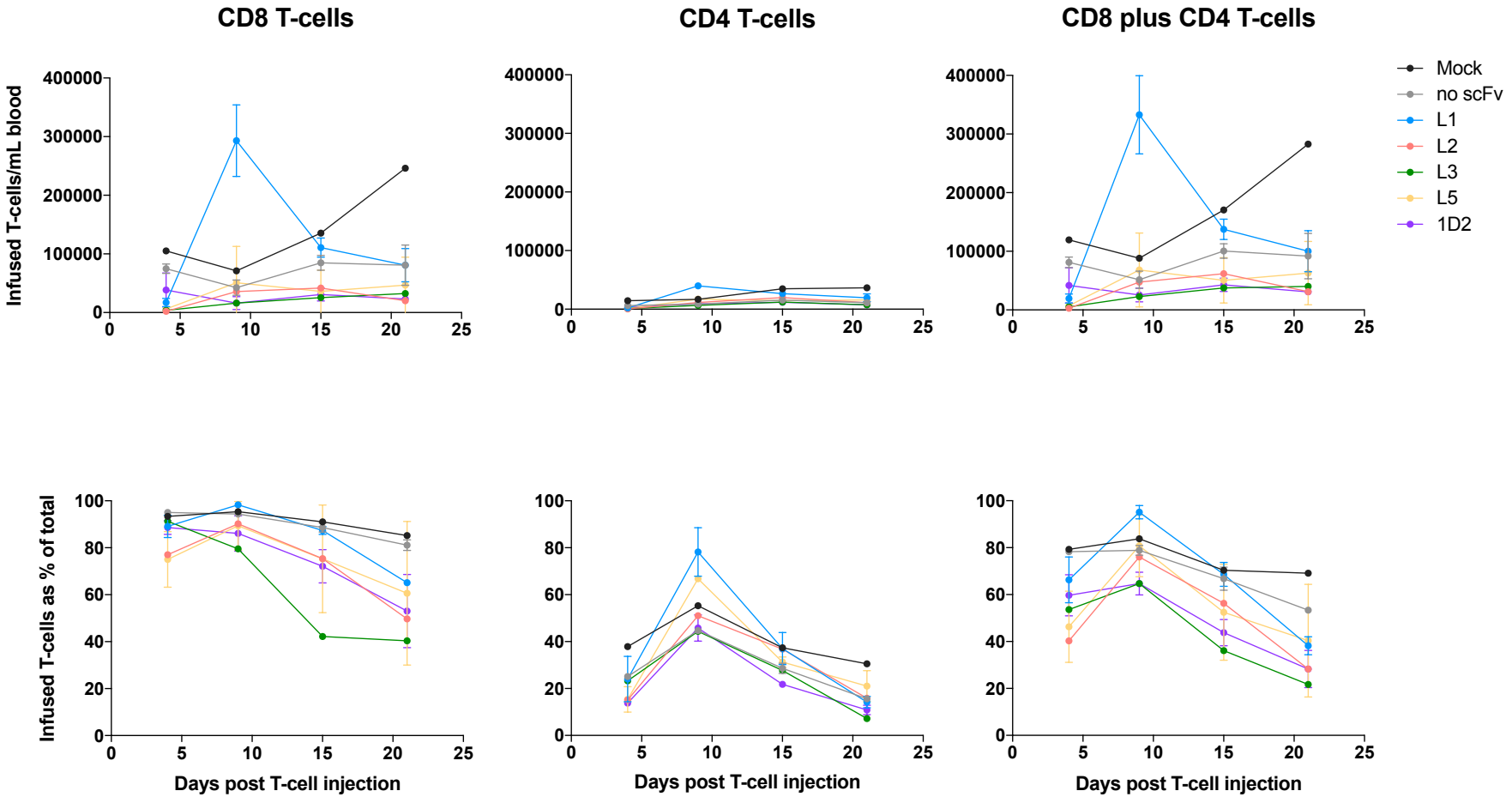

Figure 4.5 – Numbers of infused (CD45.1$^+$) T-cells in mouse peripheral blood and their proportion of the total T-cell population over time in second CAR T-cell toxicity study in C57BL/6 mice

Healthy, sublethally irradiated (5Gy) C57BL/6 mice were injected with 18-25x10^6 mock or CAR T-cells which were 76.9% (no scFv), 80.7% (L1), 85.1% (L2), 80.0% (L3), 70.1% (L5) and 83.5% (1D2) CD34$^+$ (two mice per condition, except for mock, L2 CAR

and L3 CAR T-cells – one mouse per condition). On days 4, 9, 15 and 21 after T-cell injection, tail bleed samples were collected and stained with anti-CD45.1, anti-CD8, anti-CD4 and anti-CD34 antibodies. Flow-count beads were included in the samples to calculate absolute T-cell counts during flow cytometric analysis. The analysis was performed by gating on T-cells, singlets, live cells and CD8/CD4 subsets sequentially, followed by $CD45.1^+$ gating on each subset individually and on the two together. The data are presented as numbers of infused ($CD45.1^+$) T-cells/mL blood, calculated using flow-count beads and corresponding tail bleed volumes, over time (top) or as % $CD45.1^+$ T-cells in the CD8, CD4 or both CD8 and CD4 T-cell subsets together over time (bottom). Where there were two mice per treatment, the data points are expressed as mean $\pm$ SD.

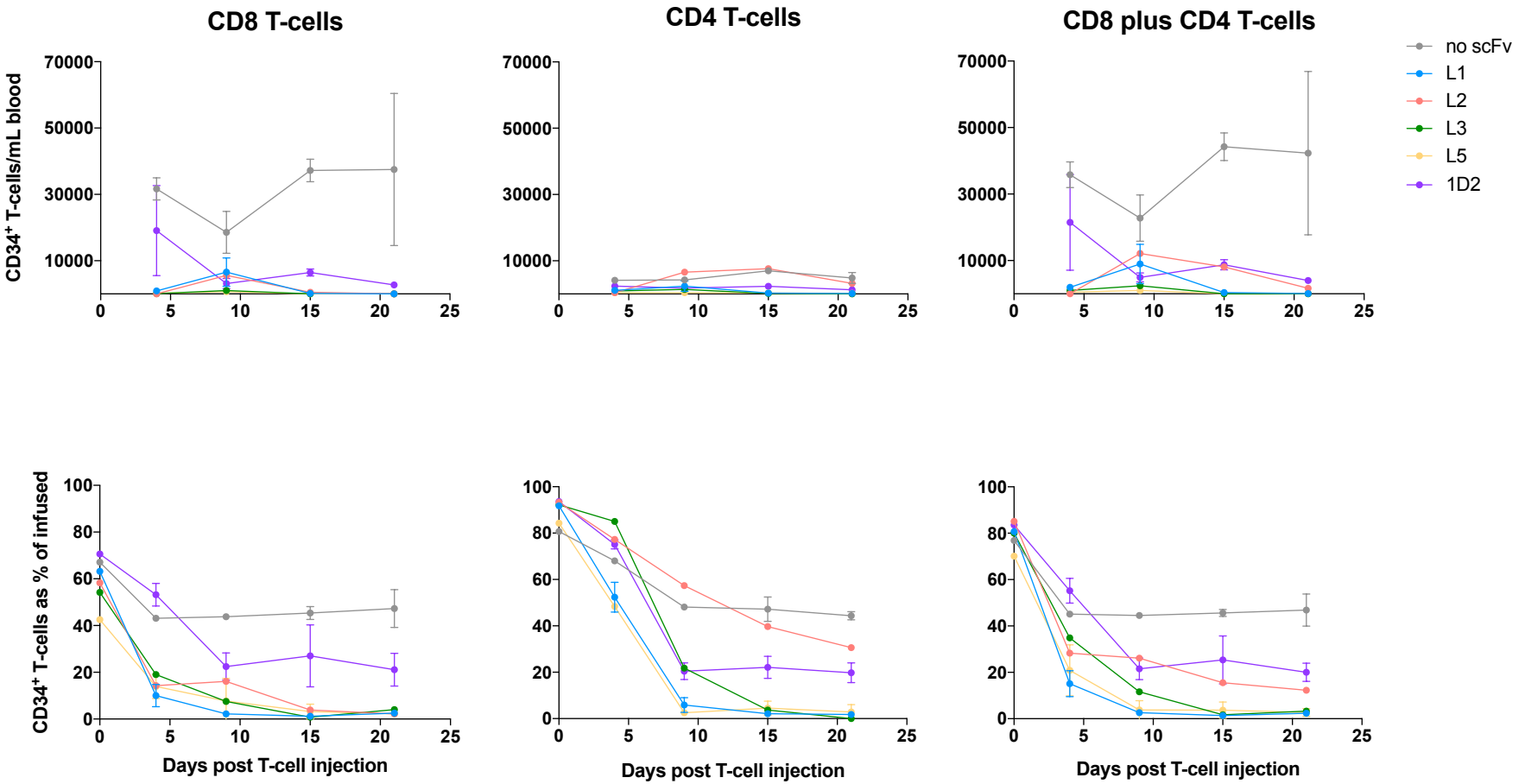

Figure 4.6 – Numbers of transduced (CD34⁺) CAR T-cells in mouse peripheral blood and their proportion of the infused T-cell population over time in second CAR T-cell toxicity study in C57BL/6 mice

Healthy, sublethally irradiated (5Gy) C57BL/6 mice were injected with 18-25x10^6 mock or CAR T-cells which were 76.9% (no scFv), 80.7% (L1), 85.1% (L2), 80.0% (L3), 70.1% (L5) and 83.5% (1D2) CD34⁺ (two mice per condition, except for mock, L2 CAR

and L3 CAR T-cells – one mouse per condition). On days 4, 9, 15 and 21 after T-cell injection, tail bleed samples were collected and stained with anti-CD45.1, anti-CD8, anti-CD4 and anti-CD34 antibodies. Flow-count beads were included in the samples to calculate absolute T-cell counts during flow cytometric analysis. The analysis was performed by gating on T-cells, singlets, live cells and CD8/CD4 subsets sequentially, followed by $CD45.1^+$ gating on each subset individually and on the two together. Each $CD45.1^+$ gate was then examined further by gating on $CD34^+$ T-cells. The data are presented as numbers of transduced ($CD34^+$) T-cells/mL blood, calculated using flow-count beads and corresponding tail bleed volumes, over time (top) or as % $CD34^+$ T-cells in the infused ($CD45.1^+$) fraction of CD8, CD4 or both CD8 and CD4 T-cell subsets together over time (bottom). In the bottom graphs, % $CD34^+$ values on day 0 correspond to the CAR transduction levels of mouse T-cells immediately prior to T-cell infusion. Where there were two mice per treatment, the data points are expressed as mean ± SD.

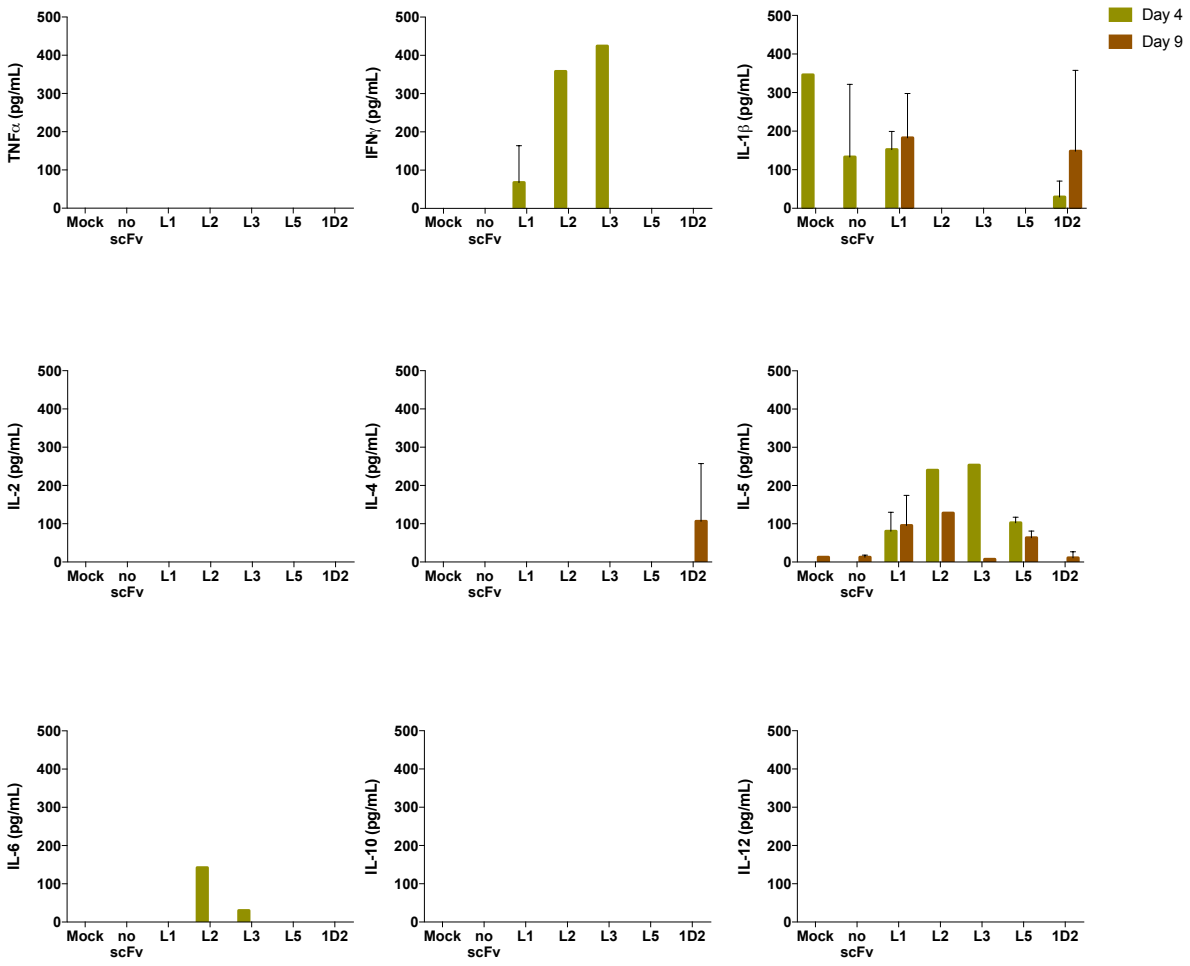

Figure 4.7 – Levels of selected cytokines measured in the plasma of C57BL/6 mice on days 4 and 9 of the second CAR T-cell toxicity study

Healthy, sublethally irradiated (5Gy) C57BL/6 mice were injected with 18-25x10^6 mock or CAR T-cells which were 76.9% (no scFv), 80.7% (L1), 85.1% (L2), 80.0% (L3), 70.1% (L5) and 83.5% (1D2) $CD34^+$ (two mice per condition, except for mock, L2 CAR and L3 CAR T-cells – one mouse per condition). On days 4, 9, 15 and 21 after T-cell injection, tail bleed samples were collected and the plasma from the first two stored for analysis. Day 4 and 9 plasma samples were subsequently analysed in a mouse multiplex cytokine assay for a panel of 26 cytokines, nine of which were considered most strongly correlated with cytokine release syndrome and are shown here. Cytokine quantities were calculated in pg/mL of plasma. Where there were two mice per treatment group, the data points are expressed as mean ± SD.

4.3 L2 CAR T-cells cause toxicity in healthy NSG mice

The promising *in vivo* persistence and safety data obtained with 1D2 CAR T-cells, and the potential for toxicity in the most highly TEM8-responsive (but also most cross-reactive) L2 CAR, prompted further investigation of these two CAR T-cell products in particular. In order to test the safety of maximising the infused CAR T-cell dose, healthy NSG mice were to be injected intravenously with three doses of $20x10^6$ L2, 1D2 or 'no scFv' CAR T-cells each on days 0, 5 and 9 of the study (three mice per treatment group). NSG mice were chosen due to the absence of an endogenous immune system and the consequent possibility of injecting them with human T-cells which, unlike murine ones, could be expanded *in vitro* to large enough numbers for multiple infusions. However, less than 24h after the first T-cell dose, all three L2 CAR-injected mice exhibited symptoms of toxicity – significantly reduced levels of activity, hunched posture, ruffled appearance and general lethargy. Experienced animal technicians in the BMSU agreed that these needed to be culled immediately. The 1D2 and 'no scFv' CAR-injected mice, however, appeared healthy and did not exhibit any adverse events even after the second and third dose of CAR T-cells. They remained active and steadily gained weight until the end of the experiment on day 16 (**Figure 4.8**).

Even though tail bleed data could not be obtained for the mice treated with the L2 CAR, the data from the rest of the mice indicated that both 1D2 and 'no scFv' CAR T-cells were able to persist and increase in number in the peripheral circulation over the course of the experiment, although naturally some of this effect may reflect the repeated infusions (**Figure 4.9**). Focusing only on the $CD34^+$ fraction of the infused T-cells, which in this experiment was comparatively lower than in the previous ones due

to using human T-cells, a similar pattern of 1D2 CAR T-cell persistence was observed once again (**Figure 4.10**). Even though absolute $CD34^+$ T-cell numbers were variable in the 'no scFv' CAR-infused mouse group, $CD34^+$ T-cell proportions of the total infused populations remained reasonably constant for both 1D2 and 'no scFv' CARs. This pattern was apparent in both CD8 and CD4 T-cell subsets and reinforced once again the *in vivo* persistence of the 1D2 CAR.

In an attempt to examine the toxicity caused by L2 CAR T-cells more closely, major organs were harvested from all three treated mice immediately after their culling and the resulting organ sections compared to those obtained from 1D2 and 'no scFv' CAR-injected mice following the end of the experiment. Despite the clearly observable toxicity in the L2 CAR-infused mice during the experiment, none of their organs showed pathology or differed in appearance to the organs of mice injected with 1D2 or 'no scFv' CARs (**Figure 4.11**). Subsequent analyses focused on the T-cells that had been prepared for infusion into the mice. The cells were tested *in vitro* for IFNγ release to titrating concentrations of recombinant human TEM8, where L2 CAR T-cells showed a much higher avidity for the target protein compared to 1D2 CAR T-cells (**Figure 4.12A**). This once again raised the possibility that L2 CAR T-cells recognised low-level TEM8 expressed on healthy mouse tissue leading to a toxic response whereas 1D2 CAR T-cells were unable to detect it, even though it was not yet clear which tissue(s) this might be. At the same time, both L2 and 1D2 CAR T-cells were shown to respond specifically to cellular targets overexpressing TEM8 *in vitro*, but L2 CAR T-cells also showed strong responses to other cell lines that appeared to express relatively little or no TEM8 (**Figure 4.12B**). These results suggested an alternative cause of the toxicity seen in

mice, namely that L2 CAR T-cells were responding to a target other than TEM8 present on healthy mouse tissue(s).

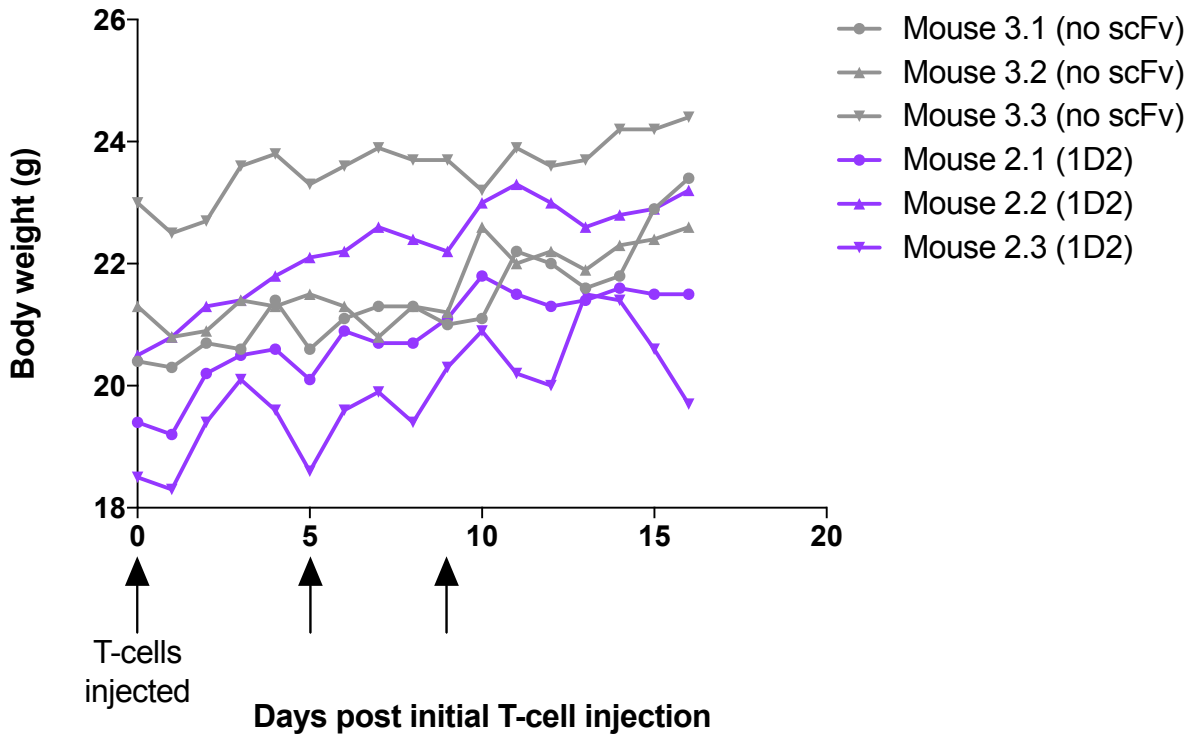

Figure 4.8 – Mouse body weights over time in multiple infusion CAR T-cell toxicity study in NSG mice

On day 0, healthy NSG mice were injected with $20x10^6$ L2, 1D2 or 'no scFv' CAR T-cells which were 21.8% (no scFv), 21.3% (L2) and 24.5% (1D2) $CD34^+$ (three mice per condition). All three L2 CAR-injected mice exhibited toxicity and were culled within the first 24h. The remaining mice were injected as before with two more T-cell doses on days 5 and 9 (represented by black arrows on the graph). The mice were weighed at regular intervals for 16 days after the first T-cell injection.

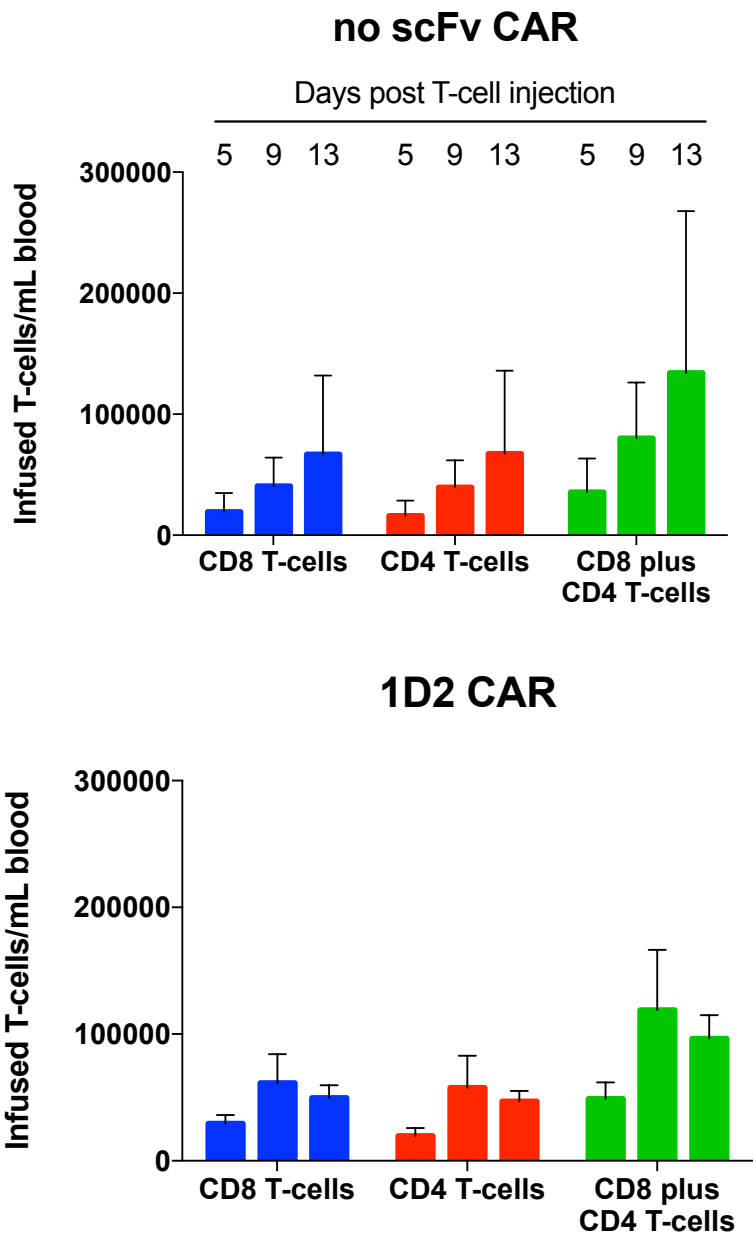

Figure 4.9 – Numbers of infused T-cells in mouse peripheral blood over time in multiple infusion CAR T-cell toxicity study in NSG mice

On day 0, healthy NSG mice were injected with $20x10^6$ L2, 1D2 or 'no scFv' CAR T-cells which were 21.8% (no scFv), 21.3% (L2) and 24.5% (1D2) $CD34^+$ (three mice per condition). All three L2 CAR-injected mice exhibited toxicity and were culled within the first 24h. The remaining mice were injected as before with two more T-cell doses on days 5 and 9. On days 5, 9 and 13 after the first T-cell injection, tail bleeds were performed (prior to T-cell infusions if these were happening on the same day), and the samples stained with anti-CD8, anti-CD4 and anti-CD34 antibodies. Flow-count beads were included in the samples to calculate absolute T-cell counts during flow cytometric analysis. The analysis

was performed by gating on T-cells, singlets, live cells and CD8/CD4 subsets sequentially. The data are presented as numbers of infused T-cells/mL blood, calculated using flow-count beads and corresponding tail bleed volumes, over time in ‘no scFv’ CAR- (top) or 1D2 CAR-injected mice (bottom). The data points are expressed as mean + SD.

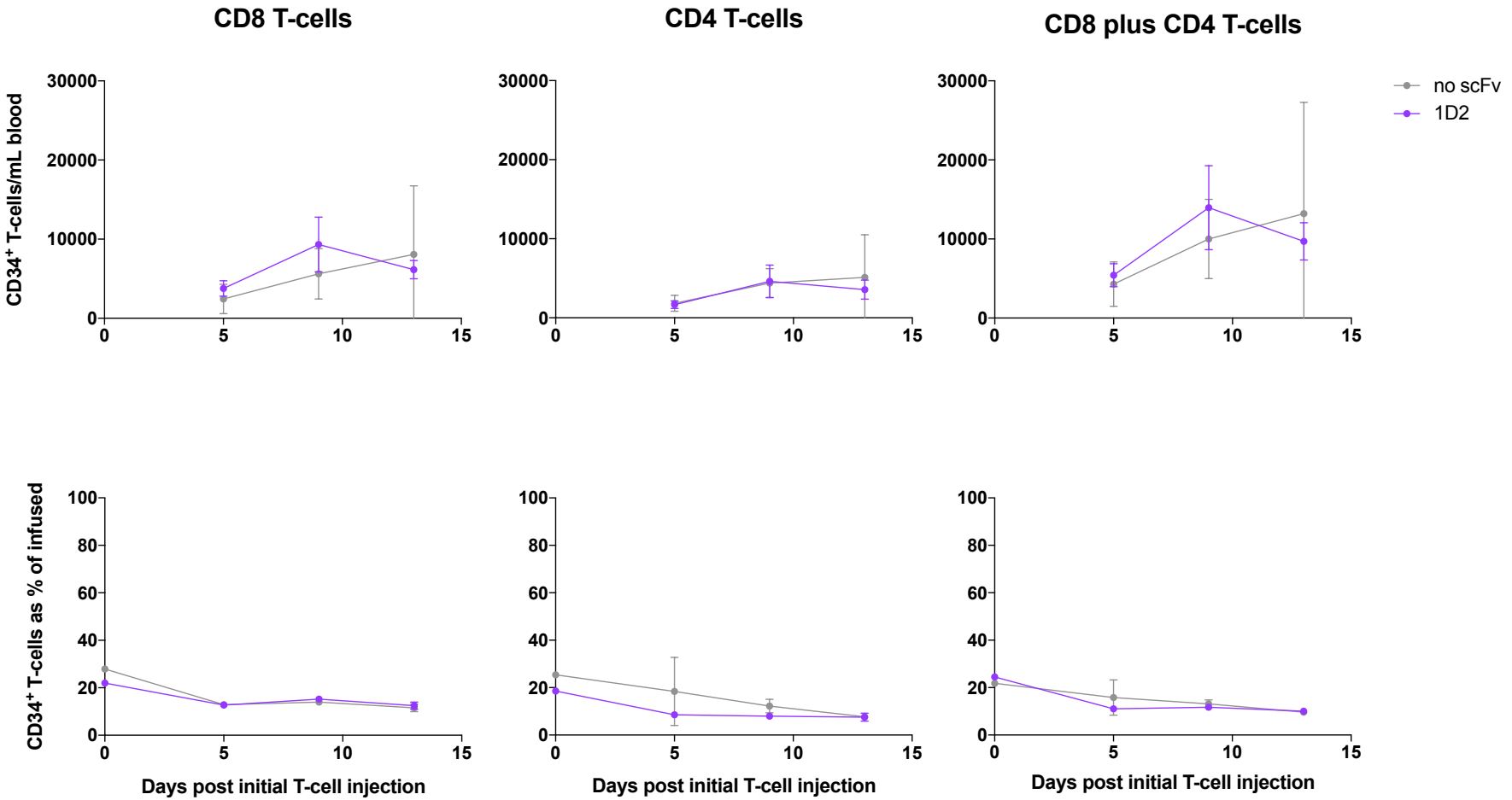

Figure 4.10 – Numbers of transduced (CD34$^+$) CAR T-cells in mouse peripheral blood and their proportion of the total infused T-cell population over time in multiple infusion CAR T-cell toxicity study in NSG mice

On day 0, healthy NSG mice were injected with 20x10^6 L2, 1D2 or 'no scFv' CAR T-cells which were 21.8% (no scFv), 21.3% (L2) and 24.5% (1D2) CD34$^+$ (three mice per condition). All three L2 CAR-injected mice exhibited toxicity and were culled within the first

24h. The remaining mice were injected as before with two more T-cell doses on days 5 and 9. On days 5, 9 and 13 after the first T-cell injection, tail bleeds were performed (prior to T-cell infusions if these were happening on the same day), and the samples stained with anti-CD8, anti-CD4 and anti-CD34 antibodies. Flow-count beads were included in the samples to calculate absolute T-cell counts during flow cytometric analysis. The analysis was performed by gating on T-cells, singlets, live cells and CD8/CD4 subsets sequentially, then examined further by gating on $CD34^+$ T-cells in each subset separately and the two together. The data are presented as numbers of transduced ($CD34^+$) T-cells/mL blood, calculated using flow-count beads and corresponding tail bleed volumes, over time (top) or as % $CD34^+$ T-cells in the infused fraction of CD8, CD4 or both CD8 and CD4 T-cell subsets together over time (bottom). In the bottom graphs, % $CD34^+$ values on day 0 correspond to the CAR transduction levels of human T-cells immediately prior to T-cell infusion. The data points are expressed as mean $\pm$ SD.

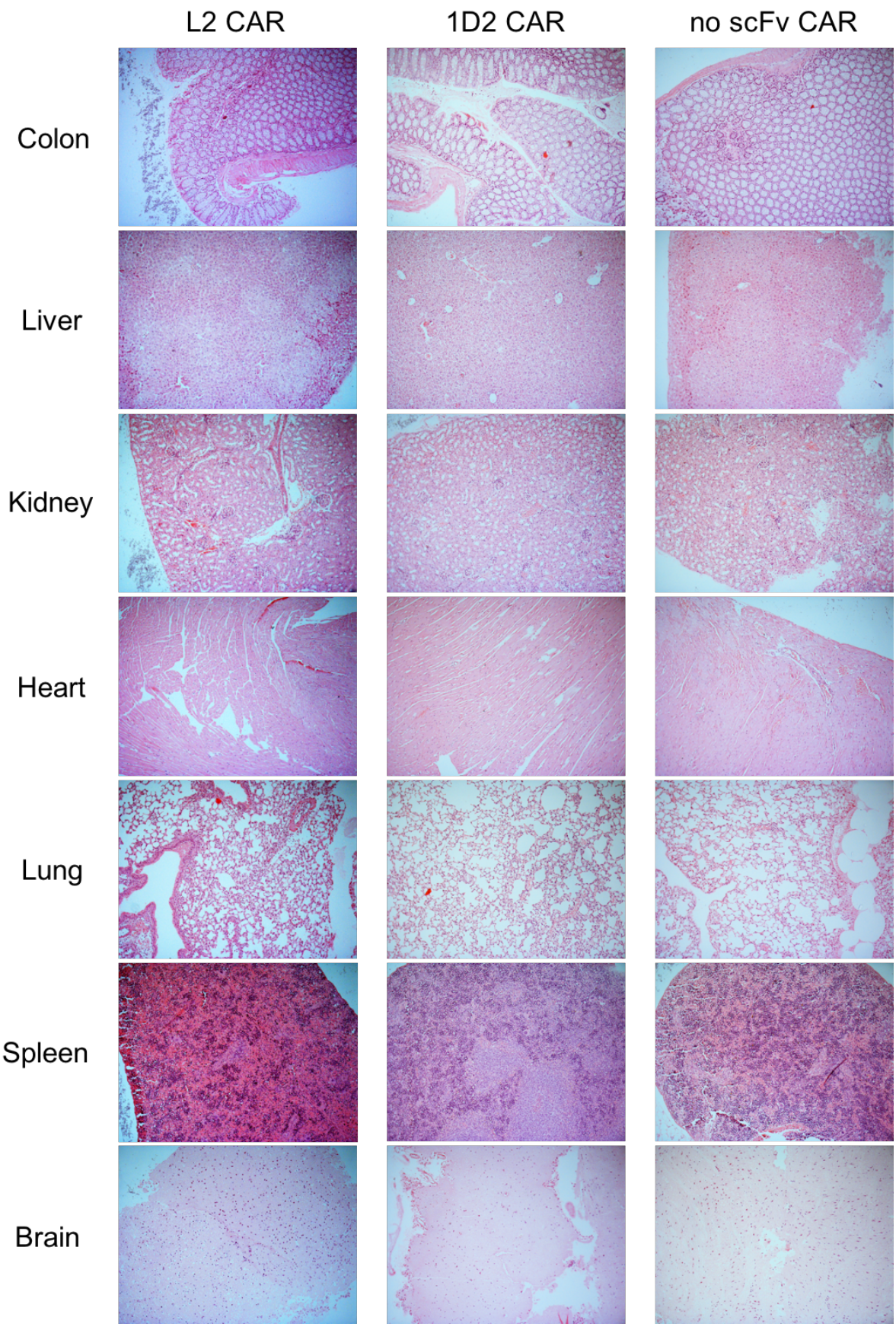
L2 CAR
1D2 CAR
no scFv CAR
Colon
Liver
Kidney
Heart
Lung
Spleen
Brain

Figure 4.11 – Representative tissue sections from NSG mice in the multiple infusion CAR T-cell toxicity study

On day 0, healthy NSG mice were injected with $20x10^6$ L2, 1D2 or 'no scFv' CAR T-cells which were 21.8% (no scFv), 21.3% (L2) and 24.5% (1D2) $CD34^+$ (three mice per condition). All three L2 CAR-injected mice exhibited toxicity and were culled within the first 24h. The remaining mice were injected as before with two more T-cell doses on days 5 and 9. Major mouse organs were harvested from L2 CAR-injected mice following their culling and from the rest of the mice at the end of the experiment, fixed in formalin and sectioned before being stained using haematoxylin and eosin (H&E) and examined for histopathology. The sections were imaged at 10X magnification on a brightfield microscope and are representative of three mice in each treatment group.

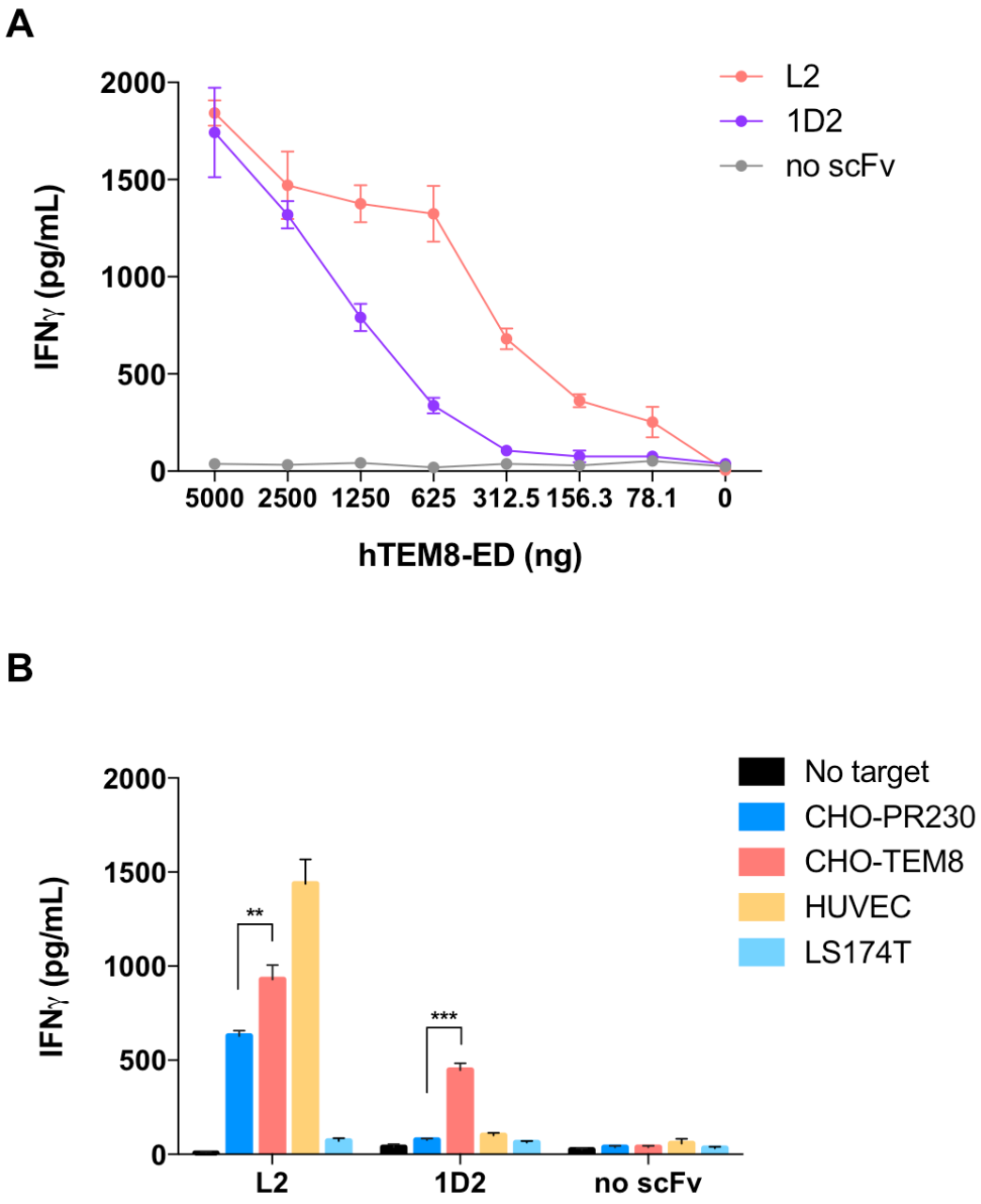

Figure 4.12 – *In vitro* hTEM8 and target cell responses by CAR T-cells used in multiple infusion CAR T-cell toxicity study in NSG mice

(A) L2, 1D2 or 'no scFv' CAR-transduced T-cells used in the multiple infusion CAR T-cell toxicity study were incubated in a 96-well plate overnight at $5x10^4$ cells/well with decreasing concentrations of human recombinant TEM8-extracellular domain (hTEM8-ED). Supernatants were assayed by IFNγ ELISA the following day and the resulting T-cell IFNγ production expressed in pg/mL. All data points were measured in triplicate and expressed as mean ± SD. **(B)** The same T-cells as in A were incubated alone or with indicated target cells ($2x10^4$ cells/well) in a 96-well plate overnight and assayed by IFNγ ELISA as in A. All data points were measured in triplicate and

expressed as mean + SD. The levels of response to CHO-TEM8 compared to those to CHO-PR230 were significantly higher for both L2 and 1D2 CAR T-cells (**, $P<0.01$; ***, $P<0.001$), as measured by Student's t-test and corrected for multiple comparisons using the Holm-Sidak method.

4.4 L2 CAR T-cells potentially target low-level TEM8 expression on healthy mouse tissue

To help ascertain the underlying cause of the observed toxicity in L2 CAR-injected mice, TEM8 KO mice on C57BL/6 background were obtained as described in section 2.6.1. They were injected with L2, 1D2 or 'no scFv' CAR T-cells alongside their C57BL/6 WT counterparts (two mice per group), with an additional WT mouse injected with mock T-cells as a further control. It was reasoned that, if toxicity arose in L2 CAR-infused WT mice, but not TEM8 KO mice, it could be concluded with reasonable certainty that this was due to L2 CAR T-cells responding to TEM8 expressed on healthy mouse tissue(s) or vasculature. If, however, the adverse reactions were to occur in both WT and KO mice, cross-reactivity of the L2 CAR with an unrelated protein would be the most likely explanation.

In this experiment, unlike the previous one, no toxicity was observed in any of the treated mice. They all appeared active and did not exhibit signs of lethargy or acute illness. The only exception was one of the TEM8 KO mice injected with 'no scFv' CAR T-cells which developed a very sore and bulging left eye within 12h of the injection, which grew progressively worse over the next two days. The animal was considered to be in distress and pain and was therefore culled on the second day after the T-cell infusion. This adverse effect was entirely unforeseen and, although it could not be adequately explained, it appeared to be related to the KO phenotype – soon after the first mouse, two more TEM8 KO mice developed the same sore and bulging eye, one of which was injected with L2 and the other with 1D2 CAR T-cells. In these two mice, however, the symptoms were somewhat milder and they were not culled; after a period

of close observation, the affected eye of each mouse returned to its normal size, but it had also developed a cloudy appearance resembling a cataract. Both mice seemed otherwise healthy and their weight, like that of the rest of the mice, either increased or remained stable until the experiment ended (**Figure 4.13**). Nevertheless, their affected eyes remained cloudy for the duration of the study.

Tail bleeds were performed during the experiment to track the fate of the injected T-cells in the peripheral circulation of all the mice. This revealed once more their proliferation and expansion over time and the decrease in their proportion of the total T-cell population as the host immune systems were gradually restored after irradiation (**Figure 4.14**). The absolute numbers of mock and 'no scFv' CAR T-cells in the circulation were always higher than those of 1D2 and especially L2 CAR T-cells in both CD8 and CD4 compartments, regardless of whether the mice were WT or TEM8 KO. This once again highlighted the tendency of the antigen-specific CARs to be eliminated early on after the T-cell injection, which was further confirmed by the $CD34^+$ T-cell data. This showed the familiar pattern of mock and 'no scFv' CAR T-cells persisting in the circulation over time, 1D2 CAR T-cells still being present at similar levels in both WT and KO mice, and L2 CAR T-cells being virtually undetectable in WT mice by day 13 (**Figure 4.15**). It was very interesting to observe, however, that unlike in WT mice, L2 CAR T-cells persisted in TEM8 KO mice to a considerable degree. The difference in numbers and proportions of $CD34^+$ T-cells between TEM8 KO mice and their WT counterparts was particularly striking on day 6 of the experiment, although it was still pronounced on day 13. This led to the conclusion that, while overt toxicity was not detected in WT mice, the injected L2 CAR-expressing T-cells had been rapidly

eliminated from the mouse circulation possibly due to the recognition of a target which was not present in TEM8 KO mice. While this result does not entirely eliminate the possibility of L2 CAR T-cells cross-reacting with an unrelated antigen, it does provide evidence that their loss from the circulation is largely a result of recognising TEM8 expressed on healthy mouse tissue(s).

Consistent with the absence of symptoms of CRS in the mice, multiplex cytokine analysis of mouse plasma samples from days 1 and 6 of the experiment revealed no upregulated cytokine levels, except IL-1β which was present in all the mice to a similar degree (**Figure 4.16**). Apart from this, and very small amounts of IL-5 detected in some plasma samples, there was no evidence of any significant cytokine response having taken place in the mice following CAR T-cell injection.

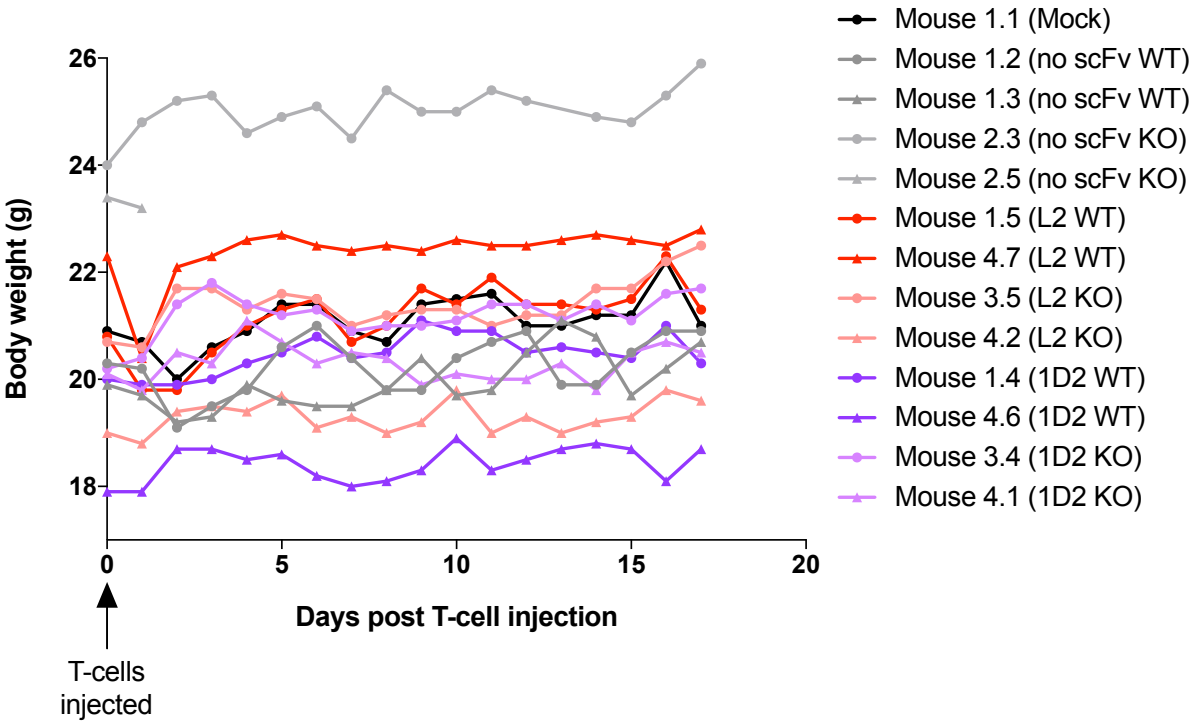

Figure 4.13 – Mouse body weights over time in CAR T-cell toxicity study in C57BL/6 WT and TEM8 KO mice

Healthy, sublethally irradiated (4Gy) C57BL/6 WT or TEM8 KO mice were injected with $13x10^6$ mock or CAR T-cells which were 93.4% (no scFv), 91.2% (L2) and 93.7% (1D2) $CD34^+$ (two WT and two KO mice per condition, except for one WT mouse injected with mock T-cells). One of each of the TEM8 KO mice injected with L2, 1D2 and 'no scFv' CAR T-cells exhibited ocular toxicity, and the 'no scFv' CAR-injected KO mouse (mouse 2.5) was culled on day 2, leaving only mouse 2.3 in this treatment group. The mice were weighed at regular intervals for 17 days after T-cell injection.

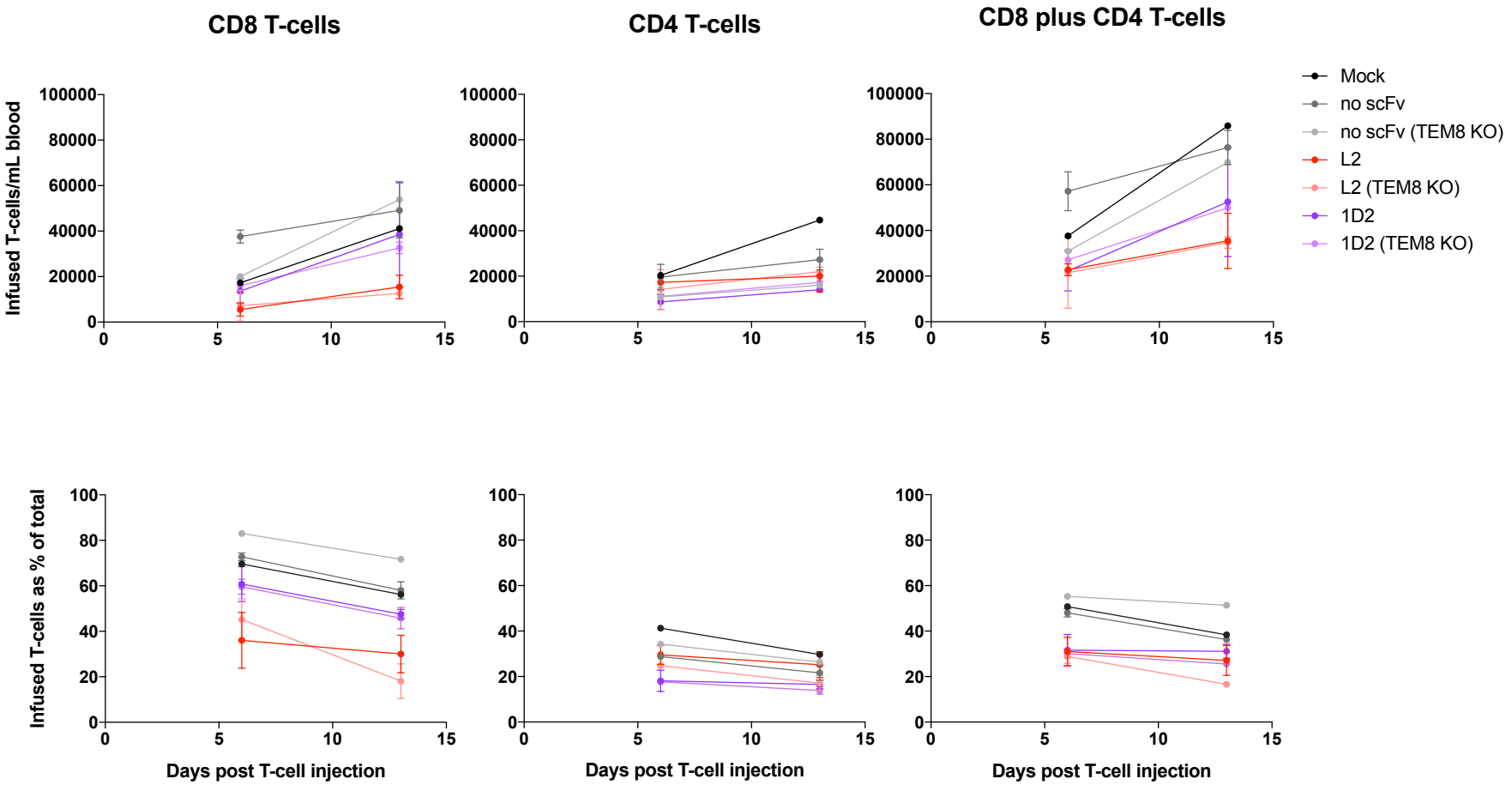

Figure 4.14 – Numbers of infused (CD45.1$^+$) T-cells in mouse peripheral blood and their proportion of the total T-cell population over time in CAR T-cell toxicity study in C57BL/6 WT and TEM8 KO mice

Healthy, sublethally irradiated (4Gy) C57BL/6 WT or TEM8 KO mice were injected with 13x10^6 mock or CAR T-cells which were 93.4% (no scFv), 91.2% (L2) and 93.7% (1D2) CD34$^+$ (two WT and two KO mice per condition, except for one WT mouse injected

with mock T-cells). One of each of the TEM8 KO mice injected with L2, 1D2 and 'no scFv' CAR T-cells exhibited ocular toxicity, and the 'no scFv' CAR-injected KO mouse was culled on day 2, leaving only one mouse in this treatment group. On days 6 and 13 after T-cell injection, tail bleed samples were collected and stained with anti-CD45.1, anti-CD8, anti-CD4 and anti-CD34 antibodies. Flow-count beads were included in the samples to calculate absolute T-cell counts during flow cytometric analysis. The analysis was performed by gating on T-cells, singlets, live cells and CD8/CD4 subsets sequentially, followed by $CD45.1^+$ gating on each subset individually and on the two together. The data are presented as numbers of infused ($CD45.1^+$) T-cells/mL blood, calculated using flow-count beads and corresponding tail bleed volumes, over time (top) or as % $CD45.1^+$ T-cells in the CD8, CD4 or both CD8 and CD4 T-cell subsets together over time (bottom). Where there were two mice per treatment, the data points are expressed as mean ± SD. Data are representative of two independent experiments.

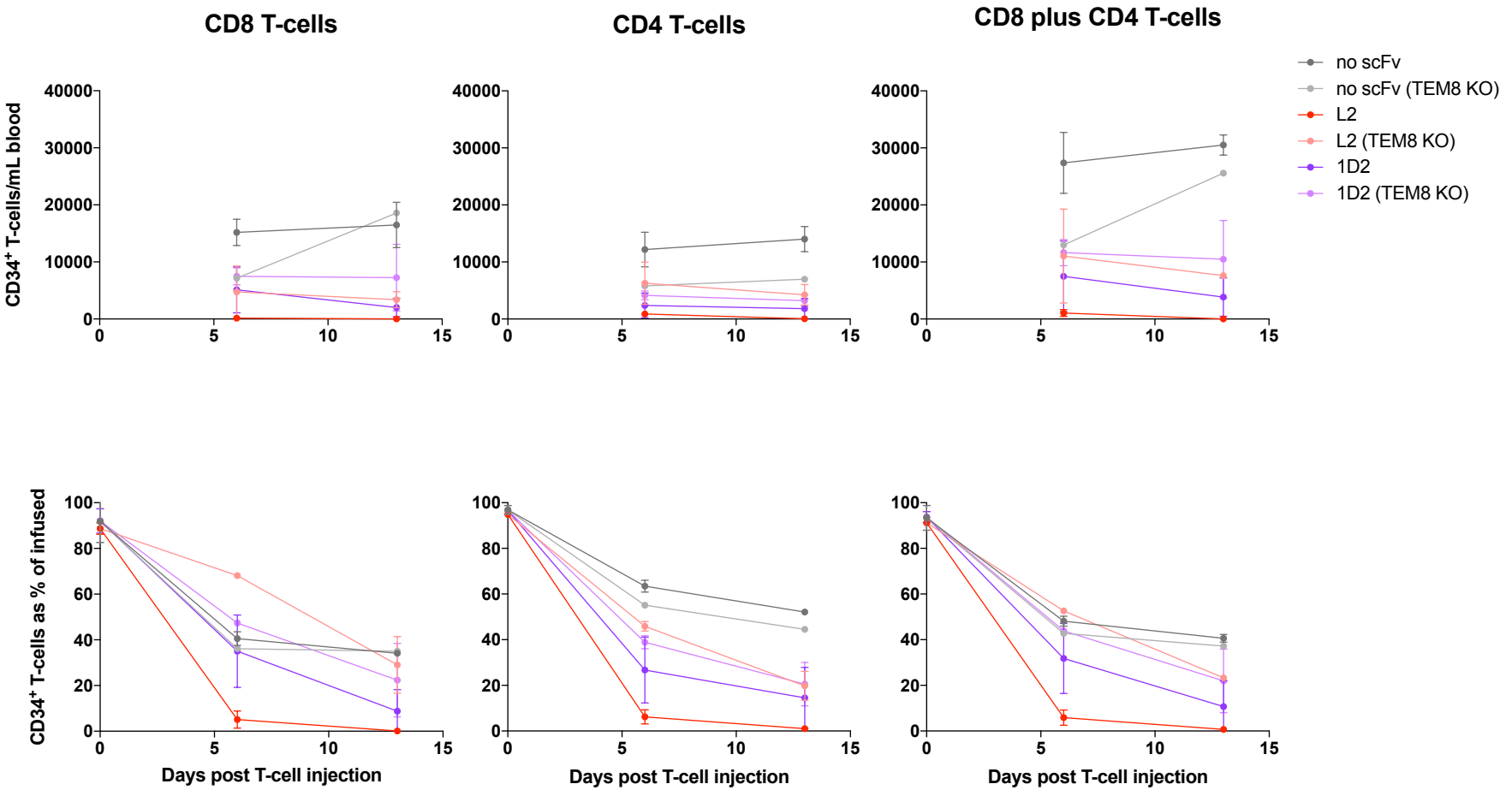

Figure 4.15 – Numbers of transduced ($CD34^+$) CAR T-cells in mouse peripheral blood and their proportion of the infused T-cell population over time in CAR T-cell toxicity study in C57BL/6 WT and TEM8 KO mice

Healthy, sublethally irradiated (4Gy) C57BL/6 WT or TEM8 KO mice were injected with $13x10^6$ mock or CAR T-cells which were 93.4% (no scFv), 91.2% (L2) and 93.7% (1D2) $CD34^+$ (two WT and two KO mice per condition, except for one WT mouse injected

with mock T-cells). One of each of the TEM8 KO mice injected with L2, 1D2 and 'no scFv' CAR T-cells exhibited ocular toxicity, and the 'no scFv' CAR-injected KO mouse was culled on day 2, leaving only one mouse in this treatment group. On days 6 and 13 after T-cell injection, tail bleed samples were collected and stained with anti-CD45.1, anti-CD8, anti-CD4 and anti-CD34 antibodies. Flow-count beads were included in the samples to calculate absolute T-cell counts during flow cytometric analysis. The analysis was performed by gating on T-cells, singlets, live cells and CD8/CD4 subsets sequentially, followed by $CD45.1^+$ gating on each subset individually and on the two together. Each $CD45.1^+$ gate was then examined further by gating on $CD34^+$ T-cells. The data are presented as numbers of transduced ($CD34^+$) T-cells/mL blood, calculated using flow-count beads and corresponding tail bleed volumes, over time (top) or as % $CD34^+$ T-cells in the infused ($CD45.1^+$) fraction of CD8, CD4 or both CD8 and CD4 T-cell subsets together over time (bottom). In the bottom graphs, % $CD34^+$ values on day 0 correspond to the CAR transduction levels of mouse T-cells immediately prior to T-cell infusion. Where there were two mice per treatment, the data points are expressed as mean ± SD. Data are representative of two independent experiments.

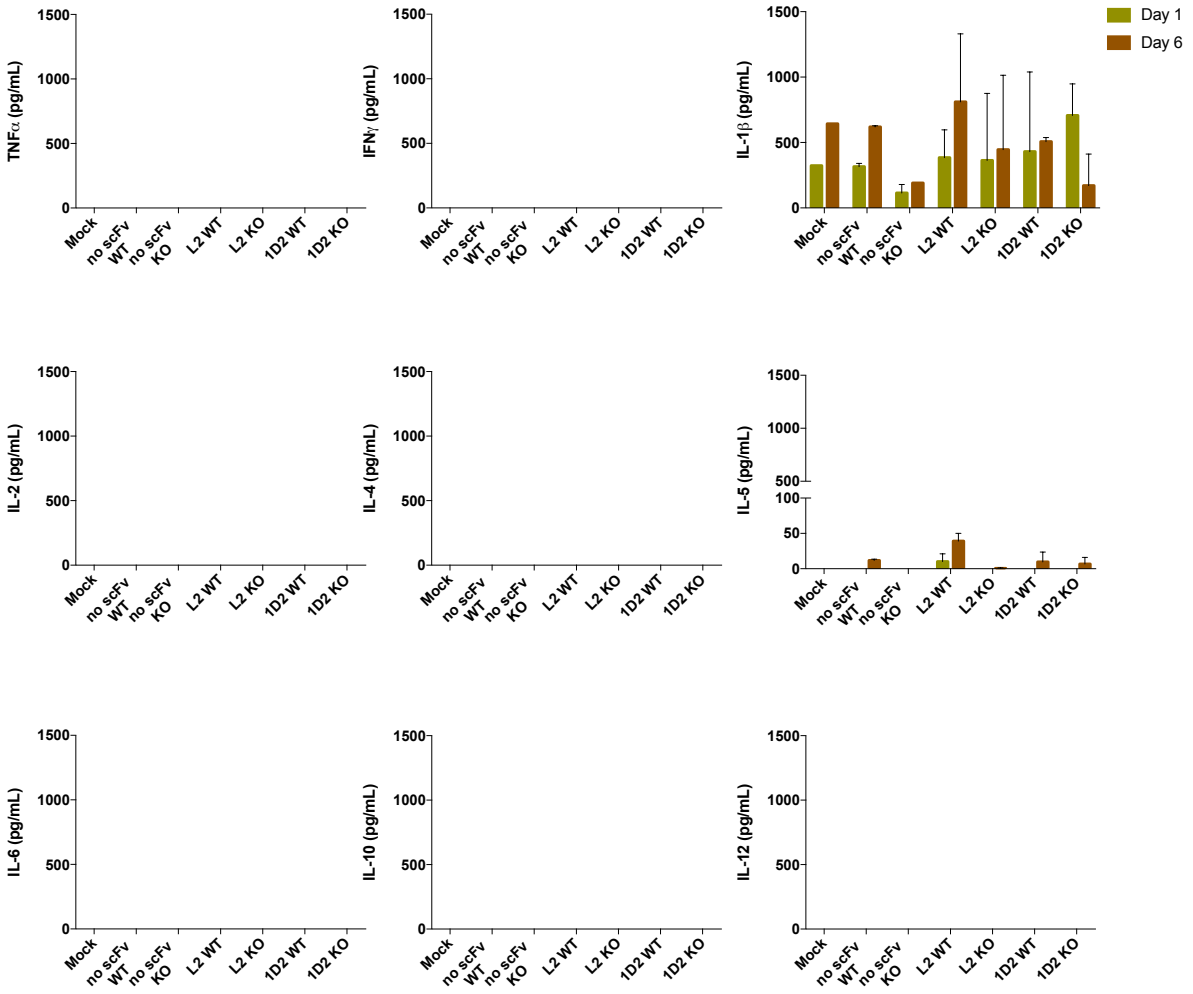

Figure 4.16 – Levels of selected cytokines measured in the plasma of C57BL/6 WT and TEM8 KO mice on days 1 and 6 of the CAR T-cell toxicity study

Healthy, sublethally irradiated (4Gy) C57BL/6 WT or TEM8 KO mice were injected with $13x10^6$ mock or CAR T-cells which were 93.4% (no scFv), 91.2% (L2) and 93.7% (1D2) $CD34^+$ (two WT and two KO mice per condition, except for one WT mouse injected with mock T-cells). One of each of the TEM8 KO mice injected with L2, 1D2 and 'no scFv' CAR T-cells exhibited ocular toxicity, and the 'no scFv' CAR-injected KO mouse was culled on day 2, leaving only one mouse in this treatment group. On days 1 and 6 after T-cell injection, tail bleed samples were collected and the plasma stored for analysis. The plasma samples were subsequently analysed in a mouse multiplex cytokine assay for a panel of 26 cytokines, nine of which were considered most strongly correlated with cytokine release syndrome and are shown here. Cytokine quantities were calculated in pg/mL of plasma. Where there were two mice per treatment group, the data points are expressed as mean ± SD.

4.5 1D2 CAR T-cells are not tumour-protective in a pilot study in NSG mice

Throughout the CAR safety studies described in preceding sections, L2 CAR T-cells injected into healthy WT mice showed a clear potential for toxicity or, if not toxic, mostly failed to persist in the peripheral circulation over time. Even though the early toxicity of L3 CAR T-cells observed in the pilot safety study was not seen again, the CAR-expressing fraction of these cells also failed to persist when examined further, along with L1 and L5 CAR T-cells. The 1D2 CAR was the only TEM8 CAR which was consistently safe and detected in the circulation at the end of each experiment, making it the most promising candidate for mouse tumour protection studies. 1D2 CAR T-cells were therefore tested against a colorectal carcinoma xenograft, DLD-1, which was itself TEM8-negative but had been shown previously to generate a TEM8-positive tumour vasculature *in vivo*[246]. As all CARs were derived from antibodies which were fully cross-reactive with both human and mouse TEM8, it was anticipated that 1D2 CAR T-cells could respond to mTEM8 on mouse tumour vasculature and lead to tumour control or regression.

In a pilot anti-tumour study, six NSG mice received subcutaneous flank injections of DLD-1 cells as described in section 2.6.4, and three days later half of them were injected with 1D2 CAR T-cells while the other half received 'no scFv' CAR T-cell controls. The mice had no adverse reactions to the T-cell treatment, with their weights being mostly steady throughout the experiment (**Figure 4.17**), and the tail bleeds performed showed expansion of infused T-cells (**Figure 4.18**) as well as persistence of the $CD34^+$ fraction in both CAR T-cell products over time (**Figure 4.19**). Despite this, however, tumour measurements in the two groups showed that 1D2 CAR T-cells had

no effect on tumour growth compared to the 'no scFv' CAR controls (**Figure 4.20A**). Even though the individual tumour volumes of 1D2 CAR-treated mice were somewhat lower than those observed in their control-treated counterparts (**Figure 4.20B**), the overall difference between the two groups was not significant. Therefore, an explanation was sought for this apparent inability of the 1D2 CAR to control tumour growth.

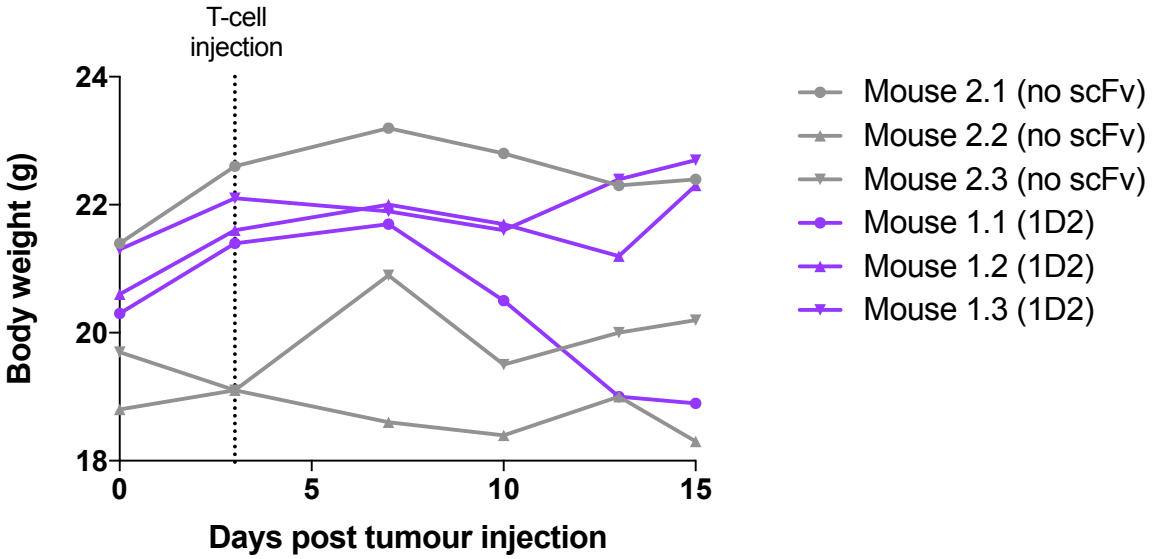

Figure 4.17 – Mouse body weights over time in DLD-1 tumour protection study in NSG mice

On day 0, six healthy NSG mice were injected subcutaneously into the flank with $2.5x10^6$ DLD-1 colorectal carcinoma cells each. On day 3, they were each injected with $20x10^6$ 1D2 or 'no scFv' CAR T-cells which were 20.0% (no scFv) and 23.2% (1D2) $CD34^+$ (three mice per treatment group). The mice were weighed at regular intervals for 15 days after tumour cell injection.

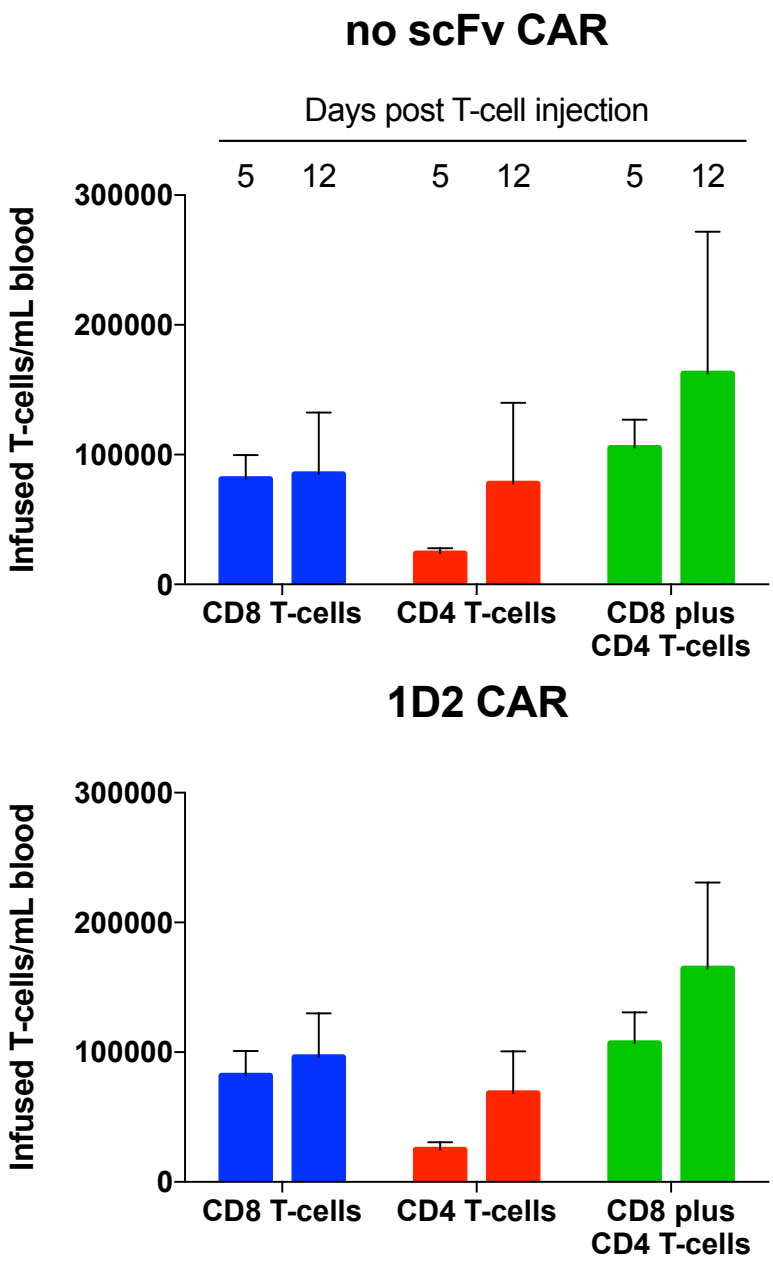

Figure 4.18 – Numbers of infused T-cells in mouse peripheral blood over time in DLD-1 tumour protection study in NSG mice

On day 0, six healthy NSG mice were injected subcutaneously into the flank with $2.5x10^6$ DLD-1 colorectal carcinoma cells each. On day 3, they were each injected with $20x10^6$ 1D2 or 'no scFv' CAR T-cells which were 20.0% (no scFv) and 23.2% (1D2) $CD34^+$ (three mice per treatment group). On days 5 and 12 after T-cell injection, tail bleed samples were collected and stained with anti-CD8, anti-CD4 and anti-CD34 antibodies. Flow-count beads were included in the samples to calculate absolute T-cell counts during flow cytometric analysis. The analysis was performed by gating on T-cells, singlets, live cells and CD8/CD4 subsets sequentially. The data are presented as numbers of infused T-

cells/mL blood, calculated using flow-count beads and corresponding tail bleed volumes, over time in ‘no scFv’ CAR- (top) or 1D2 CAR-injected mice (bottom). The data points are expressed as mean + SD.

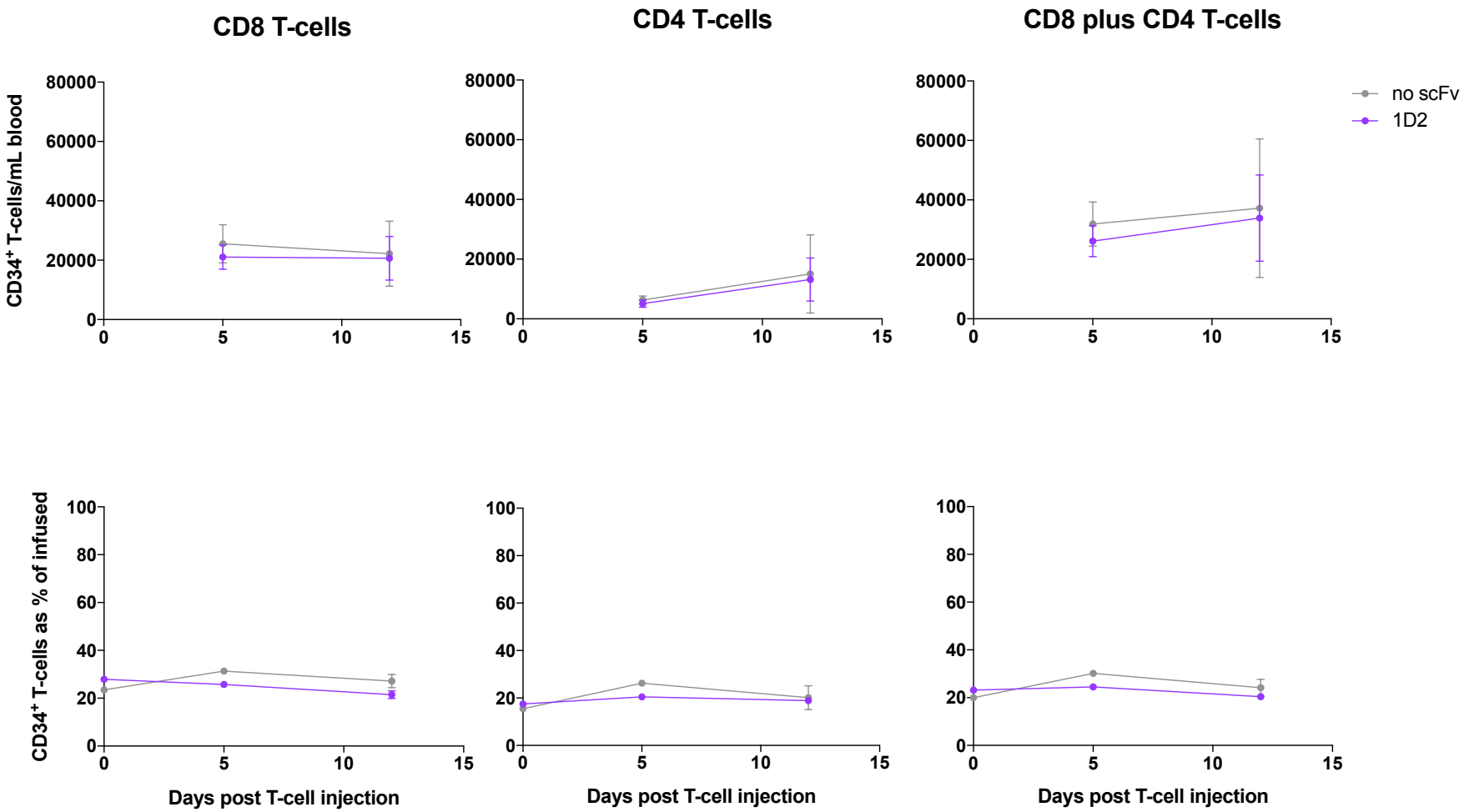

Figure 4.19 – Numbers of transduced ($CD34^+$) CAR T-cells in mouse peripheral blood and their proportion of the total infused T-cell population over time in DLD-1 tumour protection study in NSG mice

On day 0, six healthy NSG mice were injected subcutaneously into the flank with $2.5x10^6$ DLD-1 colorectal carcinoma cells each. On day 3, they were each injected with $20x10^6$ 1D2 or 'no scFv' CAR T-cells which were 20.0% (no scFv) and 23.2% (1D2) $CD34^+$ (three mice per treatment group). On days 5 and 12 after T-cell injection, tail bleed samples were collected and stained with anti-CD8, anti-CD4 and anti-CD34 antibodies. Flow-count beads were included in the samples to calculate absolute T-cell counts during flow cytometric analysis. The analysis was performed by gating on T-cells, singlets, live cells and CD8/CD4 subsets sequentially, then examined further by gating on $CD34^+$ T-cells in each subset separately and the two together. The data are presented as numbers of transduced ($CD34^+$) T-cells/mL blood, calculated using flow-count beads and corresponding tail bleed volumes, over time (top) or as % $CD34^+$ T-cells in the infused fraction of CD8, CD4 or both CD8 and CD4 T-cell subsets together over time (bottom). In the bottom graphs, % $CD34^+$ values on day 0 correspond to the CAR transduction levels of human T-cells immediately prior to T-cell infusion. The data points are expressed as mean $\pm$ SD.

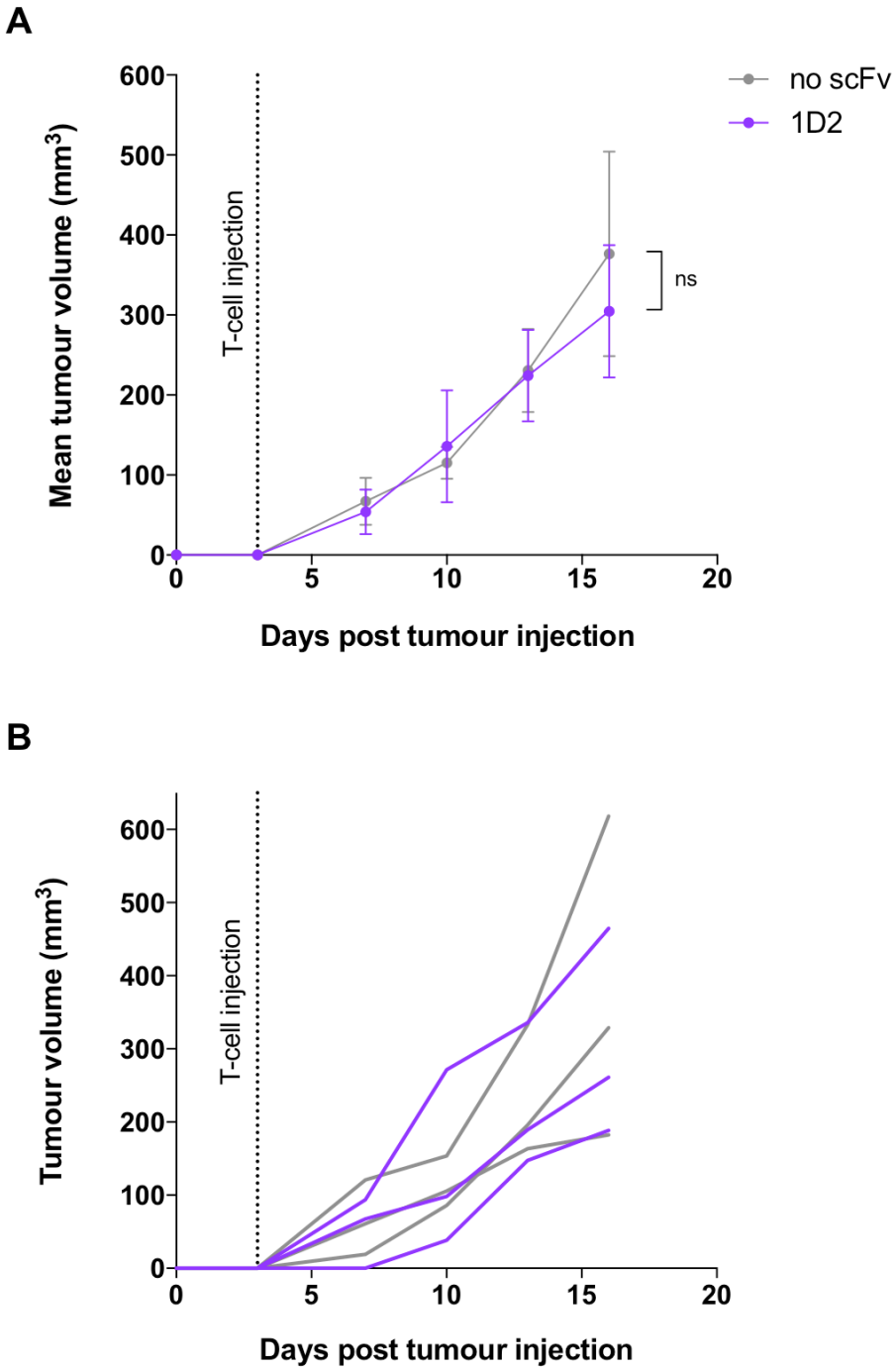

Figure 4.20 – Tumour volumes measured in mice over time in DLD-1 tumour protection study

On day 0, six healthy NSG mice were injected subcutaneously into the flank with $2.5x10^6$ DLD-1 colorectal carcinoma cells each. On day 3, they were each injected with $20x10^6$ 1D2 or 'no scFv' CAR T-cells which were 20.0% (no scFv) and 23.2% (1D2) $CD34^+$ (three mice per treatment group). Tumour size was monitored by regular calliper measurements. Data are represented as **(A)** mean tumour volume in each treatment

group, with data points expressed as mean ± SD, and as **(B)** individual tumour volume measurements in each mouse. In A, the difference in mean tumour volume between the two treatment groups was not significant at any time point, as measured by two-way analysis of variance (ANOVA) with repeated measures by columns (time points) and corrected by Sidak's multiple comparisons test.

4.6 1D2 CAR T-cells do not respond to mouse TEM8

Even though the five anti-TEM8 mAbs that were used to generate CARs bound to both human and mouse TEM8 in their original, Fab form, the affinity of 1D2 for hTEM8 was markedly lower than that of the other four antibodies. Furthermore, while the affinities of the rest of the mAbs for hTEM8 and mTEM8 were very similar, that of 1D2 for mTEM8 was four times lower than its affinity for the human version of the protein[246]. Because of this, and the apparent lack of tumour protective function of 1D2 CAR T-cells, they were tested *in vitro* for responses to both human and mouse TEM8.

In a repeat of the IFNγ ELISA assay, HEK293 cells engineered to express mTEM8 or hTEM8 on their surface were included as targets, alongside parent HEK293 cells, CHO-PR230 and CHO-TEM8. The previously observed pattern of cross-reactivity of all but 1D2 CAR T-cells with CHO-PR230 and HEK293 was seen once again, but all CARs showed a specific response to human TEM8 over the control when overexpressed in CHO cells (**Figure 4.21A**). On the other hand, responses to both human and mouse TEM8 expressed in HEK293 cells were less clear, largely due to the high background response to HEK293 cells alone. 1D2 CAR T-cells did show a weak but clear response to human TEM8, but had no response above background to HEK293 cells expressing mouse TEM8. Even when they were not diluted with mock T-cells in order to equalise their CAR transduction levels with that of the other four, the levels of IFNγ release to the mTEM8-expressing cell line were the same as those observed in the mock T-cell population (**Figure 4.21B**). Similar results were observed in a chromium release assay, where all five CARs mediated human TEM8-specific killing but mouse TEM8-specific killing was less clear because of high background

levels of lysis to HEK293 cells, even with mock T-cells (**Figure 4.22**). When tested against decreasing concentrations of recombinant hTEM8 or mTEM8 in another IFNγ ELISA (**Figure 4.23**), all CAR T-cells responded to hTEM8, some of them even exhibiting saturation and decrease in IFNγ release above a certain protein concentration. However, while all the other CARs also responded to mTEM8, 1D2 CAR T-cells exhibited extremely low or undetectable IFNγ responses even at the highest concentration of the mouse protein; this was true of both 1D2 CAR T-cells equalised for transduction efficiency and those undiluted with mock T-cells (labelled as 1D2').

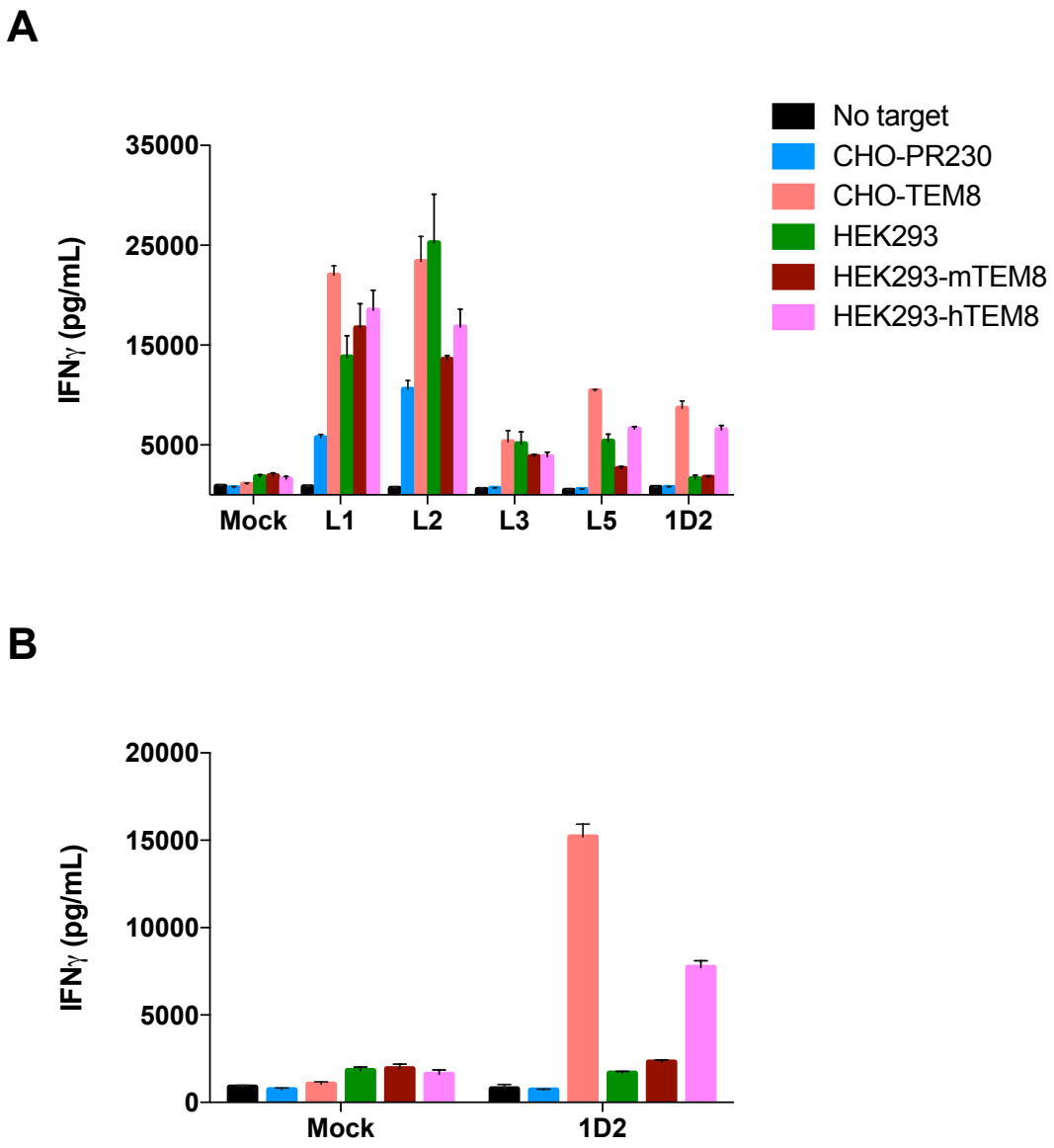

Figure 4.21 – TEM8 CAR T-cell IFNγ release in response to hTEM8 and mTEM8-expressing target cells

Mock or TEM8 CAR-transduced T-cells ($2x10^5$ cells/well) were incubated alone or with indicated target cells ($2x10^4$ cells/well) in a 96-well plate overnight. In **(A),** all CAR T-cells were equalised for CAR transduction efficiency by being diluted with appropriate amounts of mock T-cells, as normally done for all functional assays. In **(B),** 1D2 CAR T-cells undiluted with mock T-cells were also tested at the same time. Following the overnight incubation, supernatants were assayed by IFNγ ELISA and the resulting T-cell IFNγ production expressed in pg/mL. All data points were measured in triplicate and expressed as mean + SD.

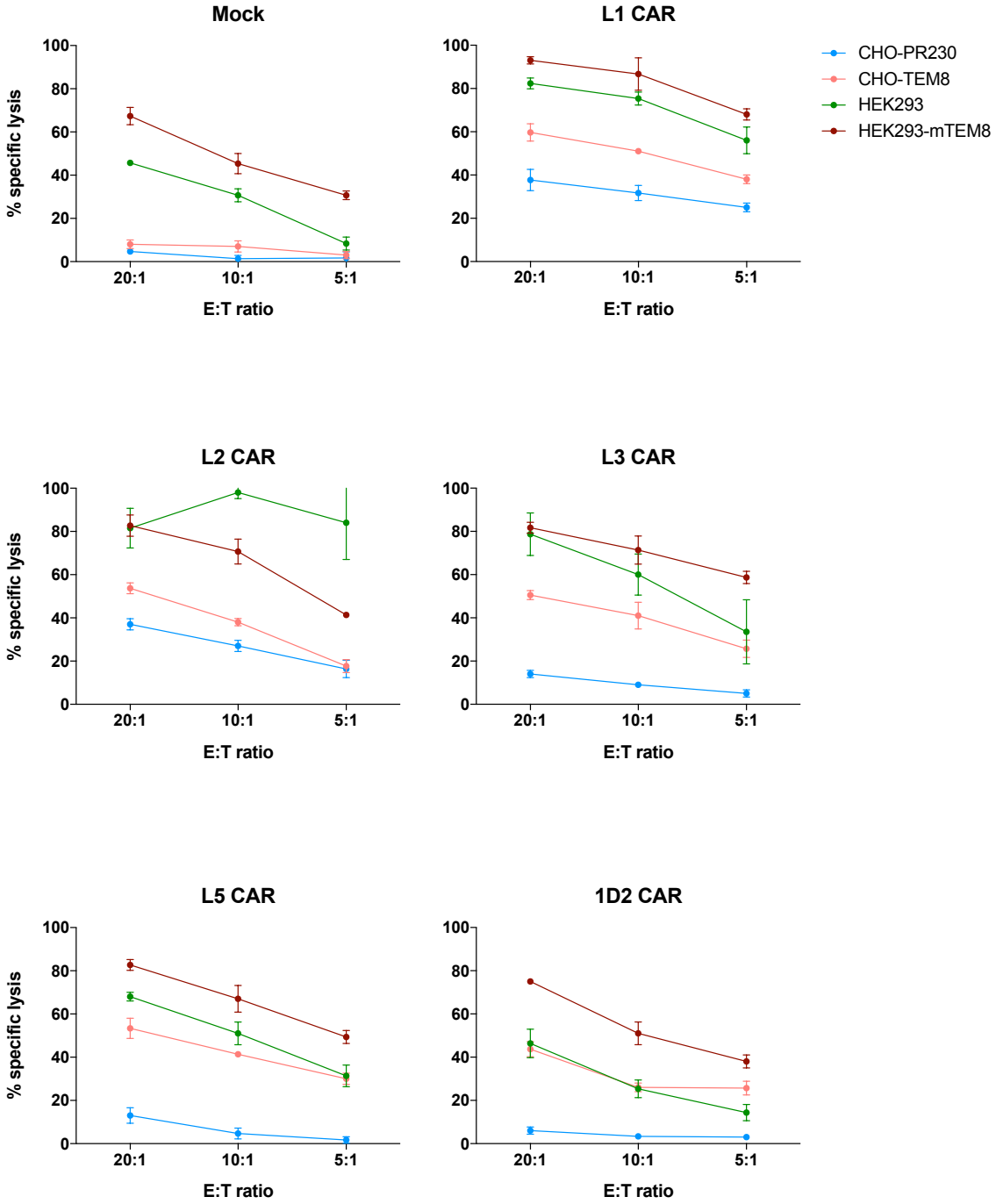

Figure 4.22 – Specific cytotoxicity of TEM8 CAR T-cells in response to hTEM8- and mTEM8-expressing target cells

Mock or TEM8 CAR-transduced T-cells were incubated at decreasing effector:target (E:T) ratios with indicated chromium-labelled target cells ($2.5x10^3$ target cells/well of a 96-well plate), and supernatants harvested and analysed for released chromium after 12 hours. % specific lysis for each target was calculated from spontaneous (targets alone) and maximum lysis values (targets incubated with 1% sodium dodecyl-sulphate). All data points were measured in triplicate and expressed as mean ± SD.

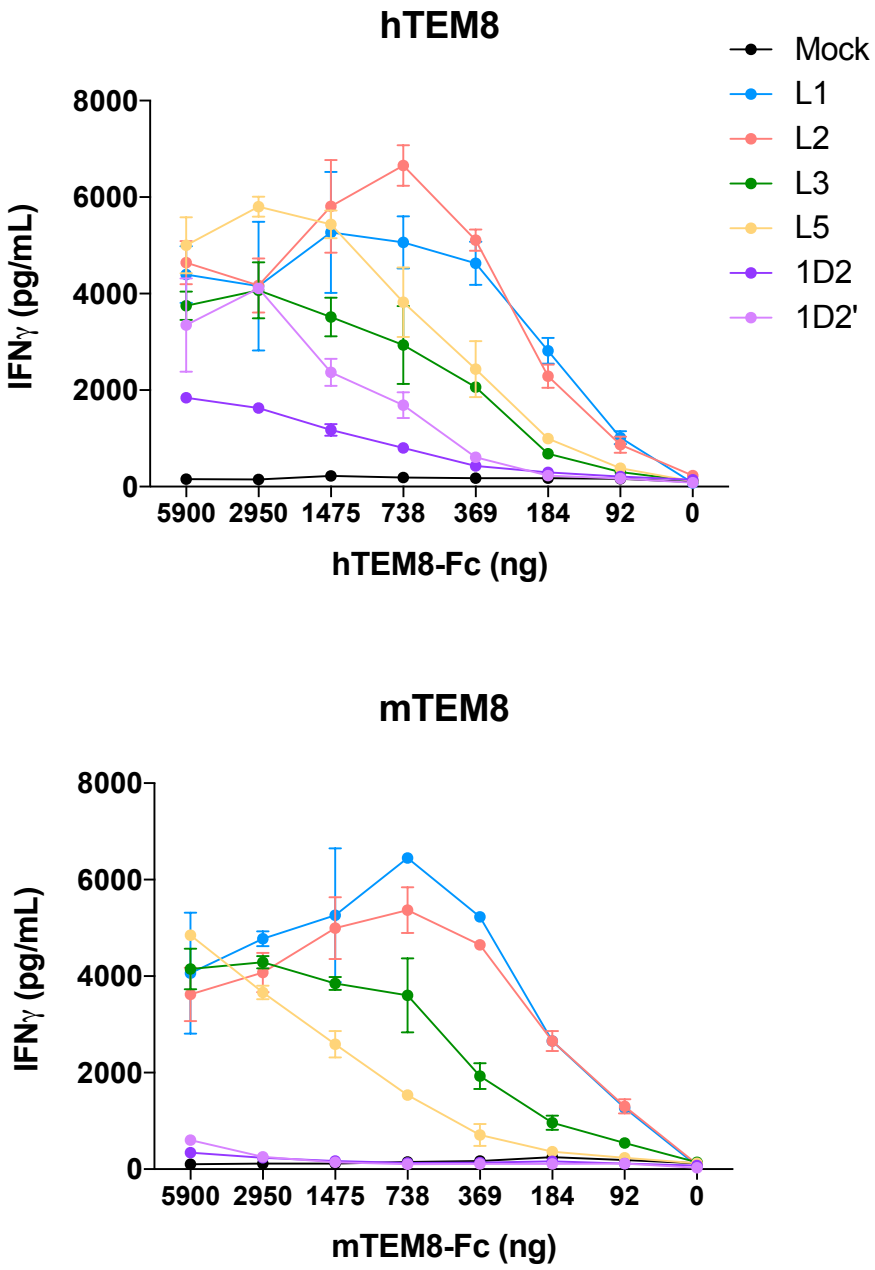

Figure 4.23 – TEM8 CAR T-cell IFNγ release in response to decreasing concentrations of recombinant hTEM8 and mTEM8 protein

Mock or TEM8 CAR-transduced T-cells ($2x10^5$ cells/well) were incubated in a 96-well plate overnight with decreasing concentrations of recombinant hTEM8-Fc (top) or mTEM8-Fc (bottom). All CAR T-cells were equalised for CAR transduction efficiency by being diluted with appropriate amounts of mock T-cells, as normally done for all functional assays, but 1D2 CAR T-cells undiluted with mock T-cells (1D2') were also tested at the same time. Following the overnight incubation, supernatants were assayed by IFNγ ELISA and the resulting T-cell IFNγ production expressed in pg/mL. All data points were measured in triplicate and expressed as mean ± SD.

In the assays described above which utilised cells as targets, a very high background T-cell response was observed to HEK293; it was therefore difficult to tell whether the CAR T-cells responded specifically to HEK293-mTEM8 or if the responses seen were due to their already high reactivity to the parent cell line. As a final test of CAR T-cell recognition (or lack thereof) of mTEM8 expressed on cell surface, LS174T cells were transduced with a GFP^+ mTEM8 lentiviral construct as described in section 2.4.3. The transduction was successful, with the newly obtained LS174T-mTEM8 cells expressing high levels of GFP post-transduction and staining positive for TEM8 surface expression using the L2 mAb (**Figure 4.24**). The parent TEM8-negative LS174T cells were the only target to which none of the TEM8 CAR T-cells previously responded, making this cell line the ideal negative control. All five CAR T-cells were then tested for IFNγ release in the presence of LS174T or LS174T-mTEM8 cells, and while none of them responded to the parent cell line, all but 1D2 CAR T-cells produced IFNγ in response to LS174T-mTEM8 (**Figure 4.25**). L1 and L2 CARs were the highest responders, as observed before, but L3 and L5 CAR T-cells also produced substantial amounts of the cytokine. On the other hand, 1D2 CAR T-cell responses to LS174T-mTEM8, whether equalised for transduction efficiency or not, were not significantly raised above background levels observed for mock T-cells. Finally, in a chromium release assay using the same T-cells and targets (**Figure 4.26**), specific cytotoxicity to the mTEM8-expressing cell line was exhibited by L1, L2, L3 and L5 CAR T-cells. The 1D2 CAR, however, did not induce specific killing of LS174T-mTEM8, confirming the inability of this CAR to elicit a T-cell response to the mouse version of the target protein. While disappointing, this result helped explain the previous lack of anti-tumour response in 1D2 CAR-treated mice,

and established that the therapeutic efficacy of 1D2 CAR T-cells would have to be tested in alternative animal models that are beyond the scope of this thesis.

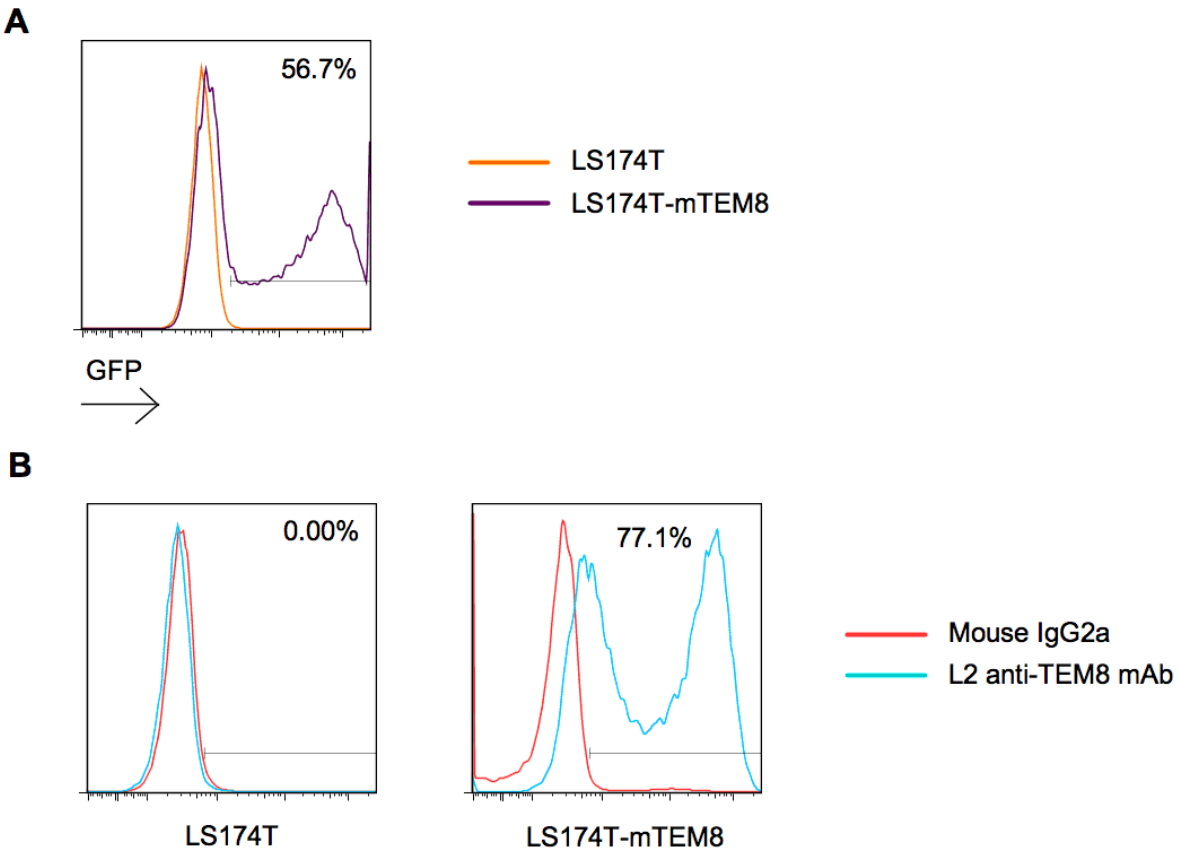

Figure 4.24 – The results of the transduction of LS174T cells with a GFP$^+$ lentiviral mTEM8 gBlock construct

LS174T cells were transduced with a green fluorescent protein (GFP)-positive mTEM8 lentiviral construct, left to recover for 2-3 days, and both the parent LS174T and the newly generated LS174T-mTEM8 cells analysed for GFP and TEM8 expression. **(A)** Both cell lines were analysed for transduction efficiency by flow cytometry. The presence of a GFP marker in the lentiviral vector allowed for the detection of successfully transduced target cells in the FITC channel. **(B)** Both cell lines were labelled with the TEM8-specific L2 mAb (cross-reactive with both human and mouse TEM8; blue line), or with the mouse IgG2a isotype control (red line), before being labelled further with the secondary fluorophore-conjugated anti-mouse IgG. TEM8 expression on the cells was then assayed by flow cytometry.

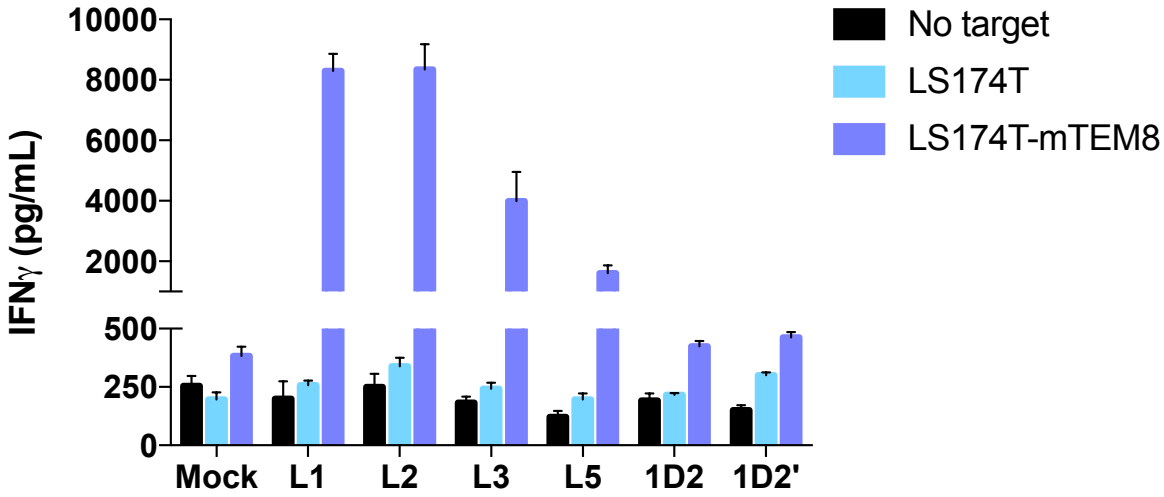

Figure 4.25 – TEM8 CAR T-cell IFNγ release in response to LS174T cells with or without surface mTEM8 expression

Mock or TEM8 CAR-transduced T-cells ($2x10^5$ cells/well) were incubated alone or with indicated target cells ($2x10^4$ cells/well) in a 96-well plate overnight. All CAR T-cells were equalised for CAR transduction efficiency by being diluted with appropriate amounts of mock T-cells, as normally done for all functional assays, but 1D2 CAR T-cells undiluted with mock T-cells (1D2') were also tested at the same time. Following the overnight incubation, supernatants were assayed by IFNγ ELISA and the resulting T-cell IFNγ production expressed in pg/mL. All data points were measured in triplicate and expressed as mean + SD.

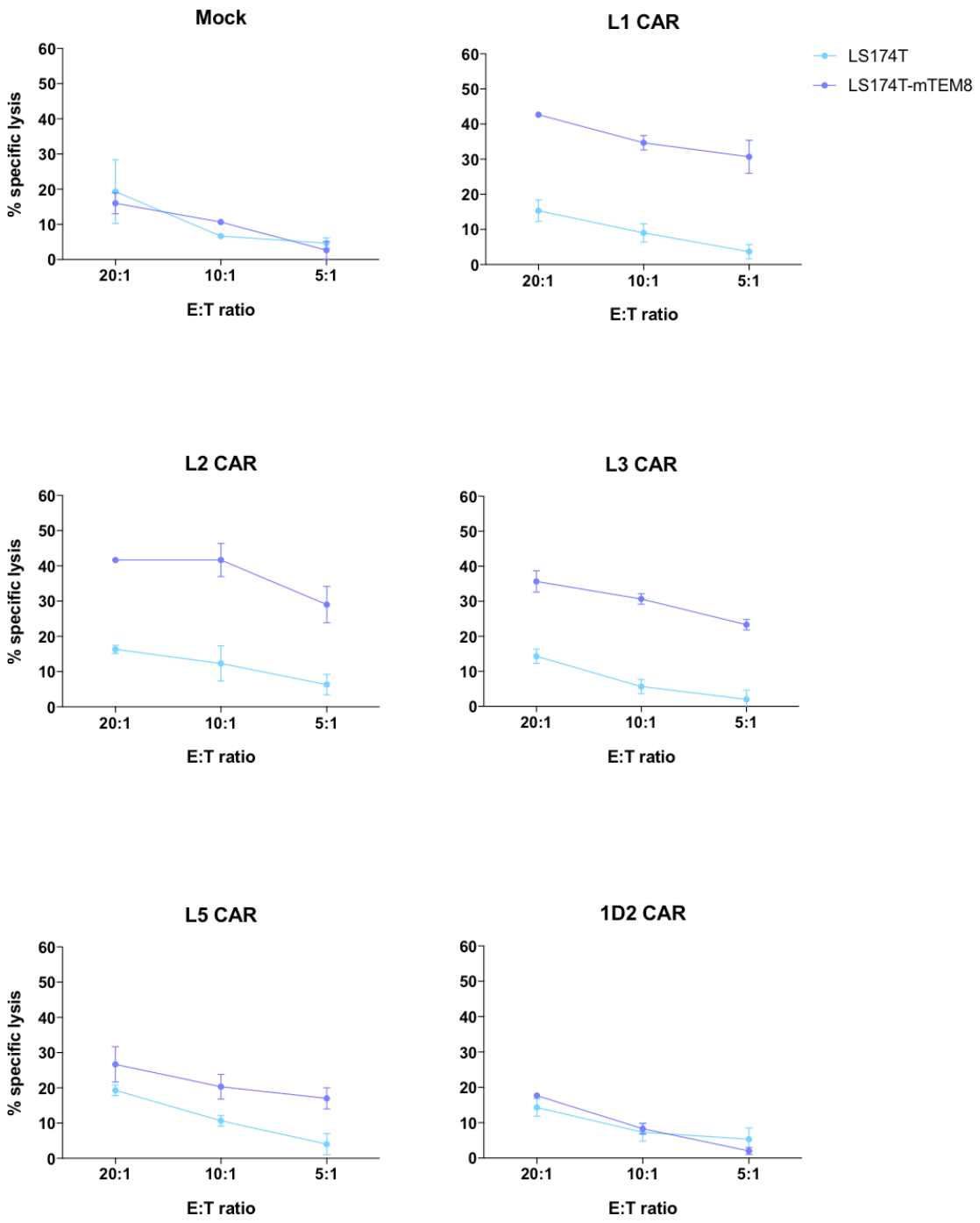

Figure 4.26 – Specific cytotoxicity of TEM8 CAR T-cells in response to LS174T cells with or without surface mTEM8 expression

Mock or TEM8 CAR-transduced T-cells were incubated at decreasing effector:target (E:T) ratios with indicated chromium-labelled target cells ($2.5x10^3$ target cells/well of a 96-well plate), and supernatants harvested and analysed for released chromium after 12 hours. % specific lysis for each target was calculated from spontaneous (targets alone) and maximum lysis values (targets incubated with 1% sodium dodecyl-sulphate). All data points were measured in triplicate and expressed as mean ± SD.

4.7 Discussion

In this chapter the five TEM8 CARs were tested for their safety and persistence in the peripheral circulation of healthy mice, demonstrating that L2 and possibly L3 CARs were occasionally toxic to the treated animals; when not exhibiting toxicity, these along with L1 and L5 CARs were for the most part lost from the circulation within several days. 1D2 CAR T-cells, on the other hand, appeared safe and persisted in the blood for the duration of each experiment. However, when they were tested in mice following a tumour challenge, they failed to confer any protection from tumour progression, which was subsequently discovered to be a possible result of the inability of 1D2 CAR T-cells to recognise the mouse version of the TEM8 protein. Although this CAR is clearly capable of responding to human TEM8, without a TEM8 knock-in mouse available it is not possible to test the therapeutic potential (and to revisit the potential toxicity) of this agent in mouse studies.

4.7.1 Toxicity of high-affinity TEM8 CARs in healthy mice

Of all the TEM8 CARs tested, the only evidence of overt toxicity was seen for the L2 and, in one instance, the L3 CAR. The severity of the observed symptoms in L2 CAR-injected mice, both in the single C57BL/6 mouse and the three NSG mice which exhibited them and had to be culled as a consequence, indicated that L2 CARs may not be a safe therapeutic option under any circumstance. However, not every toxicity study showed adverse events in L2 CAR-infused mice, much like not every treatment is toxic to each patient it is administered to – this made the establishment of the underlying cause of the toxicity an important step towards deciding whether this CAR,

or indeed any TEM8 CAR, could be safely administered in human clinical trials in the future.

The rapid onset of toxic symptoms in the affected mice suggested a possible cytokine storm. The reduced mobility, hunched posture and ruffled fur observed in all of the affected animals were in agreement with previous studies which reported similar symptoms when antibody or CAR T-cell injections given to mice resulted in CRS[307,329–331]. It was unfortunate that, due to the need for immediate culling, plasma samples for cytokine analysis could not be obtained from the four mice experiencing L2 CAR-induced toxicity. Nevertheless, the samples taken from other mice for comparison were tested as described in the preceding sections for the presence of cytokines most commonly associated with mouse CRS[307,326–330]. It was interesting to note that, even when mice did not exhibit overt toxic effects, L2, L3 and to some extent L1 CAR T-cells were still producing increased levels of IFNγ, IL-5 and IL-6 in their circulation on day 4 after T-cell injection (Figure 4.7). These cytokines were all upregulated in the studies of mice developing cytokine storms in response to anti-CD3, anti-CD28 or CAR T-cell treatment[307,329,330], with the levels reported in the CAR T-cell study[307] very similar to those observed in this thesis; IFNγ was highlighted as a particularly important mediator of CRS effects. TNFα is another cytokine observed almost universally to be raised in CRS, however it peaks early and is not normally present beyond the first few hours post-treatment[329]; this could be the reason why it is also not observed in the plasma samples analysed herein. Even though the mice that the samples came from did not actually exhibit toxicity, the presence of the cytokines in L2, L3 and to a lesser extent

L1 CAR-treated animals points to the possibility of occult responses by high-affinity TEM8 CARs even when overt toxicity is absent.

In the study of 2nd generation CD19 CAR T-cells in mice with B-cell lymphoma referred to above[307], 75% of mice receiving high CAR T-cell doses developed the previously described CRS symptoms and were culled within 2-4 days; those receiving lower doses of the CAR (<$5x10^6$ CAR-positive T-cells) developed the same symptoms in a milder form and eventually recovered. Similarly, the mice which exhibited toxicity in response to TEM8 CAR treatment in this thesis all received close to or well above $5x10^6$ CAR-expressing T-cells within the T-cell populations infused into them (sections 4.1 and 4.3) and developed signs of CRS within the first 24h. However, the highest numbers of L2 or L3 CAR T-cells given to mice did not mediate toxicity (sections 4.2 and 4.4).

Contrary to the findings in this thesis, a study of natural killer group 2D (NKG2D) CARs in various mouse models concluded that the presence of the host immune system was necessary for CRS-like symptoms to develop, reporting that NSG mice injected with $20x10^6$ NKG2D CAR T-cells remained healthy while the less immunocompromised mice developed cytokine storms[331]. This brings into question the toxicity observed in NSG mice in the experiment described here (section 4.3) suggesting that it may not have been CRS, or alternatively that the mechanisms involved may be more complex and may differ depending on the CAR and mouse model used. From the rapidity of symptom onset, appearance and behaviour of the mice and limited evidence of cytokines present in the plasma of other mice several days after treatment, CRS is still

the most likely explanation for the toxic effects observed in the animal experiments described in this chapter. This is supported by the finding that there was no observable pathology in the organs of the treated mice which exhibited adverse effects compared to those that did not (Figure 4.11) – something that has also been reported by the study referred to above[331].

Curiously, no toxicity was reported in the recently published study of 2nd and 3rd generation L2 CAR T-cells for the treatment of TNBC in mice[325]. It should be noted that, while both CARs were tested in several anti-tumour experiments with no adverse effects, only 3rd generation L2 CARs were injected into healthy immunocompromised mice and tracked as part of a toxicity study. It had already been stated that the 3rd generation L2 CARs had a higher activation threshold than their 2nd generation counterparts, requiring higher levels of antigen for response[325]. This could perhaps explain the reason why no adverse events were observed, as TEM8 expression in healthy mice, if present, is expected to be low[246]. Nonetheless, these reported findings were surprising in light of our own experience with the L2 CAR. In addition, we have heard from another group using the L2 anti-TEM8 antibody for immunotherapy studies in mice who also found toxicity, although these data are yet to be published.

4.7.2 TEM8 expression on healthy mouse tissue

Apart from CRS-like symptoms in some mice treated with L2 and L3 CARs, another consistently observed effect in the *in vivo* studies described in this thesis was the rapid selective depletion of CAR-expressing ($CD34^+$) T-cells from mouse peripheral circulation for all but 1D2 CAR T-cells. Even though all injected T-lymphocytes were

lost from the blood over time to a greater or lesser extent, 1D2 CAR T-cells were the only ones to persist at the end of each experiment, with the notable exception of the CD4 subset of L2 CAR T-cells in one mouse in the study described in section 4.2. The high *in vitro* responses of all but the 1D2 CAR to cells expressing very low levels of TEM8, coupled with their rapid loss from murine circulation, suggests that the TEM8 CAR T-cells were recognising low-level expression of their target on healthy mouse tissue and being retained in these tissue sites. In fact, it is possible that both the cytokine storms and the loss of CAR T-cells from peripheral blood were a result of TEM8 recognition by the high-affinity CARs. The possibility of TEM8 CAR T-cells responding to a target unrelated to TEM8 cannot be fully discounted – nevertheless, the persistence of the high-affinity L2 CAR T-cells in TEM8 KO mice, and their concurrent elimination from the circulation of WT animals, points to TEM8 expression in healthy tissues being at least one of the major reasons for the loss of CAR T-cells from the circulation.

Despite early studies reporting that TEM8 is solely detectable on tumour-associated vasculature, mounting evidence suggests that its expression is in fact much more widespread, even if it is comparatively low in normal tissue. TEM8 transcripts have been detected by RT-PCR on normal endothelial and smooth muscle cells[324], in various digestive tissues and on a range of vital organs including heart, lungs and brain of both humans[332] and mice[333], as well as on stem cells[334] and circulating endothelial cells[335]. It has been suggested, however, that inter-individual variability of TEM8 expression is high, and that its levels are likely to be different in various normal tissues as well as between normal and tumour tissue[332]. It is therefore reasonable to expect

low-level expression of the TEM8 protein on healthy murine cells which cannot be detected by staining techniques such as immunofluorescence[246]. As discussed already in the previous chapter, TEM8 CAR T-cells other than the low-affinity 1D2 CAR may be highly sensitive even to very low levels of target antigen undetectable by antibody staining. Therefore, the toxicity as well as the selective loss of TEM8 CAR-expressing T-cells observed in the experiments described herein are most likely a direct result of T-cell recognition of their intended target on an as yet unidentified healthy tissue.

4.7.3 Eye toxicity in TEM8 KO mice

Quite apart from the toxicity observed in WT mice, an adverse effect specific to the C57BL/6 TEM8 KO strain was the development of a swollen and sore left eye, which gradually reduced in size over time but became cloudy in appearance, resembling a cataract. This effect only became apparent after CAR T-cell injection but did not seem to be related to any one treatment, as mice injected with both TEM8 CARs and the non-specific CAR control developed the same reaction. It was also acknowledged on closer inspection that, in general, healthy TEM8 KO mice had a less elongated head and slightly more protruding eyes than their WT littermates, which became very pronounced in those that developed the eye anomaly following CAR T-cell injection. While entirely unexpected, this adverse effect can perhaps be explained by the similarities between TEM8 KO mice and patients with a rare autosomal recessive condition known as GAPO syndrome.

GAPO is the acronym derived from four principal manifestations of the condition – growth retardation, alopecia, pseudoanodontia (tooth eruption failure) and optic

atrophy – all of which arise due to mutations in human TEM8[336]. The tissues of patients with GAPO syndrome demonstrate abnormal extracellular matrix (ECM) depositions and extensive involvement of connective tissue in disease pathology[336], which is in keeping with the identified role of TEM8 in collagen binding and cell migration. In addition, ECM accumulation and dental abnormalities in GAPO patients are recapitulated in TEM8 KO mice[245] and, even though the phenotype in mice is less severe than that in humans[337], it is entirely possible that the animals can also develop the progressive optic atrophy exhibited by patients with the TEM8 mutation. In fact, a study of TEM8 KO mice has already shown that these homozygous mutants can display growth retardation, a shortened skull with a protruding forehead, and midfacial hypoplasia which is characterised by large and bulging eyes[338]. In this study the affected eyes of TEM8 KO mice also appeared cloudy[338], further confirming that optical anomalies are a very possible scenario.

The appearance of the affected TEM8 KO mice described in this thesis bore the most resemblance to a patient with GAPO syndrome with left-sided optic atrophy who was reported to have developed cerebral arterial atherosclerosis[339] as well as, curiously, to a patient with Apert syndrome who, among other things, exhibited midfacial hypoplasia and corneal opacity in the left eye[340]. The resemblance to the latter was particularly striking. Apert syndrome is caused by a mutation in the fibroblast growth factor receptor-2 (FGFR2) gene, which causes prolonged signalling of the protein and leads to the described malformations[341]. Furthermore, it has been shown that TEM8 knockout mediates complex crosstalk mechanisms in primary fibroblasts and enhances one of the signalling pathways of the FGFR2 ligand, FGF2[342]. While it is

impossible to say with certainty how, or indeed if, CAR T-cell injection triggered the ocular defects in some of the TEM8 KO mice, the described evidence points to the heavy involvement of the KO phenotype and the complex interactions of signalling molecules and growth factors brought about by the TEM8 genetic mutation.

4.7.4 Tumour protection by TEM8 CARs

Despite successful recognition of TEM8 overexpression *in vitro* by the 1D2 CAR, and the promising safety and *in vivo* persistence profile of 1D2 CAR T-cells, they failed to provide protection from tumour challenge in mice due to their subsequently discovered inability to recognise mouse TEM8. This had not been anticipated before, as human and mouse TEM8 share 99% amino acid sequence homology in the extracellular binding region (Brad St Croix, personal communication) and all five originating anti-TEM8 antibodies were fully cross-reactive with both. Nevertheless, the affinity of the 1D2 antibody in its Fab form, already much weaker for hTEM8 than that of the other four Fabs, was a further four times weaker for mTEM8 than for the human version of the protein[246] (Table 3.1). This potentially resulted in a CAR that could not recognise expression of the mouse protein at all. Even though sequence homology between hTEM8 and mTEM8 is very high, an antibody has been developed which recognises only human and not mouse TEM8 by binding a different epitope to that bound by cross-reactive antibodies[324]. This suggests that the 1D2 antibody also binds to a region that is only partially shared between human and mouse TEM8, resulting in its very low affinity for mTEM8 and the observed selectivity for hTEM8 of the derived CAR. While this prevents the 1D2 CAR from being studied in a standard mouse model, where any implanted tumour would necessarily generate vasculature expressing mouse rather

than human proteins, generating a human TEM8 knock-in mouse model could be a promising way forward for exploring the anti-tumour efficacy (and potential toxicity) of this CAR in pre-clinical studies. Should it prove successful, its low-affinity hTEM8-targeting scFv moiety may be a significant advantage, allowing it to respond only to tissues overexpressing TEM8 – such as tumour vasculature – and spare any low-level TEM8 expressed on normal cells.

In contrast to previously reported findings, a study has recently shown that the slower tumour growth in TEM8 KO mice is related to their malnutrition resulting from misaligned incisors; when soft food was provided as rescue, these mice regained both their weight and normal tumour growth rates exhibited in WT littermates[343]. Despite this, and the consequent assertion that TEM8 is not essential for tumour growth[343], targeting the vasculature of various solid tumours with both anti-TEM8 antibodies[246] and TEM8 CAR T-cells[325] has successfully resulted in tumour regression. TEM8 CAR T-cells were able to control both patient-derived TNBC xenografts and tumours formed from metastatic TNBC cells, however they were not curative[325]. Importantly, both the antibody and the CAR T-cells used in the studies above were derived from the L2 Fab. While this did not result in toxicity in its naked antibody form[246], the experimental data presented in this thesis argue that L2 CAR T-cells can be toxic due to their potent effector function and heightened sensitivity to low-level TEM8 expression on normal tissue. Because of this, and the rapid selective loss of all high-affinity TEM8 CARs from peripheral circulation of the mice, it can be argued that the lower affinity 1D2 CAR may prove to be the most effective for targeting this protein.

5 GENERATION AND SUPPRESSIVE POTENTIAL OF CAR-ENGINEERED T_{REGS} TARGETING CLEC14A IN INFLAMED LIVER

As discussed in detail in sections 1.6 and 1.7 of the Introduction, there is increasing interest in using immunotherapy to target autoimmune and inflammatory conditions, especially those with high unmet clinical need such as certain conditions of the liver. Adoptive transfer of Tregs to treat a variety of autoimmune diseases has already proven successful in animal studies and is being increasingly trialled in the clinic. Antigen-specific Tregs redirected towards a target in the inflammatory site have also proven superior to polyclonal Tregs in various mouse models of autoimmune conditions. However, the general paucity of known autoantigens or disease markers in inflammatory conditions renders the generation of antigen-specific Tregs difficult, with only the suboptimal polyclonal Treg ACT currently being tested in patients. This problem is present in autoimmune diseases of the liver too, where there is only one pilot feasibility study of autologous polyclonal Treg infusions into patients with AIH currently being carried out[344]. The aim of this part of the thesis, therefore, was to examine the therapeutic potential of antigen-specific Tregs in PSC, a debilitating inflammatory liver condition which is strongly associated with other autoimmune diseases and results in the need for liver transplantation in more than half of affected patients[255]. The expression of a novel TEM, CLEC14A, was hypothesised to be raised on the surface of liver endothelial cells in PSC due to the previously discovered association of this TEM with vasculature characterised by disturbed blood flow and low shear stress[225]. If expressed, this protein would provide a promising target for CLEC14A-specific CAR-engineered Tregs, which would in turn allow the examination

of the suppressive action of the Tregs *in vitro* and of their therapeutic efficacy in a PSC mouse model.

5.1 CLEC14A is expressed in human inflamed liver

To determine whether CLEC14A is expressed in the livers of patients with inflammatory hepatic diseases, and specifically PSC, fixed liver sections were obtained from patients with PSC, alcoholic liver disease (ALD) and from those whose donor livers were rejected for transplantation. The sections originated from four patients for each of the three conditions, with the latter two selected as additional examples of hepatic inflammation or distress for comparison with PSC. Normal (non-inflamed) liver sections from two patients were also obtained as part of tissue arrays.

Following immunohistochemical staining and imaging of all samples for the endothelial marker CD31 and for CLEC14A, as described in section 2.7.1, it was observed that normal liver sections predominantly expressed low or undetectable levels of CLEC14A on the endothelium (**Figure 5.1**). On the other hand, rejected donor livers, as well as those originating from patients with PSC and ALD, all exhibited prominent endothelial CLEC14A staining (**Figure 5.1** and **Figure 5.2**). To ensure the staining was specific, spare sections from each patient sample were treated at the same time with a concentration-matched IgG control for the anti-CLEC14A antibody – all of the control sections were completely free of staining (**Figure 5.3**).

The results obtained showed that CLEC14A was not only expressed on the hepatic endothelium in PSC, but also in other conditions characterised by liver inflammation,

even when the underlying cause of such inflammation is not necessarily known (such as in the case of donor livers which had been rejected). This confirmed the value of CLEC14A as a potential disease marker for future targeted therapies of autoimmune and inflammatory liver diseases. As the focus of this project was on PSC, it next became necessary to examine the expression of CLEC14A in the available PSC mouse model in order to assess its suitability for future studies of therapeutic Tregs.

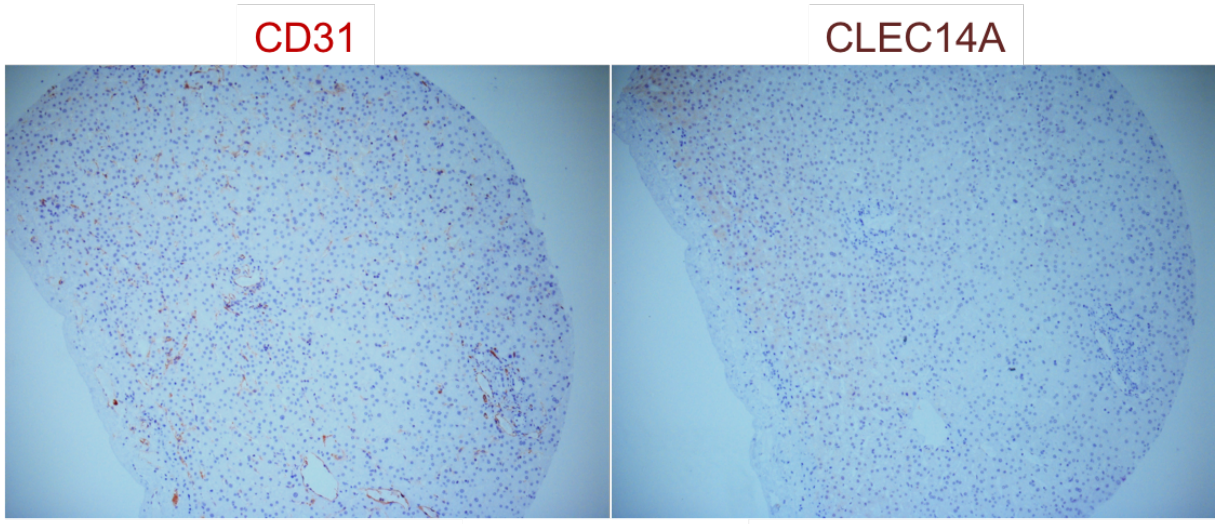

Normal liver 1

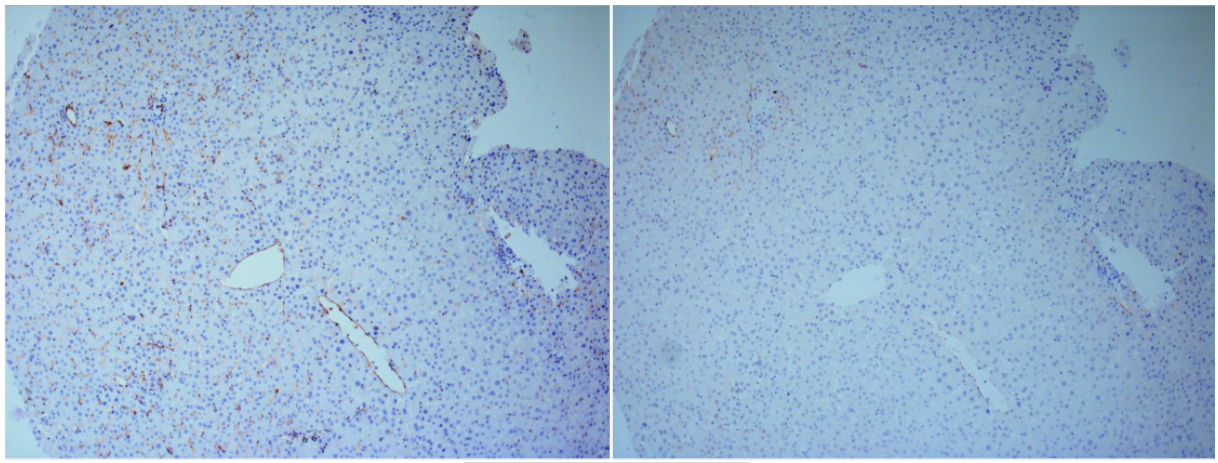

Normal liver 2

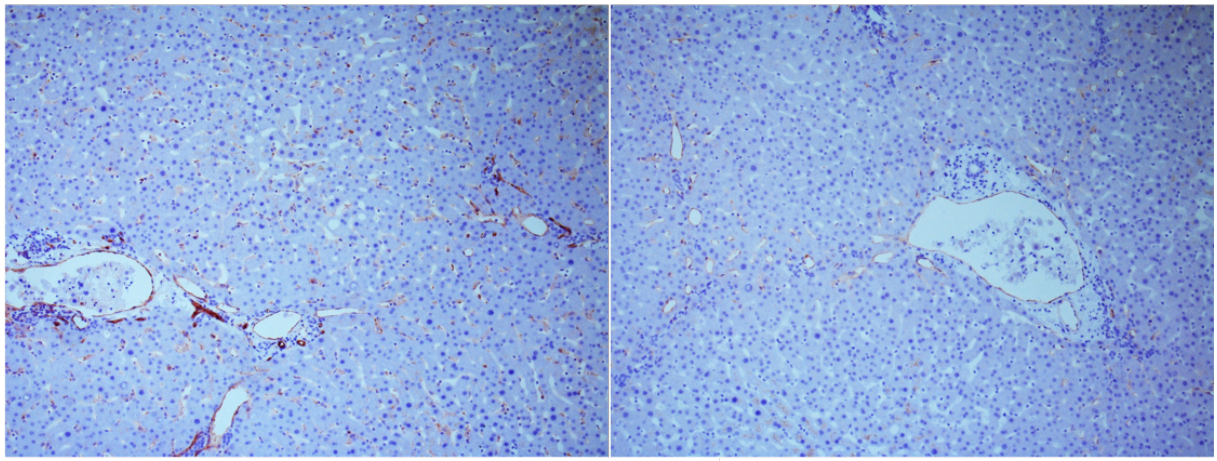

Donor liver

Figure 5.1 – Representative normal and donor human liver sections stained for CD31 and CLEC14A by immunohistochemistry

Fixed sections from non-inflamed (normal) livers and those from donor livers which had been rejected for transplantation were stained by immunohistochemistry for the endothelial marker CD31 (left) or for the C-type lectin CLEC14A (right) and examined by brightfield microscopy. Horseradish peroxidase (HRP) staining (brown) indicates the presence of endothelial cells or CLEC14A respectively. Normal liver sections 1 and 2 originated from two patients whose samples were part of tissue arrays MNO1021 and LVD481 (Pantomics) respectively. Rejected donor liver sections were provided by the Centre for Liver Research (CLR, University of Birmingham). Sections from one donor liver patient are shown here and are representative of samples from four patients.

CD31

CLEC14A

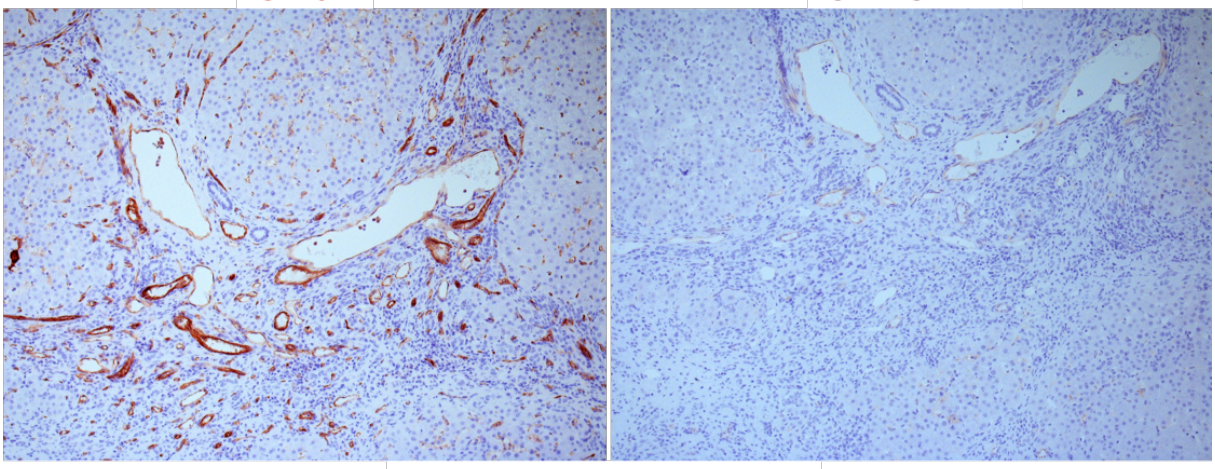

Alcoholic liver disease

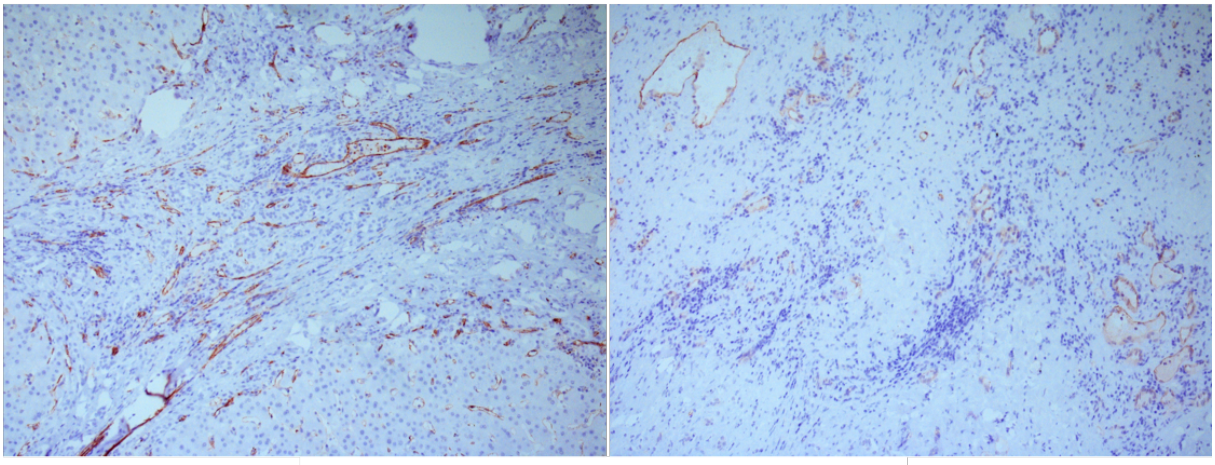

Primary sclerosing cholangitis 1

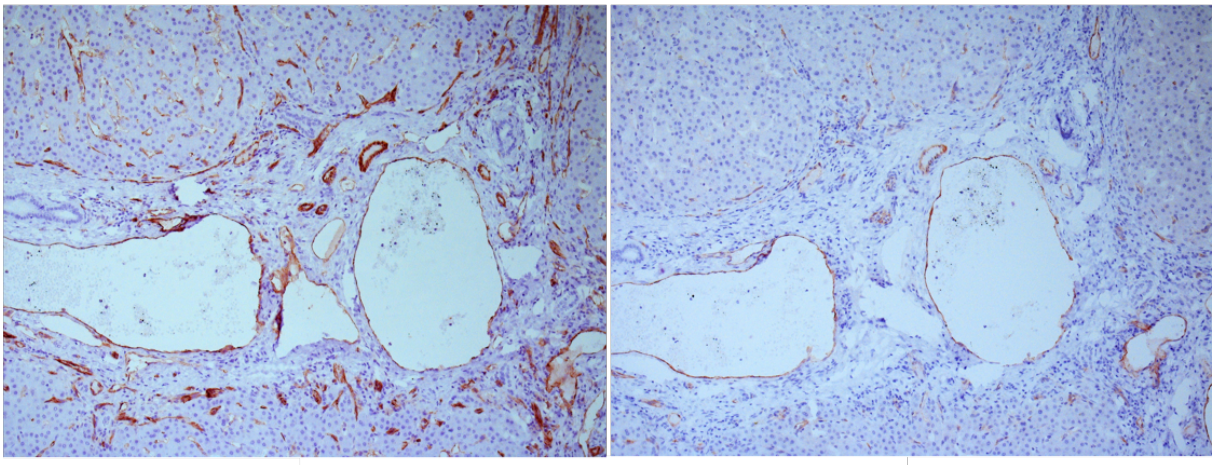

Primary sclerosing cholangitis 2

Figure 5.2 – Representative human liver sections from inflammatory liver conditions stained for CD31 and CLEC14A by immunohistochemistry

Fixed liver sections from patients with alcoholic liver disease (ALD) or primary sclerosing cholangitis (PSC) were stained by immunohistochemistry for the endothelial marker CD31 (left) or for the C-type lectin CLEC14A (right) and examined by brightfield microscopy. HRP staining (brown) indicates the presence of endothelial cells or CLEC14A respectively. All ALD and PSC sections were provided by the Centre for Liver Research (CLR, University of Birmingham). Sections from one patient with ALD and two patients with PSC are shown here and are representative of samples from four patients each.

IgG control staining

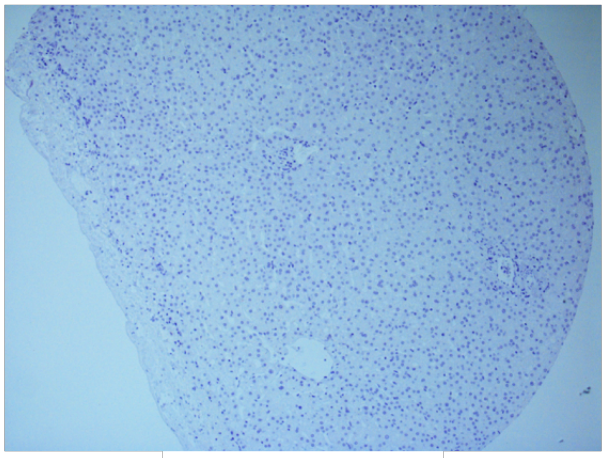

Normal liver 1

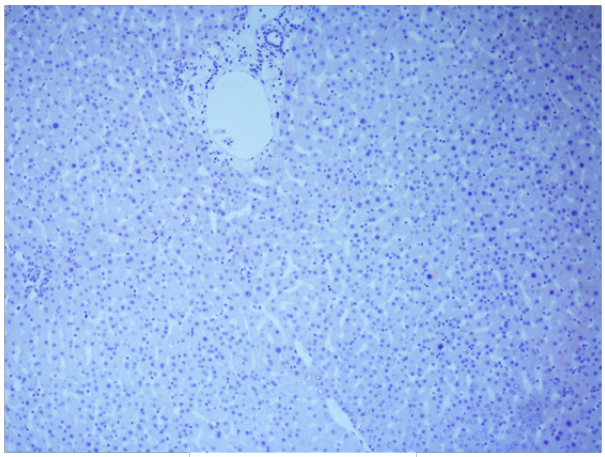

Donor liver

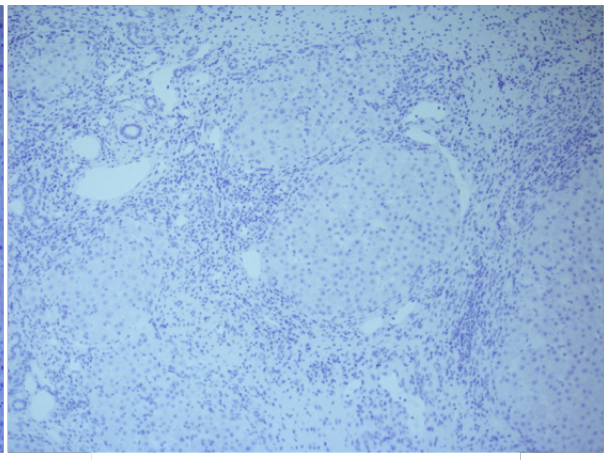

Alcoholic liver disease

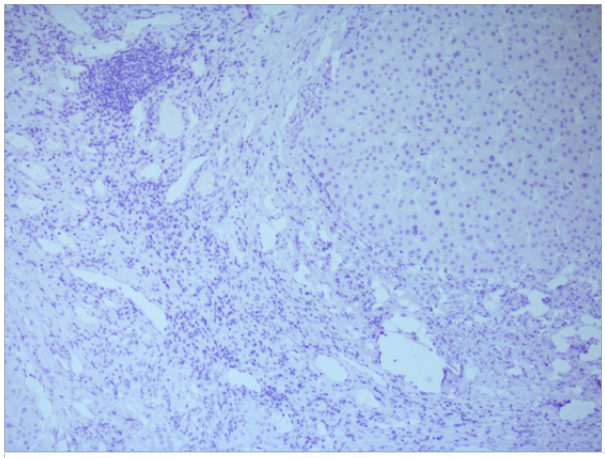

Primary sclerosing cholangitis 1

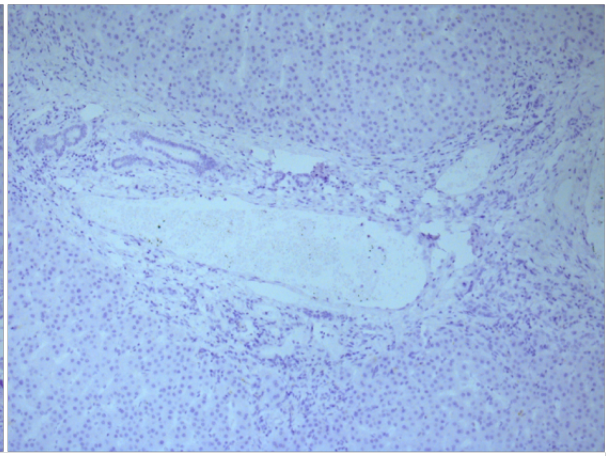

Primary sclerosing cholangitis 2

Figure 5.3 – Representative normal, donor and inflamed human liver sections stained with IgG control for CLEC14A by immunohistochemistry

Fixed sections from non-inflamed (normal) liver, donor livers which had been rejected for transplantation, and livers with ALD or PSC were stained by immunohistochemistry with a concentration-matched IgG control for the anti-CLEC14A antibody alongside corresponding CLEC14A-stained sections shown in Figure 5.1 and Figure 5.2. Donor liver, ALD and PSC sections are representative of samples from four patients each.

5.2 CLEC14A is expressed in the liver of MDR2 KO FVB mice

As described in the Introduction (section 1.6.3), none of the existing mouse models of PSC completely replicate the complex pathology and full course of the disease. Nevertheless, KO mouse models, MDR2 KO chief among them, afford the opportunity to study the condition longitudinally and test potential therapeutic approaches. MDR2 KO mice on FVB background develop a spontaneous PSC-like phenotype[265] which progresses with age and eventually results in HCC[263], making this model reasonably representative of the human condition. The availability of the animal model at the CLR meant that their liver samples were readily obtainable and could be tested for CLEC14A expression on the hepatic endothelium.

Frozen sections from the livers of male MDR2 KO FVB mice of various ages were stained by immunofluorescence for CD31 and CLEC14A as described in section 2.7.2. As evidenced by confocal microscopy imaging, these 5-10 week old mice all expressed CLEC14A on the surface of their liver vasculature, exhibiting co-localisation of the target protein with the endothelial marker CD31 (**Figure 5.4**). The intensity of CLEC14A fluorescence appeared equally strong in both younger and older mice. Mouse sections stained with the IgG control for the anti-CLEC14A antibody only exhibited low levels of non-specific staining, confirming that the CLEC14A expression observed was genuine. In addition, immunofluorescence staining of frozen liver sections from 6-8 week old FVB WT mice showed only low CLEC14A expression in these healthy controls (**Figure 5.5**). It should be noted that the FVB WT sections are only representative of two mice, and further staining of these would need to be carried out to validate the results obtained. Nevertheless, the fact that the observed staining

was similar to very low-level CLEC14A detected in human healthy liver sections (Figure 5.1) suggests that this mouse model provides a good representation of the human condition.

Taken together, these findings established that the relevant disease marker was expressed in the available PSC mouse model and could be further examined as a target for antigen-specific Treg therapy.

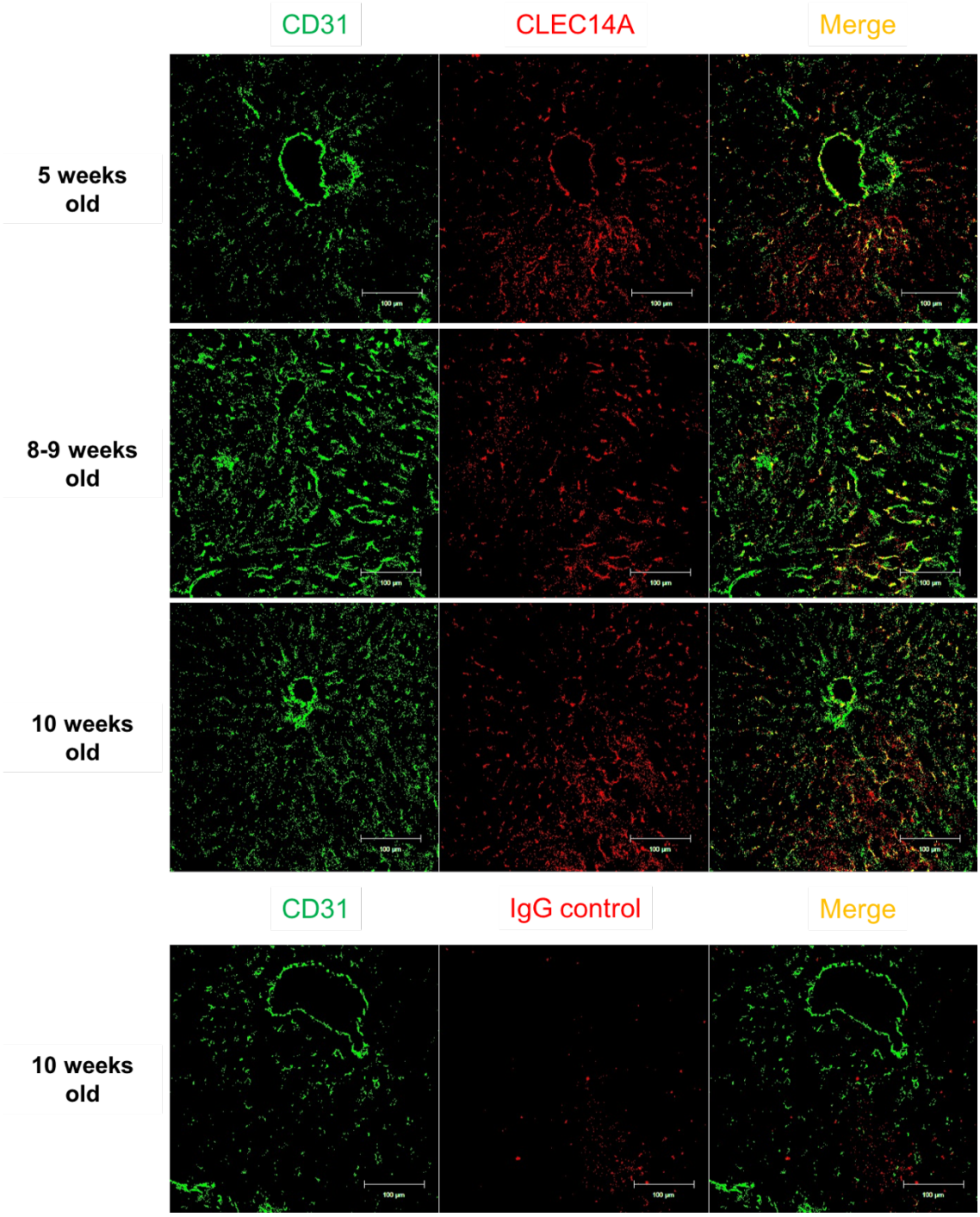

Figure 5.4 – Representative liver sections from MDR2 KO FVB mice of various ages stained for CD31 and CLEC14A by immunofluorescence

Frozen liver sections from male MDR2 KO FVB mice aged 5, 8-9 or 10 weeks were stained by immunofluorescence for the endothelial marker CD31 (green) and CLEC14A or the appropriate IgG control (red) and examined by confocal microscopy. The merged images for each sample are shown, with areas of co-localisation in yellow. The sections shown are representative of one mouse (5 weeks), two mice (8-9 weeks), or three mice (10 weeks). Scale bar, 100μm.

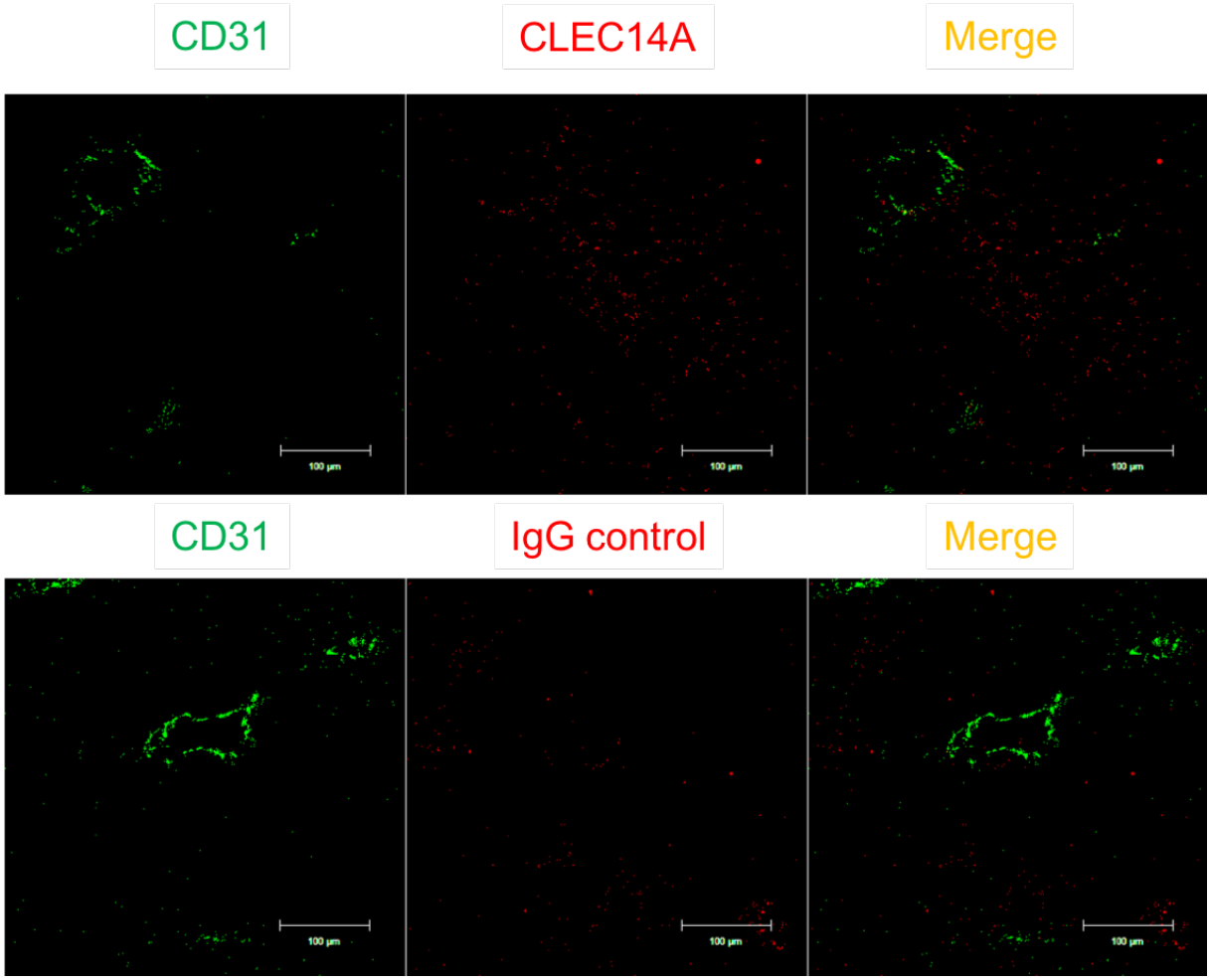

Figure 5.5 – Representative liver sections from 6-8 week old FVB WT mice stained for CD31 and CLEC14A by immunofluorescence

Frozen liver sections from male FVB WT mice aged 6-8 weeks were stained by immunofluorescence for the endothelial marker CD31 (green) and CLEC14A or the appropriate IgG control (red) and examined by confocal microscopy. The merged images for each sample are shown. The sections are representative of two mice. Scale bar, 100μm.

5.3 Human Tregs are successfully engineered to express a CLEC14A CAR

To generate CLEC14A-specific human regulatory T-cells, Tregs were isolated from a donor PBMC population and transduced with a CLEC14A CAR construct, CRT3.2, as described in sections 2.1.3 and 2.4.1 respectively. Following transduction, CAR Tregs (and, when available, mock Treg controls) were stained with a panel of antibodies to examine their phenotype and CAR transduction levels (the panel is detailed in Table 2.2). The gating strategy, together with phenotypic marker and CAR expression levels obtained in one of the representative Treg batches, are shown in **Figure 5.6**. The consistently high proportion of $CD3^+CD4^+$ T-cells obtained after Treg isolation exhibited variable amounts of $CD127^{low}Foxp3^+$ cells present, with the variability seemingly donor-dependent. Nevertheless, the Treg subset was regularly transduced successfully with the CRT3.2 CAR, as evidenced by CD34 expression of the $CD3^+CD4^+CD127^{low}Foxp3^+$ T-cell population.

As previously described in several publications[305,345,346], Treg phenotype is maintained in culture by the inclusion of rapamycin, usually at a concentration of 100nM. When at first the isolated Tregs were expanded without the addition of this immunosuppressive drug, a substantial conventional T-cell (Tconv) outgrowth was observed, as evidenced by the loss of Foxp3 expression and a conversion to a predominantly $CD127^{high}$ T-cell phenotype (**Figure 5.7**, T_{REG} BATCH 1). However, when rapamycin was introduced into a second batch of Tregs, the initial decline in Foxp3 expression which preceded its introduction was significantly slowed down, and the phenotype remained stable for several weeks in culture (**Figure 5.7**, T_{REG} BATCH 2).

Taken together, the data showed that human regulatory T-cells could be successfully isolated, transduced with the desired CAR, and maintained and expanded *in vitro*. Their suppressive potential, however, as well as their advantage over non-transduced Tregs when CLEC14A was present as a target, were yet to be tested.

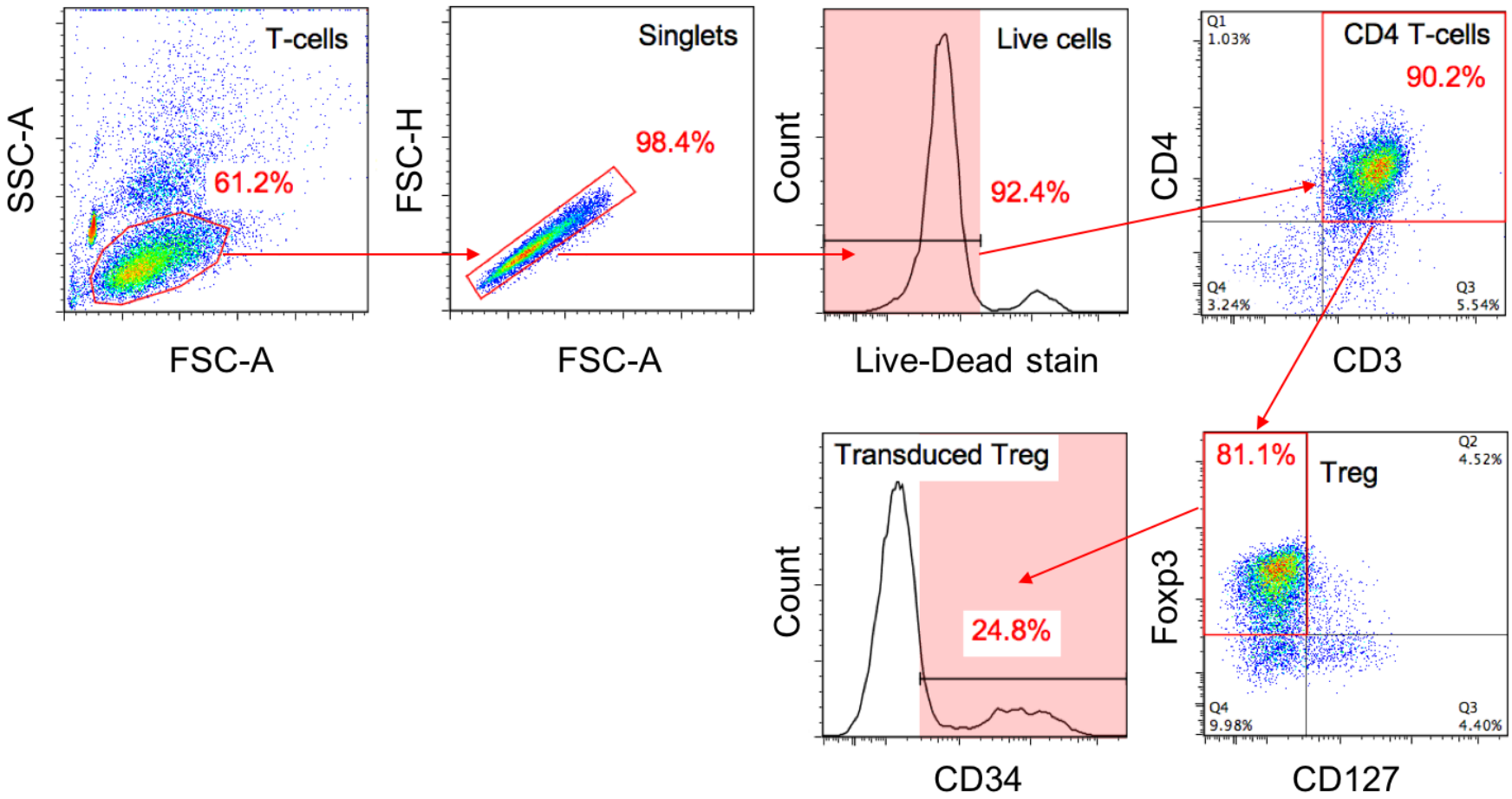

Figure 5.6 – Gating strategy to identify purified Tregs successfully transduced with a CLEC14A CAR

CRT3.2 CLEC14A CAR Tregs, and mock Treg controls if present, were stained with viability dye, anti-CD3, anti-CD4, anti-CD127 and anti-CD34 surface antibodies. The cells were then fixed, permeabilised and stained with the intracellular anti-Foxp3

antibody or its corresponding concentration-matched isotype control and analysed on the flow cytometer, with CD34 acting as a surface marker of CAR expression. The gates were put sequentially on the T-cell population, singlets (to exclude cell clumps), live cells (viability dye-negative), $CD3^{+}CD4^{+}$ and finally $CD127^{low}Foxp3^{+}$ Tregs. Within this final subset, mock Tregs or the appropriate concentration-matched anti-CD34 antibody isotype control were used to determine the position of the CD34-negative population and thus allow correct positioning of the CD34 gate. The Tregs falling within this gate were considered CAR-positive. Data are representative of four different donors.

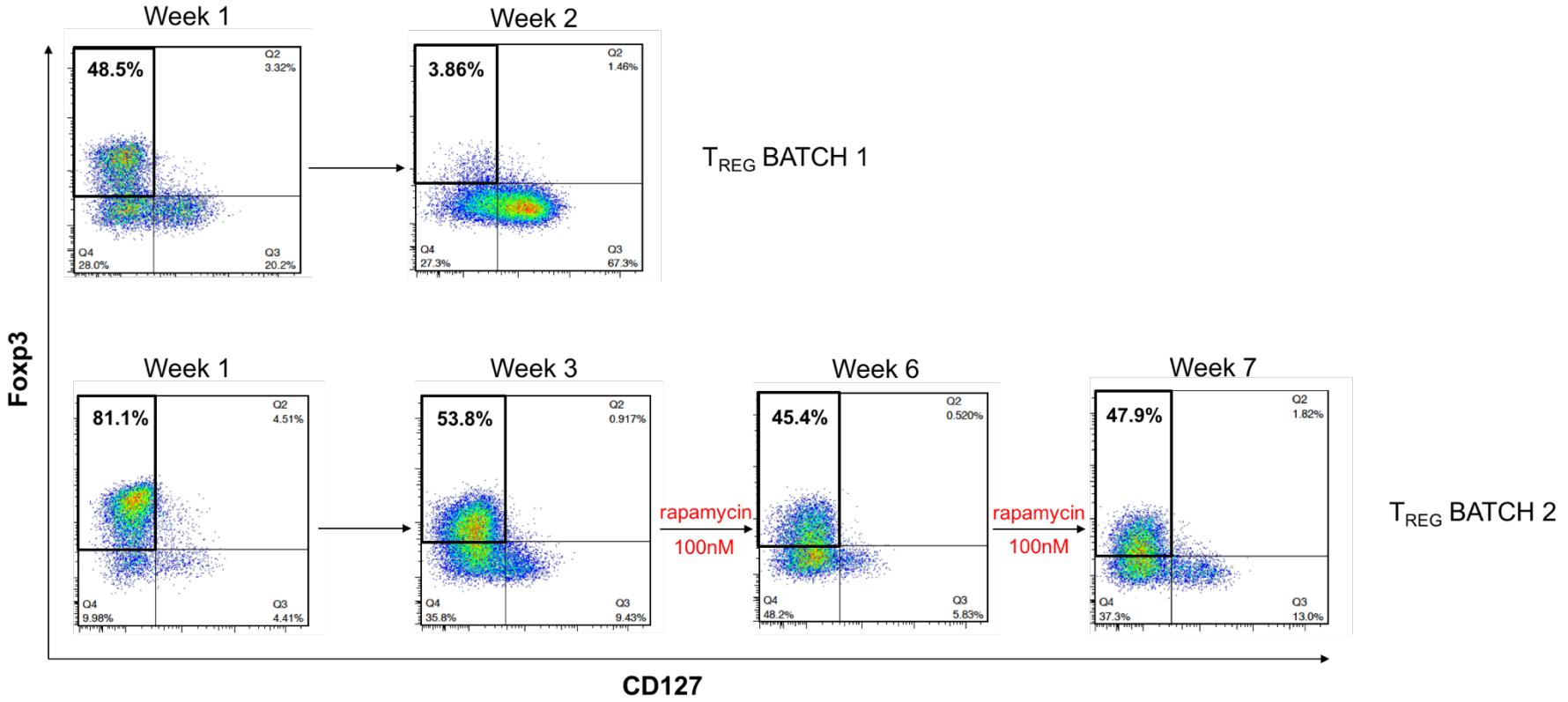

Figure 5.7 – Effect of rapamycin on the maintenance of Treg phenotype with time spent in culture

CRT3.2 CLEC14A CAR Tregs were stained and pre-gated on the $CD3^+CD4^+$ population as described in Figure 5.6. The position of the Foxp3 gate was determined by staining with the appropriate concentration-matched isotype control. The Tregs were maintained in culture in the presence of CD3/CD28 beads, 1,000 IU/mL IL-2 and either in the absence (Treg batch 1) or presence of 100nM rapamycin from week 3 onwards (Treg batch 2). All subsequent *in vitro* Treg culture included rapamycin.

5.4 Pilot studies exploring the suppressive activities of CLEC14A-specific CAR Tregs

At this stage in the project, I was approaching the end of my time in the laboratory so could only conduct some initial experiments to explore the suppressive activity of CRT3.2 CLEC14A CAR-engineered Tregs. To establish whether they were able to suppress the proliferation of autologous T-cells, the CRT3.2 CAR Tregs were first incubated with CFSE-labelled CRT3.2 CAR Tconv or their mock-transduced counterparts in the presence of recombinant human CLEC14A-Fc or the IgG-Fc control. Four different Tconv:Treg ratios and Tconv alone were tested. As described previously for T-cell proliferation assays (section 3.3), Tconv were harvested after four days and their CFSE expression examined by flow cytometry, with dilution of the dye being a direct measure of cell proliferation. It is important to note that the CFSE-negative Treg and the CFSE-positive Tconv populations exhibited significant overlap in the FITC channel instead of forming discrete peaks, possibly due to dye leakage from Tconv and its subsequent uptake by Tregs (**Figure 5.8A**). Therefore, to distinguish between these two populations, the gating was set only on the $CD8^+$ Tconv cells as this excluded any Tregs (which were all $CD4^+$). All the suppression data reported herein is therefore expressed in terms of CD8 Tconv.

As shown in **Figure 5.8B**, CAR Tregs successfully suppressed the proliferation of autologous CAR Tconv in the presence of their target, CLEC14A, at all Tconv:Treg ratios, compared to Tconv in the absence of Tregs. This proliferation was CLEC14A-specific since CAR Tconv proliferation in response to IgG-Fc was minimal. Mock Tconv, on the other hand, showed more non-specific proliferation to both CLEC14A

and Fc, but again both of these responses were suppressed in equal measure when the CAR Tregs were added. This suggested that the CLEC14A CAR on the surface of Tregs, which was expected to lead to greater suppression of non-specific Tconv proliferation in the presence of CLEC14A, did not improve the activity of the Tregs.

To explore further whether CLEC14A-specific CAR Tregs conferred any advantages over untransduced Tregs in suppressing autologous Tconv proliferation, the assay described above was repeated with the inclusion of a mock Treg control. The new assay was carried out twice – once for four days and once for a shortened period of three days – and analysed for CD8 Tconv proliferation as before. The results are shown in **Figure 5.9**. The four-day assay showed a very similar pattern to the one described above, with CAR Tregs successfully suppressing the proliferation of Tconv in the presence of CLEC14A; nevertheless, mock Tregs exhibited equal or greater suppressive capacity compared to CAR Tregs at all Tconv:Treg ratios. This was less pronounced in the 3-day assay due to less overall proliferation observed, but was still apparent. As before, CAR Tregs were also able to suppress the non-specific proliferation of mock Tconv, although in the 4-day assay this was only seen at higher Tconv:Treg ratios and was clearly not enhanced by the presence of CLEC14A.

The data shown here are limited by the fact that, due to time constraints, only two Treg batches were tested and only one of these included a mock Treg control. Nevertheless, these initial results indicate that expression of the CRT3.2 CLEC14A-specific CAR in Tregs has not increased their suppressive activity in the presence of their target antigen, since suppressive effects were equal, if not greater, using Tregs not

expressing the CAR or in the absence of CLEC14A. However, further experiments and analyses are required before definite conclusions can be drawn about the potential of targeting CLEC14A using regulatory T-cells.

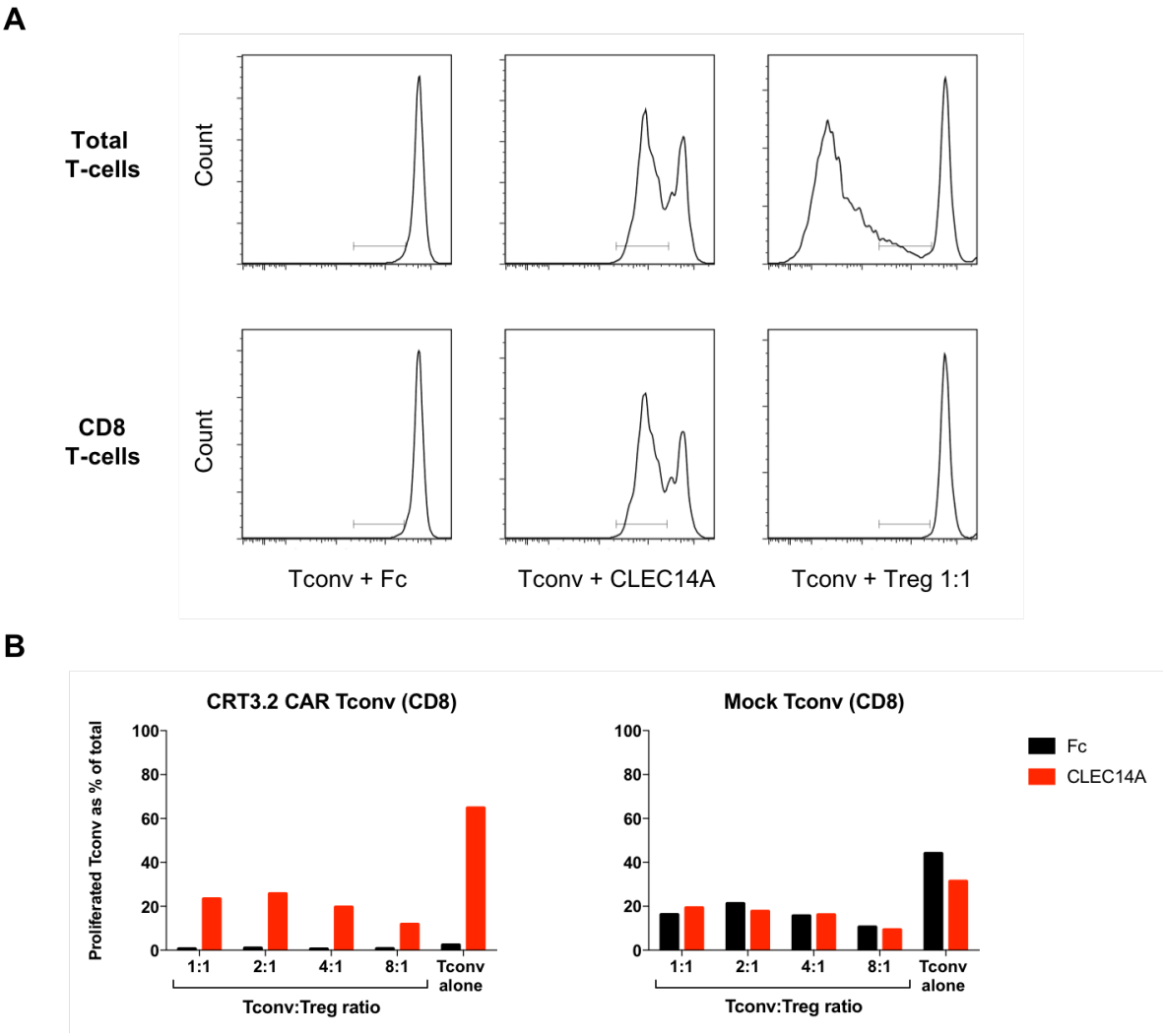

Figure 5.8 – Suppression of proliferation of one batch of conventional CD8 CAR T-cells by their autologous CAR Tregs in the presence or absence of antigen

Conventional T-cells (Tconv) transduced with the CRT3.2 CLEC14A CAR, or their mock-transduced controls, were labelled with CFSE intracellular dye and incubated alone or with autologous CRT3.2 CLEC14A Tregs at increasing Tconv:Treg ratios for four days. The cells were incubated in the presence of recombinant human CLEC14A-Fc (CLEC14A) or a concentration-matched IgG-Fc control (Fc). On day 4 the T-cells were harvested, labelled with viability dye, anti-CD8, anti-CD4 and anti-CD34 antibodies and analysed by flow cytometry. **(A)** Representative histograms of CFSE expression showing the proliferation of bulk Tconv (top) and CD8 Tconv (bottom) when incubated alone with IgG-Fc control protein (left) or CLEC14A (middle), or at 1:1 ratio with autologous Tregs in the presence of either protein (right). The overlap of Treg and Tconv peaks when Tregs were present in the bulk T-cell populations made data interpretation difficult; analysis was therefore performed using CD8 Tconv proliferation instead. **(B)** Proportion of proliferated Tconv expressed as % of the total CD8 Tconv population for CRT3.2 CLEC14A CAR Tconv (left) and mock-transduced Tconv (right).

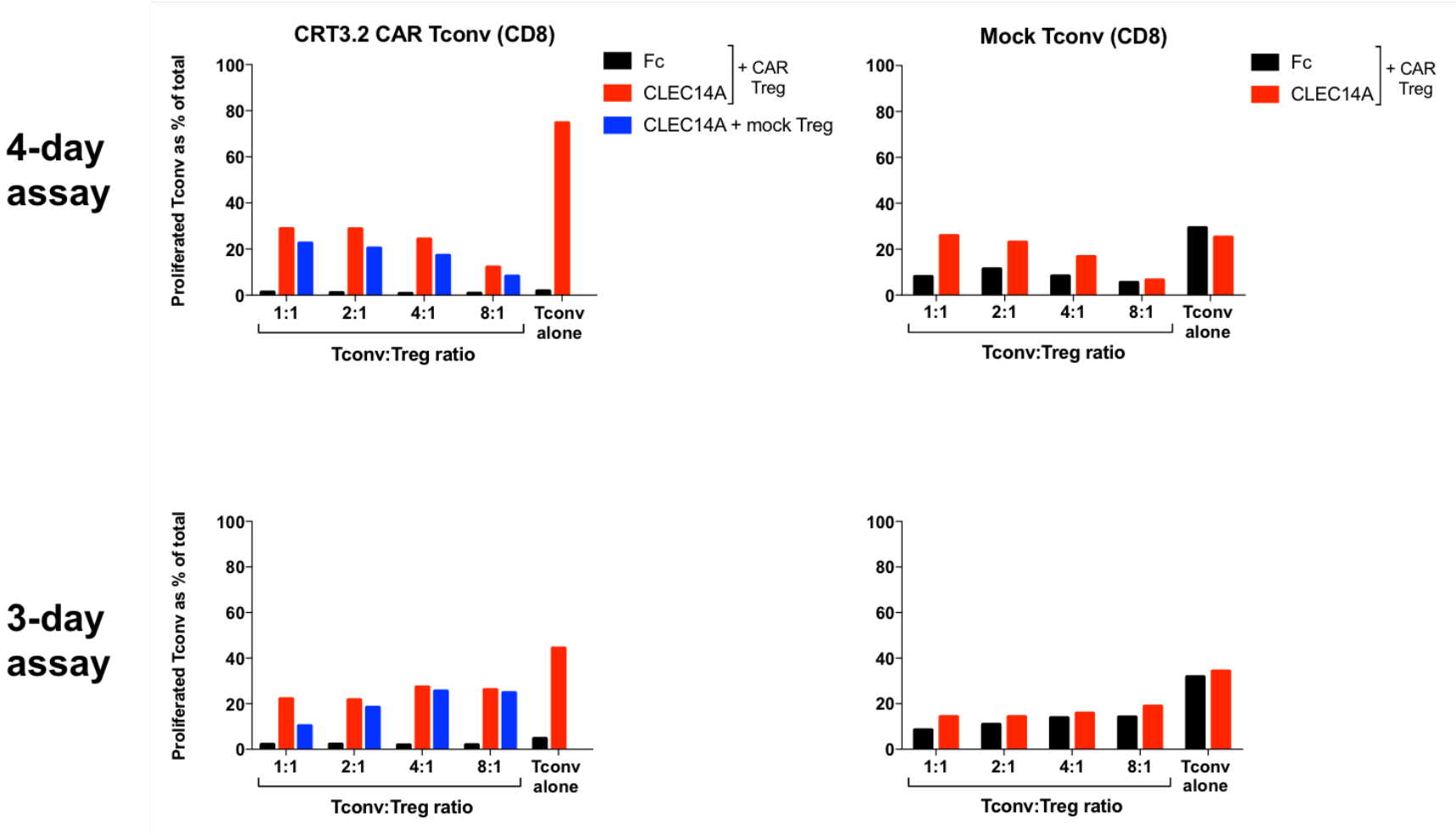

Figure 5.9 – Suppression of proliferation of a second batch of conventional CD8 CAR T-cells by their autologous CAR or mock Tregs in the presence or absence of antigen

Tconv transduced with the CRT3.2 CLEC14A CAR, or their mock-transduced controls, were labelled with CFSE intracellular dye and incubated alone or with autologous CRT3.2 CLEC14A or mock Tregs at increasing Tconv:Treg ratios for three or four days.

The cells were incubated in the presence of recombinant human CLEC14A-Fc (CLEC14A) or the IgG-Fc control (Fc). On day 3 or 4 the T-cells were harvested, labelled with viability dye, anti-CD8, anti-CD4 and anti-CD34 antibodies and analysed by flow cytometry. As explained previously, analysis was performed using CD8 Tconv proliferation only.

5.5 Discussion

This chapter presents preliminary data on CLEC14A expression on the vasculature of the inflamed PSC liver in both humans and mice, and shows that Tregs isolated from human PBMCs can be successfully transduced with a CLEC14A CAR with a view to targeting PSC inflammation with antigen-specific immunotherapy. The chapter also begins to explore the *in vitro* suppressive capacity of the generated Tregs and finds that, although successful, the CAR Tregs do not appear to suppress autologous T-cell proliferation any more than their mock-transduced counterparts. These, however, are very early data which would need to be explored in greater depth in order to give definitive answers about potential benefits of CLEC14A CAR Tregs. In addition, a pilot study of the Tregs in MDR2 KO FVB mice, although planned, was unfortunately not carried out due to time constraints. *In vivo* experiments would be the logical next step and would provide greater insight into the therapeutic potential of CLEC14A CAR Tregs in PSC, possibly paving the way for future clinical studies if successful.

5.5.1 The suitability of the MDR2 KO FVB model

As discussed already in section 1.6.3, no mouse model that completely replicates the complexity of PSC exists yet, with many producing suboptimal liver inflammation or resulting in unacceptable toxicity[263]. Knockout mouse models, however, provide the advantage of studying the disease longitudinally. For example, cystic fibrosis transmembrane conductance regulator (CFTR) KO mice spontaneously develop biliary injury resembling PSC, but this phenotype is weak unless colitis is further induced chemically and carries with it a high risk of intestinal obstruction[263,347]. Furthermore, fibrosis characteristic of PSC does not develop unless it is induced by additional

treatment with a xenobiotic[347], making the CFTR KO model suboptimal and difficult to work with. On the other hand, the MDR2 KO mouse develops progressive cholestatic hepatitis and biliary injury very similar to PSC without the need for any additional treatment, eventually progressing further to HCC[263,265]. The availability of this murine model on FVB background at the University of Birmingham meant that sections could easily be obtained for analysis, and its representative PSC-like phenotype suggested that it would lend itself well to studies of immunotherapeutic approaches that could later be applied to patients.

It is interesting to note that sections from 6 and 12 week old male MDR2 KO C57BL/6 (BL6) mice, which were also readily available, were stained alongside those from male MDR2 KO FVB mice, but did not show any evidence of CLEC14A expression despite also exhibiting PSC-like liver injury. Even though this at first suggests that CLEC14A may not be an ideal disease marker for this condition, it has been shown that MDR2 KO mice on BL6 background develop a much less severe chronic liver inflammation than those on FVB background, resulting in delayed progression to HCC; this difference is especially prominent in males[348]. MDR2 KO BL6 mice develop cholangitis and inflammation more rapidly than their age-matched FVB counterparts only in the first month of life, but while this phenotype becomes more severe over time in MDR2 KO FVB mice, it actually decreases in severity in BL6 mice by 3 months of age. In addition, 3 month old MDR2 KO FVB mice display increased fibrosis, liver enzyme disturbances, and importantly, higher levels of immune cell infiltrates – T-cells among them – than MDR2 KO BL6 mice of the same age[348]. This, therefore, correlates well with the absence of CLEC14A staining in liver sections from BL6 mice and its

concurrent presence in the sections from FVB mice of similar age. Importantly, the strong presence of a T-cell infiltrate in MDR2 KO FVB livers suggests that Treg-mediated therapies may indeed be of benefit in this model, and in PSC in general.

In order to validate CLEC14A as a marker of PSC inflammation further, it would be interesting to look at its expression on the liver vasculature of the more recently generated MDR2 KO BALB/c mouse model, which displays significantly faster rate of progression of both fibrosis and subsequent liver cancer compared to the FVB strain[349]. CLEC14A expression in these mice, if present, would provide yet another PSC model in which Treg therapy could potentially be tested in the future.

5.5.2 Treg stability and in vitro culture methods

Once isolated from PBMCs, it can be difficult for regulatory T-cells to remain stable in culture or *in vivo* due to their plasticity, which renders them very susceptible to reverting to other T-cell phenotypes. For example, a pro-inflammatory environment such as that of Crohn's disease may cause the conversion of Tregs to inflammation-promoting Th17 cells which can be deleterious therapeutically[292]. Similarly, if maintained *in vitro* with no stimulation other than through CD3 and CD28, Tregs will eventually take on the phenotype of conventional T-cells and lose their suppressive capacity. There are a number of strategies which can be employed to increase human Treg stability both *in vitro* and *in vivo*, the most utilised one being the addition of the mTOR inhibitor rapamycin to Tregs growing in culture[273]. Rapamycin has been shown to not only stabilise the regulatory phenotype and suppressive capacity of these cells, but also to promote the expansion of Tregs while selectively depleting conventional T-cell

effectors in a number of different studies[305,345,346,350]. In addition, IL-2 is necessary for Treg proliferation and overall survival and has also been routinely used in their *in vitro* culture, usually at a high dose of 1,000 IU/mL[273,345,346,350]. Both of these strategies were employed to maintain human Tregs for the purpose of this thesis, with a clear stabilisation in regulatory phenotype once rapamycin at the commonly used concentration of 100nM was introduced (Figure 5.7).

Even though the isolated Tregs were successfully cultured and maintained their suppressive capacity in the experiments described in this chapter, their phenotype can be further stabilised in future studies by additional strategies reported in the literature. Isolating $CD4^+CD25^+CD127^{low}$ T-cells is considered a good starting point for a pure Treg population – as performed herein – but CD45RA has been proposed as another important surface marker to select for in order to increase Treg proliferative capacity while keeping their suppressive potential[273,294]. It has been suggested that expanding the $CD4^+CD25^+CD127^{low}CD45RA^+$ T-cell subset results in substantial numbers of Tregs with high Foxp3 expression even in the absence of rapamycin[351], and that this subset does not convert to pro-inflammatory Th17 cells *in vitro*[292]. Another strategy that can be used is the treatment of Tregs with all-*trans* retinoic acid (atRA), the active vitamin A derivative[352]. This has been shown to inhibit Treg conversion to other T-helper phenotypes and help maintain Treg suppressive capacity in the pro-inflammatory setting of collagen-induced arthritis in mice[352], making it a potentially very effective approach to treating chronic inflammation characteristic of autoimmune disease. However, the use of rapamycin and atRA in combination rather than atRA alone may lead to the most stable Treg population for subsequent *in vivo* and clinical

use[353]. Other strategies to enrich for the most suppressive and phenotypically stable Tregs both *in vitro* and *in vivo* may include selection for Tregs expressing the co-inhibitory receptor T-cell Ig and ITIM domain (TIGIT), which is associated with lineage stability[354], or forced Treg overexpression of *Eos*, a key transcription factor which prevents regulatory T-cell reprogramming even in environments that could destabilise them[355].

5.5.3 CAR Treg suppression capacity

Tregs naturally act in a targeted, antigen-specific fashion, exerting their immunosuppressive action where appropriate. Adoptive Treg transfer has therefore been extensively explored as a way to enhance both the numbers and the suppressive function of Tregs to treat autoimmune disease[294]. However, merely increasing the dose of adoptively transferred polyclonal Tregs often isn't enough to generate a response. Even though early clinical trials have reported on their safety when infused into patients[291], these cells have a range of antigen specificities which only contain very low frequencies of the disease-relevant Tregs; large numbers of polyclonal Tregs thus need to be administered, which is not always possible[356]. Furthermore, treatment with a wide range of regulatory T-cell specificities can also lead to non-specific immunosuppression, which in turn increases the risk of infection and even reactivation of latent virus – this has already been reported[357]. On the other hand, rendering Tregs antigen-specific not only reduces the therapeutic dose required and lowers the risk of non-specific suppression, but also increases Treg potency up to 100 times compared to a polyclonal population due to specific targeting[358]. In addition, it may not be necessary to know the autoantigen responsible for aberrant T-cell responses in an

autoimmune condition for antigen-specific Tregs to be successful. As they possess the capacity for local immunosuppression of autoreactive T-cells directed against a different antigen, it may be enough to simply redirect the Tregs towards any antigen selectively expressed in the inflamed tissue[290].

In order to generate antigen-specific regulatory T-cells, one of the most promising approaches is genetic engineering with a TCR or CAR targeted to an antigen of choice. CAR-targeted Tregs have already been successful in several murine studies of autoimmune conditions[298–300], and were therapeutically superior to a non-specific Treg population in mouse models of colitis[298,299], GvHD[302] and haemophilia A[303]. Guided by this principle, the experiments reported in this thesis used human Tregs engineered with a CAR redirected towards CLEC14A, testing them for suppression in response to their target protein and comparing the observed responses to those of mock-engineered (control) Tregs. However, our initial experiments have so far not demonstrated superiority of CLEC14A CAR Tregs over non-specific Tregs with regards to their suppressive capacity (Figure 5.9). Nevertheless, the data are very preliminary and derived only from a single CAR and mock Treg batch; drawing definitive conclusions from them is therefore not possible at this stage, with further studies being required.

It was noted in the present study that, paradoxically, higher Tconv:Treg ratios resulted in greater suppression of Tconv proliferation (Figure 5.8 and Figure 5.9). It is possible that this was a result of too many cells present in the wells when the Tconv:Treg ratio was 8:1, causing exhaustion of the media and thus reduced overall Tconv proliferation.

The experiment would need to be repeated with other Treg batches to validate this observation, but it would be interesting to explore lower Treg titrations and whether they lead to a greater difference in suppression activity between CAR and mock Tregs. This may be especially relevant since it was also noted that conventional T-cells exhibited high rates of cell death during the suppression assay incubations. Competition between the two T-cell subsets for the limited IL-2 available, and the preferential use of the cytokine by the Tregs, may have led to death of some Tconv; therefore, it is necessary to improve effector T-cell survival in order to be able to interpret any future assay results correctly. It would also be beneficial to test the CLEC14A CAR Tregs in other functional assays, such as those examining cytokines released in response to antigen (e.g. the immunosuppressive cytokine IL-10) in order to elucidate their function and antigen specificity more fully. Finally, *in vitro* studies on cell lines expressing CLEC14A, as well as *in vivo* experiments in representative mouse models such as the MDR2 KO FVB strain, are all necessary to gauge the therapeutic efficacy and potency of CLEC14A-targeted regulatory T-cells in inflammatory conditions of the liver such as PSC.

6 GENERAL DISCUSSION

This thesis set out to explore the promising approach of CAR T-cell engineering in the context of solid tumours, more specifically for targeting the tumour vasculature, by testing the *in vitro* and *in vivo* functionality of CAR T-cells redirected against the tumour endothelial marker TEM8. This TEM had previously been identified as overexpressed on tumour blood vessels, but present only at very low or undetectable levels on healthy vasculature of both mice and humans[226,246]. As originally hypothesised, T-cells were amenable to transduction with TEM8 CARs and proved very effective at responding to their target protein on the surface of cells; however, four of the five CARs also exhibited extensive *in vitro* reactivity to other cell lines and either resulted in *in vivo* toxicity or were selectively lost from the peripheral circulation of the treated mice. The only TEM8 CAR to prove safe as well as persist in the blood was 1D2, but its inability to recognise mouse TEM8 expressed on murine tumour vasculature rendered any further tumour protection or toxicity studies in currently available animal models obsolete. CAR engineering of Tregs was also explored in the context of autoimmunity, namely as a potential treatment for the autoimmune liver condition primary sclerosing cholangitis. While CAR Tregs targeting the vasculature marker CLEC14A, which is expressed in the PSC liver, did not prove superior to non-specific Tregs with regards to suppressive capacity, the data are very preliminary and merit a more thorough examination of this CAR Treg approach before any definitive conclusions can be reached.

The use of CAR T-cell immunotherapy for cancer is currently the focus of intense research, and has led to successful clinical trials which recently culminated in the first

FDA approvals of CARs for the treatment of ALL[359] and large B-cell lymphoma[360]. Research continues in both haematological and solid tumours, with the latter being particularly challenging to treat due to the inherently suppressive tumour microenvironment adversely affecting any immunotherapies aimed at it. Nevertheless, here as well progress is being made, not only in the CAR T-cell field but in cancer immunotherapies in general. The knowledge obtained from targeting tumours is also increasingly applied to treating other conditions such as autoimmune disorders and transplant rejection, where CAR Tregs are especially promising. This chapter aims to discuss novel immunotherapeutic strategies using CAR-engineered T-cells, and how these might be applied to targeting the tumour vasculature using TEM8 CARs or in the treatment of liver inflammation with CLEC14A-specific CAR Tregs in the future.

6.1 Metabolic modulation of tumours and CAR T-cell treatment

The absence of T-cell infiltration and defects in the antigen processing and presentation pathways characteristic of many solid tumours render checkpoint inhibition, cancer vaccines and even standard TIL therapy ineffective. In these cases, engineering T-cells to express CARs, which recognise native surface-expressed antigens independent of any processing pathways, is a very promising approach to treating these otherwise non-immune infiltrated “cold” tumours. Nevertheless, the metabolic barriers of the tumour microenvironment (TME) still need to be overcome by CAR T-cells in order to access the tumour in the first place, rendering metabolic modulation a particularly important area of CAR research[174]. The tumour microenvironment is typically starved of nutrients, hypoxic and acidic, and the low glucose levels coupled to the lack of essential amino acids such as arginine in the TME

all act to impair normal T-cell function. To overcome nutrient starvation, for example, CAR T-cells could be further genetically engineered to overexpress glucose or amino acid transporters, thus enabling them to compete with the tumour for the limited resources available[174]. In addition, concurrent inhibition of the main transcription factor associated with low oxygen levels, hypoxia-inducible factor-1α (HIF-1α) by a drug such as tirapazamine[361], could make the tumours more sensitive to CAR T-cell treatment by providing a more hospitable environment for their anti-tumour activity. The lack of arginine, the amino acid normally necessary for T-cell activation and proliferation, could also be counteracted by administering inhibitors of the enzyme arginase which is responsible for arginine depletion in the TME[362]. An arginase inhibitor is already showing promising results in a clinical trial of patients with advanced solid tumours[363], and could provide a potent metabolic boost if administered in combination with CAR T-cells.

Another important metabolic factor that adversely affects tumour-targeting T-lymphocytes is the expression of the immunosuppressive enzyme IDO by the cells of the tumour microenvironment. IDO catalyses the degradation of the essential amino acid tryptophan; this depletion suppresses T-cell proliferation and leads to lack of T-cell accumulation at the tumour site[66]. IDO is associated with poor prognosis in several solid cancers[174] and has also been shown to lead to inhibition of CAR T-cells, resulting in their failure to control IDO-expressing tumours even when the tumour cells were positive for the antigen targeted by the CAR T-cells[364]. Therefore, co-administration of CAR T-cells and IDO inhibitors, several of which are already in clinical trials for various

solid tumour indications[365], could be of great benefit for tumours otherwise resistant to immunotherapy or standard chemotherapy.

Even though tumour vasculature-targeting CAR T-cells, such as those bearing TEM8 CARs, are not as exposed to the inhospitable TME as T-cell immunotherapies redirected against the tumour itself, tumour-associated blood vessels can themselves be a metabolic barrier and thus need to be taken into account when designing CAR T-cell strategies. To maximise the anti-tumour potential of TEM8 CAR T-cells, one or more of the approaches described above could be employed – for example, tirapazamine could be administered following CAR T-cell treatment to eliminate the remaining tumour tissue that becomes hypoxic following the destruction of some of the vasculature. Additionally, TEM8 CAR T-cells could be given a survival advantage in highly glycolytic tumours by being engineered with a 4-1BB rather than a CD28 co-stimulatory domain, which would help promote oxidative metabolism of the T-cells and give them enhanced respiratory capacity[315]. If both immediate anti-tumour activity and long-term T-cell persistence are required, however, the administration of both CD28/CD3ζ and 4-1BB/CD3ζ TEM8 CAR T-cells might be the optimal therapeutic approach. Finally, the reported expression of PD-L1 on tumour vasculature[366], which can inhibit T-cell activity by binding to PD-1 on T-cell surface, can also be exploited and reversed to provide stimulation of TEM8 CARs instead. An engineered T-cell switch receptor with a PD-1 extracellular domain has been described which, upon binding PD-L1, causes stimulation through its CD28 intracellular moiety and results in efficient activation of a desired target-specific CAR also expressed on the T-cell surface[367]. An alternative approach is the engineering of CAR T-cells to secrete anti-

PD-L1 mAbs at the tumour site, which has resulted in efficient reduction in tumour growth in humanised mouse models[368]. Whether by modifying them to locally secrete anti-PD-L1 blocking antibodies in the tumour vasculature, or by co-opting the normally inhibitory PD-L1/PD-1 binding axis using a PD-1/CD28 stimulatory construct instead, genetically engineering TEM8 CAR T-cells in this way would provide them with substantial therapeutic and survival advantages when targeting tumour blood vessels.

6.2 Antigen specificity and safety of CAR T-cells

Many alternative CAR designs are being explored with the aim of making their antigen-binding domains more structurally diverse as well as target-specific. For example, if there is no antibody available for re-formatting into a CAR, designed ankyrin repeat proteins can be similarly effective as the tumour-targeting CAR moieties[369], and if a functional scFv domain cannot be easily obtained, dual-chain CARs utilise the natural antibody configuration to bind with high affinity and selectivity to the cognate antigen[370]. The latter may be of relevance to the more highly reactive TEM8 CARs – in view of their increased avidity for TEM8 when the original antibodies are reformatted to CAR scFv domains, keeping the natural antibody configurations in the TEM8 CAR construct may increase the selectivity of the CARs for high-level TEM8 expression.

To expand the therapeutic range of the existing CAR structure, and potentially prevent antigen loss as a tumour escape mechanism, tandem CARs (TanCARs) have been described which simultaneously bind to two tumour-restricted antigens and are activated by each one individually or synergistically by both[371]. A CD28/CD3ζ TanCAR incorporating two antigen binding domains specific for HER2 and IL-13 receptor α2 in

its extracellular region has already shown superior anti-tumour efficacy compared to single CAR-expressing T-cells in a mouse model of glioblastoma[372]. This approach could also allow for targeting of both the tumour cells themselves and the tumour stroma, providing a mechanism to battle the inhospitable TME[371]. For example, TEM8 CARs could be made into TanCARs incorporating a TEM8 scFv together with a scFv recognising the fibroblast activation protein (FAP), a serine protease expressed by tumour-associated stromal cells in the vast majority of epithelial cancers[373]. In two separate studies, FAP-specific CAR T-cells mediated potent anti-tumour effects *in vivo*[374,375], especially in combination with CAR T-cells targeting an antigen expressed on the tumour cells themselves[374]. Therefore, a TEM8/FAP TanCAR could provide an effective therapeutic approach for targeting both the tumour vasculature and the immunosuppressive stroma in the remaining tumour after some of the vasculature is eliminated.

A major concern with some of the CARs in the clinic, and one that was also highlighted for TEM8 CARs by the work described in this thesis, is their safety. As previously discussed in the Introduction (sections 1.4.2 and 1.4.3), toxicities have been reported in trials of CAR T-cell treatment for both haematological and solid tumours, most of them related to on-target/off-tumour recognition and cytokine storms. In order to improve their safety profile, a number of combinatorial CAR strategies have been developed, such as the previously mentioned dissociation of CD3ζ and co-stimulatory signals into two co-expressed CARs which both need to be engaged for full T-cell activation[207,376]. For example, CARs recognising TEM8 and CLEC14A could be engineered in this way to increase the selectivity of the therapeutic T-cells for the

tumour vasculature. An elegant approach allowing for the titration of CAR T-cell response levels has also been described, whereby the antigen recognition and signalling domains of the CAR are split and their heterodimerisation made dependent on the presence of a small molecule[377]. This ON-switch CAR is therefore only activated in the presence of both its cognate antigen and the otherwise inert small molecule, the dose of the latter determining the amount of therapeutic CAR activity. Re-engineering TEM8-specific CARs to the ON-switch format could therefore provide a way to gradually titrate their dose and monitor toxicity reactions more closely, both in preclinical animal models and, provided a suitable inert small molecule can be found, in clinical trials in patients. Another method of titrating CAR T-cell response levels is by using a semisynthetic "switch" molecule that combines the desired antigen-binding antibody fragment with the inert FITC dye and acts as a bridge between the antigen itself and an anti-FITC CAR[378]. The ability to optimise the binding interactions of this intermediate bridging molecule as desired, and thus modify the immunological synapse between the CAR T-cell and the tumour cell, has already resulted in reduced toxicity *in vivo*[378] – a very important finding which could be used in future animal studies where toxicity is a concern, such as the ones using TEM8 CARs described in this thesis.

A way to increase both the specificity and safety of CAR T-cells, as well as remodel the tumour microenvironment to make it more optimal for therapeutic T-cell action, has been recently proposed by using synthetic Notch (synNotch) receptors on the surface of the T-cells[379]. Upon activation of these receptors by their target antigen, expression of a CAR specific for a second tumour antigen is induced; thus only dual antigen-expressing tumour cells are recognised while any single-antigen ones are spared,

providing high specificity and reduced off-tumour toxicity of the CAR. Additionally, synNotch receptors can customise T-cell responses within the tumour through transcriptional activation, inducing specific cytokine secretion or facilitating the localised delivery of therapeutic payloads such as antibodies[380], thus directly combatting the immunosuppressive effects of the tumour microenvironment. To increase the specificity of tumour blood vessel targeting, an anti-TEM8 scFv could be incorporated into a synNotch receptor on the T-cell surface which, upon activation, would induce the expression of a CAR recognising a second tumour vasculature-associated antigen – for example, a ligand of the NKG2D receptor. It has been shown that mouse tumour vasculature expresses the NKG2D ligand Rae1, and that NKG2D-based CAR T-cells targeting the murine tumour blood vessels led to reduced cancer angiogenesis and growth[381]. In humans, up to eight different NKG2D ligands are expressed in various primary tumours, both on the tumour cells themselves and the associated vasculature; a clinical trial of NKG2D receptor-based CAR T-cells is currently in progress in patients with one of seven different malignancies, including CRC, TNBC and pancreatic cancer[382]. A TEM8/NKG2D synNotch receptor would therefore not only provide more specific targeting of cancer-associated blood vessels and expand the range of potential tumour indications it can be used in, but also allow for favourable modulation of the tumour microenvironment through NKG2D-mediated targeting of immunosuppressive TME components such as Tregs[382].

If antigen specificity and safety of TEM8 CARs can be achieved by the strategies outlined above, further optimisation of anti-tumour effects and toxicity mitigation strategies should be implemented in any potential human clinical trials. RNA

electroporation can be used to express the desired TEM8 CAR on the T-cell surface only transiently, allowing the receptor to be extinguished spontaneously within days of the T-cell injection if toxicity arises[383]. If stable CAR surface expression by means of retro- or lentiviral transduction of the T-cells is required, however, careful dose escalation would be necessary, with potential addition of a suicide switch such as the inducible caspase 9 system to enable selective deletion of the CAR T-cell product in the event of toxicity[384]. Additional strategies to optimise the TEM8 CAR T-cells include, for example, gene editing to render them deficient for their endogenous $\alpha\beta$ TCR prior to CAR transduction, allowing for the administration of third party CAR T-cells to any patient that needs them without fear of GvHD[385]. These "off-the-shelf" CAR T-cells can also be rendered resistant to destruction by chemotherapeutic agents used in pre-conditioning regimens, such that T-cell engraftment is improved while tumour destruction is maintained. To avoid prolonged *in vitro* T-cell expansion protocols prior to reinfusion into patients, the cells could potentially be programmed for tumour recognition by using nanoparticles to introduce CAR DNA into them quickly and efficiently *in situ*; such nanoparticles are stable and cost-effective to maintain, and their use has resulted in long-term disease remission in tumour-bearing mice[386]. Alternatively, a recent breakthrough in CAR gene editing reported that targeted CD19 CAR gene delivery to the T-cell receptor α (TRAC) locus resulted in both greater potency and delayed exhaustion of the T-cells after repeated antigen exposure[387], vastly increasing their potential for sustained therapeutic activity over prolonged periods. Such an approach taken with TEM8 CAR T-cells could lead to a much more potent and long-lasting anti-tumour effect if this therapeutic modality is to be tested in patients.

6.3 Autoimmunity and CAR Tregs

The potential of the CAR platform is such that its use is now being expanded into areas other than oncology. CAR engineering of Tregs to treat inflammatory conditions, GvHD and transplant rejection was already discussed in section 1.7.3 of this thesis, and although there are as yet no human trials of CAR-engineered Tregs for any condition, the promising results from the relevant *in vitro* and *in vivo* studies will certainly lead to their clinical testing in the near future. CAR Tregs targeting inflamed vascular endothelial cells, such as the ones directed against CLEC14A and described in chapter 5 of this thesis, may also hold promise for future therapies of autoimmune diseases of the liver. Further *in vitro* data would first need to be generated before taking the cells forward to any pilot animal experiments, but the preliminary data and the existence of an appropriate mouse model are encouraging.

As with TEM8 CAR T-cells, combinatorial targeting strategies could be applied to increase the specificity and safety of CAR Tregs as well. For example, the CLEC14A CAR Tregs could be engineered further to overexpress the liver-homing chemokine receptor CXCR3, which would help direct the cells specifically to the inflamed liver vasculature where the corresponding CXCR3 ligands are upregulated[273]. Furthermore, expression of the previously mentioned NKG2D ligands is also thought to be induced in inflamed tissues such as those found in autoimmune diseases[382]. Validating their expression in autoimmune liver conditions such as PSC and, if appropriate, constructing a specific way to target the inflamed liver – for example, using a CLEC14A/NKG2D TanCAR on the surface of Tregs – could provide a novel and potent approach to treating this disease. Whatever the chosen strategy, it is important to

weigh the predicted benefits of administering liver vasculature-targeting CAR Tregs to a PSC patient against the risks and toxicity issues that could arise. Compared to life-threatening cancers, the safety concerns are much more limiting in chronic autoimmune conditions and require the benefits of treatment to substantially outweigh the risks in order for therapy to be considered viable. Nevertheless, the frequent culmination of PSC in end-stage liver disease and thus in the requirement for liver transplantation[255], coupled with the increased risk of several cancers in PSC patients[262], means that there is a high unmet need for a successful therapeutic approach to this debilitating condition. If CLEC14A-specific CAR Tregs can be rendered safe and effective in mouse models of the disease using the strategies suggested above, it can be argued that the benefits of testing them in patients would outweigh the risks that could potentially arise from their administration.

6.4 Conclusions

The main application of CARs where they have seen the most success are still haematological malignancies, although solid tumour targeting is being explored to a much greater extent than before and generating very promising data. Of particular relevance to this thesis is tumour vasculature targeting where, if successful, CARs could drastically improve rates of solid tumour destruction and help contain metastatic spread in patients suffering from many different cancers. Another emerging indication for CARs are autoimmune and inflammatory conditions, where *in vivo* studies using CAR-engineered Tregs have already shown promise; this has opened up the possibility of using CAR Tregs to target the inflamed vasculature in autoimmune liver diseases, which merits in-depth investigation. If tumour and inflamed vasculature-

targeting CARs reach clinical trials, it would be important to introduce safety measures into them due to their potential for toxicity to healthy tissue – for example, by split signalling, combinatorial antigen sensing or careful titration of the introduced dose using a small inert molecule, all of which are discussed in this chapter. If safety obstacles can be overcome, and an appropriate target with its expression restricted mostly to tumour or inflamed endothelium – such as TEM8 and CLEC14A respectively – be specifically targeted, the therapeutic potential of these CARs alone or in combination with other immunotherapies could be truly transformative.

7 LIST OF REFERENCES

1. Huston DP. The biology of the immune system. JAMA. 1997 Dec 10;278(22):1804–14.
2. Chaplin DD. Overview of the immune response. J Allergy Clin Immunol. 2010 Feb;125(2 Suppl 2):S3-23.
3. Fearon DT, Locksley RM. The Instructive Role of Innate Immunity in the Acquired Immune Response. Science (80-). 1996 Apr 5;272(5258):50–4.
4. Bonilla FA, Oettgen HC. Adaptive immunity. J Allergy Clin Immunol. 2010 Feb;125(2 Suppl 2):S33-40.
5. Doherty PC, Zinkernagel RM. A biological role for the major histocompatibility antigens. Lancet. 1975;1406–9.
6. Zinkernagel RM, Doherty PC. Immunological surveillance against altered self components by sensitised T lymphocytes in lymphocytic choriomeningitis. Nature. 1974;251:547–8.
7. Nitta T, Murata S, Ueno T, Tanaka K, Takahama Y. Thymic microenvironments for T-cell repertoire formation. Adv Immunol. 2008 Jan;99:59–94.
8. Joshi NS, Kaech SM. Effector CD8 T cell development: a balancing act between memory cell potential and terminal differentiation. J Immunol. 2008 Feb 1;180(3):1309–15.
9. Turley SJ, Inaba K, Garrett WS, Ebersold M, Unternaehrer J, Steinman RM, et al. Transport of peptide-MHC class II complexes in developing dendritic cells. Science (80-). 2000 Apr 21;288(5465):522–7.
10. Schwartz RH, Mueller DL, Jenkins MK, Quill H. T-cell clonal anergy. Cold Spring Harb Symp Quant Biol. 1989 Jan;54 Pt 2:605–10.
11. June CH, Ledbetter JA, Gillespie MM, Lindsten T, Thompson CB. T-cell proliferation involving the CD28 pathway is associated with cyclosporine-resistant interleukin 2 gene expression. Mol Cell Biol. 1987 Dec;7(12):4472–81.
12. Green JM, Noel PJ, Sperling AI, Walunas TL, Gray GS, Bluestone JA, et al. Absence of B7-dependent responses in CD28-deficient mice. Immunity. 1994 Sep;1(6):501–8.
13. Shahinian A, Pfeffer K, Lee KP, Kündig TM, Kishihara K, Wakeham A, et al. Differential T cell costimulatory requirements in CD28-deficient mice. Science (80-). 1993 Jul 30;261(5121):609–12.
14. Linsley PS, Clark EA, Ledbetter JA. T-cell antigen CD28 mediates adhesion with B cells by interacting with activation antigen B7/BB-1. Proc Natl Acad Sci U S A. 1990 Jul;87(13):5031–5.
15. Azuma M, Ito D, Yagita H, Okumura K, Phillips JH, Lanier LL, et al. B70 antigen is a second ligand for CTLA-4 and CD28. Nature. 1993 Nov 4;366(6450):76–9.

16. Linsley PS, Brady W, Urnes M, Grosmaire LS, Damle NK, Ledbetter JA. CTLA-4 is a second receptor for the B cell activation antigen B7. J Exp Med. 1991 Sep 1;174(3):561–9.
17. Rudd CE, Taylor A, Schneider H. CD28 and CTLA-4 coreceptor expression and signal transduction. Immunol Rev. 2009 May;229(1):12–26.
18. Croft M. The role of TNF superfamily members in T-cell function and diseases. Nat Rev Immunol. 2009 Apr;9(4):271–85.
19. Chen L, Flies DB. Molecular mechanisms of T cell co-stimulation and co-inhibition. Nat Rev Immunol. 2013 Apr;13(4):227–42.
20. Grakoui A, Bromley SK, Sumen C, Davis MM, Shaw AS, Allen PM, et al. The immunological synapse: a molecular machine controlling T cell activation. Science (80-). 1999 Jul 9;285(5425):221–7.
21. Sadelain M, Rivière I, Riddell S. Therapeutic T cell engineering. Nature. 2017;545(7655):423–31.
22. Huppa JB, Davis MM. T-cell-antigen recognition and the immunological synapse. Nat Rev Immunol. 2003 Dec 1;3(12):973–83.
23. Vesely MD, Kershaw MH, Schreiber RD, Smyth MJ. Natural Innate and Adaptive Immunity to Cancer. Annu Rev Immunol. 2011 Jan;29:235–71.
24. Shankaran V, Ikeda H, Bruce AT, White JM, Swanson PE, Old LJ, et al. IFNgamma and lymphocytes prevent primary tumour development and shape tumour immunogenicity. Nature. 2001 Apr 26;410(6832):1107–11.
25. Dunn GP, Bruce AT, Ikeda H, Old LJ, Schreiber RD. Cancer immunoediting: from immunosurveillance to tumor escape. Nat Immunol. 2002 Nov;3(11):991–8.
26. Dunn GP, Old LJ, Schreiber RD. The three Es of cancer immunoediting. Annu Rev Immunol. 2004 Jan;22:329–60.
27. Girardi M, Oppenheim DE, Steele CR, Lewis JM, Glusac E, Filler R, et al. Regulation of cutaneous malignancy by gammadelta T cells. Science (80-). 2001 Oct 19;294(5542):605–9.
28. Engel AM, Svane IM, Mouritsen S, Rygaard J, Clausen J, Werdelin O. Methylcholanthrene-induced sarcomas in nude mice have short induction times and relatively low levels of surface MHC class I expression. Acta Pathol Microbiol Immunol Scand. 1996 Sep;104(9):629–39.
29. Street SEA, Cretney E, Smyth MJ. Perforin and interferon-gamma activities independently control tumor initiation, growth, and metastasis. Blood. 2001 Jan 1;97(1):192–7.
30. Kaplan DH, Shankaran V, Dighe AS, Stockert E, Aguet M, Old LJ, et al. Demonstration of an interferon gamma-dependent tumor surveillance system in immunocompetent mice. Proc Natl Acad Sci U S A. 1998 Jun 23;95(13):7556–61.

31. Alimonti J, Zhang Q-J, Gabathuler R, Reid G, Chen SS, Jefferies WA. TAP expression provides a general method for improving the recognition of malignant cells in vivo. Nat Biotechnol. 2000 May;18(5):515–20.
32. Smyth MJ, Thia KY, Street SEA, MacGregor D, Godfrey DI, Trapani JA. Perforin-mediated cytotoxicity is critical for surveillance of spontaneous lymphoma. J Exp Med. 2000 Sep 4;192(5):755–60.
33. Street SEA, Hayakawa Y, Zhan Y, Lew AM, MacGregor D, Jamieson AM, et al. Innate immune surveillance of spontaneous B cell lymphomas by natural killer cells and gammadelta T cells. J Exp Med. 2004 Mar 15;199(6):879–84.
34. Chia J, Yeo KP, Whisstock JC, Dunstone MA, Trapani JA, Voskoboinik I. Temperature sensitivity of human perforin mutants unmasks subtotal loss of cytotoxicity, delayed FHL, and a predisposition to cancer. Proc Natl Acad Sci U S A. 2009 Jun 16;106(24):9809–14.
35. Finn OJ. Cancer Immunology. N Engl J Med. 2008 Jun 19;358(25):2704–15.
36. van der Bruggen P, Traversari C, Chomez P, Lurquin C, De Plaen E, van den Eynde BJ, et al. A gene encoding an antigen recognized by cytolytic T lymphocytes on a human melanoma. Science (80-). 1991 Dec 13;254(5038):1643–7.
37. Chen YT, Scanlan MJ, Sahin U, Türeci Ö, Gure AO, Tsang S, et al. A testicular antigen aberrantly expressed in human cancers detected by autologous antibody screening. Proc Natl Acad Sci U S A. 1997 Mar 4;94(5):1914–8.
38. Park TS, Groh EM, Patel K, Kerkar SP, Lee C-CR, Rosenberg SA. Expression of MAGE-A and NY-ESO-1 in Primary and Metastatic Cancers. J Immunother. 2016;39(1):1–7.
39. Kao H, Marto JA, Hoffmann TK, Shabanowitz J, Finkelstein SD, Whiteside TL, et al. Identification of Cyclin B1 as a Shared Human Epithelial Tumor-Associated Antigen Recognized by T Cells. J Exp Med. 2001 Nov 5;194(9):1313–24.
40. Boshoff C, Weiss R. AIDS-related malignancies. Nat Rev Cancer. 2002 May;2(5):373–82.
41. Chaturvedi AK, Pfeiffer RM, Chang L, Goedert JJ, Biggar RJ, Engels EA. Elevated risk of lung cancer among people with AIDS. AIDS. 2007 Jan 11;21(2):207–13.
42. Kirk GD, Merlo C, O' Driscoll P, Mehta SH, Galai N, Vlahov D, et al. HIV infection is associated with an increased risk for lung cancer, independent of smoking. Clin Infect Dis. 2007 Jul 1;45(1):103–10.
43. Roithmaier S, Haydon AM, Loi S, Esmore D, Griffiths A, Bergin P, et al. Incidence of malignancies in heart and/or lung transplant recipients: a single-institution experience. J Hear Lung Transplant. 2007 Aug;26(8):845–9.
44. Clark WH, Elder DE, Guerry D, Braitman LE, Trock BJ, Schultz D, et al. Model

predicting survival in stage I melanoma based on tumor progression. J Natl Cancer Inst. 1989 Dec 20;81(24):1893–904.
45. Clemente CG, Mihm MC, Bufalino R, Zurrida S, Collini P, Cascinelli N. Prognostic value of tumor infiltrating lymphocytes in the vertical growth phase of primary cutaneous melanoma. Cancer. 1996 Apr 1;77(7):1303–10.
46. Zhang L, Conejo-Garcia JR, Katsaros D, Gimotty PA, Massobrio M, Regnani G, et al. Intratumoral T cells, recurrence, and survival in epithelial ovarian cancer. N Engl J Med. 2003 Jan 16;348(3):203–13.
47. Galon J, Costes A, Sanchez-Cabo F, Kirilovsky A, Mlecnik B, Lagorce-Pagès C, et al. Type, density, and location of immune cells within human colorectal tumors predict clinical outcome. Science (80-). 2006 Sep 29;313(5795):1960–4.
48. Koebel CM, Vermi W, Swann JB, Zerafa N, Rodig SJ, Old LJ, et al. Adaptive immunity maintains occult cancer in an equilibrium state. Nature. 2007 Dec 6;450(7171):903–7.
49. Braumüller H, Wieder T, Brenner E, Aßmann S, Hahn M, Alkhaled M, et al. T-helper-1-cell cytokines drive cancer into senescence. Nature. 2013 Feb;494(7437):361–5.
50. Eyles J, Puaux A-L, Wang X, Toh B, Prakash C, Hong M, et al. Tumor cells disseminate early, but immunosurveillance limits metastatic outgrowth, in a mouse model of melanoma. J Clin Invest. 2010 Jun;120(6):2030–9.
51. Meng S, Tripathy D, Frenkel EP, Shete S, Naftalis EZ, Huth JF, et al. Circulating tumor cells in patients with breast cancer dormancy. Clin Cancer Res. 2004 Dec 15;10(24):8152–62.
52. Myron Kauffman H, McBride MA, Cherikh WS, Spain PC, Marks WH, Roza AM. Transplant tumor registry: donor related malignancies. Transplantation. 2002 Aug 15;74(3):358–62.
53. MacKie RM, Reid R, Junor B. Fatal melanoma transferred in a donated kidney 16 years after melanoma surgery. N Engl J Med. 2003 Feb 6;348(6):567–8.
54. Saudemont A, Quesnel B. In a model of tumor dormancy, long-term persistent leukemic cells have increased B7-H1 and B7.1 expression and resist CTL-mediated lysis. Blood. 2004 Oct 1;104(7):2124–33.
55. Matsushita H, Vesely MD, Koboldt DC, Rickert CG, Uppaluri R, Magrini VJ, et al. Cancer exome analysis reveals a T-cell-dependent mechanism of cancer immunoediting. Nature. 2012 Feb 8;482(7385):400–4.
56. Willimsky G, Blankenstein T. Sporadic immunogenic tumours avoid destruction by inducing T-cell tolerance. Nature. 2005 Sep 1;437(7055):141–6.
57. Schell TD, Knowles BB, Tevethia SS. Sequential loss of cytotoxic T lymphocyte responses to simian virus 40 large T antigen epitopes in T antigen transgenic mice developing osteosarcomas. Cancer Res. 2000 Jun 1;60(11):3002–12.

58. Restifo NP, Marincola FM, Kawakami Y, Taubenberger J, Yannelli JR, Rosenberg SA. Loss of functional beta 2-microglobulin in metastatic melanomas from five patients receiving immunotherapy. J Natl Cancer Inst. 1996 Jan 17;88(2):100–8.
59. Jäger E, Ringhoffer M, Karbach J, Arand M, Oesch F, Knuth A. Inverse relationship of melanocyte differentiation antigen expression in melanoma tissues and CD8+ cytotoxic-T-cell responses: evidence for immunoselection of antigen-loss variants in vivo. Int J Cancer. 1996 May 16;66(4):470–6.
60. Hinz S, Trauzold A, Boenicke L, Sandberg C, Beckmann S, Bayer E, et al. Bcl-XL protects pancreatic adenocarcinoma cells against CD95- and TRAIL-receptor-mediated apoptosis. Oncogene. 2000 Nov 16;19(48):5477–86.
61. Takahashi H, Feuerhake F, Kutok JL, Monti S, Dal Cin P, Neuberg D, et al. FAS death domain deletions and cellular FADD-like interleukin 1beta converting enzyme inhibitory protein (long) overexpression: alternative mechanisms for deregulating the extrinsic apoptotic pathway in diffuse large B-cell lymphoma subtypes. Clin Cancer Res. 2006 Jun 1;12(11 Pt 1):3265–71.
62. Villablanca EJ, Raccosta L, Zhou D, Fontana R, Maggioni D, Negro A, et al. Tumor-mediated liver X receptor-alpha activation inhibits CC chemokine receptor-7 expression on dendritic cells and dampens antitumor responses. Nat Med. 2010 Jan;16(1):98–105.
63. Gabrilovich DI, Ishida T, Nadaf S, Ohm JE, Carbone DP. Antibodies to vascular endothelial growth factor enhance the efficacy of cancer immunotherapy by improving endogenous dendritic cell function. Clin Cancer Res. 1999 Oct;5(10):2963–70.
64. Wrzesinski SH, Wan YY, Flavell RA. Transforming growth factor-beta and the immune response: implications for anticancer therapy. Clin Cancer Res. 2007 Sep 15;13(18 Pt 1):5262–70.
65. Munn DH, Zhou M, Attwood JT, Bondarev I, Conway SJ, Marshall B, et al. Prevention of allogeneic fetal rejection by tryptophan catabolism. Science (80-). 1998 Aug 21;281(5380):1191–3.
66. Uyttenhove C, Pilotte L, Théate I, Stroobant V, Colau D, Parmentier N, et al. Evidence for a tumoral immune resistance mechanism based on tryptophan degradation by indoleamine 2,3-dioxygenase. Nat Med. 2003 Oct;9(10):1269–74.
67. Terabe M, Berzofsky JA. Immunoregulatory T cells in tumor immunity. Curr Opin Immunol. 2004 Apr;16(2):157–62.
68. Woo EY, Chu CS, Goletz TJ, Schlienger K, Yeh H, Coukos G, et al. Regulatory CD4(+)CD25(+) T cells in tumors from patients with early-stage non-small cell lung cancer and late-stage ovarian cancer. Cancer Res. 2001 Jun 15;61(12):4766–72.

69. Fecci PE, Mitchell DA, Whitesides JF, Xie W, Friedman AH, Archer GE, et al. Increased regulatory T-cell fraction amidst a diminished CD4 compartment explains cellular immune defects in patients with malignant glioma. Cancer Res. 2006 Mar 15;66(6):3294–302.
70. Chikamatsu K, Sakakura K, Whiteside TL, Furuya N. Relationships between regulatory T cells and CD8+ effector populations in patients with squamous cell carcinoma of the head and neck. Head Neck. 2007 Feb;29(2):120–7.
71. Curiel TJ, Coukos G, Zou L, Alvarez X, Cheng P, Mottram P, et al. Specific recruitment of regulatory T cells in ovarian carcinoma fosters immune privilege and predicts reduced survival. Nat Med. 2004 Sep;10(9):942–9.
72. Hiraoka N, Onozato K, Kosuge T, Hirohashi S. Prevalence of FOXP3+ regulatory T cells increases during the progression of pancreatic ductal adenocarcinoma and its premalignant lesions. Clin Cancer Res. 2006 Sep 15;12(18):5423–34.
73. Saito T, Nishikawa H, Wada H, Nagano Y, Sugiyama D, Atarashi K, et al. Two FOXP3+CD4+ T cell subpopulations distinctly control the prognosis of colorectal cancers. Nat Med. 2016 Apr 25;22(6):679–84.
74. Overacre-Delgoffe AE, Chikina M, Dadey RE, Yano H, Brunazzi EA, Shayan G, et al. Interferon-g Drives Treg Fragility to Promote Anti-tumor Immunity. Cell. 2017;169:1130–41.
75. Yarchoan M, Johnson BA, Lutz ER, Laheru DA, Jaffee EM. Targeting neoantigens to augment antitumour immunity. Nat Rev Cancer. 2017;17(4):209–22.
76. Kwek SS, Cha E, Fong L. Unmasking the immune recognition of prostate cancer with CTLA4 blockade. Nat Rev Cancer. 2012 Apr;12(4):289–97.
77. Butts C, Murray N, Maksymiuk A, Goss G, Marshall E, Soulières D, et al. Randomized phase IIB trial of BLP25 liposome vaccine in stage IIIB and IV non-small-cell lung cancer. J Clin Oncol. 2005 Sep 20;23(27):6674–81.
78. Butts C, Maksymiuk A, Goss G, Soulières D, Marshall E, Cormier Y, et al. Updated survival analysis in patients with stage IIIB or IV non-small-cell lung cancer receiving BLP25 liposome vaccine (L-BLP25): phase IIB randomized, multicenter, open-label trial. J Cancer Res Clin Oncol. 2011 Sep;137(9):1337–42.
79. Butts C, Socinski MA, Mitchell PL, Thatcher N, Havel L, Krzakowski M, et al. Tecemotide (L-BLP25) versus placebo after chemoradiotherapy for stage III non-small-cell lung cancer (START): a randomised, double-blind, phase 3 trial. Lancet Oncol. 2014 Jan;15(1):59–68.
80. Redfern CH, Guthrie TH, Bessudo A, Densmore JJ, Holman PR, Janakiraman N, et al. Phase II trial of idiotype vaccination in previously treated patients with indolent non-Hodgkin's lymphoma resulting in durable clinical responses. J Clin

Oncol. 2006 Jul 1;24(19):3107–12.
81. Czerniecki BJ, Koski GK, Koldovsky U, Xu S, Cohen PA, Mick R, et al. Targeting HER-2/neu in early breast cancer development using dendritic cells with staged interleukin-12 burst secretion. Cancer Res. 2007 Feb 15;67(4):1842–52.
82. Sheikh NA, Petrylak D, Kantoff PW, dela Rosa C, Stewart FP, Kuan L-Y, et al. Sipuleucel-T immune parameters correlate with survival: an analysis of the randomized phase 3 clinical trials in men with castration-resistant prostate cancer. Cancer Immunol Immunother. 2013 Jan;62(1):137–47.
83. Enock A, Ndefo UA. Sipuleucel-T (Provenge) Injection: The First Immunotherapy Agent (Vaccine) For Hormone-Refractory Prostate Cancer. Pharm Ther. 2011;36(4):197–202.
84. Kantoff PW, Higano CS, Shore ND, Berger ER, Small EJ, Penson DF, et al. Sipuleucel-T immunotherapy for castration-resistant prostate cancer. N Engl J Med. 2010 Jul 29;363(5):411–22.
85. Higano CS, Schellhammer PF, Small EJ, Burch PA, Nemunaitis J, Yuh L, et al. Integrated data from 2 randomized, double-blind, placebo-controlled, phase 3 trials of active cellular immunotherapy with sipuleucel-T in advanced prostate cancer. Cancer. 2009 Aug 15;115(16):3670–9.
86. Small EJ, Schellhammer PF, Higano CS, Redfern CH, Nemunaitis JJ, Valone FH, et al. Placebo-Controlled Phase III Trial of Immunologic Therapy with Sipuleucel-T (APC8015) in Patients with Metastatic, Asymptomatic Hormone Refractory Prostate Cancer. J Clin Oncol. 2006 Jul;24(19):3089–94.
87. Restifo NP, Dudley ME, Rosenberg SA. Adoptive immunotherapy for cancer: harnessing the T cell response. Nat Rev Immunol. 2012 Apr;12(4):269–81.
88. Antonia SJ, Mirza N, Fricke I, Chiappori A, Thompson P, Williams N, et al. Combination of p53 cancer vaccine with chemotherapy in patients with extensive stage small cell lung cancer. Clin Cancer Res. 2006 Mar 1;12(3 Pt 1):878–87.
89. Mahnke K, Schönfeld K, Fondel S, Ring S, Karakhanova S, Wiedemeyer K, et al. Depletion of CD4+CD25+ human regulatory T cells in vivo: kinetics of Treg depletion and alterations in immune functions in vivo and in vitro. Int J Cancer. 2007 Jun 15;120(12):2723–33.
90. Blankenstein T, Coulie PG, Gilboa E, Jaffee EM. The determinants of tumour immunogenicity. Nat Rev Cancer. 2012 Apr;12(4):307–13.
91. Pastor F, Kolonias D, Giangrande PH, Gilboa E. Induction of tumour immunity by targeted inhibition of nonsense-mediated mRNA decay. Nature. 2010 May 13;465(7295):227–30.
92. Türeci Ö, Vormehr M, Diken M, Kreiter S, Huber C, Sahin U. Targeting the Heterogeneity of Cancer with Individualized Neoepitope Vaccines. Clin Cancer

Res. 2016;22(8):1885–96.
93. Pardoll DM. The blockade of immune checkpoints in cancer immunotherapy. Nat Rev Cancer. 2012 Apr;12(4):252–64.
94. Tivol EA, Borriello F, Schweitzer AN, Lynch WP, Bluestone JA, Sharpe AH. Loss of CTLA-4 leads to massive lymphoproliferation and fatal multiorgan tissue destruction, revealing a critical negative regulatory role of CTLA-4. Immunity. 1995 Nov;3(5):541–7.
95. Waterhouse P, Penninger JM, Timms E, Wakeham A, Shahinian A, Lee KP, et al. Lymphoproliferative disorders with early lethality in mice deficient in CTLA-4. Science (80-). 1995 Nov 10;270(5238):985–8.
96. Peggs KS, Quezada SA, Chambers CA, Korman AJ, Allison JP. Blockade of CTLA-4 on both effector and regulatory T cell compartments contributes to the antitumor activity of anti-CTLA-4 antibodies. J Exp Med. 2009 Aug 3;206(8):1717–25.
97. Leach DR, Krummel MF, Allison JP. Enhancement of antitumor immunity by CTLA-4 blockade. Science (80-). 1996 Mar 22;271(5256):1734–6.
98. Loser K, Scherer A, Krummen MBW, Varga G, Higuchi T, Schwarz T, et al. An important role of CD80/CD86-CTLA-4 signaling during photocarcinogenesis in mice. J Immunol. 2005 May 1;174(9):5298–305.
99. van Elsas A, Hurwitz AA, Allison JP. Combination immunotherapy of B16 melanoma using anti-cytotoxic T lymphocyte-associated antigen 4 (CTLA-4) and granulocyte/macrophage colony-stimulating factor (GM-CSF)-producing vaccines induces rejection of subcutaneous and metastatic tumors accompanied . J Exp Med. 1999 Aug 2;190(3):355–66.
100. Dariavach P, Mattéi MG, Golstein P, Lefranc MP. Human Ig superfamily CTLA-4 gene: chromosomal localization and identity of protein sequence between murine and human CTLA-4 cytoplasmic domains. Eur J Immunol. 1988 Dec;18(12):1901–5.
101. Hodi FS, Mihm MC, Soiffer RJ, Haluska FG, Butler M, Seiden M V, et al. Biologic activity of cytotoxic T lymphocyte-associated antigen 4 antibody blockade in previously vaccinated metastatic melanoma and ovarian carcinoma patients. Proc Natl Acad Sci U S A. 2003 Apr 15;100(8):4712–7.
102. Phan GQ, Yang JC, Sherry RM, Hwu P, Topalian SL, Schwartzentruber DJ, et al. Cancer regression and autoimmunity induced by cytotoxic T lymphocyte-associated antigen 4 blockade in patients with metastatic melanoma. Proc Natl Acad Sci U S A. 2003 Jul 8;100(14):8372–7.
103. Hodi FS, O'Day SJ, McDermott DF, Weber RW, Sosman JA, Haanen JB, et al. Improved survival with ipilimumab in patients with metastatic melanoma. N Engl J Med. 2010 Aug 19;363(8):711–23.
104. Eggermont AMM, Chiarion-Sileni V, Grob JJ, Dummer R, Wolchok JD, Schmidt

H, et al. Adjuvant ipilimumab versus placebo after complete resection of high-risk stage III melanoma (EORTC 18071): A randomised, double-blind, phase 3 trial. Lancet Oncol. 2015;16(5):522–30.
105. Coens C, Suciu S, Chiarion-Sileni V, Grob JJ, Dummer R, Wolchok JD, et al. Health-related quality of life with adjuvant ipilimumab versus placebo after complete resection of high-risk stage III melanoma (EORTC 18071): secondary outcomes of a multinational, randomised, double-blind, phase 3 trial. Lancet Oncol. 2017;18(3):393–403.
106. Sharma P. Immune Checkpoint Therapy and the Search for Predictive Biomarkers. Cancer J. 2016;22(2):68–72.
107. Barber DL, Wherry EJ, Masopust D, Zhu B, Allison JP, Sharpe AH, et al. Restoring function in exhausted CD8 T cells during chronic viral infection. Nature. 2006 Feb 9;439(7077):682–7.
108. Sfanos KS, Bruno TC, Meeker AK, De Marzo AM, Isaacs WB, Drake CG. Human prostate-infiltrating CD8+ T lymphocytes are oligoclonal and PD-1+. Prostate. 2009 Nov 1;69(15):1694–703.
109. Ahmadzadeh M, Johnson LA, Heemskerk B, Wunderlich JR, Dudley ME, White DE, et al. Tumor antigen-specific CD8 T cells infiltrating the tumor express high levels of PD-1 and are functionally impaired. Blood. 2009 Aug 20;114(8):1537–44.
110. Dong H, Strome SE, Salomao DR, Tamura H, Hirano F, Flies DB, et al. Tumor-associated B7-H1 promotes T-cell apoptosis: a potential mechanism of immune evasion. Nat Med. 2002 Aug;8(8):793–800.
111. Konishi J, Yamazaki K, Azuma M, Kinoshita I, Dosaka-Akita H, Nishimura M. B7-H1 expression on non-small cell lung cancer cells and its relationship with tumor-infiltrating lymphocytes and their PD-1 expression. Clin Cancer Res. 2004 Aug 1;10(15):5094–100.
112. Brown JA, Dorfman DM, Ma F-R, Sullivan EL, Munoz O, Wood CR, et al. Blockade of programmed death-1 ligands on dendritic cells enhances T cell activation and cytokine production. J Immunol. 2003 Feb 1;170(3):1257–66.
113. Gubin MM, Zhang X, Schuster H, Caron E, Ward JP, Noguchi T, et al. Checkpoint blockade cancer immunotherapy targets tumour-specific mutant antigens. Nature. 2014 Nov 26;515(7528):577–81.
114. Brahmer JR, Drake CG, Wollner I, Powderly JD, Picus J, Sharfman WH, et al. Phase I study of single-agent anti-programmed death-1 (MDX-1106) in refractory solid tumors: safety, clinical activity, pharmacodynamics, and immunologic correlates. J Clin Oncol. 2010 Jul 1;28(19):3167–75.
115. Topalian SL, Hodi FS, Brahmer JR, Gettinger SN, Smith DC, McDermott DF, et al. Safety, Activity, and Immune Correlates of Anti–PD-1 Antibody in Cancer. N Engl J Med. 2012 Jun 28;366(26):2443–54.

116. Weber JS, D'Angelo SP, Minor D, Hodi FS, Gutzmer R, Neyns B, et al. Nivolumab versus chemotherapy in patients with advanced melanoma who progressed after anti-CTLA-4 treatment (CheckMate 037): a randomised, controlled, open-label, phase 3 trial. Lancet Oncol. 2015 Apr;16(4):375–84.
117. Robert C, Long G V, Brady B, Dutriaux C, Maio M, Mortier L, et al. Nivolumab in Previously Untreated Melanoma without BRAF Mutation. N Engl J Med. 2015 Jan 22;372(4):320–30.
118. Motzer RJ, Escudier B, McDermott DF, George S, Hammers HJ, Srinivas S, et al. Nivolumab versus Everolimus in Advanced Renal-Cell Carcinoma. N Engl J Med. 2015 Nov 5;373(19):1803–13.
119. Brahmer J, Reckamp KL, Baas P, Crinò L, Eberhardt WEE, Poddubskaya E, et al. Nivolumab versus Docetaxel in Advanced Squamous-Cell Non–Small-Cell Lung Cancer. N Engl J Med. 2015 Jul 9;373(2):123–35.
120. Borghaei H, Paz-Ares L, Horn L, Spigel DR, Steins M, Ready NE, et al. Nivolumab versus Docetaxel in Advanced Nonsquamous Non–Small-Cell Lung Cancer. N Engl J Med. 2015 Oct 22;373(17):1627–39.
121. Horn L, Spigel DR, Vokes EE, Holgado E, Ready N, Steins M, et al. Nivolumab Versus Docetaxel in Previously Treated Patients With Advanced Non–Small-Cell Lung Cancer: Two-Year Outcomes From Two Randomized, Open-Label, Phase III Trials (CheckMate 017 and CheckMate 057). J Clin Oncol. 2017 Dec 10;35(35):3924–33.
122. Ribas A, Puzanov I, Dummer R, Schadendorf D, Hamid O, Robert C, et al. Pembrolizumab versus investigator-choice chemotherapy for ipilimumab-refractory melanoma (KEYNOTE-002): a randomised, controlled, phase 2 trial. Lancet Oncol. 2015 Aug;16(8):908–18.
123. Garon EB, Rizvi NA, Hui R, Leighl N, Balmanoukian AS, Eder JP, et al. Pembrolizumab for the Treatment of Non–Small-Cell Lung Cancer. N Engl J Med. 2015;372(21):2018–28.
124. Le DT, Uram JN, Wang H, Bartlett BR, Kemberling H, Eyring AD, et al. PD-1 Blockade in Tumors with Mismatch-Repair Deficiency. N Engl J Med. 2015;372(26):2509–20.
125. Le DT, Durham JN, Smith KN, Wang H, Bartlett BR, Aulakh LK, et al. Mismatch repair deficiency predicts response of solid tumors to PD-1 blockade. Science (80-). 2017;357(6349):409–13.
126. U.S. Food & Drug Administration. FDA approves first cancer treatment for any solid tumor with a specific genetic feature [Internet]. FDA News Release. 2017 [cited 2017 Dec 23]. Available from: https://www.fda.gov/newsevents/newsroom/pressannouncements/ucm560167.htm
127. Herbst RS, Soria J-C, Kowanetz M, Fine GD, Hamid O, Gordon MS, et al.

Predictive correlates of response to the anti-PD-L1 antibody MPDL3280A in cancer patients. Nature. 2014 Nov 26;515(7528):563–7.
128. Powles T, Eder JP, Fine GD, Braiteh FS, Loriot Y, Cruz C, et al. MPDL3280A (anti-PD-L1) treatment leads to clinical activity in metastatic bladder cancer. Nature. 2014 Nov 26;515(7528):558–62.
129. McDermott DF, Sosman JA, Sznol M, Massard C, Gordon MS, Hamid O, et al. Atezolizumab, an anti-programmed death-ligand 1 antibody, in metastatic renal cell carcinoma: Long-term safety, clinical activity, and immune correlates from a phase Ia study. J Clin Oncol. 2016;34(8):833–42.
130. Antonia SJ, Villegas A, Daniel D, Vicente D, Murakami S, Hui R, et al. Durvalumab after Chemoradiotherapy in Stage III Non–Small-Cell Lung Cancer. N Engl J Med. 2017 Nov 16;377(20):1919–29.
131. Vonderheide RH, June CH. Engineering T cells for cancer: our synthetic future. Immunol Rev. 2014 Jan;257(1):7–13.
132. Ruella M, Kalos M. Adoptive immunotherapy for cancer. Immunol Rev. 2014 Jan;257(1):14–38.
133. Greenberg PD, Reusser P, Goodrich JM, Riddell SR. Development of a treatment regimen for human cytomegalovirus (CMV) infection in bone marrow transplantation recipients by adoptive transfer of donor-derived CMV-specific T cell clones expanded in vitro. Ann N Y Acad Sci. 1991 Dec 30;636:184–95.
134. Rosenberg SA, Yannelli JR, Yang JC, Topalian SL, Schwartzentruber DJ, Weber JS, et al. Treatment of patients with metastatic melanoma with autologous tumor-infiltrating lymphocytes and interleukin 2. J Natl Cancer Inst. 1994 Aug 3;86(15):1159–66.
135. Dudley ME, Wunderlich JR, Robbins PF, Yang JC, Hwu P, Schwartzentruber DJ, et al. Cancer regression and autoimmunity in patients after clonal repopulation with antitumor lymphocytes. Science (80-). 2002 Oct 25;298(5594):850–4.
136. Dudley ME, Wunderlich JR, Yang JC, Sherry RM, Topalian SL, Restifo NP, et al. Adoptive cell transfer therapy following non-myeloablative but lymphodepleting chemotherapy for the treatment of patients with refractory metastatic melanoma. J Clin Oncol. 2005 Apr 1;23(10):2346–57.
137. Dudley ME, Yang JC, Sherry R, Hughes MS, Royal R, Kammula U, et al. Adoptive cell therapy for patients with metastatic melanoma: evaluation of intensive myeloablative chemoradiation preparative regimens. J Clin Oncol. 2008 Nov 10;26(32):5233–9.
138. Rosenberg SA, Yang JC, Sherry RM, Kammula US, Hughes MS, Phan GQ, et al. Durable Complete Responses in Heavily Pretreated Patients with Metastatic Melanoma Using T-Cell Transfer Immunotherapy. Clin Cancer Res. 2011 Apr 15;17(13):4550–7.

139. Hinrichs CS, Rosenberg SA. Exploiting the curative potential of adoptive T-cell therapy for cancer. Immunol Rev. 2014 Jan;257(1):56–71.
140. Goff SL, Dudley ME, Citrin DE, Somerville RP, Wunderlich JR, Danforth DN, et al. Randomized, Prospective Evaluation Comparing Intensity of Lymphodepletion Before Adoptive Transfer of Tumor-Infiltrating Lymphocytes for Patients With Metastatic Melanoma. J Clin Oncol. 2016 Jul 10;34(20):2389–97.
141. Dudley ME, Gross CA, Langhan MM, Garcia MR, Sherry RM, Yang JC, et al. CD8+ enriched “young” tumor infiltrating lymphocytes can mediate regression of metastatic melanoma. Clin Cancer Res. 2010 Dec 15;16(24):6122–31.
142. Gattinoni L, Klebanoff CA, Palmer DC, Wrzesinski C, Kerstann K, Yu Z, et al. Acquisition of full effector function in vitro paradoxically impairs the in vivo antitumor efficacy of adoptively transferred CD8+ T cells. J Clin Invest. 2005 Jun;115(6):1616–26.
143. Barrett DM, Grupp SA, June CH. Chimeric Antigen Receptor- and TCR-Modified T Cells Enter Main Street and Wall Street. J Immunol. 2015;195(3):755–61.
144. Dembić Z, Haas W, Weiss S, McCubrey J, Kiefer H, von Boehmer H, et al. Transfer of specificity by murine alpha and beta T-cell receptor genes. Nature. 1986;320(6059):232–8.
145. Clay TM, Custer MC, Sachs J, Hwu P, Rosenberg SA, Nishimura MI. Efficient transfer of a tumor antigen-reactive TCR to human peripheral blood lymphocytes confers anti-tumor reactivity. J Immunol. 1999 Jul 1;163(1):507–13.
146. Li Y, Moysey R, Molloy PE, Vuidepot A-L, Mahon T, Baston E, et al. Directed evolution of human T-cell receptors with picomolar affinities by phage display. Nat Biotechnol. 2005 Mar;23(3):349–54.
147. Udyavar A, Alli R, Nguyen P, Baker L, Geiger TL. Subtle affinity-enhancing mutations in a myelin oligodendrocyte glycoprotein-specific TCR alter specificity and generate new self-reactivity. J Immunol. 2009 Apr 1;182(7):4439–47.
148. Morgan RA, Dudley ME, Wunderlich JR, Hughes MS, Yang JC, Sherry RM, et al. Cancer regression in patients after transfer of genetically engineered lymphocytes. Science (80-). 2006 Oct 6;314(5796):126–9.
149. Johnson LA, Morgan RA, Dudley ME, Cassard L, Yang JC, Hughes MS, et al. Gene therapy with human and mouse T-cell receptors mediates cancer regression and targets normal tissues expressing cognate antigen. Blood. 2009 Jul 16;114(3):535–46.
150. Robbins PF, Morgan RA, Feldman SA, Yang JC, Sherry RM, Dudley ME, et al. Tumor regression in patients with metastatic synovial cell sarcoma and

melanoma using genetically engineered lymphocytes reactive with NY-ESO-1. J Clin Oncol. 2011 Mar 1;29(7):917–24.
151. Robbins PF, Kassim SH, Tran TLN, Crystal JS, Morgan RA, Feldman SA, et al. A pilot trial using lymphocytes genetically engineered with an NY-ESO-1-reactive T-cell receptor: Long-term follow-up and correlates with response. Clin Cancer Res. 2015;21(5):1019–27.
152. Rapoport AP, Stadtmauer EA, Binder-Scholl GK, Goloubeva O, Vogl DT, Lacey SF, et al. NY-ESO-1-specific TCR-engineered T cells mediate sustained antigen-specific antitumor effects in myeloma. Nat Med. 2015;21(8):914–21.
153. Morgan RA, Chinnasamy N, Abate-Daga D, Gros A, Robbins PF, Zheng Z, et al. Cancer regression and neurological toxicity following anti-MAGE-A3 TCR gene therapy. J Immunother. 2013 Feb;36(2):133–51.
154. Cameron BJ, Gerry AB, Dukes J, Harper J V, Kannan V, Bianchi FC, et al. Identification of a titin-derived HLA-A1-presented peptide as a cross-reactive target for engineered MAGE A3-directed T cells. Sci Transl Med. 2013 Aug 7;5(197):197ra103.
155. Linette GP, Stadtmauer EA, Maus M V, Rapoport AP, Levine BL, Emery L, et al. Cardiovascular toxicity and titin cross-reactivity of affinity-enhanced T cells in myeloma and melanoma. Blood. 2013 Aug 8;122(6):863–71.
156. Sadelain M, Brentjens R, Rivière I. The Basic Principles of Chimeric Antigen Receptor Design. Cancer Discov. 2013 Apr;3(4):388–98.
157. Maus M V, Grupp SA, Porter DL, June CH. Antibody-modified T cells: CARs take the front seat for hematologic malignancies. Blood. 2014;123(17):2625–35.
158. Dotti G, Gottschalk S, Savoldo B, Brenner MK. Design and development of therapies using chimeric antigen receptor-expressing T cells. Immunol Rev. 2014 Jan;257(1):107–26.
159. Guest RD, Hawkins RE, Kirillova N, Cheadle EJ, Arnold J, O'Neill A, et al. The role of extracellular spacer regions in the optimal design of chimeric immune receptors: evaluation of four different scFvs and antigens. J Immunother. 2005;28(3):203–11.
160. Brocker T, Karjalainen K. Signals through T cell receptor-zeta chain alone are insufficient to prime resting T lymphocytes. J Exp Med. 1995 May 1;181(5):1653–9.
161. Gong MC, Latouche J-B, Krause A, Heston WDW, Bander NH, Sadelain M. Cancer patient T cells genetically targeted to prostate-specific membrane antigen specifically lyse prostate cancer cells and release cytokines in response to prostate-specific membrane antigen. Neoplasia. 1999 Jun;1(2):123–7.
162. Maher J, Brentjens RJ, Gunset G, Rivière I, Sadelain M. Human T-lymphocyte

cytotoxicity and proliferation directed by a single chimeric TCRzeta/CD28 receptor. Nat Biotechnol. 2002 Jan;20(1):70–5.
163. Kowolik CM, Topp MS, Gonzalez S, Pfeiffer T, Olivares S, Gonzalez N, et al. CD28 costimulation provided through a CD19-specific chimeric antigen receptor enhances in vivo persistence and antitumor efficacy of adoptively transferred T cells. Cancer Res. 2006 Nov 15;66(22):10995–1004.
164. Brentjens RJ, Santos E, Nikhamin Y, Yeh R, Matsushita M, La Perle K, et al. Genetically targeted T cells eradicate systemic acute lymphoblastic leukemia xenografts. Clin Cancer Res. 2007 Sep 15;13(18 Pt 1):5426–35.
165. Savoldo B, Ramos CA, Liu E, Mims MP, Keating MJ, Carrum G, et al. CD28 costimulation improves expansion and persistence of chimeric antigen receptor-modified T cells in lymphoma patients. J Clin Invest. 2011 May;121(5):1822–6.
166. Zhao Z, Condomines M, van der Stegen SJC, Perna F, Kloss CC, Gunset G, et al. Structural Design of Engineered Costimulation Determines Tumor Rejection Kinetics and Persistence of CAR T Cells. Cancer Cell. 2015;28(4):415–28.
167. Zhong X-S, Matsushita M, Plotkin J, Rivière I, Sadelain M. Chimeric antigen receptors combining 4-1BB and CD28 signaling domains augment PI3kinase/AKT/Bcl-XL activation and CD8+ T cell-mediated tumor eradication. Mol Ther. 2010 Feb;18(2):413–20.
168. Tammana S, Huang X, Wong M, Milone MC, Ma L, Levine BL, et al. 4-1BB and CD28 signaling plays a synergistic role in redirecting umbilical cord blood T cells against B-cell malignancies. Hum Gene Ther. 2010 Jan;21(1):75–86.
169. Till BG, Jensen MC, Wang J, Qian X, Gopal AK, Maloney DG, et al. CD20-specific adoptive immunotherapy for lymphoma using a chimeric antigen receptor with both CD28 and 4-1BB domains: pilot clinical trial results. Blood. 2012 Apr 26;119(17):3940–50.
170. Chmielewski M, Hombach AA, Abken H. Of CARs and TRUCKs: chimeric antigen receptor (CAR) T cells engineered with an inducible cytokine to modulate the tumor stroma. Immunol Rev. 2014 Jan;257(1):83–90.
171. Pegram HJ, Lee JC, Hayman EG, Imperato GH, Tedder TF, Sadelain M, et al. Tumor-targeted T cells modified to secrete IL-12 eradicate systemic tumors without need for prior conditioning. Blood. 2012 May 3;119(18):4133–41.
172. Chinnasamy D, Yu Z, Kerkar SP, Zhang L, Morgan RA, Restifo NP, et al. Local delivery of interleukin-12 using T cells targeting VEGF receptor-2 eradicates multiple vascularized tumors in mice. Clin Cancer Res. 2012 Mar 15;18(6):1672–83.
173. Yeku OO, Brentjens RJ. Armored CAR T-cells: utilizing cytokines and pro-inflammatory ligands to enhance CAR T-cell anti-tumour efficacy. Biochem Soc Trans. 2016 Apr 15;44(2):412–8.

174. Irving M, Vuillefroy De Silly R, Scholten K, Dilek N, Coukos G. Engineering CAR T-cells for Racing in Solid Tumors; Don't Forget the Fuel. Front Immunol. 2017;8:267.
175. Brentjens RJ, Latouche J-B, Santos E, Marti F, Gong MC, Lyddane C, et al. Eradication of systemic B-cell tumors by genetically targeted human T lymphocytes co-stimulated by CD80 and interleukin-15. Nat Med. 2003 Mar;9(3):279–86.
176. June CH, O'Connor RS, Kawalekar OU, Ghassemi S, Milone MC. CAR T cell immunotherapy for human cancer. Science (80-). 2018;359:1361–5.
177. Holzinger A, Barden M, Abken H. The growing world of CAR T cell trials: a systematic review. Cancer Immunol Immunother. 2016 Dec;65(12):1433–50.
178. Kochenderfer JN, Wilson WH, Janik JE, Dudley ME, Stetler-Stevenson M, Feldman SA, et al. Eradication of B-lineage cells and regression of lymphoma in a patient treated with autologous T cells genetically engineered to recognize CD19. Blood. 2010 Nov 18;116(20):4099–102.
179. Kochenderfer JN, Dudley ME, Feldman SA, Wilson WH, Spaner DE, Maric I, et al. B-cell depletion and remissions of malignancy along with cytokine-associated toxicity in a clinical trial of anti-CD19 chimeric-antigen-receptor-transduced T cells. Blood. 2012 Mar 22;119(12):2709–20.
180. Kochenderfer JN, Dudley ME, Kassim SH, Somerville RPT, Carpenter RO, Stetler-Stevenson M, et al. Chemotherapy-refractory diffuse large B-cell lymphoma and indolent B-cell malignancies can be effectively treated with autologous T cells expressing an anti-CD19 chimeric antigen receptor. J Clin Oncol. 2015;33(6):540–9.
181. Kochenderfer JN, Somerville RPT, Lu T, Yang JC, Sherry RM, Feldman SA, et al. Long-Duration Complete Remissions of Diffuse Large B Cell Lymphoma after Anti-CD19 Chimeric Antigen Receptor T Cell Therapy. Mol Ther. 2017;25(10):2245–53.
182. Brentjens RJ, Rivière I, Park JH, Davila ML, Wang X, Stefanski J, et al. Safety and persistence of adoptively transferred autologous CD19-targeted T cells in patients with relapsed or chemotherapy refractory B-cell leukemias. Blood. 2011 Nov 3;118(18):4817–28.
183. Brentjens R, Davila ML, Rivière I, Park J, Wang X, Cowell LG, et al. CD19-targeted T cells rapidly induce molecular remissions in adults with chemotherapy-refractory acute lymphoblastic leukemia. Sci Transl Med. 2013 Mar 20;5(177):177ra38.
184. Davila ML, Rivière I, Wang X, Bartido S, Park J, Curran K, et al. Efficacy and toxicity management of 19-28z CAR T cell therapy in B cell acute lymphoblastic leukemia. Sci Transl Med. 2014;6(224):224ra25.
185. Kalos M, Levine BL, Porter DL, Katz S, Grupp SA, Bagg A, et al. T cells with

chimeric antigen receptors have potent antitumor effects and can establish memory in patients with advanced leukemia. Sci Transl Med. 2011 Aug 10;3(95):95ra73.
186. Porter DL, Levine BL, Kalos M, Bagg A, June CH. Chimeric antigen receptor-modified T cells in chronic lymphoid leukemia. N Engl J Med. 2011 Aug 25;365(8):725–33.
187. Grupp SA, Kalos M, Barrett DM, Aplenc R, Porter DL, Rheingold SR, et al. Chimeric antigen receptor-modified T cells for acute lymphoid leukemia. N Engl J Med. 2013 Apr 18;368(16):1509–18.
188. Maude SL, Frey N, Shaw PA, Aplenc R, Barrett DM, Bunin NJ, et al. Chimeric Antigen Receptor T Cells for Sustained Remissions in Leukemia. N Engl J Med. 2014 Oct 16;371(16):1507–17.
189. Porter DL, Hwang W-T, Frey N V, Lacey SF, Shaw PA, Loren AW, et al. Chimeric antigen receptor T cells persist and induce sustained remissions in relapsed refractory chronic lymphocytic leukemia. Sci Transl Med. 2015 Sep 2;7(303):303ra139.
190. Ritchie DS, Neeson PJ, Khot A, Peinert S, Tai T, Tainton K, et al. Persistence and efficacy of second generation CAR T cell against the LeY antigen in acute myeloid leukemia. Mol Ther. 2013 Nov;21(11):2122–9.
191. Ali SA, Shi V, Maric I, Wang M, Stroncek DF, Rose JJ, et al. T cells expressing an anti-B-cell maturation antigen chimeric antigen receptor cause remissions of multiple myeloma. Blood. 2016 Sep 29;128(13):1688–700.
192. Pan J, Yang JF, Deng BP, Zhao XJ, Zhang X, Lin YH, et al. High efficacy and safety of low-dose CD19-directed CAR-T cell therapy in 51 refractory or relapsed B acute lymphoblastic leukemia patients. Leukemia. 2017;31:2587–93.
193. Hombach AA, Görgens A, Chmielewski M, Murke F, Kimpel J, Giebel B, et al. Superior Therapeutic Index in Lymphoma Therapy: CD30(+) CD34(+) Hematopoietic Stem Cells Resist a Chimeric Antigen Receptor T-cell Attack. Mol Ther. 2016;24(8):1423–34.
194. Gao H, Li K, Tu H, Pan X, Jiang H, Shi B, et al. Development of T Cells Redirected to Glypican-3 for the Treatment of Hepatocellular Carcinoma. Clin Cancer Res. 2014 Dec 15;20(24):6418–28.
195. Li K, Pan X, Bi Y, Xu W, Chen C, Gao H, et al. Adoptive immunotherapy using T lymphocytes redirected to glypican-3 for the treatment of lung squamous cell carcinoma. Oncotarget. 2016 Jan 19;7(3):2496–507.
196. Posey Jr AD, Schwab RD, Boesteanu AC, Steentoft C, Mandel U, Engels B, et al. Engineered CAR T Cells Targeting the Cancer-Associated Tn-Glycoform of the Membrane Mucin MUC1 Control Adenocarcinoma. Immunity. 2016;44(6):1444–54.

197. Hong H, Brown CE, Ostberg JR, Priceman SJ, Chang W-C, Weng L, et al. L1 Cell Adhesion Molecule-Specific Chimeric Antigen Receptor-Redirected Human T Cells Exhibit Specific and Efficient Antitumor Activity against Human Ovarian Cancer in Mice. PLoS One. 2016;11(1):e0146885.
198. Owens GL, Sheard VE, Kalaitsidou M, Blount D, Lad Y, Cheadle EJ, et al. Preclinical Assessment of CAR T-Cell Therapy Targeting the Tumor Antigen 5T4 in Ovarian Cancer. J Immunother. 2018 Apr;41(3):130–40.
199. Textor A, Listopad J, Wührmann L Le, Perez C, Kruschinski A, Chmielewski M, et al. Efficacy of CAR T cell therapy in large tumors relies upon stromal targeting by IFNγ. Cancer Res. 2014 Oct 8;74(23):6796–805.
200. Chmielewski M, Abken H. CAR T Cells Releasing IL-18 Convert to T-Bet high FoxO1 low Effectors that Exhibit Augmented Activity against Advanced Solid Tumors. Cell Rep. 2017;21(11):3205–19.
201. Morgan RA, Yang JC, Kitano M, Dudley ME, Laurencot CM, Rosenberg SA. Case report of a serious adverse event following the administration of T cells transduced with a chimeric antigen receptor recognizing ERBB2. Mol Ther. 2010 Apr;18(4):843–51.
202. Lamers CHJ, Sleijfer S, van Steenbergen S, van Elzakker P, van Krimpen B, Groot C, et al. Treatment of metastatic renal cell carcinoma with CAIX CAR-engineered T cells: clinical evaluation and management of on-target toxicity. Mol Ther. 2013 Apr;21(4):904–12.
203. Maus M V, Haas AR, Beatty GL, Albelda SM, Levine BL, Liu X, et al. T cells expressing chimeric antigen receptors can cause anaphylaxis in humans. Cancer Immunol Res. 2013 Jul;1(1):26–31.
204. Tanyi JL, Stashwick C, Plesa G, Morgan MA, Porter D, Maus M V, et al. Possible Compartmental Cytokine Release Syndrome in a Patient With Recurrent Ovarian Cancer After Treatment With Mesothelin-targeted CAR-T Cells. J Immunother. 2017 Feb 23;40(3):104–7.
205. Louis CU, Savoldo B, Dotti G, Pule M, Yvon E, Myers GD, et al. Antitumor activity and long-term fate of chimeric antigen receptor-positive T cells in patients with neuroblastoma. Blood. 2011 Dec 1;118(23):6050–6.
206. Ahmed N, Brawley V, Hegde M, Bielamowicz K, Kalra M, Landi D, et al. HER2-Specific Chimeric Antigen Receptor–Modified Virus-Specific T Cells for Progressive Glioblastoma: A Phase 1 Dose-Escalation Trial. JAMA Oncol. 2017 Apr 20;21(11):2087–101.
207. Kloss CC, Condomines M, Cartellieri M, Bachmann M, Sadelain M. Combinatorial antigen recognition with balanced signaling promotes selective tumor eradication by engineered T cells. Nat Biotechnol. 2013 Jan;31(1):71–5.
208. Santoro SP, Kim S, Motz GT, Alatzoglou D, Li C, Irving M, et al. T Cells Bearing a Chimeric Antigen Receptor against Prostate-Specific Membrane

Antigen Mediate Vascular Disruption and Result in Tumor Regression. Cancer Immunol Res. 2015 Jan 1;3(1):68–84.
209. Weis SM, Cheresh DA. Tumor angiogenesis: molecular pathways and therapeutic targets. Nat Med. 2011 Jan;17(11):1359–70.
210. Samant RS, Shevde LA. Recent Advances in Anti-Angiogenic Therapy of Cancer. Oncotarget. 2011;2(3):122–34.
211. Nanda A, St Croix B. Tumor endothelial markers: new targets for cancer therapy. Curr Opin Oncol. 2004 Jan;16(1):44–9.
212. Chaudhary A, St Croix B. Selective blockade of tumor angiogenesis. Cell Cycle. 2012;11(12):2253–9.
213. Neri D, Bicknell R. Tumour vascular targeting. Nat Rev Cancer. 2005 Jun;5(6):436–46.
214. Burrows FJ, Thorpe PE. Eradication of large solid tumors in mice with an immunotoxin directed against tumor vasculature. Proc Natl Acad Sci U S A. 1993 Oct 1;90(19):8996–9000.
215. Hoff PM, Machado KK. Role of angiogenesis in the pathogenesis of cancer. Cancer Treat Rev. 2012 Nov;38(7):825–33.
216. Brekken RA, Huang X, King SW, Thorpe PE. Vascular endothelial growth factor as a marker of tumor endothelium. Cancer Res. 1998 May 1;58(9):1952–9.
217. Brekken RA, Overholser JP, Stastny VA, Waltenberger J, Minna JD, Thorpe PE. Selective inhibition of vascular endothelial growth factor (VEGF) receptor 2 (KDR/Flk-1) activity by a monoclonal anti-VEGF antibody blocks tumor growth in mice. Cancer Res. 2000 Sep 15;60(18):5117–24.
218. Ferrara N, Hillan KJ, Gerber H-P, Novotny W. Discovery and development of bevacizumab, an anti-VEGF antibody for treating cancer. Nat Rev Drug Discov. 2004 May;3(5):391–400.
219. Tew WP, Gordon M, Murren J, Dupont J, Pezzulli S, Aghajanian C, et al. Phase 1 study of aflibercept administered subcutaneously to patients with advanced solid tumors. Clin Cancer Res. 2010 Jan 1;16(1):358–66.
220. Macarulla T, Sauri T, Tabernero J. Evaluation of aflibercept in the treatment of metastatic colorectal cancer. Expert Opin Biol Ther. 2014 Oct;14(10):1493–505.
221. Liontos M, Lykka M, Dimopoulos M-A, Bamias A. Profile of trebananib (AMG386) and its potential in the treatment of ovarian cancer. Onco Targets Ther. 2014 Jan;7:1837–45.
222. Hollebecque A, Massard C, Soria J-C. Vascular disrupting agents: a delicate balance between efficacy and side effects. Curr Opin Oncol. 2012 May;24(3):305–15.
223. Lee S, Chen TT, Barber CL, Jordan MC, Murdock J, Desai S, et al. Autocrine

VEGF signaling is required for vascular homeostasis. Cell. 2007 Aug 24;130(4):691–703.
224. Huminiecki L, Gorn M, Suchting S, Poulsom R, Bicknell R. Magic roundabout is a new member of the roundabout receptor family that is endothelial specific and expressed at sites of active angiogenesis. Genomics. 2002 Apr;79(4):547–52.
225. Mura M, Swain RK, Zhuang X, Vorschmitt H, Reynolds GM, Durant S, et al. Identification and angiogenic role of the novel tumor endothelial marker CLEC14A. Oncogene. 2012 Jan 19;31:293–305.
226. St Croix B, Rago C, Velculescu V, Traverso G, Romans KE, Montgomery E, et al. Genes Expressed in Human Tumor Endothelium. Science (80-). 2000 Aug 18;289(5482):1197–202.
227. Carson-Walter EB, Watkins DN, Nanda A, Vogelstein B, Kinzler KW, St Croix B. Cell Surface Tumor Endothelial Markers Are Conserved in Mice and Humans. Cancer Res. 2001;61:6649–55.
228. Bradley KA, Mogridge J, Mourez M, Collier RJ, Young JAT. Identification of the cellular receptor for anthrax toxin. Nature. 2001 Nov 8;414(6860):225–9.
229. Scobie HM, Rainey GJA, Bradley KA, Young JAT. Human capillary morphogenesis protein 2 functions as an anthrax toxin receptor. Proc Natl Acad Sci U S A. 2003 Apr 29;100(9):5170–4.
230. Liu S, Crown D, Miller-Randolph S, Moayeri M, Wang H, Hu H, et al. Capillary morphogenesis protein-2 is the major receptor mediating lethality of anthrax toxin in vivo. Proc Natl Acad Sci U S A. 2009 Jul 28;106(30):12424–9.
231. Miles LA, Burga LN, Gardner EE, Bostina M, Poirier JT, Rudin CM. Anthrax toxin receptor 1 is the cellular receptor for Seneca Valley virus. J Clin Invest. 2017 Jun 26;25(13):1605–12.
232. Nanda A, Carson-Walter EB, Seaman S, Barber TD, Stampfl J, Singh S, et al. TEM8 Interacts with the Cleaved C5 Domain of Collagen α3(VI). Cancer Res. 2004;64:817–20.
233. Hotchkiss KA, Basile CM, Spring SC, Bonuccelli G, Lisanti MP, Terman BI. TEM8 expression stimulates endothelial cell adhesion and migration by regulating cell-matrix interactions on collagen. Exp Cell Res. 2005 Apr 15;305(1):133–44.
234. Werner E, Kowalczyk AP, Faundez V. Anthrax toxin receptor 1/tumor endothelium marker 8 mediates cell spreading by coupling extracellular ligands to the actin cytoskeleton. J Biol Chem. 2006;281(32):23227–36.
235. Andersen NJ, Boguslawski EA, Naidu AS, Szot C, Bromberg-White JL, Kits K, et al. Anthrax Toxin Receptor 1 Is Essential for Arteriogenesis in a Mouse Model of Hindlimb Ischemia. PLoS One. 2016;11(1):e0146586.
236. Bonuccelli G, Sotgia F, Frank PG, Williams TM, de Almeida CJ, Tanowitz HB,

et al. ATR/TEM8 is highly expressed in epithelial cells lining Bacillus anthracis' three sites of entry: implications for the pathogenesis of anthrax infection. Am J Physiol Cell Physiol. 2005;288:1402–10.
237. Cao C, Wang Z, Huang L, Bai L, Wang Y, Liang Y, et al. Down-regulation of tumor endothelial marker 8 suppresses cell proliferation mediated by ERK1/2 activity. Sci Rep. 2016;6:23419.
238. Xu Y, Ge K, Lu J, Huang J, Wei W, Huang Q. MicroRNA-493 suppresses hepatocellular carcinoma tumorigenesis through down-regulation of anthrax toxin receptor 1 (ANTXR1) and R-Spondin 2 (RSPO2). Biomed Pharmacother. 2017;93:334–43.
239. Gutwein LG, Al-Quran SZ, Fernando S, Fletcher BS, Copeland EM, Grobmyer SR. Tumor endothelial marker 8 expression in triple-negative breast cancer. Anticancer Res. 2011 Oct;31(10):3417–22.
240. Maurya SK, Tewari M, Kumar M, Thakur MK, Shukla HS. Expression pattern of tumor endothelial marker 8 protein in gallbladder carcinomas. Asian Pacific J Cancer Prev. 2011 Jan;12(2):507–12.
241. Duan H-F, Hu X-W, Chen J-L, Gao L-H, Xi Y-Y, Lu Y, et al. Antitumor activities of TEM8-Fc: an engineered antibody-like molecule targeting tumor endothelial marker 8. J Natl Cancer Inst. 2007 Oct 17;99(20):1551–5.
242. Ruan Z, Yang Z, Wang Y, Wang H, Chen Y, Shang X. DNA Vaccine Against Tumor Endothelial Marker 8 Inhibits Tumor Angiogenesis and Growth. J Immunother. 2009;32(5):486–91.
243. Yang X, Zhu H, Hu Z. Dendritic cells transduced with TEM8 recombinant adenovirus prevents hepatocellular carcinoma angiogenesis and inhibits cells growth. Vaccine. 2010 Oct 8;28(43):7130–5.
244. Fernando S, Fletcher BS. Targeting Tumor Endothelial Marker 8 in the Tumor Vasculature of Colorectal Carcinomas in Mice. Cancer Res. 2009 Jun 2;69(12):5126–32.
245. Cullen M, Seaman S, Chaudhary A, Yang MY, Hilton MB, Logsdon D, et al. Host-Derived Tumor Endothelial Marker 8 Promotes the Growth of Melanoma. Cancer Res. 2009 Aug 1;69(15):6021–6.
246. Chaudhary A, Hilton MB, Seaman S, Haines DC, Stevenson S, Lemotte PK, et al. TEM8/ANTXR1 blockade inhibits pathological angiogenesis and potentiates tumoricidal responses against multiple cancer types. Cancer Cell. 2012 Feb 14;21(2):212–26.
247. Chinnasamy D, Tran E, Yu Z, Morgan RA, Restifo NP, Rosenberg SA. Simultaneous targeting of tumor antigens and the tumor vasculature using T lymphocyte transfer synergize to induce regression of established tumors in mice. Cancer Res. 2013;73(11):3371–80.
248. Jenne CN, Kubes P. Immune surveillance by the liver. Nat Immunol. 2013 Sep

18;14(10):996–1006.
249. Ebe Y, Hasegawa G, Takatsuka H, Umezu H, Mitsuyama M, Arakawa M, et al. The role of Kupffer cells and regulation of neutrophil migration into the liver by macrophage inflammatory protein-2 in primary listeriosis in mice. Pathol Int. 1999 Jun 18;49(6):519–32.
250. Robinson MW, Harmon C, O'Farrelly C. Liver immunology and its role in inflammation and homeostasis. Cell Mol Immunol. 2016 May 11;13(3):267–76.
251. Norris S, Collins C, Doherty DG, Smith F, McEntee G, Traynor O, et al. Resident human hepatic lymphocytes are phenotypically different from circulating lymphocytes. J Hepatol. 1998 Jan;28(1):84–90.
252. Berg M, Wingender G, Djandji D, Hegenbarth S, Momburg F, Hämmerling G, et al. Cross-presentation of antigens from apoptotic tumor cells by liver sinusoidal endothelial cells leads to tumor-specific CD8+ T cell tolerance. Eur J Immunol. 2006 Nov 1;36(11):2960–70.
253. Chiang JYL. Bile acid metabolism and signaling. Compr Physiol. 2013 Jul;3(3):1191–212.
254. Tabibian JH, Masyuk AI, Masyuk T V, O'Hara SP, LaRusso NF. Physiology of cholangiocytes. Compr Physiol. 2013 Jan;3(1):541–65.
255. Hirschfield GM, Karlsen TH, Lindor KD, Adams DH. Primary sclerosing cholangitis. Lancet. 2013 Nov 9;382(9904):1587–99.
256. Boonstra K, Beuers U, Ponsioen CY. Epidemiology of primary sclerosing cholangitis and primary biliary cirrhosis: A systematic review. J Hepatol. 2012 May 1;56(5):1181–8.
257. Liu JZ, Roksund Hov J, Folseraas T, Ellinghaus E, Rushbrook SM, Doncheva NT, et al. Dense genotyping of immune-related disease regions identifies nine new risk loci for primary sclerosing cholangitis. Nat Genet. 2013;45(6):670–5.
258. Saarinen S, Olerup O, Broome U. Increased frequency of autoimmune diseases in patients with primary sclerosing cholangitis. Am J Gastroenterol. 2000 Nov 1;95(11):3195–9.
259. Abdalian R, Heathcote EJ. Sclerosing cholangitis: A focus on secondary causes. Hepatology. 2006 Nov 1;44(5):1063–74.
260. Goode EC, Rushbrook SM. A review of the medical treatment of primary sclerosing cholangitis in the 21st century. Ther Adv Chronic Dis. 2016 Jan;7(1):68–85.
261. Hildebrand T, Pannicke N, Dechene A, Gotthardt DN, Kirchner G, Reiter FP, et al. Biliary strictures and recurrence after liver transplantation for primary sclerosing cholangitis: A retrospective multicenter analysis. Liver Transplant. 2016 Jan 1;22(1):42–52.
262. Razumilava N, Gores GJ, Lindor KD. Cancer surveillance in patients with primary sclerosing cholangitis. Hepatology. 2011 Nov 1;54(5):1842–52.

263. Fickert P, Pollheimer MJ, Beuers U, Lackner C, Hirschfield G, Housset C, et al. Characterization of animal models for primary sclerosing cholangitis (PSC). J Hepatol. 2014 Jun 1;60(6):1290–303.
264. Smit JJM, Schinkel AH, Oude Elferink RPJ, Groen AK, Wagenaar E, van Deemter L, et al. Homozygous disruption of the murine mdr2 P-glycoprotein gene leads to a complete absence of phospholipid from bile and to liver disease. Cell. 1993 Nov 5;75(3):451–62.
265. Fickert P, Fuchsbichler A, Wagner M, Zollner G, Kaser A, Tilg H, et al. Regurgitation of Bile Acids From Leaky Bile Ducts Causes Sclerosing Cholangitis in Mdr2 (Abcb4) Knockout Mice. Gastroenterology. 2004;127:261–74.
266. Fickert P, Wagner M, Marschall H-U, Fuchsbichler A, Zollner G, Tsybrovskyy O, et al. 24-norUrsodeoxycholic acid is superior to ursodeoxycholic acid in the treatment of sclerosing cholangitis in Mdr2 (Abcb4) knockout mice. Gastroenterology. 2006;130(2):465–81.
267. Halilbasic E, Fiorotto R, Fickert P, Marschall H-U, Moustafa T, Spirli C, et al. Side chain structure determines unique physiologic and therapeutic properties of norUrsodeoxycholic acid in Mdr2−/− mice. Hepatology. 2009 Jun 1;49(6):1972–81.
268. Baghdasaryan A, Claudel T, Gumhold J, Silbert D, Adorini L, Roda A, et al. Dual farnesoid X receptor/TGR5 agonist INT-767 reduces liver injury in the Mdr2−/− (Abcb4−/−) mouse cholangiopathy model by promoting biliary HCO3− output. Hepatology. 2011 Oct 1;54(4):1303–12.
269. Noy PJ, Lodhia P, Khan K, Zhuang X, Ward DG, Verissimo AR, et al. Blocking CLEC14A-MMRN2 binding inhibits sprouting angiogenesis and tumour growth. Oncogene. 2015;34:5821–31.
270. Liaskou E, Jeffery LE, Trivedi PJ, Reynolds GM, Suresh S, Bruns T, et al. Loss of CD28 expression by liver-infiltrating T cells contributes to pathogenesis of primary sclerosing cholangitis. Gastroenterology. 2014 Jul;147(1):221–32.e7.
271. Sebode M, Peiseler M, Franke B, Schwinge D, Schoknecht T, Wortmann F, et al. Reduced FOXP3+ regulatory T cells in patients with primary sclerosing cholangitis are associated with IL2RA gene polymorphisms. J Hepatol. 2014 May 1;60(5):1010–6.
272. Chatila TA. Role of regulatory T cells in human diseases. J Allergy Clin Immunol. 2005 Nov 1;116(5):949–59.
273. Oo YH, Sakaguchi S. Regulatory T-cell directed therapies in liver diseases. J Hepatol. 2013;59(5):1127–34.
274. Yadav M, Stephan S, Bluestone JA. Peripherally induced Tregs - role in immune homeostasis and autoimmunity. Front Immunol. 2013;4:232.
275. Wildin RS, Ramsdell F, Peake J, Faravelli F, Casanova J-L, Buist N, et al. X-

linked neonatal diabetes mellitus, enteropathy and endocrinopathy syndrome is the human equivalent of mouse scurfy. Nat Genet. 2001 Jan 1;27(1):18–20.
276. Bennett CL, Christie J, Ramsdell F, Brunkow ME, Ferguson PJ, Whitesell L, et al. The immune dysregulation, polyendocrinopathy, enteropathy, X-linked syndrome (IPEX) is caused by mutations of FOXP3. Nat Genet. 2001 Jan 1;27(1):20–1.
277. Brunkow ME, Jeffery EW, Hjerrild KA, Paeper B, Clark LB, Yasayko S-A, et al. Disruption of a new forkhead/winged-helix protein, scurfin, results in the fatal lymphoproliferative disorder of the scurfy mouse. Nat Genet. 2001 Jan 1;27(1):68–73.
278. Sakaguchi S, Sakaguchi N, Asano M, Itoh M, Toda M. Immunologic self-tolerance maintained by activated T cells expressing IL-2 receptor alpha-chains (CD25). Breakdown of a single mechanism of self-tolerance causes various autoimmune diseases. J Immunol. 1995 Aug 1;155(3):1151–64.
279. Bonomo A, Kehn PJ, Shevach EM. Post-thymectomy autoimmunity: abnormal T-cell homeostasis. Immunol Today. 1995 Jan 1;16(2):61–7.
280. Samstein RM, Josefowicz SZ, Arvey A, Treuting PM, Rudensky AY. Extrathymic generation of regulatory T cells in placental mammals mitigates maternal-fetal conflict. Cell. 2012 Jul 6;150(1):29–38.
281. Longhi MS, Hussain MJ, Mitry RR, Arora SK, Mieli-Vergani G, Vergani D, et al. Functional study of CD4+CD25+ regulatory T cells in health and autoimmune hepatitis. J Immunol. 2006 Apr 1;176(7):4484–91.
282. Kriegel MA, Lohmann T, Gabler C, Blank N, Kalden JR, Lorenz H-M. Defective suppressor function of human CD4+ CD25+ regulatory T cells in autoimmune polyglandular syndrome type II. J Exp Med. 2004 May 3;199(9):1285–91.
283. Schneider A, Rieck M, Sanda S, Pihoker C, Greenbaum C, Buckner JH. The effector T cells of diabetic subjects are resistant to regulation via CD4+ FOXP3+ regulatory T cells. J Immunol. 2008 Nov 15;181(10):7350–5.
284. Chowdary Venigalla RK, Tretter T, Krienke S, Max R, Eckstein V, Blank N, et al. Reduced CD4+,CD25− T cell sensitivity to the suppressive function of CD4+, CD25 high, CD127−/low regulatory T cells in patients with active systemic lupus erythematosus. Arthritis Rheum. 2008 Jul;58(7):2120–30.
285. Viglietta V, Baecher-Allan C, Weiner HL, Hafler DA. Loss of functional suppression by CD4+CD25+ regulatory T cells in patients with multiple sclerosis. J Exp Med. 2004 Apr 5;199(7):971–9.
286. Balandina A, Lécart S, Dartevelle P, Saoudi A, Berrih-Aknin S. Functional defect of regulatory CD4(+)CD25+ T cells in the thymus of patients with autoimmune myasthenia gravis. Blood. 2005 Jan 15;105(2):735–41.
287. Ehrenstein MR, Evans JG, Singh A, Moore S, Warnes G, Isenberg DA, et al. Compromised function of regulatory T cells in rheumatoid arthritis and reversal

by anti-TNFalpha therapy. J Exp Med. 2004 Aug 2;200(3):277–85.
288. DiPaolo RJ, Brinster C, Davidson TS, Andersson J, Glass D, Shevach EM. Autoantigen-specific TGFbeta-induced Foxp3+ regulatory T cells prevent autoimmunity by inhibiting dendritic cells from activating autoreactive T cells. J Immunol. 2007 Oct 1;179(7):4685–93.
289. Stephens LA, Malpass KH, Anderton SM. Curing CNS autoimmune disease with myelin-reactive Foxp3+ Treg. Eur J Immunol. 2009 Apr 1;39(4):1108–17.
290. Wright GP, Notley CA, Xue S-A, Bendle GM, Holler A, Schumacher TN, et al. Adoptive therapy with redirected primary regulatory T cells results in antigen-specific suppression of arthritis. Proc Natl Acad Sci U S A. 2009;106(45):19078–83.
291. Bluestone JA, Buckner JH, Fitch M, Gitelman SE, Gupta S, Hellerstein MK, et al. Type 1 diabetes immunotherapy using polyclonal regulatory T cells. Sci Transl Med. 2015;7(315):315ra189.
292. Canavan JB, Scottà C, Vossenkämper A, Goldberg R, Elder MJ, Shoval I, et al. Developing in vitro expanded CD45RA+ regulatory T cells as an adoptive cell therapy for Crohn's disease. Gut. 2016;65(4):584–94.
293. Jethwa H, Adami AA, Maher J. Use of gene-modified regulatory T-cells to control autoimmune and alloimmune pathology: is now the right time? Clin Immunol. 2014 Jan;150(1):51–63.
294. McGovern JL, Wright GP, Stauss HJ. Engineering Specificity and Function of Therapeutic Regulatory T Cells. Front Immunol. 2017;8:1517.
295. Lapierre P, Béland K, Yang R, Alvarez F. Adoptive transfer of ex vivo expanded regulatory T cells in an autoimmune hepatitis murine model restores peripheral tolerance. Hepatology. 2013 Jan 1;57(1):217–27.
296. Longhi MS, Hussain MJ, Kwok WW, Mieli-Vergani G, Ma Y, Vergani D. Autoantigen-specific regulatory T cells, a potential tool for immune-tolerance reconstitution in type-2 autoimmune hepatitis. Hepatology. 2011 Feb 1;53(2):536–47.
297. Elinav E, Waks T, Eshhar Z. Redirection of regulatory T cells with predetermined specificity for the treatment of experimental colitis in mice. Gastroenterology. 2008 Jun 1;134(7):2014–24.
298. Elinav E, Adam N, Waks T, Eshhar Z. Amelioration of Colitis by Genetically Engineered Murine Regulatory T Cells Redirected by Antigen-Specific Chimeric Receptor. Gastroenterology. 2009;136(5):1721–31.
299. Blat D, Zigmond E, Alteber Z, Waks T, Eshhar Z. Suppression of murine colitis and its associated cancer by carcinoembryonic antigen-specific regulatory T cells. Mol Ther. 2014 May 1;22(5):1018–28.
300. Fransson M, Piras E, Burman J, Nilsson B, Essand M, Lu B, et al. CAR/FoxP3-engineered T regulatory cells target the CNS and suppress EAE upon

intranasal delivery. J Neuroinflammation. 2012 Dec 30;9(1):576.
301. Hombach AA, Kofler D, Rappl G, Abken H. Redirecting human CD4+CD25+ regulatory T cells from the peripheral blood with pre-defined target specificity. Gene Ther. 2009;16(9):1088–96.
302. MacDonald KG, Hoeppli RE, Huang Q, Gillies J, Luciani DS, Orban PC, et al. Alloantigen-specific regulatory T cells generated with a chimeric antigen receptor. J Clin Invest. 2016 Mar 21;126(4):1413–24.
303. Yoon J, Schmidt A, Zhang A-H, Konigs C, Kim YC, Scott DW. FVIII-specific human chimeric antigen receptor T-regulatory cells suppress T-and B-cell responses to FVIII. Blood. 2017;129(2):238–45.
304. Nolan Lab. Phoenix helper-free retrovirus producer lines [Internet]. [cited 2017 Oct 23]. Available from: https://web.stanford.edu/group/nolan/_OldWebsite/retroviral_systems/phx.html
305. Battaglia M, Stabilini A, Migliavacca B, Horejs-Hoeck J, Kaupper T, Roncarolo MG. Rapamycin Promotes Expansion of Functional CD4+CD25+FOXP3+ Regulatory T Cells of Both Healthy Subjects and Type 1 Diabetic Patients. J Immunol. 2006 Dec 15;177(12):8338–47.
306. Fehse B, Richters A, Putimtseva-Scharf K, Klump H, Li Z, Ostertag W, et al. CD34 Splice Variant: An Attractive Marker for Selection of Gene-Modified Cells. Mol Ther. 2000;1(5):448–56.
307. Cheadle EJ, Sheard V, Rothwell DG, Bridgeman JS, Ashton G, Hanson V, et al. Differential role of Th1 and Th2 cytokines in autotoxicity driven by CD19-specific second-generation chimeric antigen receptor T cells in a mouse model. J Immunol. 2014 Apr 15;192(8):3654–65.
308. Applied Biosystems. User Bulletin #2: ABI PRISM 7700 Sequence Detection System. Relative Quantitation of Gene Expression. 2001. p. 1–36.
309. Liu S, Leppla SH. Cell surface tumor endothelium marker 8 cytoplasmic tail-independent anthrax toxin binding, proteolytic processing, oligomer formation, and internalization. J Biol Chem. 2003;278(7):5227–34.
310. Engels B, Cam H, Schüler T, Indraccolo S, Gladow M, Baum C, et al. Retroviral vectors for high-level transgene expression in T lymphocytes. Hum Gene Ther. 2003 Aug 10;14(12):1155–68.
311. Hacein-Bey-Abina S, Garrigue A, Wang GP, Soulier J, Lim A, Morillon E, et al. Insertional oncogenesis in 4 patients after retrovirus-mediated gene therapy of SCID-X1. J Clin Invest. 2008 Sep;118(9):3132–42.
312. Newrzela S, Cornils K, Li Z, Baum C, Brugman MH, Hartmann M, et al. Resistance of mature T cells to oncogene transformation. Blood. 2008 Sep 15;112(6):2278–86.
313. Scholler J, Brady TL, Binder-Scholl GK, Hwang W-T, Plesa G, Hege KM, et al. Decade-long safety and function of retroviral-modified chimeric antigen

receptor T cells. Sci Transl Med. 2012 May 2;4(132):132ra53.
314. Long AH, Haso WM, Shern JF, Wanhainen KM, Murgai M, Ingaramo M, et al. 4-1BB costimulation ameliorates T cell exhaustion induced by tonic signaling of chimeric antigen receptors. Nat Med. 2015 May 4;21(6):581–90.
315. Kawalekar OU, O'Connor RS, Fraietta JA, Guo L, McGettigan SE, Posey AD, et al. Distinct Signaling of Coreceptors Regulates Specific Metabolism Pathways and Impacts Memory Development in CAR T Cells. Immunity. 2016;44(2):380–90.
316. Lamers CHJ, van Elzakker P, Langeveld SCL, Sleijfer S, Gratama JW. Process validation and clinical evaluation of a protocol to generate gene-modified T lymphocytes for imunogene therapy for metastatic renal cell carcinoma: GMP-controlled transduction and expansion of patient's T lymphocytes using a carboxy anhydrase IX-s. Cytotherapy. 2006 Jan;8(6):542–53.
317. Porter DL, Levine BL, Bunin N, Stadtmauer EA, Luger SM, Goldstein S, et al. A phase 1 trial of donor lymphocyte infusions expanded and activated ex vivo via CD3/CD28 costimulation. Blood. 2006 Feb 15;107(4):1325–31.
318. Kaartinen T, Luostarinen A, Maliniemi P, Keto J, Arvas M, Belt H, et al. Low interleukin-2 concentration favors generation of early memory T cells over effector phenotypes during chimeric antigen receptor T-cell expansion. Cytotherapy. 2017;19(6):689–702.
319. Yang S, Ji Y, Gattinoni L, Zhang L, Yu Z, Restifo NP, et al. Modulating the differentiation status of ex vivo-cultured anti-tumor T cells using cytokine cocktails. Cancer Immunol Immunother. 2013 Apr 4;62(4):727–36.
320. Caruso HG, Hurton L V, Najjar A, Rushworth D, Ang S, Olivares S, et al. Tuning sensitivity of CAR to EGFR density limits recognition of normal tissue while maintaining potent antitumor activity. Cancer Res. 2015;75(17):3505–18.
321. Chmielewski M, Hombach AA, Heuser C, Adams GP, Abken H. T Cell Activation by Antibody-Like Immunoreceptors: Increase in Affinity of the Single-Chain Fragment Domain above Threshold Does Not Increase T Cell Activation against Antigen-Positive Target Cells but Decreases Selectivity. J Immunol. 2004;173(12):7647–53.
322. Liu X, Jiang S, Fang C, Yang S, Olalere D, Pequignot EC, et al. Affinity-tuned ErbB2 or EGFR chimeric antigen receptor T cells exhibit an increased therapeutic index against tumors in mice. Cancer Res. 2015;75(17):3596–607.
323. Lever M, Lim H-S, Kruger P, Nguyen J, Trendel N, Abu-Shah E, et al. Architecture of a minimal signaling pathway explains the T-cell response to a 1 million-fold variation in antigen affinity and dose. Proc Natl Acad Sci U S A. 2017 Jan 10;114(2):E267.
324. Yang MY, Chaudhary A, Seaman S, Dunty J, Stevens J, Elzarrad MK, et al. The cell surface structure of tumor endothelial marker 8 (TEM8) is regulated by

the actin cytoskeleton. Biochim Biophys Acta. 2011 Jan;1813(1):39–49.
325. Byrd TT, Fousek K, Pignata A, Szot C, Samaha H, Seaman S, et al. TEM8/ANTXR1-Specific CAR T Cells as a Targeted Therapy for Triple-Negative Breast Cancer. Cancer Res. 2018 Jan 15;78(2):489–500.
326. Hod EA, Cadwell CM, Liepkalns JS, Zimring JC, Sokol SA, Schirmer DA, et al. Cytokine storm in a mouse model of IgG-mediated hemolytic transfusion reactions. Blood. 2008;112(3):891–4.
327. Gogishvili T, Langenhorst D, Lühder F, Elias F, Elflein K, Dennehy KM, et al. Rapid Regulatory T-Cell Response Prevents Cytokine Storm in CD28 Superagonist Treated Mice. Unutmaz D, editor. PLoS One. 2009 Feb 27;4(2):e4643.
328. Tisoncik JR, Korth MJ, Simmons CP, Farrar J, Martin TR, Katze MG. Into the eye of the cytokine storm. Microbiol Mol Biol Rev. 2012 Mar 1;76(1):16–32.
329. Brady JL, Harrison LC, Goodman DJ, Cowan PJ, Hawthorne WJ, O'Connell PJ, et al. Preclinical screening for acute toxicity of therapeutic monoclonal antibodies in a hu-SCID model. Clin Transl Immunol. 2014 Dec;3(12):e29.
330. Weißmüller S, Kronhart S, Kreuz D, Schnierle B, Kalinke U, Kirberg J, et al. TGN1412 Induces Lymphopenia and Human Cytokine Release in a Humanized Mouse Model. Stoddart CA, editor. PLoS One. 2016 Mar 9;11(3):e0149093.
331. Sentman M-L, Murad JM, Cook WJ, Wu M-R, Reder J, Baumeister SH, et al. Mechanisms of Acute Toxicity in NKG2D Chimeric Antigen Receptor T Cell–Treated Mice. J Immunol. 2016 Dec 15;197(12):4674–85.
332. Vargas M, Karamsetty R, Leppla SH, Chaudry GJ. Broad Expression Analysis of Human ANTXR1/TEM8 Transcripts Reveals Differential Expression and Novel Splice Variants. Hong W, editor. PLoS One. 2012 Aug 17;7(8):e43174.
333. Liu S, Zhang Y, Moayeri M, Liu J, Crown D, Fattah RJ, et al. Key tissue targets responsible for anthrax-toxin-induced lethality. Nature. 2013;501(7465):63–8.
334. Chen D, Bhat-Nakshatri P, Goswami C, Badve S, Nakshatri H. ANTXR1, a stem cell-enriched functional biomarker, connects collagen signaling to cancer stem-like cells and metastasis in breast cancer. Cancer Res. 2013;73:5821–33.
335. Mancuso P, Calleri A, Gregato G, Labanca V, Quarna J, Antoniotti P, et al. A subpopulation of circulating endothelial cells express CD109 and is enriched in the blood of cancer patients. PLoS One. 2014 Jan 15;9(12):e114713.
336. Stranecky V, Hoischen A, Hartmannova H, Zaki MS, Chaudhary A, Zudaire E, et al. Mutations in ANTXR1 cause GAPO syndrome. Am J Hum Genet. 2013;92(5):792–9.
337. Liu S, Moayeri M, Leppla SH. Anthrax lethal and edema toxins in anthrax pathogenesis. Trends Microbiol. 2014;22(6):317–25.
338. Besschetnova TY, Ichimura T, Katebi N, St Croix B, Bonventre J V, Olsen BR.

Regulatory mechanisms of anthrax toxin receptor 1-dependent vascular and connective tissue homeostasis. Matrix Biol. 2015 Mar;42:56–73.
339. Zeydan B, Benbir G, Uluduz D, Ince B, Goksan B, Islak C. Arterial and Venous Thrombosis of the Cerebral Vasculature in GAPO Syndrome. Am J Med Genet Part A. 2014;164A:1284–8.
340. Tiwari A, Agrawal A, Pratap A, Lakshmi RS, Narad R. Apert syndrome with septum pellucidum agenesis. Singapore Med J. 2007;48(2):e62.
341. NIH U.S. National Library of Medicine. Apert syndrome [Internet]. [cited 2018 Mar 15]. Available from: https://ghr.nlm.nih.gov/condition/apert-syndrome#genes
342. Hu K, Olsen BR, Besschetnova TY. Cell autonomous ANTXR1-mediated regulation of extracellular matrix components in primary fibroblasts. Matrix Biol. 2017;62:105–14.
343. Liu S, Liu J, Ma Q, Cao L, Fattah RJ, Yu Z, et al. Solid tumor therapy by selectively targeting stromal endothelial cells. Proc Natl Acad Sci U S A. 2016 Jul 12;113(28):E4079-87.
344. Oo YH. AUTUMN - University of Birmingham [Internet]. [cited 2018 Apr 3]. Available from: https://www.birmingham.ac.uk/research/activity/mds/trials/crctu/trials/autumn/index.aspx
345. Strauss L, Czystowska M, Szajnik M, Mandapathil M, Whiteside TL. Differential Responses of Human Regulatory T Cells (Treg) and Effector T Cells to Rapamycin. Unutmaz D, editor. PLoS One. 2009 Jun 22;4(6):e5994.
346. Tresoldi E, Dell'Albani I, Stabilini A, Jofra T, Valle A, Gagliani N, et al. Stability of human rapamycin-expanded CD4+CD25+ T regulatory cells. Haematologica. 2011;96(9):1357–65.
347. Martin CR, Zaman MM, Ketwaroo GA, Bhutta AQ, Coronel E, Popov Y, et al. CFTR dysfunction predisposes to fibrotic liver disease in a murine model. Am J Physiol Gastrointest Liver Physiol. 2012 Aug 15;303(4):G474-81.
348. Potikha T, Stoyanov E, Pappo O, Frolov A, Mizrahi L, Olam D, et al. Interstrain differences in chronic hepatitis and tumor development in a murine model of inflammation-mediated hepatocarcinogenesis. Hepatology. 2013;58(1):192–204.
349. Ikenaga N, Liu SB, Sverdlov DY, Yoshida S, Nasser I, Ke Q, et al. A New Mdr2−/− Mouse Model of Sclerosing Cholangitis with Rapid Fibrosis Progression, Early-Onset Portal Hypertension, and Liver Cancer. Am J Pathol. 2015 Feb 1;185(2):325–34.
350. Strauss L, Whiteside TL, Knights A, Bergmann C, Knuth A, Zippelius A. Selective Survival of Naturally Occurring Human CD4+CD25+Foxp3+ Regulatory T Cells Cultured with Rapamycin. J Immunol. 2007 Jan

1;178(1):320–9.
351. Putnam AL, Brusko TM, Lee MR, Liu W, Szot GL, Ghosh T, et al. Expansion of human regulatory T-cells from patients with type 1 diabetes. Diabetes. 2009 Mar;58(3):652–62.
352. Zhou X, Kong N, Wang J, Fan H, Zou H, Horwitz D, et al. Cutting Edge: All-Trans Retinoic Acid Sustains the Stability and Function of Natural Regulatory T Cells in an Inflammatory Milieu. J Immunol. 2010;185(5):2675–9.
353. Scottà C, Esposito M, Fazekasova H, Fanelli G, Edozie FC, Ali N, et al. Differential effects of rapamycin and retinoic acid on expansion, stability and suppressive qualities of human CD4+CD25+FOXP3+ T regulatory cell subpopulations. Haematologica. 2013;98(8):1291–9.
354. Fuhrman CA, Yeh W-I, Seay HR, Saikumar Lakshmi P, Chopra G, Zhang L, et al. Divergent Phenotypes of Human Regulatory T Cells Expressing the Receptors TIGIT and CD226. J Immunol. 2015 Jul 1;195(1):145–55.
355. Pan F, Yu H, Dang E V, Barbi J, Pan X, Grosso JF, et al. Eos mediates Foxp3-dependent gene silencing in regulatory T cells. Science (80-). 2009;325(5944):1142–6.
356. Scott DW. From IgG Fusion Proteins to Engineered-Specific Human Regulatory T Cells: A Life of Tolerance. Front Immunol. 2017;8:1576.
357. Brunstein CG, Blazar BR, Miller JS, Cao Q, Hippen KL, McKenna DH, et al. Adoptive transfer of umbilical cord blood-derived regulatory T cells and early viral reactivation. Biol Blood Marrow Transplant. 2013 Aug 1;19(8):1271–3.
358. Dawson NAJ, Vent-Schmidt J, Levings MK. Engineered Tolerance: Tailoring Development, Function, and Antigen-Specificity of Regulatory T Cells. Front Immunol. 2017 Nov 3;8:1460.
359. Mullard A. FDA approves first CAR T therapy. Nat Rev Drug Discov. 2017 Sep 29;16(10):669.
360. FDA Approves Second CAR T-cell Therapy. Cancer Discov. 2018 Jan;8(1):5–6.
361. Cai T-Y, Liu X-W, Zhu H, Cao J, Zhang J, Ding L, et al. Tirapazamine sensitizes hepatocellular carcinoma cells to topoisomerase I inhibitors via cooperative modulation of hypoxia-inducible factor-1α. Mol Cancer Ther. 2014 Mar 1;13(3):630–42.
362. Ananieva E. Targeting amino acid metabolism in cancer growth and anti-tumor immune response. World J Biol Chem. 2015 Nov 26;6(4):281–9.
363. Papadopoulos KP, Tsai FY-C, Bauer TM, Muigai L, Liang Y, Bennett MK, et al. CX-1158-101: A first-in-human phase 1 study of CB-1158, a small molecule inhibitor of arginase, as monotherapy and in combination with an anti-PD-1 checkpoint inhibitor in patients (pts) with solid tumors. J Clin Oncol. 2017;35:15_suppl, 3005.

364. Ninomiya S, Narala N, Huye L, Yagyu S, Savoldo B, Dotti G, et al. Tumor indoleamine 2,3-dioxygenase (IDO) inhibits CD19-CAR T cells and is downregulated by lymphodepleting drugs. Blood. 2015 Jun 18;125(25):3905–16.
365. Marin-Acevedo JA, Soyano AE, Dholaria B, Knutson KL, Lou Y. Cancer immunotherapy beyond immune checkpoint inhibitors. J Hematol Oncol. 2018;11(1):8.
366. Lanitis E, Irving M, Coukos G. Targeting the tumor vasculature to enhance T cell activity. Curr Opin Immunol. 2015;33:55–63.
367. Liu X, Ranganathan R, Jiang S, Fang C, Sun J, Kim S, et al. A Chimeric Switch-Receptor Targeting PD1 Augments the Efficacy of Second-Generation CAR T Cells in Advanced Solid Tumors. Cancer Res. 2016;76(6):1578–90.
368. Suarez ER, Chang D-K, Sun J, Sui J, Freeman GJ, Signoretti S, et al. Chimeric antigen receptor T cells secreting anti-PD-L1 antibodies more effectively regress renal cell carcinoma in a humanized mouse model. Oncotarget. 2016 Jun 7;7(23):34341–55.
369. Hammill JA, VanSeggelen H, Helsen CW, Denisova GF, Evelegh C, Tantalo DGM, et al. Designed ankyrin repeat proteins are effective targeting elements for chimeric antigen receptors. J Immunother Cancer. 2015;3(1):55.
370. Faitschuk E, Nagy V, Hombach AA, Abken H. A dual chain chimeric antigen receptor (CAR) in the native antibody format for targeting immune cells towards cancer cells without the need of an scFv. Gene Ther. 2016 Oct 14;23(10):718–26.
371. Grada Z, Hegde M, Byrd T, Shaffer DR, Ghazi A, Brawley VS, et al. TanCAR: A Novel Bispecific Chimeric Antigen Receptor for Cancer Immunotherapy. Mol Ther - Nucleic Acids. 2013;2:e105.
372. Hegde M, Mukherjee M, Grada Z, Pignata A, Landi D, Navai SA, et al. Tandem CAR T cells targeting HER2 and IL13Rα2 mitigate tumor antigen escape. J Clin Invest. 2016 Aug 1;126(8):3036–52.
373. Garin-Chesa P, Old LJ, Rettig WJ. Cell surface glycoprotein of reactive stromal fibroblasts as a potential antibody target in human epithelial cancers. Proc Natl Acad Sci U S A. 1990 Sep 1;87(18):7235–9.
374. Kakarla S, Chow KKH, Mata M, Shaffer DR, Song X-T, Wu M-F, et al. Antitumor effects of chimeric receptor engineered human T cells directed to tumor stroma. Mol Ther. 2013 Aug 1;21(8):1611–20.
375. Schuberth PC, Hagedorn C, Jensen SM, Gulati P, van den Broek M, Mischo A, et al. Treatment of malignant pleural mesothelioma by fibroblast activation protein-specific re-directed T cells. J Transl Med. 2013 Aug 12;11(1):187.
376. Lanitis E, Poussin M, Klattenhoff AW, Song D, Sandaltzopoulos R, June CH, et al. Chimeric Antigen Receptor T Cells with Dissociated Signaling Domains

Exhibit Focused Antitumor Activity with Reduced Potential for Toxicity In Vivo. Cancer Immunol Res. 2013;1(1):43–53.
377. Wu C-Y, Roybal KT, Puchner EM, Onuffer J, Lim WA. Remote control of therapeutic T cells through a small molecule-gated chimeric receptor. Science (80-). 2015 Oct 16;350(6258):aab4077.
378. Ma JSY, Kim JY, Kazane SA, Choi S, Yun HY, Kim MS, et al. Versatile strategy for controlling the specificity and activity of engineered T cells. Proc Natl Acad Sci U S A. 2016 Jan 26;113(4):E450-8.
379. Roybal KT, Rupp LJ, Morsut L, Walker WJ, McNally KA, Park JS, et al. Precision Tumor Recognition by T Cells With Combinatorial Antigen-Sensing Circuits. Cell. 2016;164(4):770–9.
380. Roybal KT, Williams JZ, Morsut L, Rupp LJ, Kolinko I, Choe JH, et al. Engineering T Cells with Customized Therapeutic Response Programs Using Synthetic Notch Receptors. Cell. 2016;167(2):419–32.
381. Zhang T, Sentman CL. Mouse tumor vasculature expresses NKG2D ligands and can be targeted by chimeric NKG2D-modified T cells. J Immunol. 2013 Mar 1;190(5):2455–63.
382. Lonez C, Verma B, Hendlisz A, Aftimos P, Awada A, Van Den Neste E, et al. Study protocol for THINK: a multinational open-label phase I study to assess the safety and clinical activity of multiple administrations of NKR-2 in patients with different metastatic tumour types. BMJ Open. 2017;7(11):e017075.
383. Zhao Y, Moon E, Carpenito C, Paulos CM, Liu X, Brennan AL, et al. Multiple injections of electroporated autologous T cells expressing a chimeric antigen receptor mediate regression of human disseminated tumor. Cancer Res. 2010 Nov 15;70(22):9053–61.
384. Gargett T, Brown MP. The inducible caspase-9 suicide gene system as a “safety switch” to limit on-target, off-tumor toxicities of chimeric antigen receptor T cells. Front Pharmacol. 2014 Oct 28;5:235.
385. Poirot L, Philip B, Schiffer-Mannioui C, Le Clerre D, Chion-Sotinel I, Derniame S, et al. Multiplex genome-edited T-cell manufacturing platform for “off-the-shelf” adoptive T-cell immunotherapies. Cancer Res. 2015;75(18):3853–64.
386. Smith TT, Stephan SB, Moffett HF, McKnight LE, Ji W, Reiman D, et al. In situ programming of leukaemia-specific T cells using synthetic DNA nanocarriers. Nat Nanotechnol. 2017 Apr 17;12(8):813–20.
387. Eyquem J, Mansilla-Soto J, Giavridis T, van der Stegen SJC, Hamieh M, Cunanan KM, et al. Targeting a CAR to the TRAC locus with CRISPR/Cas9 enhances tumour rejection. Nature. 2017 Mar 22;543(7643):113–7.